2. HOLE 504B, LEG 83[1]

Shipboard Scientific Party[2]

Hole:	504B (Leg 83)	504B (Total, Legs 69, 70, 83)
Date occupied:	22 Nov. 1981	—
Date departed:	2 Jan. 1982	—
Time on hole:	983.2 hr.	1610.1 hr.
Position:	01°13.63'N; 83°43.81'W	01°13.63'N; 83°43.81'W
Water depth (sea level; corrected m, echo-sounding):	3460	3460
Water depth (rig floor; corrected m, echo-sounding):	3470	3470
Bottom felt (m, drill pipe):	3473.5	3473.5
Penetration (m):	1350	1350
Number of cores:	71	141
Total length of cored section (m):	514	1088.5
Total core recovery (m):	106.9	276.3
Percentage recovered:	20.8	25.4
Oldest sediment cored:		
Depth sub-bottom (m):	274.5	274.5
Nature:	Chert and siliceous limestone	Chert and siliceous limestone
Age (estimated from magnetic anomalies)	5.9 m.y.	5.9 m.y.
Measured velocity (km/s):	—	—
Basement:		
Top of basement (depth sub-bottom, m):	274.5	274.5
Meters of basement drilled:	514	1075.5
Nature:	Basalt pillows, flows, and dikes	Basalt pillows, flows, and dikes
Velocity range (km/s):	5.1–6.9	5.1–6.9

Principal results: Leg 83 deepened Hole 504B in the Costa Rica Rift to 1350 m, including 1075.5 m in the basement. The lowest 300 m appear to correspond to a dike complex. Zeolite- and greenschist-facies mineral assemblages are identified from 614 to 920 m sub-basement but no rocks are completely recrystallized or reequilibrated under any metamorphic facies. Between 800 and 1000 m, the rocks are altered less extensively but under widely varying conditions. Below 1 km, the material recovered consists of highly altered dikes displaying greenschist- and zeolite-facies metamorphism. Stockwork-like mineralization with pyrite, chalcopyrite, and sphalerite are observed in metamorphic silicate veins and disseminated in the rocks from 636 to 654 m sub-basement.

Downhole temperatures indicate continued flow of ocean bottom water into the upper 100 m of the basement and conductive heat flow below at a rate of 190 mW/m^2. The maximum measured temperature before reequilibration was 133°C. The formation-water chemistry varies downhole; the Mg content decreases to half of seawater at a depth of 519 m sub-basement and a temperature of 115°C. This is the largest chemical anomaly yet measured in basement-formation waters. The pH decreases and the Ca, NH_3, and H_2S contents increase with depth. Ca gain exceeds Mg loss, implying a loss of Na or K.

A strong correlation between magnetic susceptibility, NRM intensity, and alteration of titanomagnetite is shown by a marked decrease in susceptibility from 740 to 90 $\times 10^{-5}$ cgs and a decrease in intensity from 40 to 1.5 $\times 10^{-5}$ emu/cm^3, which corresponds to progressive replacement of titanomagnetite by sphene, starting at 624 m sub-basement and complete at 636 m. Higher average susceptibility and intensity values below 757 m sub-basement correspond to lesser alteration of coarser-grained, massive dike rocks.

Full suites of successful televiewer, temperature, neutron, caliper, multichannel sonic, and resistivity logs were obtained. The large-scale resistivity log was also successful, indicating an extreme gradient in resistivity below 625 m sub-basement and suggesting a strong decrease of bulk porosity to about 1% near the bottom of the hole. The packer experiment was successful, indicating that the drop in permeability with depth in the upper ocean crust was on the scale of three orders of magnitude.

An S-wave log was run for the first time in the ocean floor. Fracture and clay content estimates from televiewer logs correlate quantitatively with all logs, particularly body wave energy and Poisson's ratio.

---

[1] Anderson, R. N., Honnorez, J., Becker, K., et al., *Init. Repts. DSDP*, 83: Washington (U.S. Govt. Printing Office).

[2] Roger N. Anderson (Co-Chief Scientist), Lamont-Doherty Geological Observatory, Columbia University, Palisades, New York 10964; Jose Honnorez (Co-Chief Scientist), Rosenstiel School of Marine and Atmospheric Science, University of Miami, Miami, Florida 33149; Keir Becker, Deep Sea Drilling Project, Scripps Institution of Oceanography, La Jolla, California 92093; Andrew C. Adamson, Department of Geology, The University, Newcastle-upon-Tyne NE1 7RU, United Kingdom (present address: Ocean Drilling Program, Texas A&M University, College Station, TX 77843-3469); Jeffrey C. Alt, Rosenstiel School of Marine and Atmospheric Science, University of Miami, Miami, Florida 33149 (present address: Dept. of Earth and Planetary Sciences, Campus Box 1169, Washington University, St. Louis, MO 63130); Rolf Emmermann, Mineralogisch-Petrologisches Institut, Justus-Liebig-Universität, D-6300 Giessen, Federal Republic of Germany; Pamela D. Kempton, Department of Geological Sciences, Southern Methodist University, Dallas, Texas (present address: NASA–Johnson Space Center, Mail Code SN2, Houston, TX 77058); Hajimu Kinoshita, Department of Earth Sciences, Chiba University, Chiba 260, Japan; Christine Laverne, Laboratoire de Geologie, Université de l'Océan Indien, 97490 Ste. Clotilde (Réunion), France (present address: Laboratoire de Géologie, Faculté des Sciences et Techniques, 3038 SFAX, Tunisia); Michael J. Mottl, Department of Chemistry, Woods Hole Oceanographic Institution, Woods Hole, Massachusetts 02543; Robin Newmark, Lamont-Doherty Geological Observatory, Palisades, New York 10964.

BACKGROUND AND OBJECTIVES

During Leg 83 of the Deep Sea Drilling Project (DSDP), the *Glomar Challenger* devoted nearly two months to the most successful basement hole in the oceanic crust, Hole 504B. Located in 5.9 m.y. old crust about 200 km south of the spreading axis of the Costa Rica Rift (Figs. 1 and 2), Hole 504B had been cored to a depth of 836 m beneath the seafloor during Legs 69 and 70 in late 1979 (CRRUST, 1982; Cann, Langseth, Honnorez, Von Herzen, White, et al., 1983). Legs 69 and 70 had achieved a total basement penetration of 561.5 m, only 22 m short of the record. (During Leg 37, 583 m of basement was cored in Hole 332B on the western flank of the Mid-Atlantic Ridge at 36°N.) Thus, Leg 83 scientists approached Hole 504B with the unique opportunity to pioneer in the direct sampling of and experimentation within the deeper oceanic basement.

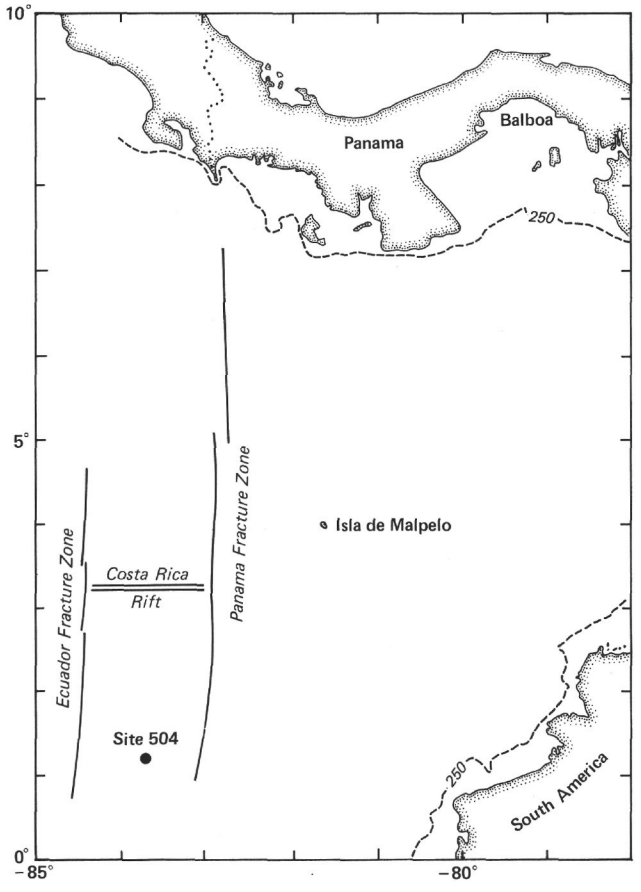

Figure 1. Location of Hole 504B in the eastern equatorial Pacific.

In a broad sense, the main reason for the return to Hole 504B on Leg 83 was to extend our knowledge of the nature of the oceanic crust to the zone underlying the interlayered basaltic pillow-lava flow formation previously encountered in every basement hole cored by DSDP. Hole 504B was doubly interesting, in that it was cored in relatively young crust, capped by a thick sediment layer (274.5 m). Thus it provided the opportunity to study the *in situ* state of young oceanic crust, with particular focus on the petrological, geochemical, and physical signature of hydrothermal circulation in the porous, igneous basement near a spreading center.

Leg 83 was specifically planned to deepen Hole 504B in order to sample and conduct geophysical experiments in the lower levels of Layer 2. Leg 83 was conducted in four distinct phases, with the following specific objectives:

1. Immediately after the hole was reentered, equilibrium temperatures were measured and undisturbed pore water samples were collected from throughout the existing 836 m hole depth. Because the hole had been undisturbed for nearly two years since Leg 70, thermal equilibrium should have been reached, and the water in the borehole should have approached chemical equilibrium with the basement pore fluids. The temperature measurements were designed to test the conclusions, based on data from Legs 69 and 70, that ocean bottom water was being drawn down the hole into an underpressured reservoir in the upper basement, and that a nearly conductive geothermal gradient (0.11°C/m) existed in the basement below 400 m. The purpose of the water sampling program was to obtain representative basement pore

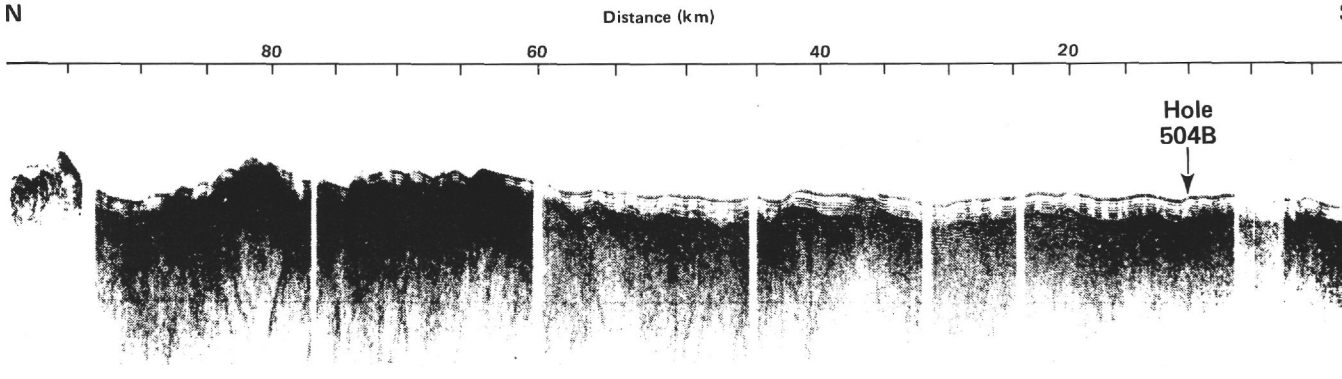

Figure 2. North-south seismic profile through Site 504, showing basement topography and sediment thickness. The axis of the Costa Rica Rift is located about 110 km north of this profile.

fluids, in order to study the chemical interactions between seawater and basalt at the temperatures now prevailing in the hole.

2. Twenty-two days were then spent coring Hole 504B, deepening the hole to 1287.5 m, or 1013 m into basement. (See Table 1. An additional 62.5 m was cored during the last four days on site.) The total basement penetration achieved was nearly double that of any other DSDP hole to date. Moreover, Leg 83 cored for the first time into the sheeted dikes and massive units of Layer 2C (Anderson et al., 1982). Thus the basalt samples recovered during Leg 83 provided a unique opportunity to study the petrologic, geochemical, and physical nature of the deeper parts of Layer 2, in particular the transition from pillow lavas and minor flows in Layer 2B to the sheeted dike complex in Layer 2C.

3. After Hole 504B had been cored to 1287.5 m (i.e., over 1 km into basement), 12 days were devoted to the most extensive set of *in situ* geophysical experiments ever conducted in the oceanic crust. These included temperature logs, borehole televiewer, sonic logs (compressional and shear waves), a full site of Schlumberger logs, large-scale resistivity experiment, water sampling, and permeability measurements. Particular attention was directed toward (1) documenting the changes in *in situ* properties with depth, especially at the Layer 2B/2C transition, (2) relating these measurements to laboratory measurements of physical properties of samples, and (3) synthesizing the experimental results with lithological and petrological studies on recovered samples.

4. After the experimental phase, four more days were devoted to coring, during which the hole was deepened to 1350 m beneath the seafloor, 1075.5 m into basement.

Specific objectives of the studies of recovered samples are discussed in greater detail in subsequent sections of this chapter. Briefly, these objectives included:

1. Determination of the lithostratigraphy and structure of the lower portion of Layer 2.

2. Determination of the geochemical nature of the recovered basalts, with particular focus on the chemical variability with depth of both unaltered and altered rocks and on the magmatic origin and formation of the basement.

3. Study of the alteration mineralogy and geochemistry and its variation with depth, with emphasis on understanding the history of alteration since crustal accretion at the spreading axis, and on comparison with models of alteration based on studies of ophiolites.

4. Measurement of various physical properties of recovered basalts, including sonic velocities, density, porosity, magnetic intensity and susceptibility, and thermal and electrical conductivities, and relating these laboratory measurements to the bulk properties of the oceanic crust.

All of our objectives were successfully fulfilled. This chapter presents the results of shipboard analyses only. In many cases, shore-based studies and detailed analyses of shipboard analyses are presented in separate later chapters. A short summary of the shipboard results was given by Anderson et al. (1982).

OPERATIONS

Leg 83 commenced on 14 November 1981 at Balboa Harbor, Panama, and terminated on 5 January 1982, again at Balboa Harbor. The total length of the leg was 52 days, of which 41 days were spent on site, 5 days on the scheduled port call and 6 days in transit (Fig. 3).

Hole 504B: Reentry No. 1

After the ship returned to the beacon location the dynamic positioning system was switched to its automatic mode. The coring bottomhole assembly was picked up and drill pipe was run to 7 m above the mudline depth reported during Legs 69 and 70. While drill pipe was being run, the ship was moved to the hole location, 1°13.63′N, 83°43.81′W, with the aid of satellite navigation fixes. The scanning sonar equipment was run and scanning began after the tool landed at the bit. The tool appeared to be working well but no echo from a cone was detected.

Finding Hole 504B was complicated by the close proximity of the reentry Hole 504A, 1000 ft. to the west. An expanding rectangle search pattern was adopted to locate the cone of either hole. After the ship was offset 1000 ft. west, 200 ft. south, and then 400 ft. east, and echo from a cone was detected.

At this point the scanning tool was found to have an effective range of 150 ft. instead of the usual 300 ft.—thus the failure to locate the cone during the initial 1000-ft. offset west. After an additional 3.5 hr. during which the ship was moved short distances to swing the drill pipe, the hole was reentered at 0632 hr., 23 November. Drill pipe was run 50 m below seafloor (BSF) to confirm reentry.

Temperature Survey and Borehole Water Sampling Program

The dual aim of the first suite of experiments was: (1) to determine, using a temperature profile of the hole, whether bottom water was still being drawn down the hole into a "capped" reservoir system (as was observed two years earlier during Legs 69 and 70) and, (2) to obtain borehole water samples for geochemical studies from several successive points down the hole.

After reentry was verified, the temperature survey and borehole water sampling tool (Barnes-Uyeda tool) was dropped down the drill pipe to the bit. The drill pipe was then run to 194 m BSF in one-stand intervals (28.5 m) with a 10 min. stop at each depth interval. At the final depth a borehole water sample was taken, the tool recovered, and the results analyzed.

The temperatures recorded were similar to those obtained during Leg 70, indicating a continuing flow of bottom water into the reservoir system. In addition, a 50 ml borehole water sample was recovered. In light of the results a large-volume sample was not desired at this depth, because only bottom water would have been collected.

The Barnes-Uyeda tool was again run in a similar manner to 451 m BSF, and both temperature data and a 125 ml water sample were obtained. At this depth in the

Table 1. Coring summary, Hole 504B, Leg 83.

Core no.	Date	Time 1845	Depth from drill floor (m) Top	Depth from drill floor (m) Bottom	Depth below sea floor (m) Top	Depth below sea floor (m) Bottom	Length cored (m)	Length recovered (m)	Percentage recovered
71	24 Nov. 81	2135	4309.5	4317.0	836.0	843.0	7.5	0.98	13
72	25 Nov.	0110	4317.0	4326.0	843.5	852.5	9.0	3.94	44
73	25	0456	4326.0	4335.0	852.5	861.5	9.0	2.15	24
74	25	0805	4335.0	4344.0	861.5	870.5	9.0	0.98	11
75	25	1057	4344.0	4353.0	870.5	879.5	9.0	1.46	16
76	25	1408	4353.0	4362.0	879.5	888.5	9.0	0.78	9
77	25	1726	4362.0	4371.0	888.5	897.5	9.0	3.00	33
78	26 Nov.	0456	4371.0	4378.0	897.5	904.5	7.0	2.70	39
79	26	1022	4378.0	4383.5	904.5	910.0	5.5	3.07	56
80	26	1429	4383.5	4393.0	910.0	919.5	9.5	4.00	42
81	26	1900	4393.0	4402.0	919.5	928.5	9.0	1.18	12
82	26	2342	4402.0	4411.0	928.5	937.5	9.0	2.81	31
83	27 Nov.	0328	4411.0	4420.0	937.5	946.5	9.0	1.20	13
84	27	0730	4420.0	4429.0	946.5	955.5	9.0	2.08	23
85	27	1210	4429.0	4438.0	955.5	964.5	9.0	3.19	35
RT: Change drill bit									
86	28 Nov.	1833	4438.0	4440.5	964.5	967.0	2.5	0.45	18
87	29 Nov.	0058	4440.5	4450.0	967.0	976.5	9.5	1.73	18
88	29	0429	4450.0	4459.0	976.5	985.5	9.0	1.23	14
89	29	0800	4459.0	4468.0	985.5	994.5	9.0	1.91	21
90	29	1210	4468.0	4477.0	994.5	1003.5	9.0	4.94	55
91	29	1620	4477.0	4486.0	1003.5	1012.5	9.0	3.70	41
92	29	2120	4486.0	4495.0	1012.5	1021.5	9.0	3.64	40
93	30 Nov.	0210	4495.0	4504.0	1021.5	1030.5	9.0	1.48	16
94	30	0543	4504.0	4513.0	1030.5	1039.5	9.0	3.00	33
95	30	0944	4513.0	4522.0	1039.5	1048.5	9.0	1.13	13
96	30	1710	4522.0	4531.0	1048.5	1057.5	9.0	0.90	10
Recover broken pipe									
97	03 Dec.	1305	4531.0	4535.5	1057.5	1062.0	4.5	2.93	65
98	04 Dec.	1800	4535.5	4545.0	1062.0	1071.5	9.5	0.80	08
99	04	2122	4545.0	4554.0	1071.5	1080.5	9.0	1.99	22
100	05 Dec.	0245	4554.0	4563.0	1080.5	1089.5	9.0	2.94	33
101	05	0620	4563.0	4572.0	1089.5	1098.5	9.0	2.27	25
102	05	1014	4572.0	4581.0	1098.5	1107.5	9.0	0.90	10
103	05	1443	4581.0	4590.0	1107.5	1116.5	9.0	0.90	10
104	05	2316	4590.0	4599.0	1116.5	1125.5	9.0	2.55	28
105	06 Dec.	0430	4599.0	4608.0	1125.5	1134.5	9.0	0.82	9
106	06	0805	4608.0	4617.0	1134.5	1143.5	9.0	0.70	8
107	06	1220	4617.5	4626.0	1143.5	1152.5	9.0	1.50	17
108	06	1650	4626.0	4627.0	1152.5	1153.5	1.0	0.74	74
109	06	2135	4627.0	4630.5	1153.5	1157.0	3.5	0.70	20
110	07 Dec.	0037	4630.5	4635.0	1157.0	1161.5	4.5	0.37	8
111	07	0541	4635.0	4639.5	1161.5	1166.0	4.5	1.10	24
RT: Change drill bit									
112	08 Dec.	1150	4639.5	4644.5	1166.0	1171.0	5.0	0.57	11
113	08	1734	4644.5	4649.5	1171.0	1176.0	5.0	1.19	24
114	08	2205	4649.5	4654.0	1176.0	1180.5	4.5	0.20	4
115	09 Dec.	0106	4654.0	4658.5	1180.5	1185.0	4.5	0.20	4
116	09	0413	4658.5	4663.0	1185.0	1189.5	4.5	1.17	26
117	09	0808	4663.0	4667.5	1189.5	1194.0	4.5	1.19	26
118	09	1110	4667.5	4672.0	1194.0	1198.5	4.5	0.53	12
119	09	1606	4672.0	4676.5	1198.5	1203.0	4.5	0.04	1
120	09	2155	4676.5	4681.0	1203.0	1207.5	4.5	0.25	6
RT: Change drill bit									
121	11 Dec.	0857	4681.0	4687.0	1207.5	1213.5	6.0	0.81	14
122	11	1252	4687.0	4696.0	1213.5	1222.5	9.0	1.50	17
123	11	1600	4696.5	4705.0	1222.5	1231.5	9.0	1.60	18
124	11	2235	4705.0	4714.0	1231.5	1240.5	9.0	1.00	11
125	12 Dec.	0220	4714.0	4723.0	1240.5	1249.5	9.0	0.42	5
126	12	0905	4723.0	4727.0	1249.5	1253.5	4.0	0.40	10
RT: Change drill bit									
127	13 Dec.	1605	4727.0	4734.5	1253.5	1261.0	7.5	0.80	11
128	13	2050	4734.5	4743.5	1261.0	1270.0	9.0	1.27	14
129	14 Dec.	0215	4743.5	4752.5	1270.0	1279.0	9.0	3.33	38
Fish broken drill string									
130	15 Dec.	1626	4752.5	4761.0	1279.0	1287.5	8.5	3.06	36
Logging and experiments			16 Dec.–28 Dec.						
131	28 Dec.	1743	4761.0	4768.5	1287.5	1295.0	7.5	1.53	20
132	28	2233	4768.5	4777.5	1295.0	1304.0	9.0	1.25	14
133	29 Dec.	0650	4777.5	4786.5	1304.0	1313.0	9.0	1.52	17
134	29	1642	4786.5	4792.5	1313.0	1319.0	6.0	0.96	16
135	29	2337	4792.5	4795.5	1319.0	1322.0	3.0	0.03	1
RT: Change drill bit									
136	31 Dec.	1500	4795.5	4800.5	1322.0	1327.0	5.0	0.60	12
137	31	2025	4800.5	4805.5	1327.0	1332.0	5.0	0.95	19
138	1 Jan. 82	0220	4805.5	4810.0	1332.0	1336.5	4.5	0.45	10
139	1	0707	4810.0	4814.5	1336.5	1341.0	4.5	0.40	9
140	1	1145	4814.5	4819.0	1341.0	1345.5	4.5	0.34	8
141	1	1815	4819.0	4823.5	1345.5	1350.0	4.5	0.50	11

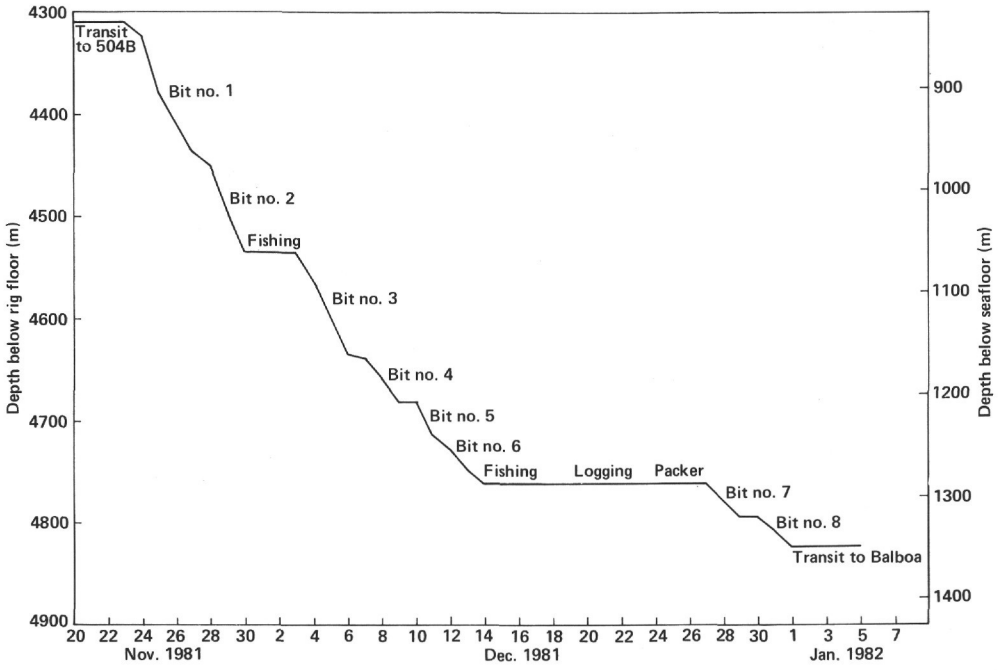

Figure 3. Summary of Leg 83 operations at Hole 504B.

hole the borehole water was stagnant, being below the reservoir, and a large-volume sample was acquired using the packer sample go-devil. The tool was dropped and its seating confirmed, the pipe was then lowered to 479 m BSF, and the sample taken. The tool was recovered with a 10-gal. water sample.

The third Barnes-Uyeda run was to a depth of 650.5 m BSF; again good temperature data were obtained but no sample was collected because of a faulty amphenol connector. The fourth and last run of the Barnes-Uyeda tool was to a depth of 736 m BSF, but because of a faulty switch no temperature data were recorded; when the sample chamber was opened it contained 150 ml of steaming water.

The sampler go-devil was again dropped and seated in the drill bit. The pipe was lowered to 793 m BSF, 43 m above the reported total depth of the hole, and the sample chamber opened. A 10-gal. water sample was recovered. A maximum-reading thermometer had also been attached to the go-devil and the maximum temperature recorded on the run was 115°C.

The second run of the sampler go-devil completed the suite of experiments scheduled to be run before the hole was drilled deeper.

Hole 504B: Bit No. 1

To retrieve the sampler go-devil after its second run, the drawworks sand line was used; the coring sand line unit was inoperative because the Bowen Hydraulic Unit had lost hydraulic pressure. A total of 5.75 hr. was lost in trying to find the cause of the pressure loss. To enable coring operations to begin, a hydraulic pump used to operate the pipe racking system was reassigned to the heave compensator. The loss of pressure was subsequently found to have been caused by small pieces of a plastic-like material which clogged various check and relief valves.

The heave compensator and power sub were picked up, an inner core barrel dropped, and the pipe was washed to bottom. Loose fill 4 m deep was circulated out and coring operations began at 1845 hr. on 24 November at a depth of 836 m BSF.

After 68.5 m had been cored, a leak in the stem between the power sub and swivel revealed a one-inch lateral crack four inches below the box end of the power sub stem. To eliminate the risk of the pipe sticking in the uncased section of the hole when the power sub was changed out, the drill pipe was pulled to position the bit inside the 11-3/4 in. casing. In all, 12 hr. were lost in replacing the swivel and power sub, including time to pull the bit into the casing and run back to bottom.

Coring operations continued to 964.5 m BSF, when the rotary torque began to increase and behave erratically. It was decided to pull the drill pipe and install a new core bit. A total of 15 cores were cut (Cores 71–85) over an interval of 128.5 m and 33.52 m of core were recovered, resulting in a 26.1% recovery rate.

The rocks recovered consisted of moderately to extensively altered pillow and massive basalts. The basalt in Cores 71 through 76 appear to have been altered at relatively low temperatures (less than 150°C), whereas the basalts in Cores 77 through 85 appear to have been more extensively altered as a result of temperature reactions ranging from 150° to 250°C. A zone of abundant sulfides was encountered in Cores 80 and 81.

After the bit had cleared the mudline, a drill string motion experiment was run by dropping a Drill Bit Motion Indicator (DBMI) package to the drill bit, installing an Instrumented Drill String Sub (IDSS) in the drill string at the rig floor, and recording the ship's motion by a Ship Motion Data System (SMDS) installed on the bridge. Various parameters were recorded by each instrument simultaneously over a 15-min. period. The data produced

were returned to DSDP to be analyzed and compared with a computer model.

Hole 504B: Reentry No. 2, Bit No. 2

After the hydraulic bit release had been replaced with a bit sub and a new drill bit installed, the drill string was run to the reentry depth 3 m above the cone.

The EDO reentry tool was run and seated at the drill bit. After 1 hr., 20 min. of maneuvering the ship, the pipe was stabbed in the cone at 1135 hr. on 28 November. Reentry was confirmed, the drill string was run to bottom, and coring operations resumed.

Coring proceeded smoothly until the inner core barrel (ICB) retrieving tool was run to retrieve Core 96. The tool was run in the hole, latched to the ICB, and pulled to the surface. It was found that the swivel connection at the top of the ICB had "backed off," leaving the barrel and core liner down the hole.

The pin end of an inner barrel sub was tapered and assembled on the end of an ICB. After the fishing assembly was pumped down the drill pipe with the intent of wedging the tapered pin in the box connection at the top of the ICB, the retrieving tool was run and the assembly pulled out of the hole. This first attempt failed and a new fishing assembly, consisting of a wireline spear attached to the end of an ICB, was pumped down the drill pipe; a retrieving tool was then run and latched to the fishing assembly. The spear was "spudded" down in order to wedge it inside the ICB. Both assemblies were pulled out of the hole and coring operations resumed.

Coring continued to 1062 m BSF, when a sudden drop in pump pressure occurred and the drill pipe jumped slightly. The drill string weight indicator showed a 75,000 lb. reduction in string weight, indicating that the drill pipe had been severed well above the drill collars. The Totco drilling recorder revealed that, over a 30 min. period prior to the failure, the pump pressure had dropped 250 psi and the pump rate had increased by 15 strokes/min.

The drill pipe was pulled out of the hole and inspection of the severed joint showed that failure was caused by a horizontal transverse crack whose outer edge was highly polished. The fatigue area measured one quarter of the circumference. The severed piece of pipe recovered measured 9.21 m, leaving in the hole an estimated 0.4 m of the joint (0.3 m of which was a tool joint). The "fish" consisted of the bottom-hole assembly and 39 joints of drill pipe.

Because there was only a short 0.1 m stub of 5 in. tube left on top of the tool joint, it was decided to run an overshot fishing tool which would catch the 7 in. tool joint. The fishing assembly picked up was the following: a 9-1/2 in. Bowen Series 150 overshot with 7 in. mill control guide and basket grapple, crossover sub, three 8-1/4 in. drill collars (DC), crossover sub, jars, crossover sub, three 8-1/4 in. DCs, two bumper subs, two 8-1/4 in. DCs, crossover sub, one 7-1/4 in. DC and drill pipe.

Hole 504B: Reentry No. 3 (fishing)

The drill string was run to the reentry depth and the EDO scanning tool run down the drill pipe and landed at the overshot. After 1 hr., 55 min. of maneuvering the ship, the pipe was stabbed at 2310 hr. on 1 December. With reentry confirmed, the pipe was run to the top of the fish at 575 m BSF. While the crew continued pumping and rotating the pipe slowly, the overshot was lowered over the drill pipe connection at the top of the fish. The drill pipe was then raised, and a weight 50,000 lbs. over string weight had been reached when the tool joint slipped out of the grapple. Subsequent attempts to latch the tool joint in the overshot were unsuccessful. The drill pipe was pulled out of the hole to modify the overshot assembly.

Hole 504B: Reentry No. 4 (fishing)

Measurement of tool joints in the drill string just above the severed joint and visual inspection of the 7-in. grapple led to the conclusions that the diameter of the tool joints at the top of the fish had been reduced with use and that they were approximately 6-13/16 in. The 7-in. grapple used on the first run was designed to catch a minimum diameter of 6-29/32 in.

A grapple able to catch 6-13/16 in. was not available on the ship, and a 7-in. grapple was modified to catch a reduced diameter and assembled in the overshot. The same assembly used in the first run was lowered to the reentry position, and after 1 hr., 30 min., the hole was reentered at 2010 hr., 2 December.

Again, while the crew continued rotating the pipe and pumping slowly, the overshot was lowered over the top of the fish. The drill pipe was raised and the fish was picked up off the bottom of the hole. The pipe had to be worked through an area of high drag 5 m off bottom. Both the coring and fishing assemblies were pulled without incident. The fishing assembly was disassembled and the four bottom drill collars of the coring assembly were found to be plugged with finely ground basalt. A total of 2-1/2 days were expended on the fishing operation.

Twelve cores (Cores 86 through 97) were cut by bit No. 2 prior to the drill string failure. An interval of 97.5 m was cored and 27.02 m recovered, giving a 27.7% recovery rate. The average rate of penetration for the cored interval was 3.1 m/hr.

The basalts drilled were a series of massive units interspaced with pillow lavas. All showed varying degrees of brecciation, which was more evident in the pillow sections. The massive units tended to be coarse grained, with only occasional fining of the grain size.

Hole 504B: Reentry No. 5, Bit No. 3

The new bit, No. 3, was attached to the coring assembly and the drill string was run to the reentry depth. Forty-four joints of drill pipe above the BHA were left out of the string and the difference was made up with used pipe from the rack. The EDO reentry tool was run and seated at the bit. The transducer would not rotate when seated, although it did so when the tool was raised 1 m. We could not solve the problem and pulled the tool to the surface.

No fault could be found in the EDO tool, so an inner core barrel fitted with a stinger, which would protrude

through the bit, was pumped down to drill pipe. The first attempt to retrieve the core barrel was unsuccessful because a retrieving tool was faulty. A replacement retrieving tool was run and latched onto the core barrel. After the barrel was unseated with an unusually large overpull of 2000 lbs, it was retrieved (no cause for the overpull was found). The EDO tool was run again and rotated without difficulty. The hole was re-entered at 0643 hr. on 4 December, after 53 min. of scanning.

After the pipe reached bottom, coring operations proceeded without incident until Core 104 had been cut. Then, as when Core 96 was being retrieved, the swivel connection at the top of the inner core barrel unscrewed, leaving the inner barrel and core liner at the bit. An inner core barrel with wireline spear attached was again used to retrieve the fish.

Coring with bit No. 3 was terminated at 1166 m BSF after 14 cores (Cores 98 through 111) had been cut. A total of 104 m were cored and 19.28 m recovered, giving a recovery rate of 18.54%. The bit was rotated for 41 hr., 14 min. with an average penetration rate of 2.52 m/hr.

Massive basaltic units formed all the material recovered. Chilled intrusive margins became common and the grain size became finer in many of the coarse units. The change probably represented the top of the dike section in the oceanic crust.

When the bit cleared the mudline, the drill string motion experiment was conducted for a second time. Again, useful data were successfully collected. On completion of the experiment the bit was pulled to the surface for replacement.

Hole 504B: Reentry No. 6, Bit No. 4

The new bit selected, an F94CK, unlike the previous three bits, had a core guide with a diameter of 2-1/8 rather than 2-7/16 in., in an effort to improve the falling recovery rate. After the new bit was installed, the pipe was run to the reentry position and was stabbed at 0207 hr. on 8 December, after 1 hr., 33 min. of scanning.

In this reentry, nine cores were cut, each 4.5 m long rather than the usual 9.0 m, in a further attempt to improve the recovery rate. Neither the reduced core diameter nor the reduced core length produced any improvement, the recovery rate from this section being 12.9%.

The rock recovered consisted of massive fine- to medium-grained basalts. Alteration remained relatively minor. The chilled margins, which were common, suggest a dike instead of a pillow structure.

After the drilling rate dropped below 1 m/hr., the drill bit was pulled to be replaced. The drill string motion experiment again yielded useful results when run with the bit above the mudline.

Site 504B: Reentry No. 7, Bit No. 5

The smaller core guide of Bit No. 4 offered no improvement in recovery, and may even have contributed to a reduction. Bit No. 5 reverted back to the 2-7/16 in size used in the first three bits. After 3 hr. of scanning the pipe was stabbed at 2054 hr., 10 December. The bit was run to bottom and 100 barrels of 12.0 lbs./gal. mud was circulated to remove any of the tungsten carbide inserts which had broken off the previous bit and which might still be at the bottom of the hole.

Coring operations proceeded smoothly to 1253.5 m BSF, when a decreased rate of penetration and increased torque indicated that the bit required replacing. Overall, the recovery rate was still a disappointing 12.5%, but the rate of penetration rose to 2.19 m/hr.

The basic lithology of the cored section remained similar to that encountered over the bit no. 4 interval, that is, massive fine- to medium-grained basalts with minor alteration. Chilled margins suggesting a dike structure continued to occur.

The fourth run of the drill string motion experiment again yielded good results. When the bit was inspected, it was found that the middle rows of tungsten carbide inserts on each core were broken off. Both bits nos. 3 and 4 had similarly lost teeth, because of the very hard basalts being cored.

Hole 504B: Reentry No. 8, Bit No. 6

With a new F94CK core bit installed, the drill string was run to the reentry depth. The EDO reentry tool was tested, lowered, and landed in the bit. After only three minutes of scanning, the hole was reentered at 0247 hr., 13 December, thus breaking the previous reentry record of 5 min. held by Leg 50.

The 13.5 kHz beacon dropped on arrival at the location was sending a rapidly decaying signal, so a 16 kHz Benthos double-life beacon was launched during the reentry procedure.

Coring operations proceeded smoothly to about the end of the fourth core cut by bit No. 6. Half a meter of core remained to be cut when a sudden drop in pump pressure was observed and the drill string was raised. A 45,000 lb. drop in total weight signified that the drill pipe had failed just above the bottom-hole assembly.

The drill pipe was pulled out of the hole and was found to have been severed 0.5 m below a female drill pipe thread connection. Thus the "fish" consisted of 9.0 m of the severed joint, 10 additional joints, and the bottom-hole assembly. The failure was similar to that which occurred earlier in the leg, that is, a horizontal fatigue crack which covered one quarter of the tube circumference. The wall of the tube was thin and badly pitted in the crack area.

Hole 504B: Reentry No. 9 (fishing)

An overshot was assembled to catch the approximately 8.5 m of the 5 in. drill pipe tube at the top of the fish. The full assembly consisted of an 8-7/8 in. Bowen Series 150 FS overshot with a 5 in. mill control and basket grapple, bit sub, three 8-1/4 in. DC, crossover, jars, crossover, three 8-1/4 in. DC, one bumper sub, two 8-1/4 in. DC, crossover, and one 7-1/4 in. DC.

After the fishing assembly was run to the reentry depth, the pipe was stabbed at 0048 hr., 14 December, after 54 min. of scanning. When the overshot was positioned just above the top of the fish, the Bowen power sub was picked up and used to pump and rotate the pipe

slowly while the overshot was lowered. The third attempt to latch the fish was successful and it was raised off the bottom with little problem.

When the ten joints and piece of drill pipe at the top of the fish were laid down, an additional fatigue crack was found in the severed joint and one each in three other joints. The time lost while retrieving the second fish was 1-1/2 days, and two days were added to the leg to make up in part time lost during the fishing operations.

The recovery of the bottom-hole assembly made it possible to retrieve the fourth and last core cut by bit no. 6. The total interval cored was 34.0 m, 8.46 m of which was recovered, resulting in a much improved 24.9% rate of recovery. The bit was rotated 16 hr. for a rate of penetration of a 2.12 m/hr.

The basalts were again massive, fine to medium grained; the second last core (Core 129) produced the coarsest-grained basalts seen so far in Hole 504B.

Hole 504B: Reentry No. 10 (logging)

The full suite of logs and the experiment phase were undertaken at this point, rather than at the end of the coring phase as had been planned originally, for a combination of reasons. First, it was felt that valuable lithological data were missing as a result of the very low recovery rate. Secondly, the drill pipe's reliability was questioned in light of the two fatigue crack failures and the additional cracks in the pipe immediately above the bottom-hole assembly.

A slightly modified bottom-hole assembly was used for the logging program. Authorization was received to pick up a limited number of joints of new pipe and to cull any joints which looked suspect. Twelve joints of new drill pipe were positioned immediately above the BHA. All the drill pipe which had been below the cone when drilling was completed was left out of the string. The difference was made up with pipe already on the rack and with another 12 joints of new pipe at the top of the string.

After the logging assembly was positioned at the reentry depth, the EDO reentry tool was lowered and landed in the clean-out bit. After 105 min. of scanning, the hole was reentered at 0820 hr., 16 December. Reentry was confirmed and the drill string was lowered to the bottom of the hole. Fifty barrels of 12.0 lbs./gal. mud was pumped and displaced out of the hole with seawater. The water circulated was equal to twice the hole volume and not only cleaned the hole but cooled it.

The bit was pulled up inside the casing after circulation was completed and a temperature survey conducted using the Schlumberger temperature sonde. The maximum temperature recorded at the bottom of the hole was 95°C, the measurement being taken 5 hr., 15 min. after circulation stopped.

After the temperature survey, a trip was made to the bottom to cool the hole prior to running the temperature-sensitive borehole televiewer. The tool functioned properly at the surface, but failed when a routine check was made in open hole. Subsequently the failure was found to have been caused by three set screws on the transducer motor shaft slip ring which had become unscrewed and damaged a teflon washer. Also, insulation on a transducer cable had been damaged, causing the signal to be shorted out.

While the televiewer was being repaired, a Dual Laterolog sonde was run, but because of a faulty capacitor in the electronics package the data were false. A Dual Induction sonde was run next and a good log was obtained. After the sonde had been laid down, the televiewer was checked at the surface and found to be working again.

Prior to the second attempt with the televiewer, the hole was cooled again. Very good quality pictures were obtained from the open hole section, apart from the bottom 200 m, where the compass did not operate consistently because of high temperatures. Compass information was recovered over this lowest interval from processed video tapes. Pictures from the top 422 m were recorded on Polaroid film only, because the video recorder had broken down when logging up the hole.

While the tool was being run in the hole to rerecord the bottom 200 m, resistance within it increased with temperature. The power limit of the surface equipment was reached and the tool would no longer rotate.

Following the televiewer, the long-spaced sonic sonde was run. A P-wave calibration log was obtained, but the tool failed during the P-wave digitization log. When the sonde was being pulled out of the hole, it became stuck in the clean-out bit and no movement of the tool was possible.

To avoid endangering the hole, the drill string was pulled clear of the mud line while the cable was "stripped" (that is, clamped and cut every 28.5 m as the stands of drill pipe were pulled). After the ship had been offset from the hole, a circulating head was installed (the cable also was clamped at the surface) and an attempt was made to pump the sonde free. When this failed, the cable was tensioned to see if the tool could be pulled up, but the weak point in the cable head parted with 9000 lbs. pull. This risk was taken in light of the probability that the sonde would remain wedged in the bit when the cable parted.

The cut piece of logging cable was spooled onto the logging winch drum and the drill string was pulled. The centralizers at the top and bottom of the sonde consist of three bow springs in each assembly. One bow spring on each centralizer was broken and it was the bottom spring which was wedged in the bit. One half of a bow spring was missing and was either in the hole or on the seabed.

Approximately 12,000 ft. of logging cable was dropped a good distance from the cone and the 2200 ft. length of teflon cable was reheaded to the remaining 19,000 ft. of cable on the drum.

Hole 504B: Reentry No. 11 (logging)

The logging assembly was run to the reentry depth and, after 2 hr., 53 min. of scanning, the hole was reentered at 0805 hr., 20 December.

After the bit was positioned just inside the casing, the Schlumberger temperature sonde was used to obtain a downhole temperature profile. The temperatures remained low in and above the reservoir, showing that bottom water continued to be drawn down the hole. The

maximum temperature at the bottom of the hole was 133°C, the measurement having been taken 58 hr. after circulation was completed.

A nuclear log was made after the temperature profile was completed and then a Schlumberger water sampler was run. Because of its light weight the tool repeatedly "hung up" as it was lowered down the open hole and would not go below 978.5 m BSF. The sample chamber was opened and 650 ml of fluid was collected.

The temperature probe was run to obtain the final profile, but it failed while being lowered in the drill pipe. After a broken wire in the cablehead was found and quickly repaired, good temperature data were recorded; the maximum temperature at the bottom of the hole was 135°C, 82 hr. after the hole was last circulated.

Before the long-spaced sonic sonde was rerun, the hole was cooled. The P-wave digitization and S-wave logs were recorded, this being the first time an S-wave log had been obtained in a submarine hole. One of the bow springs in the top centralizer broke during the run and a 0.5-m piece was lost in the hole.

The equipment used in the large-scale resistivity experiment was able to withstand a maximum temperature around 100°C, so a trip to bottom was made to cool the hole. Good data were collected from the complete open-hole section.

The resistivity experiment completed the logging plan for the hole and the drill string was pulled to change the BHA for the packer experiments.

Hole 504B: Reentry No. 12 (Packer Run No. 1)

The Lynes inflatable formation packer was made up in the BHA, tested successfully, and lowered to the reentry depth. The EDO tool was landed in the logging shoe and the pipe was stabbed after 45 min., at 1443 hr., 23 December.

The drill string was lowered to the bottom of the hole, then the heave compensator and power sub were picked up. A 40-barrel gel mud pill was circulated around the hole to get it as clean of cuttings as possible.

With the packer positioned 2 m from the bottom, the "sampler go-devil" was pumped down with the rig pumps and seated in the packer. The system was pressurized to 1000 psi to inflate the packer and after 15 min. pressure was increased to 1960 psi to open the sample chamber. Because of a small leak, additional pumping was required to maintain the pressure for the one hour needed to collect the sample.

The packer deflated and the sample chamber closed when the pressure was bled off. Two attempts were made to unseat the go-devil, but in each case the safety pins of the inner core barrel retrieving tool sheared.

The second approach to unseat the go-devil without having the drill pipe clear the mudline was to pull 14 stands (400 m) of drill pipe and immediately run 10 stands (285 m) back in the hole. This created a 400 psi differential pressure acting below the go-devil. An attempt to pull the tool was unsuccessful and the only option left was pulling the drill string and break the go-devil out on the rig floor.

A thick mixture of thread dope and rust was found to have wedged the go-devil into the packer. The packer element was punctured and was replaced prior to being rerun. Thirteen gallons of water were recovered by the go-devil.

Hole 504B: Reentry No. 13 (Packer Run No. 2)

The packer was satisfactorily surface tested after being redressed and the drill string was lowered to the reentry depth. After 63 min., the hole was reentered at 0106 hr., 25 December.

The packer was positioned at 534.2 m BSF (bottom of the element) and the heave compensator and power sub were picked up. The "safety" go-devil was dropped and pumped down using the rig pumps. After the go-devil was seated, the packer was inflated by increasing pump pressure to 1500 psi. Pressure was held 10 min. to allow the packer to inflate and then increased to 2000 psi, when the shear plug opened and exposed the formation to the drill pipe pressure.

The pressure was allowed to decay for 15 min. before being built to 370 psi. The decay was recorded for 15 min., the pressure increased to 147 psi, and a third decay of 12 min. obtained.

Finally, a steady-rate flow test was conducted. A flow rate of 105 gal./min. with a 440 psi surface pressure (325 psi downhole) was maintained for 15 min. and the pressure decay recorded for 34 min. Excellent decay curves were obtained but fluid appeared to leak past the packer elements when the surface pressure reached approximately 400 psi.

The packer was deflated, the go-devil retrieved, and the drill pipe was run to reposition the packer at 1013.5 m BSF. The "safety" go-devil was dropped and seated in the packer. The drill string was pressurized to 1500 psi to inflate the packer and, to check that full inflation had occurred, a pull of 10,000 lbs. was applied.

At 1800 psi the shear plug opened, but the pressure bled to zero immediately. A pump test confirmed that the packer element had failed. The go-devil was retrieved and the drill string pulled to replace the damaged element. When recovered, the top of the element was belled out and punctured because the packer body had moved up during the pull test.

Hole 504B: Reentry No. 14 (Packer Run No. 3)

The damaged element was quickly replaced and the drill string rerun to the reentry depth. The pipe was stabbed at 0952 hr., 26 December, after 45 min. of scanning.

The packer was positioned at 1013.5 m BSF and the "safety" go-devil was pumped down and seated in the packer. A pressure of 1600 psi was applied and held for 5 min. to allow the packer to inflate. At 1750 psi the shear plug opened, but the pressure immediately dropped to zero. A low circulating pressure during pumping meant that the packer had either failed or had not inflated.

The go-devil was retrieved and the pins which shear when deflating the packer were found to have failed, either when the go-devil was dropped or when it landed in the packer.

Stronger shear pins were installed and the go-devil was run again. As before, 1500 psi was applied to inflate the packer, but the pressure dropped slowly. An increase

in the pressure to 1750 psi blew the shear plug and the pressure dropped to zero immediately. During circulation, the pump pressure was again low. Inspection of the deflate shear pins revealed that they were intact, and the only reasonable conclusion was that the packer element had been damaged.

When recovered, the rubber outer jacket of the packer element was completely missing, as if it had "peeled off," yet the steel belt remained intact—further evidence to support the developing argument that the elements were substandard.

The time allocated to the experimental phase had almost all been used and the packer could not be rerun. The remaining time was utilized in running the drill string to the bottom and obtaining a 650 ml water sample at 1273.5 m BSF with the Schlumberger water sampler.

After the hole was coated, the bit was positioned inside the casing, the televiewer was rerun over the bottom 200 m, and good pictures were recorded. This concluded the experimental phase, and the drill string was pulled to change to a coring bottom-hole assembly.

Hole 504B: Reentry No. 15, Bit No. 7

The same bottom-hole assembly and type of bit, an F94CK used earlier in the leg, was made up and run to the reentry depth. The pipe was stabbed at 0536 hr., 28 December, after only 2 min. of scanning, breaking the record set by the eighth reentry.

The bit was run to within 15 m of bottom, the heave compensator and power sub were picked up, and 100 barrels of mud were circulated while the bit was rotated to bottom. The pipe torqued up twice because of the junk in the hole, but was pulled free easily.

When bottom was reached, coring operations commenced, the pieces of spring and the rubber element posed no further problems. Coring proceeded relatively smoothly apart from one point when some large cuttings stuck the pipe and 100,000 lbs. overpull was required to free it.

Five cores, 131 through 135, were cut before the penetration rate dropped below 0.5 m/hr. because the bit was worn out. It had cored 34.5 m, 5.29 m of which were recovered for a 15.33% recovery. The formation continued to be massive, fine- to medium-grained basalts and alteration increased with depth.

When the mudline was cleared while being pulled out of the hole, the drill string motion experiment was conducted for the fifth time; as before, good data were collected. The bottom-hole assembly and Bowen power sub were both magnafluxed on this trip and no cracks were found in any of the connections.

Hole 504B: Reentry No. 16, Bit No. 8

On completion of the magnafluxing, a new bit was installed and the drill string was run in preparation for reentry. The pipe was stabbed at 0030 hr., 31 December, after 13 min.

The coring proceeded with no problems over an interval of 28.0 m, cut in six sections; 3.24 m of core was recovered and the final depth of the hole was 1350 m BSF. No significant changes in formation occurred: the rocks still were massive, fine- to medium-grained basalts. Bit No. 8 was the final one run on Leg 83. Before we left the hole it was flushed with a gel mud pill and circulated clean with seawater.

The ship departed from Site 504 at 1352 hr., 2 January 1982. Leg 83 officially ended at 1554 hr., 5 January, 1982, at Balboa Harbor.

Coring Equipment

Essentially only one coring assembly was used during the entire leg. The only small change was in the first assembly used, when a "locked out" hydraulic bit release and a bit reference sub were substituted for the bit sub and head sub.

The coring assembly consisted of a 9-7/8 in. bit, bit sub, head sub, outer core barrel, top sub, head sub, four 8-1/4 in. DC, one bumper sub, three 8-1/4 in. DC, two bumper subs, two 8-1/4 in. DC, crossover sub, and one 7-1/4 in. DC. The hydraulic bit release, with set screws installed to ensure that it would not release, was used to provide a landing profile for the "sampler" go-devil.

The main source of problems during coring was not the actual coring equipment but the 5 in. drill pipe. Two fatigue failures occurred and four days were spent on the fishing operations. Fortunately they were both relatively straightforward, but to achieve the first one the unrecommended practice of cutting and welding a basket grapple was necessary. In addition to the failures, four other cracks were found in the joints of drill pipe included in the second fish. One hundred fifty-seven joints of drill pipe were removed from the string and the difference was made up with 24 new joints and used drill pipe already made up on the rack.

The other periods of lost time occurred in repairing the Bowen hydraulic unit, which had become clogged with a plasticlike material; in replacing the cracked power sub; and in fishing the inner core barrel twice after the swivel had unscrewed during coring.

The various methods used to improve the rate of recovery were as follows:

1. Using a bit with a reduced core guide diameter: recovery actually decreased.
2. Cutting short sections, generally 4.5 m (half a knobby joint): this seemed to help, especially if a piece of core jammed at the beginning of a section.
3. Leaving out the plastic core liner: this also helped reduce the core jamming problem, but made handling of the core at the surface more difficult.
4. Rotating the pipe slowly with light weight on the bit (20,000 lbs. weight and 55 RPM): this combination was the best for extending bit life and maintaining a reasonable rate of penetration (approx. 1 m/hr.).

Bits

The core bit used exclusively on Leg 83 was the 9-7/8 in. F94CK. The only difference was in the diameter of the core guide: bit no. 4 had a 2-1/8 in. guide compared with 2-7/16 in. for the others. It was hoped that the reduced diameter would help eliminate core jamming and thus increase recovery, but the opposite seemed to occur.

The basalts cored became harder with depth and, as a result, more difficult to drill. The average rate of penetration progressively dropped and after about 30 rotat-

ing hours, the middle rows of teeth on each cone would have been broken off. In drilling hard basalts in the future, cones with more rounded inserts in the middle rows would be useful.

Logging

An extensive suite of logs was run during the leg. The Barnes-Uyeda and "sampler" go-devil were run before coring commenced and the full set of logs between the sixth and seventh bit runs. Twenty runs were made with varying degrees of success. The Dual Laterolog was the only problem sonde which could not be rerun as a temporary repair was not made until near the end of our time at the site.

The televiewer continued to be a rather delicate tool, but despite the problems the pictures were the best ever recorded at sea. The MCD caliper-centralizers on the long-spaced sonic sonde were a problem (they also caused problems on Leg 82) because of three bow spring failures. The broken springs on the first run resulted in the destruction of 12,000 ft. of logging cable when the sonde stuck in the BHA.

The high-temperature cable spliced to the existing wireline at the beginning of the leg served its purpose, but the splice had to be cut out and replaced with a torpedo connection because of a seawater leak.

The bottom-hole assembly used for the main logging period consisted of a 9-1/4 in. clean-out bit, five 8-1/4 in. DC, one bumper sub, three 8-1/4 in. DC, two bumper subs, two 8-1/4 in. DC, crossover sub, one 7-1/4 in. DC. The tungsten carbide matrix on the clean-out bit extended into the bore and may have contributed to the bore spring failure. The bit was modified after the logging program so as to provide a smoother profile.

Packer Equipment

Three runs were made with the Lynes inflatable formation packer, but with only limited success. On the first run, the "sampler" go-devil became wedged into the packer bore with a mixture of rust and pipe dope. When recovered, the element was found to have been punctured at some stage in the experiment.

The first seating of the packer during the second run provided the only useful information concerning the physical properties of the rock. Using the "safety" go-devil, four decay curves were obtained which were used to calculate the permeability of the formation. Unfortunately, the fluid leaked past the element when the differential pressure across it exceeded 400 psi and it was not possible to attempt to fracture the rock.

Both the last two attempts to seat the packer failed because the element burst each time the shear plug blew. The most likely explanation of the problem is that the elements had not been vulcanized properly during manufacture.

The bottom-hole assembly used on the first run was a logging shoe, mechanical bit release, head sub, packer, jars, crossover sub, two bumper subs, three 8-1/4 in. DC, one bumper sub, five 8-1/4 in. DC, crossover sub, one 7-1/4 in. DC. On the second and third runs, three of the group of five 8-1/4 in. DC's were moved down between the crossover sub and the two bumper subs.

All in all, the packer experiments were a big disappointment, although some good data were collected.

BASEMENT LITHOSTRATIGRAPHY

Of the 514.0 m of basement cored during Leg 83, 106.9 m of basalts were recovered, corresponding to an average recovery rate of 20.8%. Of this, 13 cores had less than 10% recovery (two with less than 1%), and 32 cores between 10 and 20% recovery.

The low recovery in several cores made the location of boundaries and definition of units particularly difficult. Generally, a combination of several different megascopic parameters was used to divide cores into separate units: principally, changing grain size and/or occurrence of glassy rims (reflecting exposed surfaces of cooling units), massive or fractured appearance, and the assemblages and amounts of phenocrysts present.

Two major textural divisions are readily recognized using grain size alone: basalts that are medium-grained and massive in appearance, and those that are finer-grained, with glassy margins and adjacent hyaloclastic breccias (i.e., brecciated pillows consisting of glass and fine-grained material from pillow margins). Where basalts were of a more uniform, medium-coarse in grain, and where no apparent cooling margins were retrieved, the term *massive* has been applied in the following report. Such units could be thick lava flows or intrusions, but the lack of additional evidence precludes their allocation to either type. In those cases where an intrusive contact was recognized by a fine-grained/chilled rock adjacent to a coarser host the term *dike* has been applied (detailed descriptions of both hand specimen and corresponding thin sections are available in the section on Petrographic Classification of Basalts). Thin-section study of such contacts has confirmed their intrusive nature in cases where it was doubtful whether the sample represented a pillow margin/breccia contact or some other ambiguous relationship. When fine-grained rocks with numerous glassy pillow margins (see Petrographic Classification of Basalts) and hyaloclastic breccias were encountered, the term *pillow lava* has been used. All visually defined units have been revised, as necessary, on the basis of thin-section phenocryst assemblage criteria and XRF chemical data.

The different units were designated by numbers, beginning with 47. Units 4–46 in the upper portion of the hole were previously defined by Cann, Langseth, Honnorez, Von Herzen, White, et al. (1983). The petrological descriptions in this section are not complete; only parameters which are relevant to defining the units are included. For the complete petrological description on the basalts (including massive versus pillow basalt textures) see the following section, on petrographic classification of basalts. The lithologic units accordingly defined as shown in Figures 4 and 5. The descriptions of these units appear with the Visual Core Descriptions at the end of this chapter.

Discussion

The upper 571.5 m of basement in Hole 504B (i.e., 274.5–846 m beneath seafloor), which includes the basement drilled during Legs 69 and 70 and the top of 10 m

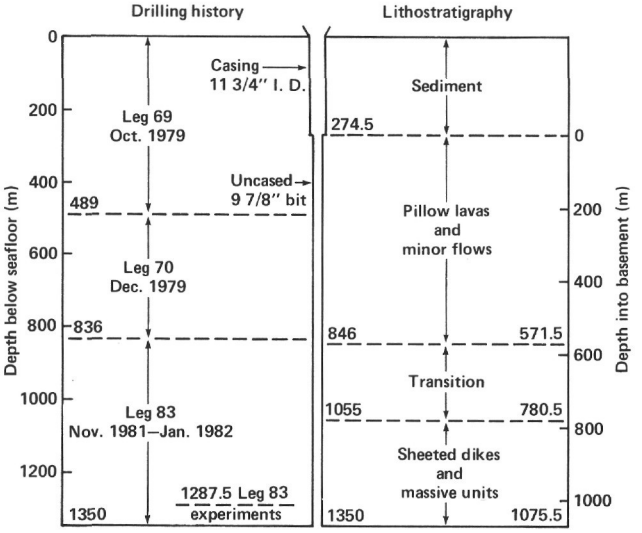

Figure 4. Schematic of drilling history and generalized lithostratigraphy at Hole 504B.

of basement recovered during Leg 83, consists of intercalated pillow lavas, pillow breccia and hyaloclastites, minor flows, and localized flow breccias (Figs. 4 and 5). This upper section of basement is underlain by a transition zone consisting of approximately 210 m of pillows, minor flows, and dikes. The upper boundary of the transition zone has been placed at a depth of 846 m BSF, where three dikes occur within 55 m of each other (Units 48, 55, and 58). Deeper than this, dike recovery becomes progressively more common. Lithologically, pillow sequences are more abundant, continuous, and heavily brecciated at the top of this transition zone than at the bottom. Fracturing is particularly extensive from about 910 to 930 m BSF within a pillow sequence where a mineralized stockwork occurs. Toward the base of the transition zone the pillow units become thinner, and chilled pillow margins are not so frequently recovered; the lavas are less convincingly identified as pillows and are generally recognizable only by their rubbly, brecciated, fine-grained character. Massive units and/or dikes progressively increase in abundance and frequency toward the base of the transition zone. These massive units cannot be identified explicitly as dikes since they lack chilled margins. In fact, in two cases the top surfaces are brecciated and the grain size fines toward the base, suggesting that these are probably flows (Units 59 and 63). However, dike chilled margins do occur at the base of the transition zone, which implies that at least some of the massive units throughout the layer are dikes.

The last pillow recovered was identified at a depth of 1055 m BSF. This marks the upper boundary of an underlying zone composed predominantly of massive units and dikes in which no pillows were recognized (sheeted dike complex?). The dikes were recovered with one, and rarely two, chilled margins, most of which were steeply inclined (50–60°) to near vertical. Some of these chilled margins were highly brecciated—the result of forceful dike intrusion? However, the zone as a whole is far less brecciated than those overlying it. Most of the lavas recovered from the lower zone are regarded as massive. Many of these exhibit significant grain size variation, fining toward one or both of their implied margins. Such units are probably dikes, although, with regard to the definitions in the petrography section, no chilled margins were recovered. However, the remainder of the units maintained a constant grain size over the recovered interval and their mode of emplacement can only be speculated.

The low recovery has seriously affected any attempt to draw an accurate lithological column to represent the rocks drilled in Hole 504B (Figs. 4 and 5). Throughout the hole, low recovery has exaggerated the more massive units. In the upper part of the hole, pillow lavas are probably much more prominent in the sequence than the diagram suggests, and massive flows form less of the total section than presently shown. Similar exaggeration in the dike formation expands the apparent thicknesses of individual dikes to many meters, whereas dikes generally average about one meter in thickness in typical ophiolites (e.g., Cyprus Ophiolite, Moores and Vine, 1971; Bay of Island Ophiolite, Williams and Malpas, 1972).

The ophiiolite model predicts that pillow lavas and massive flow sequences should have been the dominant lithologies encountered in the upper portion of Hole 504B. Visual observation of DSDP basement cores has shown that highly brecciated material is particularly common in pillow units as hyaloclastic debris/breccia, and as rubble surfaces of more massive flows. Drilled sections where such material is predominant would have a low recovery, with only the most competent and cemented material being retrieved. Recovery could be expected to rise in those sections where fracturing was less intense, cementing by alteration minerals more pervasive, and the basement by character more massive, such as in a dike sequence at increased depth. However, recovery rates from the lower section of Hole 504B, where intrusive contacts were more common (approximately Core 96 onward, i.e., the sheeted dike unit?), have in fact recorded some of the worst recoveries at this site. (Compare the average recovery recorded for the lower section of the hole, Cores 96–141, approximately 16.6%, with the average recoveries from the upper section of the hole, Cores 71–95, and that for the hole in total, 26.7% and 20.8%, respectively.) The reasons for this are unclear, but obviously the drilling of closely spaced, chilled, intrusive margins inclined at almost vertical angles is not conducive to core recovery (two vertical intrusive contacts were recovered during drilling—Cores 107 and 122—and several contacts inclined at 50° or more from elsewhere in the dike formation). Chilled margins are by character extremely hard but brittle, and experience shows they can fracture and be lost during drilling. The inclination of the dikes is such as to increase the relative amount of margin rock drilled; this is then presumably not recovered. Dike centers could be expected to form the major part of material retrieved in such cases, but recovery of even coarse-grained rock is low. It would appear the drill bit is literally pulverizing any re-

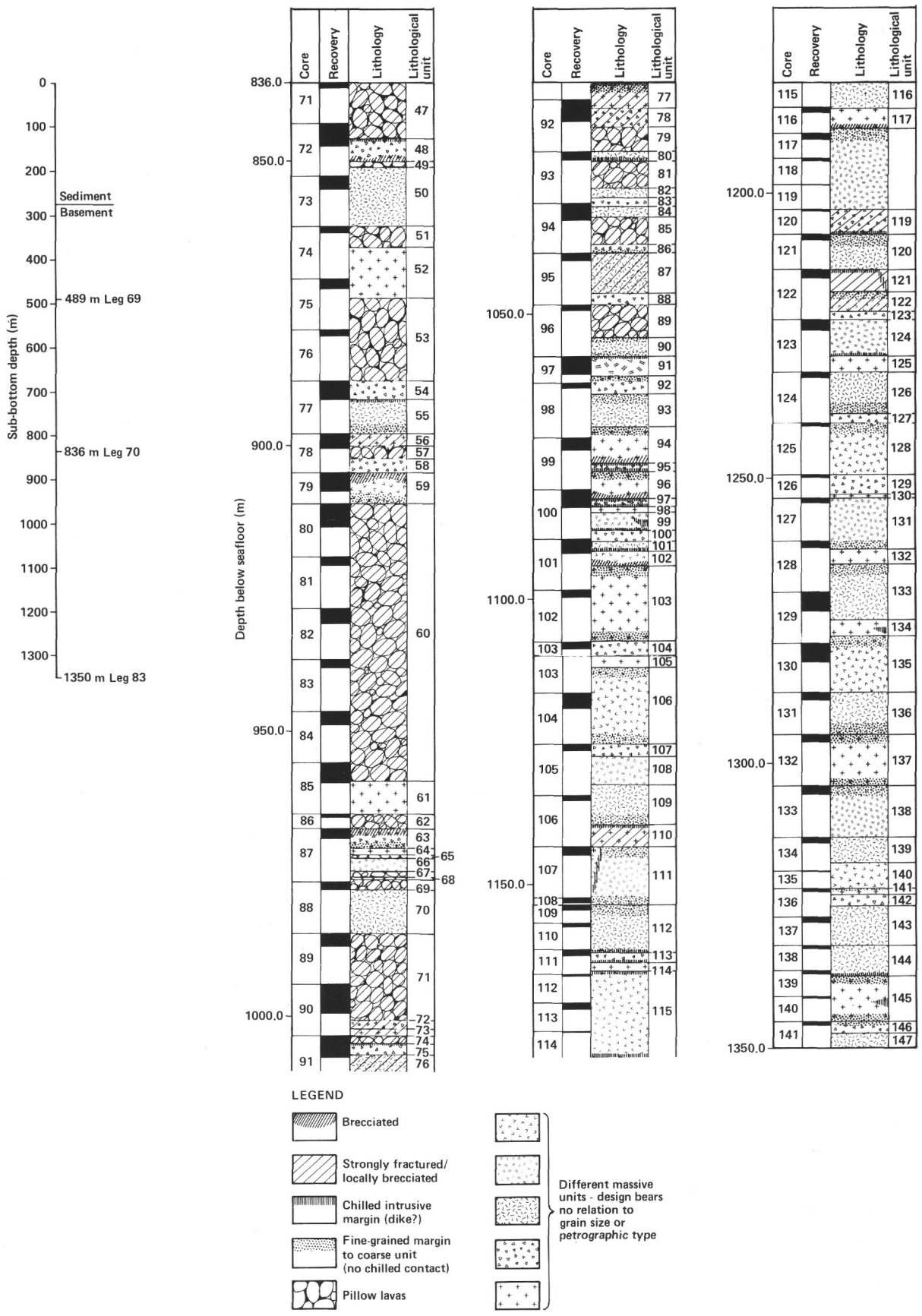

Figure 5. Lithostratigraphy of the section of Hole 504B drilled during Leg 83.

coverable material to basaltic sand, which is then flushed out of the hole and lost.

Preliminary studies of the BHTV pictures have shown the presence of many softer (fractured and brecciated) horizons distributed through the dike unit. Very few highly fractured or brecciated lithological units were recovered in those sections of the hole corresponding to the softer areas seen on the BHTV. This would suggest that such horizons are preferentially missed during coring, thereby adding to the overall low recovery experienced in the lower part of the hole.

Previous statistical analyses of dike units, conducted on ophiolite complexes (Kidd and Cann, 1974), have shown that a relationship exists between the direction of chilling of dikes, and the direction in which the spreading axis lies. Unfortunately, the particularly low recovery experienced in the deeper sections of the hole (dike unit?) has made it impossible to conduct statistical analysis on the directions of chilling which individual dikes exhibit.

PETROGRAPHIC CLASSIFICATION OF BASALTS

Introduction and Review

The petrographic aspects of basalts recovered from Hole 504B during Leg 83 were studied for two purposes: (1) to define the distinct petrographic groups present, and (2) to determine, where possible, whether material recovered from chilled margins indicated occurrence as dikes or as pillows. This latter interpretation was questionable from hand-specimen criteria because of the low core recovery during Leg 83. Fortunately, the uniqueness of crystal morphologies produced in pillows and dikes permitted us to distinguish these two modes of emplacement. The criteria employed in recognizing these are described by Kempton (this volume).

With regard to the first objective, four distinct petrographic groups have been identified from basalts collected in Hole 504B. The petrographic units were defined strictly by the presence of a particular phenocryst mineral or mineral assemblage—not the relative abundance of each phase. For this reason, the groups are labeled according to the first letter of each occurring phenocryst mineral:

OPC: *o*livine, *p*lagioclase, *c*linopyroxene phyric basalt;

OP: *o*livine, *p*lagioclase phyric basalt;

SV: accessory chrome *s*pinel with *v*ariable plagioclase, olivine, and clinopyroxene phyric basalt;

A: *a*phyric basalt.

The textural terminology used in describing these basalts is basically that outlined during Leg 70 (Table 2).

At this point it is necessary, in the interest of continuity, to review the petrographic groups previously created to describe the basalts from the upper 561.5 m of basement in Hole 504B recovered during Legs 69 and 70. Unfortunately, each leg produced its own separate petrographic classification. These, as well as the groupings reported by CRRUST (1982), are reproduced here and their suggested correlation with the present system is given in Figure 6.

Table 2. Textural terminology used to describe Leg 83 basalts.

A. Quench textures

1. *Glassy:*—matrix is amorphous, basaltic glass with no visible, incipient crystallization.
2. *Variolitic* or *spherulitic:*—texture characterized by the presence of spherulites or varioles, which are spherical bodies, usually consisting of radiating plagioclase and/or clinopyroxene microlites or crystals; individual crystals are indistinguishable with the microscope.
3. *Subvariolitic* or *subspherulitic:*—texture in which varioles coalesce.
4. *Immature sheaf:*—a bundled arrangement of small crystals (which cannot be individually distinguished with the microscope) assuming a sheaflike appearance; a central axis of crystal growth often occurs.
5. *Mature sheaf:*—same as above, but discrete skeletal crystals can be distinguished with the microscope (usually greater than 0.005 mm wide).
6. *Plumose-, plume-* or *featherlike* arrangement of microlites or crystals: may grade from immature to mature (as in sheaf texture) according to crystal size.

B. Groundmass textural terms

1. *Ophitic:*—a term applied to textural characteristic in which euhedral or subhedral crystals of plagioclase appear to be entirely enclosed in anhedral to subhedral augite.
2. *Subophitic:*—said of the ophitic texture of an igneous rock in which the feldspar crystals are approximately the same size as the pyroxene and are only partially included by them.
3. *Intergranular:*—a term applied to volcanic rocks in which there is an aggregation of grains of clinopyroxene, not in parallel optical continuity (as in subophitic texture), between a network of feldspar laths which may be divergent, subradial, or subparallel. Distinguished from an intersertal texture by the absence of interstitial glass or other quenched phases which may fill the interstices between the feldspar laths.
4. *Intersertal:*—a term applied to volcanic rocks wherein a base (mesostasis or glass and small crystals) fills the interstices between unoriented feldspar laths, the base forming a relatively small proportion of the rock. When the amount of the base increases and the feldspar laths decrease, the texture becomes *hyalophitic* and with a still greater increase in the amount of the base, the texture becomes *hyalopilitic.*

C. Phenocryst classification

1. *Phyric:*—a term describing igneous rocks in which larger crystals (phenocrysts) are set in a finer groundmass which may be crystalline or glassy, or both. *Aphyric:* no phenocrysts. *Sparsely phyric:* 1–2% phenocrysts. *Moderately phyric:* 2–10% phenocrysts. *Highly phyric:* more than 10% phenocrysts.
2. *Glomerocrystic:*—a term applied to phyric rocks containing clusters of equant crystals larger than the matrix crystals.

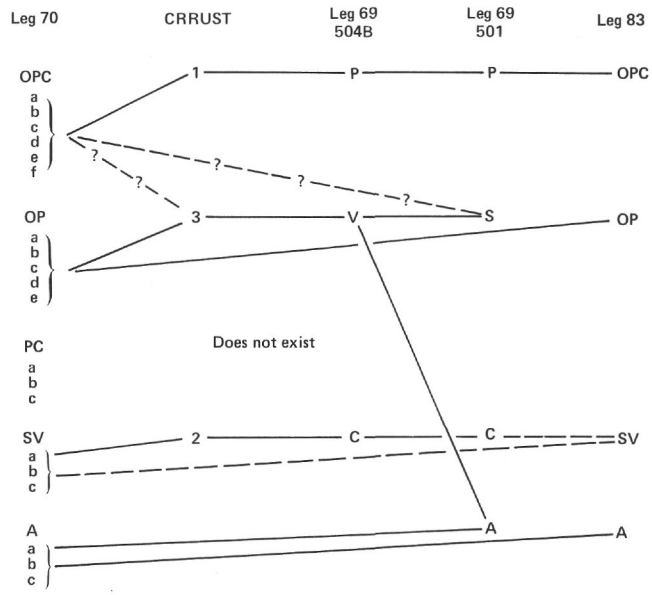

Figure 6. Correspondence among the petrographic classification schemes used during the three legs which cored Hole 504B. See text for explanation of key.

Leg 69

Type V: *v*ariably plagioclase–olivine–augite phyric basalt; augite in glomerocrystic clumps with plagioclase. (This type is actually an amalgamation of Type S and Type A defined for Hole 501 on Leg 69. Type S is a sparsely plagioclase–olivine–clinopyroxene phyric basalt and Type A is aphyric.)

Type C: moderately plagioclase–olivine phyric basalt with accessory *c*hrome spinel.

Type P: *p*lagioclase–clinopyroxene–olivine phyric basalt (emerald green clinopyroxene as isolated phenocrysts).

Leg 70

Type OPC: olivine–plagioclase–clinopyroxene phyric basalt

a. Glassy to variolitic
b. Hyalopilitic to hyalophitic
c. Intersertal to subophitic
d. Ophitic to intergranular
e. Glomerophyric to subglomerophyric
f. Brecciated

Type OP: olivine–plagioclase phyric basalt

a. Glassy to variolitic
b. Hyalopilitic to hyalophitic
c. Intersertal to subophitic
d. Ophitic to intergranular
e. Glomerophyric

Type PC: plagioclase–clinopyroxene phyric basalt

a. Glassy to variolitic
b. Intersertal to subophitic
c. Ophitic

Type SV: spinel phyric basalt, with variable percentages of olivine, plagioclase, and clinopyroxene phenocrysts (spinels range from less than 1 to 1% by volume).

a. Hyalophitic
b. Subglomerophyric
c. Ophitic

Type A: aphyric basalt

a. Hyalopilitic to hyalophitic
b. Intersertal to subophitic
c. Intergranular

CRRUST (1982)

1. Basalts with conspicuous phenocrysts of plagioclase (An_{75}), sparser pale green olivine, and rare, large, rectangular, green clinopyroxene;

2. Moderately phyric basalts containing plagioclase phenocrysts (An_{75}), less common olivine phenocrysts, and small, scattered microphenocrysts of brown chrome spinel, sometimes altered to magnetite around their edges;

3. Sparsely to moderately phyric basalts with phenocrysts of plagioclase and olivine, and sometimes glomerophyric clumps of plagioclase and augite.

Inspection of the correlations given in Figure 6 will show that the olivine, plagioclase, clinopyroxene group exists pretty much intact in each classification. However, a distinction was made on Leg 69 between clinopyroxene which occurred in glomerocrysts and that occurring as emerald green, isolated phenocrysts, that is, Type V vs. Type P. This is a pertinent observation, but does not, in our estimation, warrant classification of these two occurrences as separate groups. It is unsafe to classify a clinopyroxene phyric lava in a category characterized by olivine and plagioclase alone on the liquidus prior to groundmass crystallization, for the sole reason that the clinopyroxene occurs as glomerocrysts. Therefore, this distinction has been abandoned and all units which indicate that olivine, plagioclase, and clinopyroxene were crystallizing together before groundmass crystallization are classified as OPC, regardless of the clinopyroxene association. Only Type V (Leg 69) without clinopyroxene in glomerocrystic aggregates can be equated to Type OP (Legs 70 and 83); Type V with clinopyroxene in glomerocrysts becomes Type OPC in the Leg 70 and 83 classifications.

It should also be pointed out that Type PC (Leg 70) does not have an equivalent in Legs 69 and 83. This may simply be a statistical sampling problem; phenocrysts presents in small amounts may not ultimately become incorporated in a single thin section of the lithologic unit being described—particularly for coarse-grained rocks. Therefore, petrographic groups were also checked against hand-specimen phenocryst identification. If a phase was recognized in hand specimen, but not in thin section, it was assumed to be present and the appropriate petrographic group assigned. Thus, even though a few samples were described which had plagioclase and clinopyroxene as the only phenocryst phases, the hand specimens were obviously olivine phyric and the unit was assigned to OPC.

Type A from Leg 70 and 83 are presumably identical. However, this group is insufficiently described for the correlation to be adequately assessed. Type A (Leg 83) does not correlate precisely with anything from Leg 69. Type V was described as containing aphyric members as well as sparsely olivine, plagioclase ± clinopyroxene phyric members, but the single aphyric unit was apparently a thin, chilled layer, unlike the predominantly fine- to medium-grained units recovered in Leg 83.

The category SV is an additional one used to indicate the presence of trace amounts of chrome spinel regardless of the phenocryst assemblage. The spinel occurs in units otherwise representative of each other group. Therefore, to characterize this petrographic group more fully, the appropriate phenocryst assemblage is indicated in parentheses following the SV designation. The validity of separating these units out as a distinct group as well as the similarities and dissimilarities of SV (Leg 83), SV (Leg 70), and C (Leg 69) will be discussed more fully later.

In the description of petrographic groups to follow, many of the characteristics of the phenocryst phases are shared by all groups. The discussion will, therefore, be collective. Parameters that may be unique to a particular group will be so specified; otherwise, the information applies to all phenocryst-bearing categories.

Within a given petrographic group, the majority of textural variants are simply the result of differences in cooling history. For this reason, the details of every groundmass textural variation will not be recounted—only the most commonly encountered features will be described for each petrographic group.

Phenocrysts: Types OPC, OP, and SV

Plagioclase, olivine, and clinopyroxene constitute the phenocryst phases identified from Hole 504B basalts. The salient characteristics of each phase are summarized in Table 3 and described in more detail below.

Plagioclase (phenocrysts and/or glomerocrysts) ranges in size from 0.2 to 3.0 mm and constitutes 0.5 to 5% of the rock. Crystals are typically subhedral, although euhedral forms occur. Polysynthetic albite twinning is essentially ubiquitous. Anorthite contents could not be measured in most cases because of the degree of alteration of most feldspars (for the details of the alteration petrography see Basement Alteration Petrography section, later). Where appropriate compositions were determined, plagioclase varied from bytownite to labradorite compositions. Zoning is normal; cores are more calcic than rims, but the range in anorthite content is apparently not large. Subtle oscillatory zoning occurs, but only rarely (504B-73-1, 130 cm, Type OPC). Occasional sharp core/rim boundaries, recognized by abrupt changes in extinction angle (504B-115-1, 12 cm, 504B-100-1, 139 cm, 504B-73-1, 130 cm, 504B-94-3, 90 cm, all type OPC), indicate a somewhat greater change in anorthite content in later stages of crystallization.

Unlike the observation made from Legs 69 and 70, glomerocrystic aggregates are extremely common—usually consisting of clumps of 2 to 15 plagioclase crystals in random orientations, partially enclosed or enclosing each other. Olivine and/or clinopyroxene occasionally occur with plagioclase in these clusters; however, plagioclase alone is by far the most common. Rare synneusis[3] growth can be observed in clots similar in appearance to glomerocrysts (504B-123-1, 39 cm, Type OPC).

Larger plagioclases may have circular to oval-shaped holes, predominantly in the core area of the crystals. In more extreme cases the core has a skeletal appearance whereas the rim appears homogeneous and intact (Fig. 7). We have interpreted this as evidence for resorption. Such crystals may occur either as phenocrysts (504B-104-2, 82 cm, Type A; 504B-122-1, 116 cm, Type OP; 504B-113-1, 73 cm, Type OP; 504B-104-3, 51 cm, Type A) or in glomerocrystic clusters (504B-72-2,57 cm, Type SV). This feature was not observed in Type OPC.

Olivine forms 0.5 to 2% of the rocks. It ranges in size from 0.3 to 6 mm; 1 to 2 mm, however, is most common. It nearly always displays a euhedral crystal morphology, but may be subhedral and rarely skeletal (504B-101-1, 77 cm, Type OPC). The primary chemistry of the olivine phenocrysts in these rocks cannot be assessed since they are always replaced by saponite, talc, or chlorite.

Clinopyroxene phenocrysts occur only in types OPC and SV. They comprise 0.5 to 5% of the rock and range in size from 0.4 to 4.8 mm. The crystal morphology is typically subhedral and euhedral. They are often twinned (504B-71-1, 112 cm, Type SV (OPC); 504B-100-1, 139 cm, Type OPC), and may be zoned (504B-121-1, 73 cm, Type A).

In samples where the groundmass is coarse grained enough to form subophitic textures, the clinopyroxene phenocrysts have highly irregular boundaries. This results from the combined effect of nucleation and growth of groundmass plagioclase on the surface of the clinopyroxene while the clinopyroxene itself continues to crystallize.

Clinopyroxene also occurs with plagioclase in clusters which have been interpreted as xenoliths (504B-81-1, 82 cm, Type OP; 504B-73-1, 130 cm, Type OPC). These aggregates are generally composed of crystals in ophitic to subophitic relationships. The size of the individual crystals is commonly larger than those in the groundmass or sometimes even the phenocryst phases. Probably the most distinctive feature of the xenoliths is that the crystals involved have a sievelike texture analogous to that described previously for plagioclase. This resorption texture is an indication that the aggregates are in disequilibrium with the host material. The primary texture and grain size of these inclusions are similar to many of the massive, aphyric units and they may have been ripped from the dike wall during ascent of the host magma.

Clinopyroxene of phenocryst dimensions may contain euhedral feldspar laths in ophitic or subophitic relationship. The enclosed feldspars are generally in random orientation, as opposed to the radiate cluster pattern normally produced in the groundmass [504B-84-1, 74 cm, Type SV (OPC)]. Although not all clinopyroxene phenocrysts in the same rock exhibit this texture, they give no indication of being xenolithic material and are probably phenocrysts.

Table 3. Phenocryst phases in Hole 504B basalts.

Group	Phenocryst phase	Estimated percentage	Maximum size range (mm)	Crystal morphology
OPC	Olivine	0.5–2.0	0.3–3.5	Euhedral
	Plagioclase	1.0–5.0	0.5–3.0	Subhedral
	Clinopyroxene	1.0–5.0	0.4–4.8	Anhedral
OP	Olivine	0.5–3.0	1.0–2.5	Euhedral
	Plagioclase	0.5–5.0	1.2–2.0	Subhedral
SV	Olivine	0–5.0	0.5–4.0	Euhedral
	Plagioclase	1.0–10.0	1.0–2.5	Subhedral
	Clinopyroxene	0–1.0	0.8–1.5	Anhedral
	Spinel	$\ll 1$	0.01–0.2	Euhedral

Groundmass: Type OP

The plagioclase–olivine phyric basalts of Type OP are predominantly fine to medium grained. Groundmass texture varies from subophitic to intergranular and rarely plumose. The groundmass plagioclase is typically more elongate than the phenocrysts—length to width ratios are about 8:1 as compared to 2:1 in the phenocrysts. Plagioclase forms 40–60% of the groundmass and occurs as subhedral laths 0.08 to 1 mm in size. None are skeletal in morphology. They may occur in random orientation or in radiate aggregates of two to four crystals.

[3] The term *synneusis* comes from a Greek word meaning "to swim together." In a synneusis relationship, crystals which have crystallized independently for a length of time cluster together at some point and continue to grow as a single unit. That is, the aggregate (as a total unit) crystallizes a rim of material which is in optical continuity. The individual crystals within this rim are not in the same crystallographic orientation.

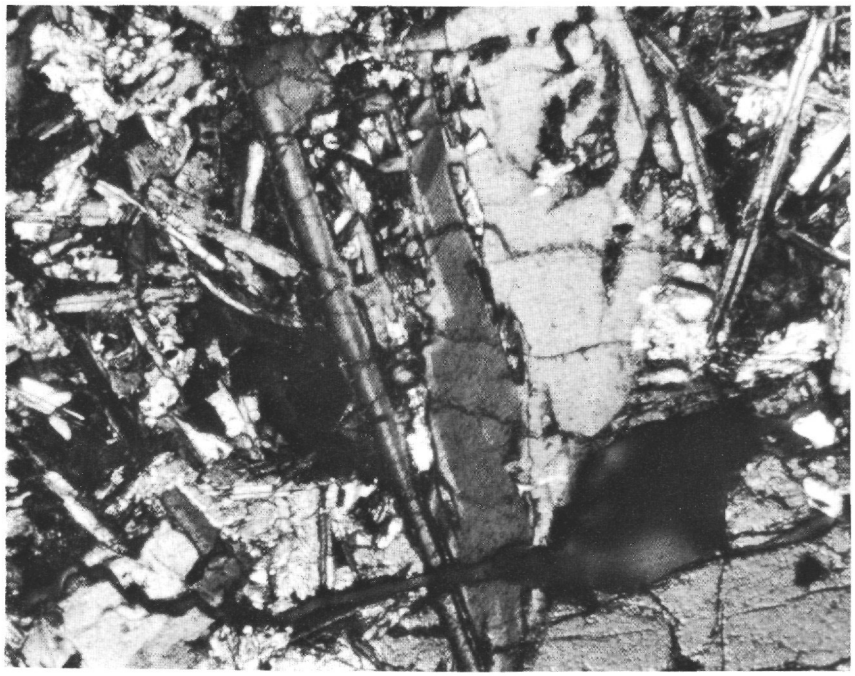

Figure 7. Resorbed plagioclase, Sample 504B-72-2, 57 cm. Field of view is 3.1 mm.

Olivine occurs in the groundmass in proportions of up to 10%, but pervasive alteration of interstitial areas to clays or chlorite makes identification of crystal morphology and abundance difficult.

Clinopyroxene forms 30–45% of the groundmass and occurs as subhedral to anhedral crystals usually less than 1 mm in size. They are located in the interspace between plagioclase laths, most commonly in subophitic relationship. However, equant granules and plumose and skeletal quench morphologies also occur. Frequently, palmate shapes of dimensions equivalent to that of the plagioclase occur in the radiate clusters. Here the clinopyroxene morphology is apparently dictated by the plagioclase laths, because these crystals taper and converge toward the center of the cluster. Extinction often takes place in an undulose or sweeping pattern, within what appears to be a single crystal. This may be due to zoning or, more probably, to a slight structural reorientation because of the interference with plagioclase during growth.

FeTi oxides, or their pseudomorphs by alteration to sphene, form 3–5% of the rock. They are nearly always euhedral, equant grains 0.02 to 0.05 mm in size. They are located in the interstices between plagioclase and clinopyroxene.

Interstitial areas forms less than 3% of the bulk and are generally filled with clays or chlorite. It is thus not possible to ascertain whether they were originally filled by glass, were quench crystals, or were actually voids.

Groundmass: Type OPC

The olivine–plagioclase–clinopyroxene phyric Type OPC ranges in grain size from glassy to medium grained. The groundmass textures encountered are, thus, the most variable of any group. Quench crystallization textures such as variolitic, sheaf, and plumose occur as frequently as coarser-grained subophitic and intergranular textures.

Plagioclase varies from 30 to 60% in the groundmass and ranges in size from submicroscopic to 0.5 mm in size. Morphologies may be subhedral laths, skeletal, or advanced quench textures, that is, variolitic and sheaf. As in Type OP, groundmass plagioclase crystals tend to be more elongate than the phenocrysts.

Clinopyroxene constitutes 30–50% of the groundmass and is submicroscopic to 0.5 mm in size. Anhedral, equant morphologies occur in intergranular or subophitic relationship with radiate plagioclase clusters, but skeletal and plumose textures also occur in the interspaces. Undulose or sweeping extinction is common and is similar to that described under Type OP.

Olivine pseudomorphs are present in the groundmass in amounts of 2–5%. They are generally less than 0.5 mm in size and are most commonly euhedral. Olivine was not recognized in quenched textures and could not be identified with assurance until the grain size coarsened to the point that subophitic or intergranular textures were produced.

FeTi oxides, or their sphene pseudomorphs, occur in abundances of 3–5%. They are typically less than 0.1 mm in size and have equant, euhedral morphologies.

Groundmass: Type SV

Type SV contains chrome spinel as an accessory phase in units which would otherwise be classified as OPC, OP, and A. Since the presence of spinel is the only characteristic which distinguishes these lavas from the

others, the descriptions of phenocrysts and groundmass textures for members of this group are given under the appropriate alternate category.

The spinel is usually present in abundances of less than 1%—usually only 2 or 3 grains 0.01 to 0.2 mm in size were detected throughout any slide. Euhedral, diamond shapes are the common morphology, although a few skeletal or wormy crystals occurred [504B-80-3, 133 cm, Type SV (OP); 504B-92-2, 121 cm, Type SV (OP); 504B-111-1, 104 cm, Type SV (OPC)]. Sometimes the spinel has a thin, dark rim which suggests alteration to magnetite.

Although spinel has been observed in all group types, it is rare in Type A (only two occurrences); even when present in this group, it is included in or attached to feldspar. In other groups it is also commonly attached to olivine pseudomorphs but was never observed to be enclosed within olivine (Fig. 8). Spinel occurs as commonly in samples that are clinopyroxene phyric as in those that are not. It is interesting to note that of the 19 lavas observed to contain spinel, 12 are from chilled margins of dikes or pillows; the reason for this is unknown.

It could reasonably be questioned whether these samples form a meaningful petrographic group distinct from the others, particularly since the occurrence of a mineral in such trace amounts could easily miss detection. The presence of spinel is nonetheless a significant observation, because it does not commonly occur in ocean basalts.

Groundmass: Type A

The aphyric group contains less than 1% of crystals which could qualify as phenocrysts. The texture is predominantly subophitic to intergranular. Rare ophitic as well as quench sheaf textures occur in samples taken from the chilled borders of typical aphyric units. Grain size is predominantly fine to medium; members of this group are frequently coarser-grained than samples from any other group, making it somewhat distinct from the A group devised in Leg 69 and presumably in Leg 70, where quench textures were more often encountered.

Plagioclase and clinopyroxene form the bulk of these units. Plagioclase constitutes 35–60% of the rocks and ranges in size from 0.4 to 1.6 mm. Subhedral to euhedral laths (length: width ratio approximately 8:1) are the most common crystal morphology. In the quenched samples, plagioclase generally forms immature sheaf or plumose textures in which skeletal microlites less than 0.3 mm in size form the centers of the sheafs.

Zoning is normal to faintly oscillatory in some of the larger crystals; occasionally distinct core/rim boundaries can be observed. Twinning is most commonly the polysynthetic albite type.

Although phenocrysts are not present by definition, rare clusters of plagioclase with stubbier shapes and slightly greater size than the groundmass form aggregates suggestive of an earlier stage where plagioclases were arranged in glomerocrystic relationships. These plagioclases often have a sievelike texture created by the presence of numerous oval to circular patches. As discussed earlier, this texture is probably an indication of disequilibrium and melting.

In general, plagioclase forms radiate aggregates of two to four crystals; otherwise, random orientations prevail. There is no indication of preferred parallel alignment of laths. Crystal faces often have scalloped edges because of interference with the clinopyroxene that crystallizes between adjacent plagioclase laths.

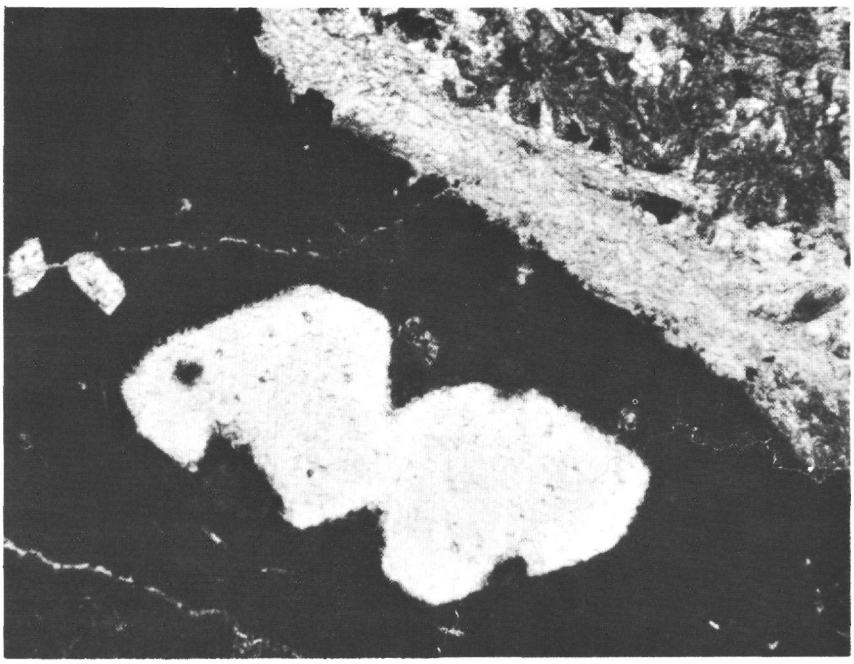

Figure 8. Chrome spinel attached to rims of euhedral olivines in dike margin, Sample 504B-111-1, 104 cm. Spinels have dark alteration (magnetite?) at rims. Photo is in uncrossed polars; field of view is 3.1 mm.

Clinopyroxene forms 30–50% of these units and ranges in size from 0.2 to 2.5 mm, although most crystals are less than 1 mm. Clinopyroxene crystal morphologies are the most variable of any mineral phase in this group. Morphologies include equant, anhedral crystals in subophitic or ophitic relationship with plagioclase or granular aggregates which fill triangular interstices between the laths. Elongate sprays similar to those described in Types OPC and OP may also occur.

The clinopyroxene commonly displays a sweeping, radiate extinction (504B-91-4, 33 cm), but it is less common and less pronounced than that found in the other groups. Occasionally, the groundmass subophitic pyroxenes are enlarged nearly to the size of phenocrysts. These may be twinned, but always have irregular crystal boundaries where plagioclase interfered with their growth during the later stages of crystallization.

Olivine forms 1–15% and ranges in size from 0.05 to 2.0 mm; it averages about 5%, 0.5 to 0.6 mm. It is nearly always euhedral and occasionally subhedral.

FeTi oxides are equant, euhedral, and interstitial when present and unaltered. Most, however, have been replaced by sphene and have lost their euhedral crystal outlines.

Type A has been recovered only from units which have been interpreted as massive bodies or dikes. A few chilled margins of these units have been thin sectioned and these display quench crystal morphologies. Since chilled margins constitute only a small percentage of the total and since these will be included in a more detailed discussion of the difference in dike and pillow textures given in Kempton (this volume), they will not be elaborated upon here.

Synthesis

Basalts from Hole 504B (Leg 83) can be divided into four petrographic groups:

OPC: olivine–plagioclase–clinopyroxene phyric basalt;

OP: olivine–plagioclase phyric basalt;

SV: accessory chrome spinel with variable olivine–plagioclase–clinopyroxene phyric basalt;

A: aphyric basalt

The plagioclase–clinopyroxene phyric basalts (Type PC, Leg 70) were not observed.

Estimates of the relative abundance of each group were made based on the number of meters of core assigned to each petrographic group. From this perspective, OPC forms 29% of the total column; OP, 13%; SV (OPC), 8%; SV (OP), 9%; SV (A), 2%, A, 40%. These estimates were determined by assuming that the petrographic group assigned to a lithologic unit is the same throughout the unit unless demonstrated otherwise by additional sampling and petrography. This is probably a safe assumption for the massive units, but is almost certainly not for the lithologic units defined as pillow sequences, that is, those containing more than one pillow.

These four groups appear to have experienced similar crystallization histories. The differences which are observed probably result from slightly different appearance temperatures of the phases and the subtle details of the cooling histories.

The following textural observations have been used to define a possible petrogenetic crystallization sequence:

1. Spinel occurs enclosed in plagioclase and frequently attached to the rims of olivine pseudomorphs.
2. Olivine and plagioclase are always present as phenocryst phases in the phyric lavas; clinopyroxene, however, may be absent.
3. The quench mineralogies observed in chilled margins include plagioclase or plagioclase plus clinopyroxene; however, olivine was never observed as a quenched phase. (That is, unfortunately, not conclusive evidence, because of the state of alteration in the samples observed.)
4. Plagioclase is always the most abundant phenocryst phase.
5. FeTi oxides or their sphene pseudomorphs are commonly absent in chilled margins and are always interstitial in the coarser-grained units.

From these observations, the surmised sequence of crystallization begins with spinel. Whether olivine or plagioclase is the next phase to enter after spinel cannot be determined unequivocally from the existing petrographic data. However, the greater modal abundance of plagioclase suggests that the bulk composition of the lavas falls in the plagioclase stability field and would, therefore, begin crystallization of plagioclase prior to olivine. Because of its absence as a phenocryst phase in numerous lavas and its common habit of ophitically or subophitically enclosing plagioclase, clinopyroxene must crystallize after olivine and plagioclase. FeTi oxides are always the last major phase to enter the crystallization sequence.

The common occurrence of medium- to coarsely crystalline aphyric units suggests that the lavas from Hole 504B are frequently multiply saturated. (Plagioclase, olivine, and clinopyroxene crystallize together throughout the crystallization sequence.) Such a condition is generally taken as an indication that the magmas are relatively evolved. However, the presence of spinel indicates that the lavas are relatively unfractionated, since spinel frequently ceases to crystallize at an early stage during the evolution of common basaltic magmas. Resolution of this discrepancy will require detailed analysis of compositional variations in bulk-rock major and trace elements, combined with phenocryst mineral chemistries.

BASEMENT GEOCHEMISTRY

During Leg 83 whole-rock analyses of basalts were carried out aboard *Glomar Challenger*. The concentrations of Si, Ti, Al, Fe, Mg, Ca, K, and P were determined by X-ray fluorescence analysis using the Siemens VRS spectrometer provided by the Centre National pour l'Exploitation des Océans. In addition, H_2O^+ and CO_2 determinations were performed on a Hewlett-Packard CHN analyzer available in the chemistry lab. Detailed descriptions of the methods applied are given in the reports of Legs 45 and 52, by Bougault (1977), Melson et al. (1979), and Emmermann and Puchelt (1980).

According to the systematic studies of the analytical error resulting from sample preparation, instrumental parameters, measuring conditions, and the like which were carried out on Leg 52 (Emmermann and Puchelt,

1980), the precisions—expressed as ±S.D. in wt.%—of the components are approximately as follows: ± 0.4 wt.% for SiO_2, ± 0.02 wt.% for TiO_2, ± 0.20 wt.% for Al_2O_3, ± 0.10 wt.% for Fe_2O_3, ± 0.15 wt.% for MgO, ± 0.15 wt.% for CaO, ± 0.01 wt.% for K_2O, ± 0.01 wt.% for P_2O_5, ± 0.2 wt.% for H_2O^+, and ± 0.01 wt.% for CO_2.

The accuracy of the values obtained by XRF analysis was ensured by using the reference rocks PCC-1, BR, BCR-1, AGV-1, DRN, GSP-1, and GH for the construction of the calibration curve. This was always checked by measuring the reference basalt MAR as an "unknown" along with each set of samples. A similar procedure was applied for H_2O^+ and CO_2. Here, the calibration curve was set up by the reference rocks UBN, M4-1, PO-1D-3, and GH, and the rock AGS was measured as "unknown."

Altogether, 52 basalt samples were analyzed on board the ship during Leg 83. Each sample represents the dominant rock type of the respective units. Care was taken always to select the "freshest" possible material for analysis, that is, material void of veins or veinlets, which appeared in hand specimen the least affected by alteration.

The XRF analyses of these samples are summarized in Table 4. Since these values were obtained on ignited rock powder, they still have to be corrected in order to derive the actual chemical composition of the rocks. To achieve this, it would be necessary also to determine Na_2O, MnO, and FeO and to recalculate all oxides to a sum of 100% including H_2O^+, CO_2, and FeO as they were measured on dry rock powder. As these data were not available, we adopted the following correction procedure:

1. 90% of the Fe_2O_3 content analyzed was arbitrarily converted to FeO (to approximate measured Fe_2O_3/FeO ratios in fresh ocean ridge basalt glasses).

2. All oxides including FeO were recalculated to a sum of 97.5% (assuming that the actual Na_2O + MnO content of these rocks is constant and averages 2.5 wt.%; see later).

This correction reduces apparent chemical variations that are due to analytical errors. It also provides data which can be compared to the whole rock analyses of the upper part of Hole 504B and which are directly comparable to magma compositions. The water and CO_2-free normalized data are given in Table 4.

Legs 69 and 70 Review

Before discussing these data we will briefly summarize some of the pertinent geochemical results obtained on "fresh" basaltic material recovered from the upper part of Hole 504B during Legs 69 and 70. Chemical data for Legs 69/70 are summarized from Hubberten et al. (1983). From the large number of chemical analyses available, three main points emerged:

1. The remarkable compositional uniformity of the basement section drilled.

2. The rather primitive character of the basalts recovered.

3. The exceptional chemistry of two subordinate lava flows, Units 5 and 36 of Legs 69 and 70.

Except for basalts from Lithologic Units 5 and 36, which differ significantly from all other basalts recovered from this hole, almost no chemical variation down hole could be established. Most of the basalts are relatively MgO-rich (MgO ≥ 8 wt.%) and have mg-values of about 0.64 which clearly indicate that the respective magmas experienced only a small degree of crystal fractionation before erupting onto the seafloor. According to their normative mineralogies, most of the rocks have to be classified as olivine tholeiites, with a few samples plotting close to the Diopside–Hypersthene join of the projected "basalt tetrahedron."

For the major oxides the following ranges of variation were found (wt.%):

SiO_2	47.7–50.9	MgO	6.8–9.4
TiO_2	0.78–1.40	CaO	11.2–14.0
Al_2O_3	14.0–17.3	Na_2O	1.98–2.75
FeO_t	7.2–11.0	K_2O	0.01–0.40
MnO	0.14–0.22	P_2O_5	0.03–0.20

However, the majority of the samples show a much more restricted chemical variation, close to the following averages:

SiO_2	50.0	MgO	8.4
TiO_2	0.92	CaO	12.8
Al_2O_3	15.5	Na_2O	2.29
FeO_t	9.2	K_2O	0.04
MnO	0.17	P_2O_5	0.07

When the samples were recalculated to a dry weight basis and Fe_2O_3/FeO corrected according to the procedure described above, the following averages were obtained:

SiO_2	50.3		
TiO_2	0.93	MgO	8.45
Al_2O_3	15.6	CaO	12.9
Fe_2O_3	1.03	Na_2O	2.31
FeO	8.08	K_2O	0.04
MnO	0.17	P_2O_5	0.07

The same averages also apply to basalts from Units 5 and 36, except for TiO_2 and P_2O_5. However, Units 5 and 36 basalts can be clearly distinguished from all other basalts recovered from this hole by their marked enrichment in both TiO_2 and P_2O_5. Their TiO_2 concentrations are between 1.25 and 1.40 wt.% and their P_2O_5 between 0.14 and 0.20 wt.%.

The differences between Unit 5 and 36 basalts and all the other basalts from Hole 504B are even more pronounced in their trace element pattern. Although majority of the basalts are strongly depleted in LIL-elements and display a "MORB"-type trace element chemistry, basalts from Units 5 and 36 are significantly higher in "magmatophile" elements. The difference between these two chemical groups is especially well documented by their rare earth element (REE) distribution curves. Figure 9 shows the chondrite-normalized REE distribution patterns for the two basalt types. Curve "a" repre-

sents the dominant basalt type, which is characterized by a strong depletion of light REE (La/Sm enrichment factor [e.f.] 0.4) and has a low overall enrichment of REE (Yb e.f. 13). In contrast, basalts from Units 5 and 36 are higher in REE (Yb e.f. 18) and exhibit chondritic or even light REE enriched patterns, which normally are regarded as typical for "plume"-derived basaltic magmas.

The pronounced mineralogical alteration and the downhole variation of two different alteration types are not reflected in significant concentration changes of most of the elements analyzed. The otherwise very sensitive "freshness" parameters H_2O^+ and CO_2 show relatively low concentrations clustering around 0.8 wt.% for H_2O^+ and 0.1 wt.% for CO_2 and do not vary systematically with depth. A significant difference between the oxidative (upper) and nonoxidative (lower) type of alteration was found only for the K_2O contents of the rocks, which are more variable (0.02 to 0.40 wt.%) and on average higher (0.20 wt.%) under the oxidative alteration conditions. In the lower part of the basement section drilled during Legs 69 and 70, K_2O contents are rather uniform with an average of 0.03 wt.%. Also, statistically, the iron oxidation state [expressed as $Fe_2O_3/(Fe_2O_3 + FeO)$ in wt.%] reflects the two types of alteration, being 0.4 in the upper part of the Hole and 0.3 in the lower part. The sulfur contents of the basalts were found to vary between 180 and 1100 ppm. On average, they are lower (300 ppm) in the oxidative zone than in the nonoxidative zone (700 ppm).

Leg 83 Results

The chemical results obtained on basalts from the basement section drilled during Legs 69 and 70 provide the background for the following evaluation and discussion of our chemical data. The questions we tried to answer were:

1. What is the chemical variability of the basaltic rocks drilled during Leg 83?
2. How do they compare to the basalts recovered from the upper part of the hole?
3. Is there any evidence for the occurrence of chemically exceptional types as represented by Lithologic Units 5 and 36?
4. Does the alteration effect a significant redistribution of the major oxides?
5. What conclusions can be drawn about the formation of the rocks recovered during Leg 83?

A close scrutiny of Table 4 reveals that the basaltic rocks analyzed during Leg 83 also display a rather limited compositional variation in their major element chemistry. The corrected concentration ranges found (wt.%) are:

SiO_2	46.9–52.8	MgO	7.58–9.78
TiO_2	0.74–1.06	CaO	11.6–13.5
Al_2O_3	14.4–17.7	K_2O	0.02–0.06
FeO_t	8.20–10.3	P_2O_5	0.05–0.11

However, as with the basalts recovered from the upper part of Hole 504B, the majority of the Leg 83 samples vary within much narrower limits than above and cluster around a mean value. This is illustrated in Figure 10 by an oxide frequency distribution plot, which shows a marked concentration maximum for all elements determined by XRF. Even for TiO_2 and P_2O_5 there is no evidence of a bimodal distribution as would be the case if basalt types like Units 5 and 36 basalts had been analyzed. Therefore, the major oxide composition of the Leg 83 samples can be characterized (wt.%) by the following averages:

SiO_2	49.9 (± 0.89)	MgO	8.80 (± 0.51)
TiO_2	0.90 (± 0.09)	CaO	12.9 (± 0.29)
Al_2O_3	15.7 (± 0.82)	K_2O	in most cases ≤0.02
FeO_t	9.04 (± 0.45)	P_2O_5	0.08 (± 0.02)

The small standard deviations, which are given as ± 1s in brackets, underline the very narrow frequency distribution curves of the respective oxides. They also indicate that the lava flows and dikes encountered have the same overall major element composition and cannot be distinguished chemically.

The averages obtained for all components are very close to those found in basalts from the upper part of the hole and their confidence limits in all cases overlap. From this it follows that, in their major oxide compositions, no significant differences can be established between basalts recovered during Legs 69 and 70 and the basement section drilled during Leg 83. The only noticeable exception might be MgO, which, according to the shipboard analyses, seems to be systematically higher in the Leg 83 part of the hole, where it averages 8.8 wt.% in contrast to 8.45 wt.% in the upper part. This point is discussed by Emmermann (this volume).

In keeping with their high MgO contents, the basaltic rocks analyzed are characterized by relatively high mg-values, that is, Mg^{2+} to $Mg^{2+} + Fe^{2+}$ atomic ratios. The $Mg^{2+}/(Mg^{2+} + Fe^{2+})$ values were calculated by assuming that the primary FeO content of the rocks was 85% of their FeO_t. They range from 0.70 to 0.62 and average 0.67. Since it has been demonstrated that tholeiitic liquids in equilibrium with their peridotitic mantle source will have mg-values ranging from 0.68 to 0.75, Leg 83 mg-values suggest that the rocks encountered were crystallized from rather primitive, that is, unevolved, basaltic melts. Thus, if the analytical data obtained represent magma compositions, it can be concluded that the respective melts experienced only a very small degree of crystal fractionation prior to their eruption or intrusion, respectively. However, determination of Ni, Cr, and other trace elements is required to derive a more precise statement about the fractionation history of the rocks (see Emmermann, this volume).

The potassium contents of the Leg 83 samples were found to be very low. On average they are even lower than those of basalts altered in the nonoxidative zone of the Leg 70 section of the hole.

This might also be true for CO_2. The values obtained on board the ship vary between 0.09 and ≤0.02 wt.%. They are on average lower than in the Leg 70 section of the hole and seem to decrease systematically with depth. In the lowermost part of the hole they are in most cases below 0.04 wt.%. This corresponds well to the very rare

Table 4. XRF analyses of basalt samples from Hole 524B, Leg 83.

Depth below seafloor (m)	Core-Section (interval in cm[a])	Lithologic unit	Rock type[b]	Uncorrected XRD analyses						
				SiO_2	TiO_2	Al_2O_3	Fe_2O_3	MgO	CaO	K_2O
850.4	72-3, 41–43(5a)	48	SV(OPC)	49.1	0.83	15.7	9.76	8.70	12.7	<0.02
858.7	73-1, 43–46(5a)	50	OPC	49.1	0.84	15.2	9.78	9.30	12.5	<0.02
875.4	75-1, 119–121(6)	53	SV(OP)	49.0	0.93	16.3	9.91	8.02	13.2	<0.02
890.0	77-1, 71–74(4)	54	A	49.6	0.96	15.9	10.1	8.48	12.3	<0.02
894.3	77-2, 123–126(10)	54	A	49.4	1.03	14.5	10.0	8.56	12.3	<0.02
903.8	78-2, 52–54(11)	57	A	48.7	0.94	16.4	10.3	8.65	13.0	<0.02
905.8	79-1, 93–100(14)	58	OP	48.5	0.91	16.9	10.1	8.02	13.2	<0.02
918.5	80-3, 132–134(8f)	59	SV(OP)	48.2	0.81	17.5	9.82	7.48	13.3	<0.02
936.6	82-3, 44–46(5)	59	SV(OP)	49.9	0.92	15.6	9.65	9.01	12.7	0.02
945.0	83-2, 2–5(1)	59	SV(OP)	49.6	1.01	15.5	9.42	8.85	12.9	<0.02
950.0	84-1, 105–107(6)	59	SV(OP)	49.7	0.89	15.1	9.56	9.31	12.1	<0.02
961.6	85-2, 113–117(4d)	60	SV(OP)	49.4	0.99	15.2	10.3	8.71	13.1	<0.02
964.9	86-1, 6–4(1)	61	A	49.6	0.88	14.9	10.8	8.52	12.8	0.06
970.3	87-1, 93–95(6d)	62	OPC	49.1	1.01	14.6	11.0	8.24	12.1	<0.02
979.5	88-1, 48–50(2d)	69	n.a.	49.1	1.05	15.6	10.6	8.75	12.7	<0.02
987.8	89-1, 67–69(7)	70	A	48.6	0.83	16.8	9.82	9.33	12.6	<0.02
1001.7	90-4, 69–71(6c)	71	A	51.2	0.89	15.6	9.98	8.60	11.5	<0.02
1006.0	91-1, 134–137(18)	73	n.a.	49.0	0.75	15.9	10.1	9.24	13.5	<0.02
1014.9	92-2, 118–121(11e)	78	OPC	48.6	0.83	15.7	9.79	8.67	12.6	<0.02
1011.9	92-3, 64–67(8)	78	OPC	49.6	0.95	14.7	11.0	8.22	13.1	<0.02
1025.8	93-2, 33–35(3)	78	OPC	52.2	0.90	14.6	10.2	7.97	11.5	<0.02
1031.3	94-1, 38–41(5)	81	OP	49.7	0.96	15.5	10.5	8.32	12.9	<0.02
1034.8	94.2, 65–67(3)	82	n.a.	49.2	0.90	15.9	10.1	8.93	13.0	<0.02
1038.5	94-3, 100–103(11)	83	n.a.	49.6	0.91	15.8	10.3	8.56	12.8	<0.02
1057.9	97-2, 26–29(3a)	88	n.a.	50.1	0.96	14.3	10.8	8.32	12.9	<0.02
1061.5	98-1, 75–77(11)	91	A	47.5	0.93	16.7	9.98	9.63	12.4	<0.02
1072.7	99-2, 61–63(7)	93	A	49.9	1.01	14.3	11.3	8.32	12.7	<0.02
1083.5	100-1, 139–144(16)	94	A	49.1	0.83	16.5	9.56	7.86	12.6	<0.02
1095.8	101-2, 39–43(5)	100	n.a.	50.4	1.05	14.4	11.4	7.95	12.6	<0.02
1102.6	102-1, 48–51(5a)	102	OPC	49.4	0.84	15.4	9.94	8.96	13.1	<0.02
1121.2	104-2, 85–87(4d)	103	A	48.3	0.91	16.6	10.1	8.34	12.5	<0.02
1129.8	105-1, 61–63(9)	105	n.a.	49.2	0.82	15.0	10.2	9.22	12.9	<0.02
1137.6	106-1, 35–37(4)	106	A	49.3	0.85	15.3	9.85	8.92	13.1	<0.02
1148.1	107-1, 116–119(15)	108	SV(OPC)	49.9	0.82	14.9	9.70	8.64	12.9	<0.02
1153.2	108-1, 57–60(7)	108	SV(OPC)	50.3	0.77	14.6	10.1	8.66	12.7	<0.02
1159.4	110-1, 34–39(5)	109	A	49.5	0.94	14.9	10.5	8.34	12.6	<0.02
1164.1	111-1, 86–89(9)	110	n.a.	46.5	0.94	17.4	10.5	9.70	12.6	0.06
1173.3	113-1, 68–70(6)	112	A	49.4	0.77	15.6	9.74	9.39	13.3	<0.02
1185.6	116-1, 24–27(4)	114	OPC	49.9	0.83	14.7	10.4	9.12	12.8	<0.02
1196.2	118-1, 33–35(2c)	115	OP	50.5	0.95	14.8	10.5	8.78	12.6	<0.02
1216.4	122-1, 116–119(9)	121	n.a.	49.0	0.91	16.2	9.52	7.99	13.0	<0.02
1224.1	123-1, 39–42(5a)	124	OPC	49.1	0.85	15.8	10.1	8.38	13.1	<0.02
1251.6	126-1, 30–34(4b)	126	n.a.	49.1	0.76	16.1	9.21	9.05	13.2	<0.02
1257.2	127-1, 50–56(6)	128	n.a.	49.4	0.76	16.1	9.24	9.26	13.2	<0.02
1263.7	128-1, 47–49(4)	132	OPC	49.8	0.83	16.1	9.50	8.79	13.3	<0.02
1270.8	129-1, 35–39(3b)	133	OPC	49.0	0.73	16.5	9.05	9.34	13.0	<0.02
1275.7	129-2, 118–121(10)	134	A	50.5	0.90	14.6	10.2	8.53	13.0	<0.02
1282.5	130-2, 9–12(1a)	135	OPC	49.1	0.74	15.8	9.06	9.23	13.1	<0.02
1289.8	131-1, 67–70(7)	136	OPC	49.7	0.77	15.8	9.19	9.43	13.3	<0.02
1298.1	132-1, 59–61(8)	136	OPC	49.6	0.82	16.1	9.35	8.90	13.3	<0.02
—	97-1 sand	Sand sample		49.7	0.99	13.9	11.5	8.62	11.7	<0.02
—	121-1, 69–72(5)	Altered (brecciated)		50.3	1.07	13.8	13.3	8.08	10.4	<0.02

[a] Piece number in parentheses.

[b] n.a. = Not available (rock type not determined).

[c] LOI = Loss on ignition.

occurrence of calcite in Leg 83 rocks as compared to Legs 69 and 70 rocks, where it seems to be more abundant.

Despite the overall chemical uniformity of the rocks analyzed, there is some minor downhole variation which can be related to specific lithological units (Fig. 11). As suggested by the more or less complementary pattern of the MgO and FeO_t concentrations, these variations may be at least in part due to slightly different degrees of fractional crystallization of the respective magmas. This interpretation is also supported by the FM-variation plots of CaO, MgO, FeO_t, and TiO_2 shown in Figure 12. The FM-index, which provides a suitable differentiation parameter of basaltic melts, is calculated as the ratio $100 \times FeO_t/(FeO_t + MgO)$ in wt. % and is given along with the corrected mg-values in Table 4. In principle, there are correlations which are to be expected when crystal fractionation processes are operative. However, the considerable scatter which is to be observed for CaO and TiO_2 might either be a result of chemical redistribution through alteration or might indicate that the rocks were crystallized from parental magmas of slightly different starting compositions. To explain this observation properly, additional trace element data are needed.

Table 4. (Continued).

Uncorrected XRD analyses			XRD analyses corrected to water and CO_2 free conditions												
P_2O_5	Total	LOI[c]	SiO_2	TiO_2	Al_2O_3	Fe_2O_3	FeO	MgO	CaO	K_2O	P_2O_5	H_2O^+	CO_2	mg	FM	TiO_2/Al_2O_3
0.08	96.27	1.81	49.9	0.84	16.0	1.00	7.94	8.84	12.9	<0.02	0.08	1.08	0.05	0.68	49.9	0.05
0.07	96.79	1.06	49.9	0.85	15.5	1.00	7.96	9.46	12.7	<0.02	0.07	1.02	0.07	0.69	48.3	0.06
0.08	97.44	1.94	49.5	0.94	16.5	1.00	8.01	8.10	13.3	<0.02	0.08	1.35	0.09	0.65	52.4	0.06
0.08	97.48	1.56	50.1	0.97	16.1	1.03	8.17	8.56	12.4	<0.02	0.08	1.43	0.04	0.66	51.4	0.06
0.11	95.90	1.43	50.7	1.06	14.9	1.02	8.23	8.79	12.6	<0.02	0.11	1.41	0.04	0.64	54.0	0.07
0.08	98.07	2.10	48.9	0.94	16.5	1.03	8.29	8.69	13.1	<0.02	0.08	1.54	0.04	0.66	51.4	0.06
0.07	97.70	1.94	48.9	0.92	17.0	1.01	8.14	8.08	13.3	<0.02	0.07	1.55	0.04	0.65	52.8	0.05
0.09	97.20	2.47	48.8	0.82	17.7	0.98	7.97	7.58	13.5	<0.02	0.09	1.80	0.04	0.64	53.9	0.05
0.10	97.90	1.56	50.2	0.93	15.7	0.97	7.78	9.06	12.8	0.02	0.10	1.83	0.03	0.69	48.8	0.06
0.08	97.36	2.05	50.1	1.02	15.7	0.94	7.62	8.94	13.0	<0.02	0.08	1.70	0.03	0.69	48.6	0.07
0.09	96.75	2.15	50.5	0.91	15.4	0.97	7.80	9.48	12.3	<0.02	0.09	1.99	0.05	0.70	47.8	0.06
0.11	97.81	1.96	49.7	1.00	15.3	1.04	8.32	8.77	13.2	<0.02	0.11	1.79	0.03	0.66	51.3	0.07
0.08	97.64	0.70	50.1	0.89	15.0	1.09	8.73	8.61	12.9	0.06	0.08	0.46	0.04	0.68	53.0	0.06
0.08	95.13	1.40	50.3	1.04	15.0	1.13	8.94	8.45	12.5	<0.02	0.08	1.48	0.02	0.64	54.4	0.07
0.12	97.92	2.70	49.4	1.06	15.7	1.07	8.54	8.80	12.8	<0.02	0.12	2.59	0.02	0.66	52.0	0.07
0.07	98.05	2.30	48.8	0.83	16.9	0.98	7.90	9.37	12.7	<0.02	0.07	2.13	0.03	0.69	48.4	0.05
0.08	97.25	3.10	51.5	0.89	15.7	1.00	8.04	8.65	11.6	<0.02	0.08	2.85	0.02	0.67	50.8	0.05
0.06	98.55	1.90	49.0	0.75	15.9	1.01	8.09	9.22	13.5	<0.02	0.06	1.78	0.02	0.68	49.3	0.05
0.05	96.24	2.50	49.8	0.85	16.1	1.00	8.03	8.88	12.9	<0.02	0.05	2.41	<0.02	0.67	50.1	0.05
0.08	97.65	1.50	50.1	0.96	14.8	1.11	8.90	8.30	13.2	<0.02	0.08	1.66	0.02	0.64	54.3	0.06
0.08	97.45	1.80	52.8	0.91	14.7	1.03	8.25	8.05	11.6	<0.02	0.08	2.35	0.02	0.65	53.3	0.06
0.10	97.98	1.50	49.9	0.96	15.6	1.06	8.48	8.36	13.0	<0.02	0.10	0.99	0.05	0.65	53.0	0.06
0.08	98.11	2.90	49.4	0.90	16.0	1.01	8.09	8.96	13.1	<0.02	0.08	2.54	0.02	0.67	50.1	0.06
0.08	98.05	1.20	49.9	0.91	15.9	1.04	8.16	8.60	12.9	<0.02	0.08	0.84	0.02	0.66	51.6	0.05
0.08	97.46	1.00	50.7	0.97	14.5	1.09	8.74	8.43	13.1	<0.02	0.08	0.72	<0.02	0.64	53.6	0.07
0.08	97.22	3.90	48.2	0.94	16.9	1.00	8.10	9.76	12.6	<0.02	0.08	3.39	0.04	0.69	48.0	0.06
0.10	97.63	1.10	50.4	1.02	14.4	1.14	9.14	8.40	12.8	<0.02	0.10	1.36	<0.02	0.63	54.7	0.07
0.07	96.52	1.70	50.2	0.85	16.8	0.96	7.81	8.02	12.9	<0.02	0.07	1.49	<0.02	0.66	52.0	0.05
0.07	97.87	1.30	50.9	1.06	14.5	1.15	9.17	7.98	12.7	<0.02	0.07	1.21	<0.02	0.62	56.0	0.07
0.08	97.72	1.70	49.8	0.85	15.5	1.00	8.03	9.04	13.2	<0.02	0.08	1.38	0.02	0.68	49.7	0.05
0.08	96.83	2.10	49.1	0.92	16.9	1.03	8.27	8.49	12.7	<0.02	0.08	1.57	<0.02	0.66	52.0	0.05
0.07	97.41	1.10	49.7	0.83	15.2	1.03	8.26	9.32	13.0	<0.02	0.07	1.18	<0.02	0.68	49.6	0.05
0.06	97.38	1.80	49.8	0.86	15.5	1.00	7.98	9.03	13.3	<0.02	0.06	1.74	<0.02	0.68	49.6	0.06
0.08	96.94	1.30	50.6	0.83	15.2	0.99	7.91	8.79	13.1	<0.02	0.08	0.91	<0.02	0.68	50.0	0.05
0.07	97.80	1.00	51.0	0.78	14.8	1.03	8.21	8.78	12.9	<0.02	0.07	0.60	<0.02	0.67	51.0	0.05
0.08	96.86	1.40	50.4	0.96	15.2	1.07	8.56	8.49	12.8	<0.02	0.08	1.37	<0.02	0.65	52.9	0.06
0.09	97.79	3.80	46.9	0.95	17.5	1.06	8.48	9.78	12.7	0.06	0.09	2.62	0.02	0.68	49.1	0.05
0.06	98.26	1.00	49.5	0.77	15.6	0.97	7.83	9.42	13.3	<0.02	0.06	—	—	0.69	48.0	0.05
0.08	97.83	0.70	50.2	0.84	14.8	1.05	8.39	9.18	12.7	<0.02	0.08	—	—	0.67	50.4	0.06
0.11	98.24	0.85	50.2	0.95	14.8	1.05	8.44	8.81	12.6	<0.02	0.11	—	—	0.66	51.6	0.06
0.07	96.69	1.90	49.4	0.92	16.3	0.96	7.69	8.05	13.1	<0.02	0.07	—	—	0.66	51.5	0.06
0.06	97.39	1.20	49.6	0.86	16.0	1.02	8.18	8.47	13.2	<0.02	0.06	—	—	0.66	51.7	0.05
0.07	97.49	1.10	49.5	0.77	16.2	0.93	7.44	9.12	13.3	<0.02	0.07	—	—	0.70	47.5	0.05
0.06	98.02	1.20	49.7	0.76	16.2	0.92	7.45	9.32	13.3	<0.02	0.06	—	—	0.70	47.0	0.05
0.06	98.38	1.30	49.9	0.83	16.1	0.95	7.64	8.80	13.3	<0.02	0.06	—	—	0.68	49.0	0.05
0.06	97.68	1.60	49.4	0.74	16.6	0.92	7.29	9.41	13.1	<0.02	0.06	—	—	0.70	46.3	0.04
0.06	97.79	1.00	50.9	0.91	14.7	1.03	8.21	8.60	13.1	<0.02	0.06	—	—	0.66	51.5	0.06
0.05	97.08	1.30	49.9	0.75	16.0	0.92	7.32	9.37	13.2	<0.02	0.05	—	—	0.70	46.6	0.05
0.06	98.25	1.10	49.8	0.77	15.8	0.92	7.36	9.43	13.3	<0.02	0.06	—	—	0.70	46.5	0.05
0.07	98.14	1.20	49.8	0.82	16.2	0.94	7.52	8.95	13.3	<0.02	0.07	—	—	0.69	48.3	0.05
0.08	96.49	2.50														
0.09	97.04	4.90														

The only component which shows a pronounced variation with depth is H_2O^+. The corrected shipboard values range from 0.46 to 3.39 wt.% (see Table 4). In the uppermost part of the Leg 83 basement section (i.e., from 836 to about 880 m BSF) they vary between 1.0 and 1.5% and correspond to the values obtained in basalts from the lower part of the Leg 70 section. However, in the interval between 980 and 1070 m BSF (Cores 88 to 97) they reach a maximum and are mostly above 2.0 wt.%. This maximum may be due to the more extensive alteration of the rocks encountered in this part of the hole (see section on basement alteration petrography). Deeper, the H_2O^+ contents decrease again and vary around 1.5 wt.%. In some samples, they are remarkably low ($\leq$ 0.6 wt.%).

Summary and Conclusions

The basement drilled in Hole 504B consists of basaltic rocks formed by a number of discrete eruptive and intrusive events. With respect to their major oxide composition these rocks are rather uniform from top to bottom of the hole and no chemical distinctions can be made between lava flows, which make up the upper part of the basement, and dikes, which prevail in the lower (Leg 83) part.

Within the 1 km of basement cored, two subordinate lava flow units 14 and 18 m thick, respectively (Units 5 and 36 of Legs 69/70), differed significantly from all other rocks. Among the major oxides the concentrations of TiO_2 and P_2O_5 can be used as discriminants

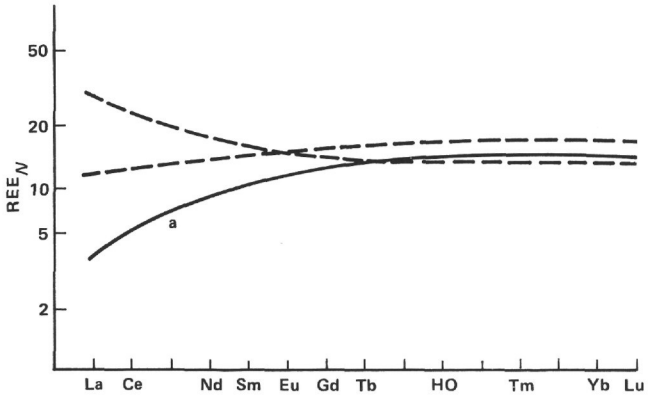

Figure 9. Chondrite-normalized distribution pattern of rare earth elements for Hole 504B basalts cored during Legs 69 and 70 (274.5–836 m below seafloor).

which are both markedly enriched in Units 5 and 36 basalts. In the trace element chemistry Units 5 and 36 basalts are distinguished by relatively high contents of incompatible elements and flat- to light-REE-enriched, chondrite-normalized REE-distribution patterns, whereas the majority of the rocks are strongly depleted in "magmatophile" elements and display light-REE-depleted patterns typical of "normal" ocean ridge basalts.

Among the basaltic rocks drilled during Leg 83 no chemically exceptional types, as represented by Units 5 and 36 basalts, were encountered in shipboard analyses because they were not sampled (see Emmermann, this volume). The rocks analyzed vary within narrow compositional limits and their oxide frequency distributions show pronounced maxima. The oxide means closely correspond to those of Legs 69 and 70 basalts. In all cases they overlap with their respective confidence limits. However, on average, MgO is higher and K_2O is lower than in basalts recovered from the upper part of the hole. According to the shipboard results there might be a systematic MgO increase and an associated K_2O decrease with depth. The significance of these trends is discussed by Emmermann, this volume).

The shipboard data also indicate downhole variation of H_2O^+ and CO_2. In the uppermost part of the Leg 83 section of the hole (Cores 71 through 78), the H_2O^+ contents are relatively low (about 1.0 wt.%) and correspond to those obtained on Leg 70 basalts. They increase with depth and reach a maximum (up to 3.39 wt.%) at a depth between 980 and 1070 m BSF, that is, in Cores 88 through 97, where actinolite is present. This maximum can be explained by an extensive alteration of the basement rocks within this depth range. Toward the bottom of the hole, the H_2O^+ contents decrease again and vary around 1.5 wt.%. The CO_2 contents are, in general, very low, and range from 0.09 to 0.02 wt.%. They seem to decrease systematically with depth. In the lower part of the Leg 83 section of the hole, CO_2 was in most cases found to be below the detection limit, that is, less than 0.02 wt.%. This corresponds well to the extremely rare occurrences of calcite in Leg 83 rocks, whereas calcite and/or aragonite are relatively frequent in basalts from Legs 69 and 70.

For all other components measured, no systematic downhole variations were observed. There might be some small-scale but irregular compositional variations with depth, which can be related to specific litholigic units and can be explained by a slightly different degree of crystal fractionation of the respective melts.

A general characteristic of the Leg 83 rocks is their high MgO (up to 9.78 wt.%) and their extremely low K_2O content. All the rocks contain olivine in the norm and according to their normative mineralogies have to be classified as olivine tholeiites. Since they display almost the same major element composition as Legs 69 and 70 basalts, it is tempting to assume that they are al-

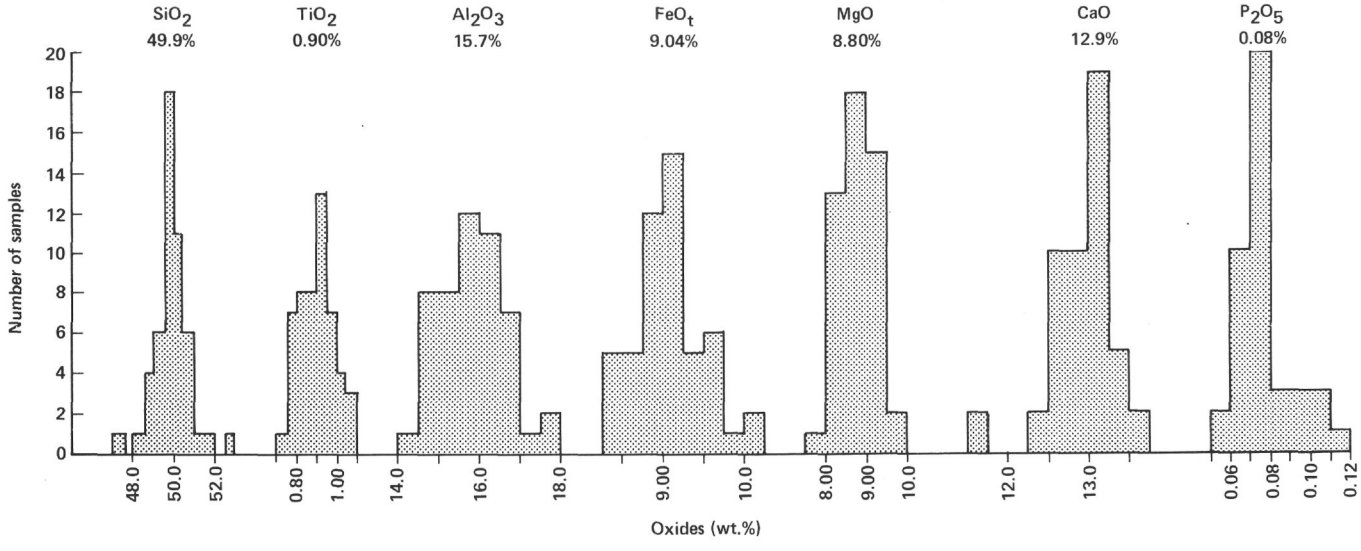

Figure 10. Oxide frequency distribution plots for Leg 83 samples analyzed by XRF.

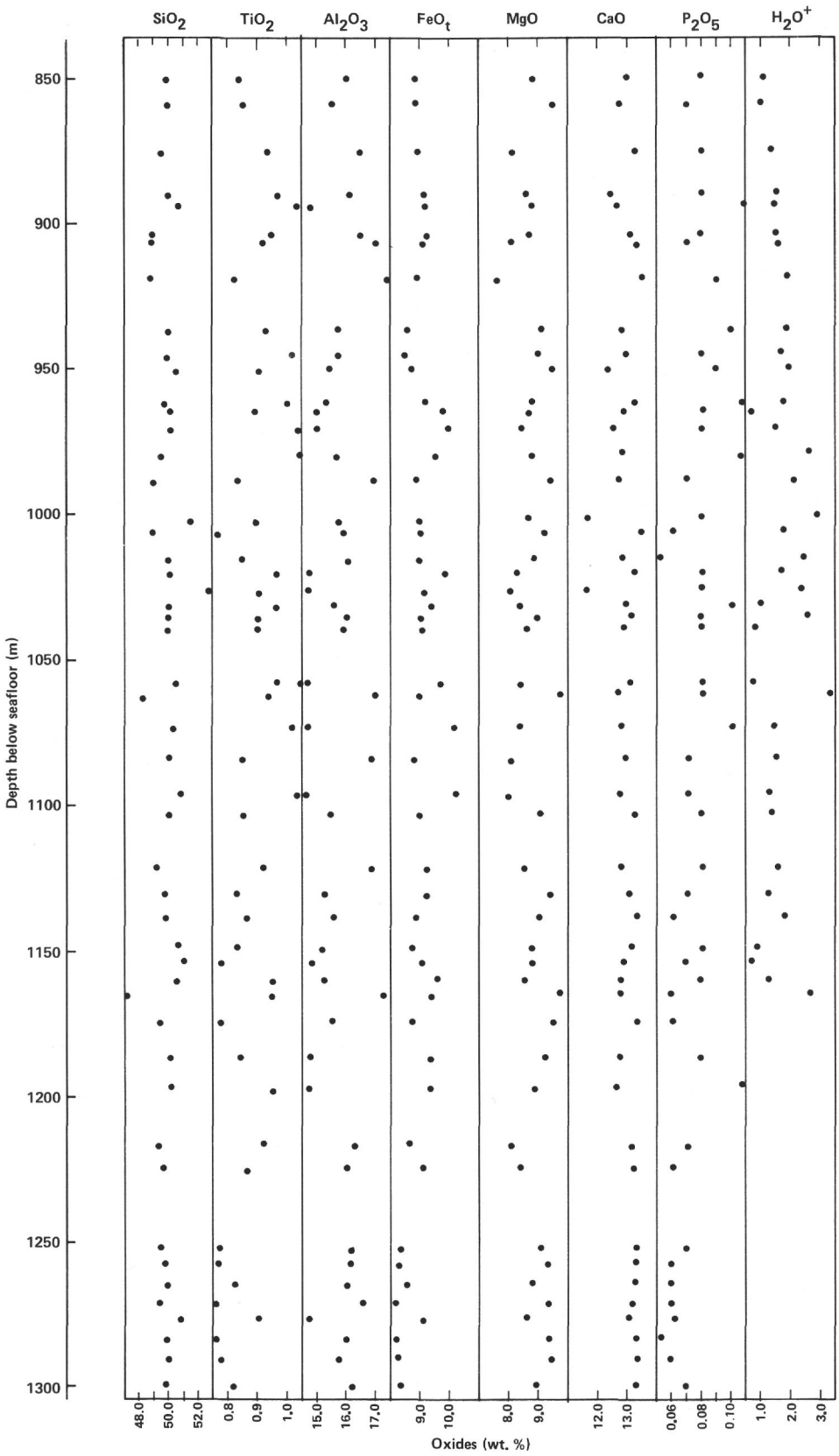

Figure 11. Downhole variation of major element chemistry of Leg 83 basalt samples.

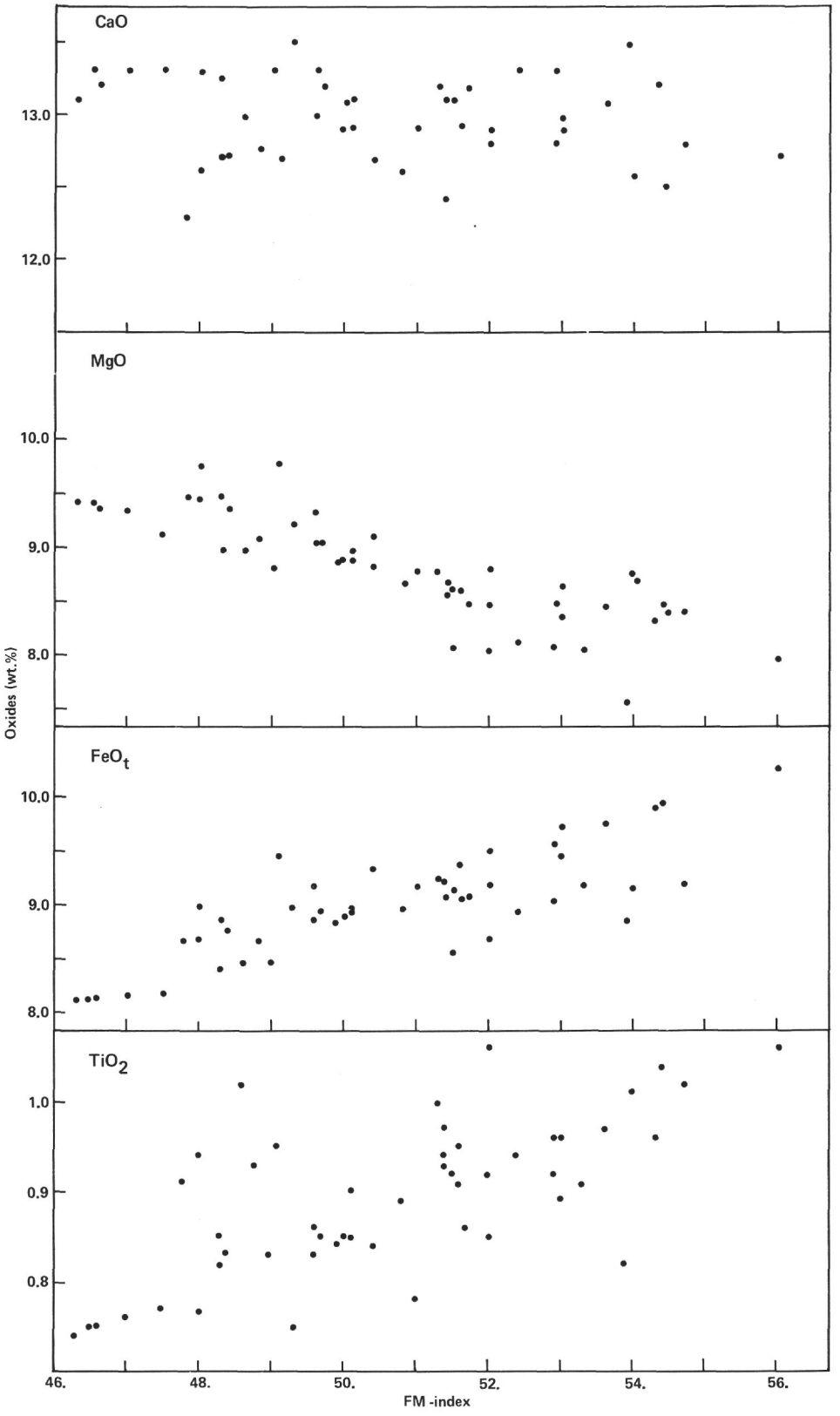

Figure 12. Variation of CaO, MgO, FeO_t, and TiO_2 with FM-index for Leg 83 basalt samples.

so characterized by similar trace element abundances, that is, that they are strongly depleted in incompatible elements.

The conformity in the major element chemistry between Leg 83 rocks and Legs 69 and 70 basalts, the very narrow oxide frequency distribution curves, and the marked compositional maxima suggest that there were no major chemical redistributions caused by alteration, although magnesium and potassium might be slightly affected by hydrothermal processes. This conclusion is strongly supported by the fact that major oxide analyses of fresh basaltic glasses from the upper part of the hole (Natland et al., 1983) for all components show almost identical ranges of variations as those determined on Leg 83 rocks. The respective concentration ranges obtained on the glasses (in wt.%) are:

SiO_2	48.4–51.7	MgO	7.55–9.31
TiO_2	0.83–1.08	CaO	12.4–13.2
Al_2O_3	14.2–17.0	K_2O	0.01–0.08
FeO_t	8.43–10.2	P_2O_5	0.06–0.11.

From this it follows that our dry-weight normalized data most likely represent the primary composition of the rocks and could even represent magma compositions. The latter "working hypothesis" is additionally substantiated by a comparison between our oxide averages and the respective values obtained on zero-age basalts dredged at different localities along the Galapagos spreading center. It can be demonstrated that the Leg 83 averages closely match the major oxide composition of fresh zero-age basalt glasses having the same mg-values (Puchelt and Emmermann, in press).

Based on the high mg-values, which average 0.67, Leg 83 rocks are among the least evolved basalt types recovered so far from the ocean floor. The values found clearly indicate that the respective melts were rather primitive and had experienced only a small degree of crystal fractionation prior to their eruption or intrusion, respectively. The correlations observed betwen the concentrations of CaO, MgO, FeO, TiO_2, and the FM-index suggest that limited shallow-depth fractionation processes were operative. These processes are reflected in the minor chemical downhole variations mentioned above. In general, however, the magmas were erupted or intruded before large-scale fractionation processes could take place. One possible explanation for this might be a relatively short residence time of the magmas within the magma chamber. Another possibility is that a large magma chamber was steadily replenished with hot new magmas.

The trace element composition of the Legs 69 and 70 basalts indicates that the basaltic liquids were derived from a LIL-element-depleted mantle source. This explanation might also hold true for the Leg 83 rocks. For the occurrence of the exceptional Units 5 and 36 basalts, no satisfactory model can be offered at the moment. As a working hypothesis we assume that they might have been generated within pockets of more primitive, less depleted mantle material.

BASEMENT ALTERATION PETROGRAPHY

Introduction

Alteration of the oceanic crust at various temperatures has been shown to have a significant effect on seawater composition. Alteration and associated cementation of cracks and breccias with secondary minerals probably affects seismic velocity, basement permeability, and magnetic properties. The generally accepted model of alteration of the oceanic crust, based on studies of ophiolites, suggests a progressively increasing metamorphic grade with depth. In this model, pillow basalts are altered at low temperature (i.e., weathering at 0 to about 50°C) in the uppermost part, ranging to zeolite facies at greater depths and then to greenschist-facies conditions at the pillow/dike transition. Dikes are altered under greenschist-facies conditions up to amphibolite-facies conditions near the dike/gabbro transition, and some gabbros are metamorphosed in the amphibolite facies. Deep-sea drilling has generally only recovered basalts altered at low temperatures (weathering at 0 to 50°C), whereas basalts altered under greenschist-facies conditions have commonly been dredged from rift valleys and transform faults. Descriptions of oceanic basalts altered under the zeolite and prehnite-pumpellyite-facies conditions are rarely found in the literature. Incomplete recrystallization and nonequilibrium mineral assemblages are the general rule for oceanic basalts. The objectives of Leg 83 were to deepen Hole 504B in order to test existing models of the structure, composition, and alteration of the oceanic crust. The question addressed in this section is the timing of alteration and how the alteration varies with depth, and specifically whether the grade of alteration progressively increases with depth.

Review of Legs 69 and 70

A brief description of the alteration observed in cores recovered from Hole 504B during Legs 69 and 70 (summarized from Cann, Langseth, Honnorez, Von Herzen, White, et al., 1983) is given below to compare with the results obtained during Leg 83.

Secondary minerals present in the uppermost 266 m of basement consist mostly of "iddingsite" (mixture of Fe-hydroxides and clay minerals), K, Fe-rich clay minerals (celadonite–nontronite), and saponite replacing olivine; and phillipsite, calcite, aragonite, and minor sulfides (essentially pyrite) in veins. These minerals are generally accepted as products of various low-temperature (less than about 50°C) alteration processes.

A zone of abundant Na-rich zeolites occurs from 266 to 300 m sub-basement. Minerals found in the veins of this zone include analcite, natrolite–mesolite, thomsonite, talc, calcite, aragonite, minor apophyllite, smectite, and Fe-hydroxides. Saponite, Fe-rich orange clay minerals, and iddingsite replace olivine. All of these minerals can form at relatively low temperatures (less than about 50°C), but are stable to somewhat higher temperatures.

Alteration minerals in the remaining rocks to a depth of 556 m sub-basement consist mainly of Fe-rich sapo-

nite replacing olivine and found in veins; and quartz, talc, mixed-layer smectite–chlorite(?), calcite, sulfides, and rare anhydrite, melanite, aegirine–augite, and gyrolite in veins. The extent of alteration and abundance of sulfides appear to gradually increase with depth. Preliminary oxygen isotopic work suggests that these minerals formed at temperatures in the range of 60–110°C (Cann, Langseth, Honnorez, Von Herzen, White, et al., 1983).

From these observations one could conclude that the alteration of the uppermost part of the oceanic crust at Hole 504B generally fits that of the ophiolite model. Results from Leg 83, however, indicate that alteration does not progressively increase with greater depths, but rather that the grade (i.e., temperature and extent) of alteration can vary with depth on the scale of tens of meters.

Leg 83 Results

The following description of alteration of basalts recovered from Hole 504B during Leg 83 has been divided into depth intervals based on the appearance or disappearance of specific secondary minerals, the abundance of fractures and veins, and the general aspect of alteration in each interval. The descriptions are based on visual observation of the cores and examination of more than 70 thin sections. Thin sections were also used for description of igneous petrography and hence were chosen to be representative of the basalt in general. Thin sections thus avoided the most interesting alteration features, that is, veins and alteration halos around veins were generally not sampled. Mineralogy was determined by X-ray diffraction analysis of selected samples (Table 5). The description of alteration with depth in the hole is followed by a general description of veins, a summary of the secondary mineral paragenetic sequence, and a discussion of the conditions and processes of alteration.

Cores 71–76 (561.5–614 m into basement; 836–888.5 m BSF)

Cores 71 through 76 display alteration similar to that observed in cores recovered from the lower portion of Hole 504B during Leg 70. In general, the rocks exhibit a fairly uniform dark greenish gray color. Lighter greenish gray alteration zones, about 5 mm wide, occasionally occur along veins, however, and fine-grained material close to pillow rims is often altered to a light gray color. Two pieces in Core 76 also exhibit 5 to 10 mm wide bands of reddish coloration.

Olivine is replaced by a pleochroic brown to yellow clay mineral with second-order interference colors, probably saponite, possibly mixed with talc. These minerals were identified as replacing olivine by both microprobe and X-ray diffraction in Leg 70, Hole 504B samples (Cann, Langseth, Honnorez, Von Herzen, White, et al., 1983). Minor amounts of sulfides (probably pyrite) also occur with the clay minerals replacing olivine phenocrysts, which are generally totally altered, although minor relict fragments of olivine are occasionally observed. Minor amounts of secondary sulfides (probably pyrite) are also fairly commonly disseminated in the groundmass. Plagioclase and clinopyroxene are generally unaltered; however plagioclase occasionally exhibits very minor alteration to clay minerals along cracks. Primary void space is also filled with pleochroic yellow brown clay minerals. Basaltic glass at pillow rims is always altered to dark green clay minerals. Titanomagnetite retains its original skeletal outlines, but may be partially maghemitized.

Veins are common, and range in width from less than 1–8 mm, but average about 1–2 mm. Veins are generally filled with dark green clay minerals which are pleochroic yellow to green in thin section. A paler green clay mineral from a vein in Sample 504B-73-2, 40–42 cm exhibits XRD peaks of trioctahedral smectite. Pyrite is also common in veins intergrown with clay minerals. White minerals (calcite and possible zeolite) occasionally occur in veins with clay minerals, generally at the center of clay-rimmed veins. A white fibrous mineral (possibly a zeolite) with a radial structure occurs in Sections 504B-71-1 and 504B-74-1 at the center of clay-rimmed veins. Calcite was also identified by XRD in a vein from Section 504B-73-2.

Cores 77–79 (614-635.5 m into basement; 888.5–910 m BSF)

Cores 77 through 79 generally exhibit a dark greenish gray color, although finer-grained pillow rims often display a lighter gray color, occasionally only in zones a few cm wide along veins.

Greenschist-facies minerals were first identified in thin section in Core 77 and were confirmed by XRD. Olivine is completely replaced by chlorite and minor pyrite, and magnetite is partly replaced by sphene. Plagioclase is occasionally slightly altered to albite and chlorite along cracks in the crystals and in small (several mm) patches, whereas clinopyroxene and fine-grained groundmass are unaltered. Primary void space is filled with clorite, and disseminated pyrite is more common in the groundmass than in Cores 71–76.

Small (less than 1 mm) pyrite crystals are common in abundant 1 to 2 mm wide veins of dark green clay minerals. Chlorite and smectite could not be distinguished in hand specimen; however, chlorite has been identified by XRD in bulk rock in Sections 504B-77-1 and 504B-79-1, and the presence of chlorite replacing olivine in Core 77 rocks suggests that at least some of the clay minerals in veins of Core 77 are also chlorite. White minerals are also occasionally observed in veins and possibly consist of variable mixtures of laumontite, quartz, and calcite, which were identified by XRD in Section 504B-80-1 and below. White minerals generally either cut clay mineral (chlorite?) + sulfide veins or occur at the centers of these veins.

Epidote was first observed as a minor component in veins in highly fractured rocks of Section 504B-78-1.

In Section 504B-78-2, no chlorite was observed in thin section or detected by XRD in the sample studied. Olivine is replaced with a pale brownish clay mineral. Plagioclase exhibits only minor alteration to clay minerals, and clinopyroxene is unaltered. Titanomagnetite is also less altered than in Section 504B-78-1. This mineralogy and alteration is similar to that observed in Cores 71 through 76 and in the lower part of the Leg 70 sec-

Table 5. Minerology determined by XRD for selected samples from Hole 504B, Leg 83.

Core-Section (interval in cm)	Description	XRD identification[a]
72-3, 41-43	Bulk rock	Smectite
73-1, 43-46	Bulk rock	No clay peaks visible
73-2, 40-42	White mineral in vein	Calcite
73-2, 40-42	Pale green clay mineral in vein	Trioctahedral smectite
75-1, 119-121	Bulk rock	Smectite
77-1, 71-74	Bulk rock	Chlorite
78-1, 107-112	Yellowish green mineral in vein	Epidote
78-2, 52-54	Bulk rock	Smectite
79-1, 98-100	Bulk rock	Chlorite
80-1,	Dark green clay mineral in vein	Chlorite
80-1,	Black octahedral mineral in vein	Sphalerite
80-1,	White platy mineral in vein	Talc
80-1,	White minerals in vein	Quartz + laumontite + talc?
80-3, 132-134	Bulk rock	Chlorite + minor smectite or mixture smectite/chlorite
85-2, 113-117	Bulk rock	Chlorite
86-1,	Dark green clay mineral in vein	Chlorite
87-1, 50-52	Yellowish green mineral in vein	Epidote
87-2, 30-32	Vein	Epidote + quartz + laumonite + talc
90-1, 40-42	White fibrous mineral in vein	Laumonite + quartz
90-1, 60-62	White blocky mineral	Calcite (+ quartz?)
90-4, 69-71	Bulk rock	Actinolite + chlorite + quartz + sphene + plagioclase + clinopyroxene
91-2, 45-46	Pinkish mineral in vein	Quartz?
92-2, 118-121	Bulk rock	Chlorite
94-1, 38-41	Bulk rock	Smectite + chlorite
94-3, 100-102	Bulk rock	Chlorite + talc (or laumonite?) + possible smectite
97-1, 88-90	White radiated mineral in vein	Laumonite
97-2, 26-29	Bulk rock	Smectite + chlorite
100-1, 139-144	Bulk rock	Chlorite + possible minor smectite
101-1, 50-52	White elongated mineral in vein	Laumonite + mica
102-1, 25-27	White radiated mineral in vein	Scolecite
104-1, 105-107	White mineral in vein	Unidentified
104-2, 85-87	Bulk rock	Chlorite + minor smectite or mixture smectite/chlorite
105-1, 61-63	Bulk rock	Chlorite + smectite + possible talc
106-1, 35-37	Bulk rock	Chlorite + actinolite
107-1, 116-119	Bulk rock	Chlorite + minor smectite
108-1, 57-60	Bulk rock	Chlorite + smectite
110-1, 34-39	Bulk rock	Chlorite
111-1, 28-30	White fibroradiated mineral in vein	Laumontite?
111-1, 86-89	Bulk rock	Chlorite + smectite
113-1, 68-70	Bulk rock	Chlorite + smectite
114-1, 23-25	White soft radiated mineral in vein	Laumontite?
118-1, 33-35	Bulk rock	Chlorite + possible smectite
122-1, 2-4	White mineral in vein	Anhydrite
123-1, 39-42	Bulk rock	Chlorite + smectite + talc + actinolite
126-1, 33-35	Minerals replacing olivine phenocrysts	Smectite + talc
126-1, 30-24	Bulk rock	Smectite + talc + chlorite
129-2, 25-29	Minerals replacing olivine phenocrysts	Smectite + mica
130-1, 120-122	Blue green mineral in vein	Chlorite + smectite
133-1, 100-102	White mineral in vein	Laumontite
141-1, 65-66	Whitish transport mineral in vein	Anhydrite

[a] Smectite identification based on expansion of 14 Å 001 peak after treatment with ethylene glycol.

tion of Hole 504B. Veins of clay minerals (unidentified, probably smectite or chlorite) and pyrite are common in Section 504B-78-2, however, and veins containing white minerals (possibly quartz, laumontite, and calcite) and epidote are also present.

Alteration in Section 504B-79-1 again consists of greenschist-facies minerals in both veins and rocks, similar to that described for Section 504B-77-1 and 504B-78-1.

Cores 80 and 81 (635.5–654 m into basement; 910–928.5 m BSF)

Cores 80 and 81 recovered a highly fractured pillow sequence with abundant hyaloclastic breccias and are characterized by the presence of abundant veins of white minerals and large crystals of sulfides, up to 1 cm in size. This zone is referred to as a "stockwork," meaning a network of mineralized veins. No economic value is implied.

The rocks generally are greenish in color. The finer-grained rocks exhibit a paler bluish green color, either over an area up to a few cm from veins or pervasively. Fine-grained rocks also frequently exhibit darker green alteration halos, about 5 mm wide along chlorite veins, superimposed on the paler green alteration color.

Alteration of the basalts is generally similar to that described above for Core 77 and Section 504B-78-1, but laumontite, in addition to albite and chlorite, partially replaces plagioclase. Glass in breccias is totally replaced by chlorite, and chlorite and intergrown pyrite generally cement breccias and fill fractures in the rocks. Large veins (up to several cm wide) of chlorite, laumontite, quartz, various sulfides, and minor calcite are also common, especially in the breccias, and appear to postdate the chlorite and pyrite veins. Laumontite, quartz, and calcite are often intergrown and generally cannot be distinguished in hand specimen; hence these minerals were simply described as "white minerals." Laumontite can occasionally be distinguished in hand specimen, however, and occurs as aggregates of radiating prismatic crystals, up to several mm in length. Abundant and large crystals of pyrite, up to 1 cm in size, occur both in chlorite and chlorite + white mineral veins, and are especially common in the breccias. Minor sphalerite occurs in small (1 mm) veinlets in the rocks, and occasionally may be either intergrown with or occur as an overgrowth on pyrite. Pyrite is also abundantly disseminated in the rocks and is particularly noticeable replacing olivine phenocrysts in association with chlorite.

The magnetic susceptibility decreases from Cores 77 through 80, where it reaches a minimum value, which generally persists deeper into the hole. This interval also corresponds to that where titanomagnetite becomes extensively replaced with sphene.

Cores 82–86 (654–692.5 m into basement; 928.5–967 m BSF)

The alteration described for Cores 80 and 81 above persists with increasing depth, but the amount and size of sulfides and white mineral veins gradually decrease below Core 81.

Fine-grained rocks in Cores 82–86 exhibit coloration similar to those in Cores 80 and 81. Coarser-grained rocks (massive cooling units) generally display a dark greenish gray color, with occasional 5–10 mm wide paler greenish gray alteration zones along chlorite veins.

Minor amounts of an unidentified, massive, very fine grained red mineral occur in narrow veinlets (less than 1 mm) in Cores 83 and 84. Epidote, which was not observed in Cores 80 and 81, is present in veins in Cores 82 through 86.

Cores 87–93 (692.5–756 m into basement; 967–1030.5 m BSF)

Below Core 86, pyrite becomes less abundant, but is still common in veins and disseminated in the rock. Minor amounts of chalcopyrite and sphalerite are also present in veins. Epidote generally increases in abundance with depth, particularly in association with quartz and laumontite (+ minor calcite?) in breccias, and becomes especially abundant in Core 91. Epidote occurs as acicular or blocky crystals, up to 5 mm long, often preceding white minerals in veins. Below Core 91 epidote is less abundant but is still fairly common. A massive, fine-grained tan to pinkish mineral occurs disseminated in hyaloclastic breccias in Core 91. XRD reveals peaks of quartz and some unidentified peaks. This mineral may be laumontite, which can have a pinkish color, but this remains speculative.

Actinolite was first observed in minor amounts in Core 87 as narrow reaction rims on clinopyroxene in a massive cooling unit. Actinolite continues to be present with depth and is generally only observed as overgrowths on or replacing clinopyroxene in the massive cooling units. Actinolite is often abundant adjacent to veins, where clinopyroxene may be almost totally replaced by actinolite within about 1 mm of the vein (e.g., 504B-90-4, 67 cm). The extent of replacement of clinopyroxene then decreases away from the vein.

At 504B-87-1, 104 cm, wall rock is totally replaced by chlorite and minor sphene for about 1 mm around a chlorite + laumontite + epidote vein. The extent of chloritization of the wall rock then decreases with increasing distance from the vein.

The wall rock within about 1 mm of a chlorite + laumontite + epidote vein at 504B-89-2, 58 cm is highly altered. Olivine is totally replaced with chlorite, and clinopyroxene and plagioclase are partially replaced by chlorite and minor amounts of epidote. The extent of wall rock alteration then decreases away from the vein. This is the only observed occurrence of epidote replacing a primary igneous phase.

Cores 94–97 (756–787.5 m into basement; 1030.5–1062 m BSF)

In general the rocks recovered in Cores 94 through 97 have a dark greenish gray color, although Core 94 is generally more dark gray in color. Lighter-colored alteration zones, about 1 cm wide, also occasionally occur around veins in Cores 94 through 97. In Section 504B-97-1 light greenish alteration zones, up to about 3 cm wide, occur

around laumontite-filled vugs, several cm in size, in two pieces of massive basalt.

Several pieces consist of breccias cemented mostly by chlorite, but also containing epidote and minor sulfides. At 504B-94-3, 90 cm, a chlorite-cemented breccia has apparently been "rebrecciated" and cemented with later epidote.

Veins are fairly common and range from 0.5–8 mm in width, but average about 1–2 mm. Chlorite + sulfide veins are the most common, with pyrite the most common sulfide. Minor sphalerite occurs in Section 504B-94-1 and possibly in 504B-97-1, and chalcopyrite in 504B-94-3. White mineral (laumontite + quartz) + minor epidote veins cross-cut chlorite + sulfide veins. White minerals also occasionally occur at the centers of chlorite + white mineral veins in 504B-97-3.

Alteration in Sections 504B-94-1, 504B-94-2, Core 95, and Core 96 is in general quite similar to that described above for Cores 87 through 94. At 504B-95-1, 34 cm, wall rock within about 1 mm of an epidote + chlorite vein in almost completely altered to actinolite + chlorite + sphene. Farther from the vein the host rock is progressively less altered.

No actinolite was observed in thin sections from Sections 504B-94-1 and 504B-97-1, however. Olivine in these sections is replaced with a pleochroic olive brown to olive green to yellowish clay mineral with second-order interference colors. Primary void space is filled with chlorite, and plagioclase is partly replaced with a clay mineral, possibly chlorite. Magnetite is also only slightly altered, possibly to sphene. Bulk-rock XRD indicates that both chlorite and smectite are present in these two samples. The brownish clay replacing olivine is probably smectite, but it may be randomly interlayered or mixed with chlorite. Sections 504B-92-1 and 504B-97-1 also contain many fewer veins than 504B-94-2, 504B-94-3, Core 95, and Core 96. Magnetic susceptibility of Core 94 is slightly higher than in Cores 95, 96, and those above. No significant differences in grain size exist among these cores.

Cores 98–104 (787.5–851 m into basement; 1062–1125.5 m BSF)

Cores 98 through 104 consist of massive cooling units, in general uniformly dark greenish gray. A light greenish gray alteration zone, 5 cm wide, occurs around a 3-mm vein of a dark green mineral (probably chlorite) in 504B-104-2, 48–55 cm, however. In Section 504B-99-2 one piece (42–50 cm) of fine-grained basalt exhibits a pale greenish gray color and displays dark green alteration zones, 5 mm wide, around chlorite veins, similar to those observed in fine-grained rocks above Core 98.

Alteration of primary igneous phases is similar to that described above for Cores 87 through 93. Bulk-rock XRD, however, indicates that smectite is possibly present, along with chlorite, in 504B-100-1, 139 cm, although none was observed in the thin section of the same sample. The 14 Å peak of chlorite–smectite is very small, but apparently broadens with glycolation. Titanomagnetite is extensively altered to sphene in Cores 98 and 99, but is less extensively altered in Cores 100 through 104.

Veins are fairly common, but decrease in abundance with depth. Very few veins were observed in Sections 504B-101-2, 504B-102-1 and Core 104. Veins consist mostly of chlorite and pyrite. Chlorite also cements several pieces of fine-grained breccia in Core 98 through Section 504B-101-1. Quartz, laumontite, and epidote occasionally occur in veins and often fill the centers of chlorite-rimmed veins. No epidote was observed in Cores 102 through 104, however. The presence of a 10.1 Å peak in the X-ray diffractogram of a chlorite + laumontite + epidote vein in 504B-101-1, 40–55 cm was interpreted as indicating the presence of a mica. Mica was not identified in thin section from this core; however, the thin section did not include the vein analyzed by XRD. Radiating acicular crystals, up to a few cm in length, of a colorless to white mineral coating a fracture surface at 504B-102-1, 22–30 cm were identified by XRD as scolecite.

Needlelike overgrowths of actinolite on clinopyroxene in wall rock were observed in veins at 504B-99-2, 64 cm and 504B-103-1, 9 cm, and appear to be intergrown with quartz and laumontite in the center of the vein in Section 504B-103-1. At 504B-99-2, 64 cm, actinolite occurs as overgrowths on clinopyroxene projecting into a 1-mm vein and as needles apparently intergrown with chlorite in the center of the same vein. This vein was later reopened and filled with chlorite and quartz. Within a few mm of the vein, magnetite is almost completely replaced by sphene, and clinopyroxene and plagioclase are extensively replaced with chlorite. Farther from the vein, the extent of alteration of magnetite, plagioclase, and clinopyroxene decreases.

Cores 105–114 (851–906 m into basement; 1125.5–1180.5 m BSF)

Cores 105 through 114 consist of gray to dark gray massive basalts, with few thin veins generally less than 1 mm in thickness. The general appearance of the rocks from this portion of the hole is that of slightly altered basalts.

Alteration halos are occasionally observed around veins in Cores 105, 106, 107, and 111. In Cores 105, 107 and 111, the alteration halos (about 5 mm wide) are located around dark green (probably chlorite) veins and are light gray to light greenish gray, whereas the remainder of the basalt is dark gray. In Core 105, the zonation is either similar to that described above, or inverse, that is, the dark greenish gray area is directly adjacent to the vein. Piece 2 (10–20 cm) exhibits both types of zonation. At 504B-106-1, 80–90 cm, a 5-mm-wide vein consists of a dark green mineral (probably chlorite) lining the walls and unidentified white to grayish minerals filling the center. A 5–10-mm-wide, dark green, alteration zone occurs around this vein, whereas the remainder of the rock is dark gray.

Alteration of primary igneous phases in Cores 107 through 114 is slightly less pronounced than in Cores 98 through 106. Olivine is always completely replaced by chlorite or by an olive brown smectite, which has been identified together with chlorite by bulk-rock XRD at 504B-105-1, 61–63 cm; 504B-107-1, 116–119 cm; 504B-

108-1, 57–60 cm; 504B-111-1, 86–89 cm; and 504B-113-1, 68–70 cm. Possible talc has been found by bulk-rock XRD in Section 504B-105-1, but its mode of occurrence is not known. Moreover, no smectite was observed in thin section in 504B-105-1, whereas XRD indicates that expandable clay minerals occur in this sample. Some unidentified opaque grains are associated with smectite that has replaced olivine. Plagioclase is only partly (10%) replaced by albite in Cores 105, 106, 110, and 111, sometimes along with minor chlorite and laumontite. Clinopyroxene is partially replaced by actinolite along its rims, and is more extensively replaced near chlorite-filled veins and vugs. Titanomagnetite is generally only partly altered to sphene, as in Cores 100 through 104, but titanomagnetite is extensively altered within a few mm of a chlorite + actinolite vein at 504B-113-1, 73 cm. Rare, disseminated sulfides are observed throughout Cores 105 through 114.

Veins are scarce in Cores 105 through 114, as they were in Sections 504B-101-2, 504B-102-1 and Core 104 above. Veins are always less than 1 mm wide, except in Section 504B-106-1, where a 1–5-mm-wide vein filled with a white mineral (probably laumontite) was observed. Veins consist mostly of chlorite and, to a lesser extent, white minerals. Quartz occurs in veins in Cores 108 and 109, and laumontite is often associated with actinolite needles in veins in Cores 98 through 104. Cores 105 through 114 have been distinguished from Cores 98 through 104 by the occurrence of prehnite, which is associated with spherules of a brown unidentified mineral in veins and vugs (504B-105-1, 46–49 cm and 504B-111-1, 104–107 cm. These spherules are 0.5 mm in diameter and are composed of radial fibers which are white in hand specimen and brown in thin section. They exhibit first-order yellow to red interference colors. Prehnite occurs as prisms or fibers up to 0.20 mm long. In Sample 504B-105-1, 46-49 cm, a large vug is rimmed with chlorite and needles of actinolite. In the inner part of the vug, actinolite is apparently intergrown with probable laumontite, and prehnite fibers surround previously described brown spherules. This sample contains other vugs of intergrown chlorite and actinolite, with several brown spherules at the center, but without prehnite. In Sample 504B-111-1, 104–107 cm, a vein is rimmed with chlorite, followed by prehnite and brown spherules at the center. In some cases, a brown spherule surrounds a tabular crystal (0.1 mm long) of prehnite. The wall rock around these veins and vugs is highly altered to actinolite and chlorite.

A chlorite vein, 0.5 mm wide, is reopened and filled with epidote in Section 504B-105-1. The wide vein with the dark green alteration halo in 504B-106-1, 80-90 cm, described above, is offset by an epidote-filled crack, and similar material (504B-106-1, 91–100 cm) is brecciated and cut by later epidote veins. These are the only occurrence of epidote in Cores 105 though 114, except an occurrence of possible epidote associated with probable chlorite in the cement of a breccia (Section 504B-107-1).

A vein filled with a light green mineral (possibly clay) and apparently different from chlorite veins was observed in hand specimen in Core 111.

In a 3-mm-wide area around a vein of chlorite and intergrown actinolite in Sample 504B-113-1, 73–76 cm, olivine is replaced by chlorite associated with a fine-grained, unidentified, tan mineral (yellow first-order interference color). No pyrite has been observed in this type of replacement. Outside this alteration halo, olivine is replaced by olive brown smectite (identified by XRD) and pyrite. Both these types of replacements can be distinguished in thin section without a microscope.

Cores 115–130 (906–1013 m into basement; 1180.5–1287.5 m BSF)

Basalts from Cores 115 through 130 exhibit the same uniform gray to dark gray color and the same slightly altered appearance as Cores 105–114. Veins are generally thin (1 mm, max. 13 mm) and are scarce except in Sections 504B-112-1 and 504B-129-2, where they are common.

Pale green to pale gray alteration halos (1 to 5 mm wide) occur in the lower part of this section, that is, in Sections 504B-124-1, -125-1, -128-2, -129-2, and -130-1, around veins and/or vugs. These veins and vugs are filled essentially with dark green mineral (chlorite and/or smectite), whereas accessory pyrite, anhydrite, and white minerals also occur in veins. In Section 504B-128-2, olivine phenocryst pseudomorphs are light green in the alteration halo, and dark green in the dark gray remainder of the rock. In Section 504B-125-1, alteration halos (3 mm in thickness) also occur around olivine phenocrysts.

Alteration of igneous phases in Cores 115 through 130 significantly differs from that of Cores 105 through 114. In Cores 115, 116, and 121, olivine is replaced by chlorite, but a different type of olivine replacement generally occurs from Core 118 to 130. The internal parts of the olivine phenocrysts are replaced by an olive brown clay mineral (probably saponite), whereas the external rims are replaced by talc and small opaque grains (probably magnetite). In Sample 504B-129-1, 35–39 cm, secondary magnetite grains are arranged along concentric lines which are parallel to the boundary between smectite and talc. Both talc and the brown clay mineral can be distinguished in hand specimen. In the rocks where olivine phenocrysts are replaced by the brown clay mineral, talc, and opaques, olivine microcrysts are in general completely replaced by talc and magnetite, without the brown clay mineral. The material replacing olivine phenocrysts was analyzed by XRD in two hand-picked samples of olivine phenocryst pseudomorphs: an expandable clay mineral and talc were identified in Sample 504B-126-1, 30–40 cm, thus confirming the observation in thin section. An expandable clay mineral and mica were identified in Sample 504B-129-2, 25–29 cm, but mica could not be found in the nearest thin section (504B-129-2, 118–121 cm). Bulk-rock XRD analyses indicate the occurrence of chlorite and possible smectite in Sample 504B-118-1, 29–32 cm; and of chlorite, an expandable clay mineral, and talc in 504B-123-1, 39–42 cm and 504B-126-1, 30–34 cm.

Plagioclase is slightly altered to albite, chlorite, and probable laumontite in Cores 115 and 116, and to albite

and clay minerals in Cores 121 and 122. Below Core 122, plagioclase is either very slightly altered to clay minerals or completely fresh.

Clinopyroxene is generally fresh. It is only very slightly altered to actinolite when in contact with chlorite veins. In some rare cases (504B-129-2, 118–121 cm), clinopyroxene bordering a vug filled with chlorite is replaced by actinolite and chlorite.

Primary titanomagnetite is partly (10–40%) replaced by sphene in all of the thin sections of Cores 115 through 130.

Veins are not very common. Most of them are filled with a dark green mineral (probably chlorite) and pyrite. Chlorite associated with an expandable clay mineral was identified by XRD in a vein of Sample 504B-130-2, 120–122 cm. The association of prehnite with brown fibroradial spherules of an unidentified mineral occurring in Cores 105 through 114 is still present in Sample 504B-116-1, 126–129 cm. Brown spherules also occur in 504B-122-1, 116–118 cm. Veins in general become rare in the massive basalt recovered from Sections 504B-129-2 to 504B-130-3.

Very irregularly shaped vugs in Sample 504B-129-2, 118–121 cm are filled with chlorite at the rim and probable quartz at the center. This would be the only occurrence of quartz observed in Cores 115 through 130.

Cores 131–141 (1013–1075.5 m into basement; 1287.5–1350 m BSF)

This interval is characterized by the frequent presence of "patchy" alteration zones. The rocks are generally dark gray in color, but frequently exhibit irregularly shaped, dark greenish patches, up to a few cm in diameter. These patches are surrounded by light grayish green halos, up to 1 cm wide, and make up most of the hand specimen in a few cases (e.g., 504B-132-1, 110–120 cm). Light greenish gray alteration halos are also occasionally present around veins in dark gray rocks.

No thin sections were made of cores below Core 134 because lab operations shut down at the end of the leg. Thin-section descriptions are thus based on five thin sections from Cores 131 through 134.

In the dark gray rocks which make up most of this interval olivine is completely replaced by chlorite and minor pyrite; titanomagnetite is partly replaced by sphene; plagioclase is partly replaced by chlorite and albite; and clinopyroxene is occasionally partly replaced by actinolite. Minor sulfides are also disseminated in the rock. At 504B-132-1, 96 cm olivine is replaced by talc and magnetite at the rim, and by chlorite at the center.

In the patchy greenish alteration zones, clinopyroxene is extensively replaced by actinolite and probably chlorite. Interstitial areas (glasses or vugs?) are filled with chlorite; plagioclase is extensively replaced by chlorite and albite; titanomagnetite is extensively replaced by sphene; and olivine is totally replaced by chlorite. In the light greenish gray halos around these patches alteration is similar to that in the centers, but is less extensive.

Veins in this interval are generally scarce, but are more abundant in Cores 139 through 141. Veins are generally narrow (1 mm) and are filled with a dark green clay mineral (probably chlorite, which was observed in a vein in thin section from 504B-131-2, 57 cm). White minerals occur at the centers of chlorite veins, or in veins crosscutting chlorite veins. Anhydrite was identified by XRD in a large (1 cm) vein in Sample 504B-141-1, 65–66 cm and laumontite was identified by XRD in a vein from Sample 504B-133-1, 100–102 cm. A white mineral also occurs in vugs at the centers of patchy alteration zones at 504B-136-1, 25 cm.

Hand specimens from 504B-141-1, 50–70 cm are bluish green; they appear extensively altered and thus different from the rest of Cores 131 through 141. No thin sections were made of these samples, however.

In general, Cores 131 through 141 are more extensively altered than Cores 118 through 130. Moreover, Cores 131 through 141 do not exhibit the effects of a stage of low-temperature alteration (i.e., no smectite was observed, although no thin sections below Core 134 were studied), as do Cores 118 through 130. This is consistent with the previous conclusion that the rocks in the hole do not exhibit a progressive increase in alteration "grade" (temperature and extent of alteration) with depth, but it also indicates that the alteration "grade" varies locally on a scale of 10 to 100 m. Thus, alteration "grade" may be much more closely related to local permeability than to a simple geothermal gradient.

Secondary Mineral Paragenetic Sequence

Many types of veins can be recognized in the rocks from Cores 71 through 130: (1) trioctahedral smectite only; (2) chlorite only; (3) quartz only; (4) intergrown chlorite and quartz; (5) chlorite + laumontite ± epidote ± quartz, where chlorite lines the walls of the veins and is intergrown with laumontite farther from the vein walls (epidote is often intergrown with laumontite at the center of the vein and quartz also is occasionally intergrown with the various minerals or as isolated patches); (6) quartz + laumontite + epidote, where quartz and laumontite are intergrown, and epidote is intergrown with both minerals at the center of the vein; (7) epidote + chlorite, where epidote occurs at the edges of the vein and is intergrown with chlorite at the center; (8) epidote + "white minerals" (laumontite, quartz, scolecite, and calcite), where epidote lines the walls of the vein and white minerals fill the center; (9) calcite only; (10) chlorite + scolecite, where chlorite lines the walls and scolecite fills the center of the vein; (11) chlorite + actinolite + laumontite ± prehnite, where chlorite and actinolite are apparently intergrown and either fill the entire vein or occur at the edges of the vein (in the latter case laumontite is apparently intergrown with actinolite needles at the center of the vein and in several cases prehnite + brown spherules also occur there with laumontite; (12) anhydrite, where anhydrite fills reopened chlorite veins; and (13) chlorite + smectite mixtures. Sulfides (mostly pyrite, but also minor amounts of sphalerite and chalcopyrite) were observed in at least one example of most of the various types of veins.

Smectite (brownish, expandable clay mineral) is the only vein mineral observed in Cores 71 through 76. In Cores 79 through about 123, chlorite is the most com-

mon vein filling, and vein types 2 through 5 make up the majority of the veins in this section. Chlorite + smectite mixtures probably make up most of the veins in Cores 125 through 130. Wall rock around chlorite and actinolite + chlorite (type 11) veins is often extensively altered for up to a few mm from the vein (see earlier description of alteration with depth).

Actinolite, chlorite, and sulfides are generally the first minerals deposited in veins, as is indicated by zoned veins and cross-cutting vein relationships. Chlorite and actinolite appear to be intergrown in some cases; hence some chlorite may have formed simultaneously with actinolite. However, at least two generations of chlorite exist, as is evidenced by chlorite and chlorite + actinolite veins which are cut by chlorite + quartz or chlorite + laumontite + epidote veins.

Quartz generally occurs later than chlorite, as is indicated by quartz veins commonly cutting chlorite veins, but quartz also occurs intergrown with chlorite. Several generations of quartz deposition are also suggested by multiple quartz fillings of veins (Section 504B-90-4).

Laumontite, epidote, scolecite, and anhydrite generally formed later than chlorite, as indicated by vein-filling sequences from wall to center. Laumontite is often apparently intergrown with chlorite near the walls of veins, however, suggesting that in these cases the two minerals may have formed at the same time. In some cases actinolite needles are apparently intergrown with laumontite. If the temperature of first appearance of actinolite in Icelandic geothermal areas (280°C; Kristmansdottir, 1975) is taken as a minimum temperature of formation for actinolite, then laumonite and actinolite could not have formed in equilibrium, since laumontite should dehydrate to form wairakite at about 235°C (0.5 kbar P_{H_2O}; Liou, 1971). Actinolite most likely does not postdate laumontite formation, because the laumontite would have dehydrated at the temperatures required to form actinolite. Thus laumontite must have formed later than actinolite.

In one instance (504B-95-1, 34 cm) chlorite occurs intergrown with epidote at the center of an epidote vein, indicating a sequence of formation opposite to that described above. In the same vein, an apparent discontinuity between fine-grained epidote lining the walls of the vein and coarser-grained epidote intergrown with chlorite at the center suggests different stages of epidote formation. Epidote also occurs at a later cement in "rebrecciated" chlorite-cemented breccias (504B-94-3, 10–30 cm; 504B-106-1, 91–100 cm), and in a crack that displaces a chlorite + unidentified white mineral vein (504B-106-1, 80–90 cm).

Calcite occurs as rare, narrow, cross-cutting veinlets filling voids in quartz veins, suggesting a late stage of formation.

Prehnite and the brown spherules probably formed simultaneously. Prehnite occurs both as a nucleus of spherules and as overgrowths on the spherules. Both these minerals postdate actinolite and chlorite formation and may have formed concurrently with associated laumontite, although this relationship is not clear. (Alt et al., this volume, demonstrate that the brown spherules are prehnite also.)

The time at which smectite and smectite + chlorite veins formed cannot be directly related to the other minerals because these veins are unzoned and no cross-cutting relationships with other veins were observed.

Discussion

It is inferred that the alteration of Cores 71 through 76 (561.5 to 614 m into basement) occurred under conditions similar to those in the lower part of Hole 504B recovered during Leg 70 (300 to 556 m into basement; Cann, Langseth, Honnorez, Von Herzen, White, et al., 1983). Reactions occurred at relatively low temperatures (less than 150°C) and under suboxic to anoxic conditions, either with seawater at low water/rock ratios, or at slightly higher water/rock ratios with seawater-derived fluids whose composition had been altered by previous reactions with basalts.

Cores 77 through 79 (614 to 635.5 m into basement) represent a transition zone between overlying basalts altered at relatively low temperature (Cores 71–76) and the stockwork below (Cores 80 and 81, 635.5 to 654 m into basement). The occurrence of chlorite replacing olivine, sphene replacing titanomagnetite, and epidote forming veins reflects a higher temperature than that responsible for the alteration of basalts in Cores 71 through 76. This higher temperature could be related to hydrothermal fluid circulation in the subjacent sulfide-rich zone. One must keep in mind that an expandable clay mineral is still present in Cores 77 through 79, probably as an olivine replacement in some rocks, and that only a small proportion of magmatic minerals is replaced. It is not very clear how this transition occurs, and further studies should enable the determination of the parameters involved (permeability, temperature, etc.).

Two processes can explain the precipitation of the abundant sulfides (pyrite + minor sphalerite) in veins of the stockwork (Cores 80 and 81, 635.5 to 654 m into basement): (1) the mixing of a metal-, S-, and SiO_2-rich hydrothermal fluid with seawater, or (2) a drop in the temperature (and/or pressure) of this solution because of its rise and loss of heat to wall rock. The higher permeability of this zone prior to mineralization would localize the hydrothermal fluid circulation and facilitate the entry of seawater and the mixing of solutions. Experimental studies predict the presence of abundant quartz with sulfides. Sulfides are associated with "white minerals" (laumontite, quartz, and calcite) in veins, but the relationships among these minerals are not known. The veins of the stockwork exhibit two stages of crystallization: (1) chlorite + sulfides, (2) "white minerals" including laumontite, quartz, and calcite (+ chlorite + sulfides). Shore-based studies demonstrated the presence of three stages in the veins of the stockwork zone (Honnorez et al., this volume).

Cores 82 through 86 (654 m to 692.5 m into basement) exhibit similar alteration to the stockwork with numerous veins of quartz, laumontite, and calcite, but with lesser amounts of sulfide.

Cores 87 through 104 (692.5 to 851 m into basement) are characterized by the occurrence of actinolite partly replacing clinopyroxene, whereas clinopyroxene is always apparently completely fresh in the basalts recovered above Core 86. The presence of actinolite suggests that these rocks reached higher temperatures than overlying rocks, that is, greater than 300°C. The extent of the alteration is often greater immediately adjacent to the veins, where wall rock is occasionally totally altered to a mixture of actinolite, chlorite, sphene, and albite. Veins also occasionally exhibit higher-temperature secondary minerals than the host rock. Moreover, relict minerals form a large proportion of the altered basalts. These points indicate that equilibrium was occasionally reached only locally, on a scale of less than one millimeter. In several areas chlorite occurs in veins, whereas smectite is still present in the rock. This was particularly observed in massive units and could be explained by the smaller number of cracks and thus lower permeability.

Alteration from 654 to 920 m into basement probably occurred in two stages: (1) a high-temperature stage ($\geq$290°C) during which chlorite and actinolite crystallized; and (2) a lower-temperature stage ($\leq$250°C), where laumontite, scolecite, and possibly chlorite formed. Epidote could have crystallized during both these stages. Changing solution chemistry probably also was an important effect on these two alteration stages.

In Cores 105 and 106 (851 to 869 m into basement) the disappearance of epidote in veins roughly corresponds to the appearance of prehnite. This may be a significant indication of change of temperature and/or chemical conditions, or of other parameters.

The association of talc and magnetite replacing the outer rims of olivine phenocrysts with brownish clay mineral (saponite?) replacing the cores of the phenocrysts indicate two stages of alteration in Cores 118 through 130 (919.5 to 1013 m into basement). It is suggested that talc and magnetite formed first, because the outer rims of olivine phenocrysts are generally altered first. These stages can be characterized by

1. A first stage involving only slight chemical changes and the formation of talc and magnetite. (Formation of talc from olivine could occur either by addition of H_2O and SiO_2, or by addition of H_2O and loss of Mg. Fe released by talc formation could then form secondary magnetite.) The scarcity of cracks and the probably low permeability of these rocks could account for the small extent of reaction and chemical changes involved.

2. A later stage involving greater chemical changes and formation of a brownish clay mineral from remaining olivine by addition of Al, Si, and H_2O. This would have been facilitated by continued reactions in the surrounding rocks, supplying this material.

Experimental seawater–basalt reactions predict that anhydrite should form from Ca-enriched heated seawater at about 150°C. Since this temperature is reached in the hole at the present time, and formation waters are enriched in Ca, anhydrite could be in equilibrium with formation waters in Cores 115–130 (906 to 1013 m into basement). Anhydrite may also form by other means, for example, by mixing of Ca-enriched hydrothermal fluids with seawater. Oxygen isotopic data on anhydrite from Leg 70 samples suggest that anhydrite also forms locally at lower temperatures (100°C). Both stages of olivine replacement could also occur at this temperature.

The fact that chlorite coexists with an expandable clay mineral in the veins of Core 130 (XRD data) can be explained in three ways: (1) different stages of alteration temperature, or (2) a temperature equal to the temperature of transition between smectite and chlorite, or (3) kinetic effects.

The presence of secondary magnetite in Cores 118 through 130 could contribute to the relatively high magnetic susceptibilities measured in these cores, although igneous titanomagnetite is only slightly altered and is more likely the major magnetic mineral.

Calcite is rare in the basalts recovered during Leg 83 and was not observed below Core 94 (765 m into basement). This is in accordance with the low CO_2 contents measured in the basalts (see Basement Geochemistry section) and suggests low pCO_2 and low pH fluids.

Conclusions

In contrast to regionally metamorphosed rocks, the rocks recovered from Hole 504B generally exhibit only a very small degree of recrystallization. Moreover, these rocks apparently do not show a systematic, progressive increase in metamorphic grade with depth as predicted by ophiolite models.

Changing temperature and solution composition with time has probably produced sequences of minerals of differing "metamorphic grade" within single veins. From 0 to 614 m into basement secondary mineralogy suggests temperatures of alteration less than about 150°C. From 692.5 to 919.5 m into basement alteration occurred in at least two stages: (1) a higher-temperature stage (at least 290°C); and (2) a lower-temperature stage (less than 250°C).

From 919.5 to 1013 m into basement alteration also occurred in at least two stages, although the second stage may have occurred at lower temperature than that in the interval above (1) a higher-temperature stage (at least 290°C); and (2) a lower-temperature stage (less than about 150°C?).

The rocks below Core 77 do not exhibit a regular increase in alteration "grade" with depth. Rather, the "grade" of alteration varies on a scale of tens of meters and is probably controlled by variations in permeability.

We have established tentative secondary-mineral paragenetic sequences; however, the timing of alteration relative to the formation of the crust remains uncertain. Alteration could have occurred, first, at the spreading center, and later on the ridge flank in an upwelling limb of a hydrothermal convection cell.

BOREHOLE WATER CHEMISTRY

Hole 504B has provided the best opportunity to date for sampling formation water from oceanic basement, because both active and passive sampling techniques have been available for use in this hole. In addition, its setting in an area of reheated crust has allowed us to study the chemical interaction of basalt with ever warmer sea-

water, up to moderately elevated temperatures. Integrating the data on solution composition versus temperature with that on rock alteration should allow us to understand a great deal about the thermal and chemical history of this piece of oceanic crust, as well as to evaluate the geochemical effects of basalt–seawater interaction along mid-ocean ridge flanks.

In the passive sampling technique, water occupying the borehole is recovered some time after the circulation of drilling fluid (surface seawater) through the hole has stopped. For Hole 504B, this elapsed time varied from one day for samples taken after drilling on Legs 69, 70, and 83, to 43 days prior to renewed drilling on Leg 70, to 2 yr. prior to Leg 83. In the active technique, the borehole is sealed off using the Lynes retrievable formation tester packer and a 51 L sample is drawn under negative pressure from the bottom of the borehole and the interstices of the rocks surrounding the hole. The sampler is segmented by one-way valves and thus obtains a series of aliquots consisting of varying proportions of borehole water and interstitial water, from which the composition of the interstitial water can be inferred by extrapolation of the mixing lines.

Five water samples were taken from Hole 504B on Leg 83 prior to renewed drilling, and three more were taken during the experimental phase of Leg 83 after the hole had been drilled to 1287.5 m (1013 m into basement). Shipboard analyses of the Leg 83 samples, along with previous data from the six samples taken on Legs 69 and 70, led to the following conclusions:

1. Two samples taken on Legs 70 and 83 from the upper part of the hole (at 194 and 355 m BSF), where temperatures are depressed, consist largely or entirely of bottom seawater which is flowing down the hole into a permeable, underpressured zone in the upper basement.

2. Samples from below this zone probably all include some admixture of seawater pushed down the hole by the sampling operation. The samples which contain the least amount of extraneous solution are the packer samples PA-1 and PA-2, because of their large volume. Their lowest or "D" aliquots, which show the largest discrepancy from seawater composition of all the samples, represent largely undiluted borehole water at 80 and 115°C, respectively.

3. The samples taken from 451 to 793 m BSF before drilling on Leg 83, 2 yr. after drilling had stopped on Leg 70, show an increase in Ca over the seawater value which exceeds their decrease in Mg on a molar basis. The Ca versus Mg relationship in the Leg 83 samples from 80°C duplicates that found in a sample taken 2 yr. ago from nearly the same depth prior to Leg 70 drilling, 43 days after Leg 69 drilling had stopped, suggesting that the relationship represents equilibrium at 80°C.

4. That Ca is gained in excess of Mg lost implies that an additional cation has been lost from solution to the altered rocks. This is presumably Na and/or K, in the total amount of at least 11 mmol/L at 80°C and 17.5 mmol/L at 115°C. If sulfate has been lost from solution at either temperature because of sulfate reduction or anhydrite precipitation, then these values would be even larger.

5. The Ca versus Mg relationship in the samples taken before drilling on Legs 70 and 83 (from 451 to 793 m BSF) contrasts markedly with the mole-for-mole exchange of Mg for Ca found in the samples taken from the same depth interval on Legs 69 and 70 after drilling had started. The mole-for-mole relationship was also found in laboratory experiments at 70°C and apparently represents only the initial stage of surprisingly rapid reaction between seawater and basalt at 70–80°C, before appreciable loss of Na and/or K.

6. The samples taken 43 days (Leg 70) to 2 yr. (Leg 83) after drilling had stopped show a change in composition with increasing depth over the interval 451 to 793 m which is presumably related to temperature. The Mg concentration decreases with increasing depth to only half the seawater value at 115°C. The pH (as measured at 25°C) and the salinity also decrease slightly. The concentrations of Ca, NH_3, and H_2S increase with depth. The Ca versus Mg relationship also changes: the excess of Ca gain over Mg loss decreases with depth. The latter change is related to depth-related changes in the net transfer of Na, K, and/or sulfate between rocks and solution.

7. The three samples taken near the end of Leg 83 at 100–133°C show a systematic decrease with temperature in the amount of Ca gained relative to Mg lost, implying that anhydrite has precipitated from the solutions at 130°C and above.

Shore-based analyses and interpretation of these samples are discussed by Mottl et al. elsewhere in this volume.

PALEOMAGNETISM

Site 504, at 1°13.63′N and 83°43.81′W, is located on the negative magnetic anomaly lying between Anomalies 3A and 4, where the estimated crustal age is 5.9×10^6 yr. (Hobart et al., this volume). This report is based exclusively on the paleomagnetic and rock magnetic data obtained on board the *Glomar Challenger* during Leg 83. Occasional references will be made to results of Legs 69 and 70 for comparison to the upper part of the hole.

The results of the paleomagnetic measurements are shown in Table 6 and Figure 13. Natural remanent magnetization was measured on the Digico spinner magnetometer. Low field susceptibility (k) was measured with a Bison Instructions, Inc. susceptibility meter (model 3101 A). No AF demagnetization was carried out on samples on board since a complete rock magnetic analysis was expected to be performed in a shore laboratory and the low core recovery kept sampling to a minimum, thus preventing duplicate sampling. Measurements were made on minicores 2.5 cm in diameter and 2.4 cm long, oriented by a scribe line parallel to the edge of the large core. In most cases, two samples were taken from each core. An effort was made to obtain samples from each petrologic unit, but this proved difficult because much of the recovered core was fractured and veined. Thus the rocks from which the paleomagnetic samples were taken generally represent the most unbroken, unveined, and often most unaltered fraction of the recovered cores. Intensity of natural remanent magnetization (J_{NRM}) values are highly scattered, ranging from 283 to 0.2×10^{-5} emu/cm^3. This is consistent with the scattered values re-

Table 6. Paleomagnetic results, Hole 504B, Leg 83.

Core-Section (interval in cm)	Depth below seafloor (m)	NRM J_n ($\times 10^{-5}$ emu/cm^3)	NRM I	k ($\times 10^{-5}$ cgs)	Magnetic unit
71-1, 127-129	837.27	239.302	84.5	940	1
72-1, 93-95	844.44	101.360	−2.1	744	
72-2, 105-107	846.0	114.980	−21.7	589	
73-1, 87-89	853.38	145.537	−13.4	532	2
73-2, 93-95	854.94	36.809	−5.2	729	
74-1, 94-96	862.45	99.900	−10.0	812	
75-1, 9-11	870.6	97.379	−42.1	721	
77-1, 23-25	888.74	46.874	0.9	744	3
77-3, 14-16	891.61	20.730	56.5	880	
78-1, 42-44	897.93	55.253	−13.3	676	
79-1, 96-98	905.47	61.536	−3.9	315	4
79-3, 110-112	908.57	26.949	−15.1	219	
80-1, 122-124	911.23	2.687	−12.3	20	
81-1, 114-116	920.65	4.472	−38.9	52	
82-1, 21-23	928.72	1.052	−2.4	38	
82-2, 111-113	931.07	7.956	−18.9	132	5
83-1, 33-35	937.84	0.252	−31.9	46	
84-1, 134-136	947.85	0.182	−55.2	40	
85-2, 75-77	957.59	60.993	−1.9	323	6
87-1, 85-87	967.86	17.304	−42.8	62	
87-2, 8-10	968.59	14.447	−50.2	115	
88-1, 15-17	976.66	0.008	−11.5	77	7
89-1, 100-102	986.01	4.139	−54.1	35	
90-2, 101-103	996.98	58.830	−60.7	357	
90-4, 143-145	1000.35	2.680	−71.4	44	
92-3, 67-69	1016.30	17.172	−8.2	80	
93-2, 81-83	1023.82	38.198	−22.0	73	
93-3, 66-68	1025.17	3.04	1.3	43	
94-1, 107-109	1031.58	48.055	1.2	374	8
94-3, 82-84	1034.33	50.681	4.8	494	
95-1, 100-102	1040.51	77.589	9.8	185	
98-1, 78-80	1062.79	14.261	−31.7	66	
99-1, 69-71	1071.57	283.306	−35.5	317	9
100-1, 21-23	1080.82	56.559	−29.1	50	
100-3, 20-22	1083.71	36.382	3.4	77	
101-1, 120-122	1090.71	28.776	2.5	113	10
101-2, 90-92	1091.91	65.878	16.1	401	
103-1, 51-53	1108.02	1.046	−28.0	28	
104-2, 124-126	1119.25	144.472	−10.7	508	11
104-3, 27-29	1119.76	78.025	17.9	274	
105-1, 116-118	1126.65	92.228	8.8	548	
107-2, 11-13	1145.04	103.098	−14.8	539	
108-1, 62-64	1153.13	113.503	−8.1	431	
109-1, 21-23	1153.72	143.205	−7.3	625	
111-1, 73-75	1162.24	160.990	−5.8	391	12
112-1, 63-65	1166.64	177.046	7.4	414	
113-1, 5-7	1171.06	182.652	−15.4	613	
113-1, 109-111	1172.10	109.032	−15.3	397	
117-1, 121-123	1190.72	84.431	−23.3	388	
118-1, 25-27	1194.26	91.077	−18.9	418	13
121-1, 33-35	1207.84	54.282	−29.9	483	
123-1, 52-54	1223.03	60.759	29.7	455	14
126-1, 151-153	1251.02	103.789	8.4	277	15
127-1, 83-85	1254.34	62.205	15.6	279	
128-1, 27-29	1261.28	131.366	−0.3	345	
129-1, 93-95	1270.94	49.119	−12.3	360	16
129-2, 18-20	1271.69	61.413	−18.2	405	
130-1, 77-79	1279.78	48.726	−15.1	314	
131-1, 129-131	1288.80	57.762	3.7	364	
132-2, 22-24	1296.68	25.089	15.2	471	
133-1, 88-90	1304.89	246.860	22.1	410	
133-2, 17-19	1305.59	175.206	24.5	307	17
134-1, 47-49	1313.48	292.747	21.1	574	
136-1, 82-84	1322.83	149.421	32.5	339	
137-1, 54-56	1327.55	173.314	36.9	451	
138-1, 28-30	1332.29	150.085	−38.6	429	18

corded during Legs 69 and 70. J_{NRM} versus depth is plotted in Figure 13. As was found in Leg 70, J_{NRM} does not appear to be depth dependent. Susceptibility (k) also is highly scattered, ranging from 940 to 20 $\times 10^{-5}$ cgs. Susceptibility versus depth is also plotted in Figure 13.

Because of the poor recovery, the average values of J_{NRM} and k obtained in this study may be artificially high, because the unrecovered section of the hole probably consists of a relatively larger fraction of breccia and altered units, whose J_{NRM} and k values are likely to be

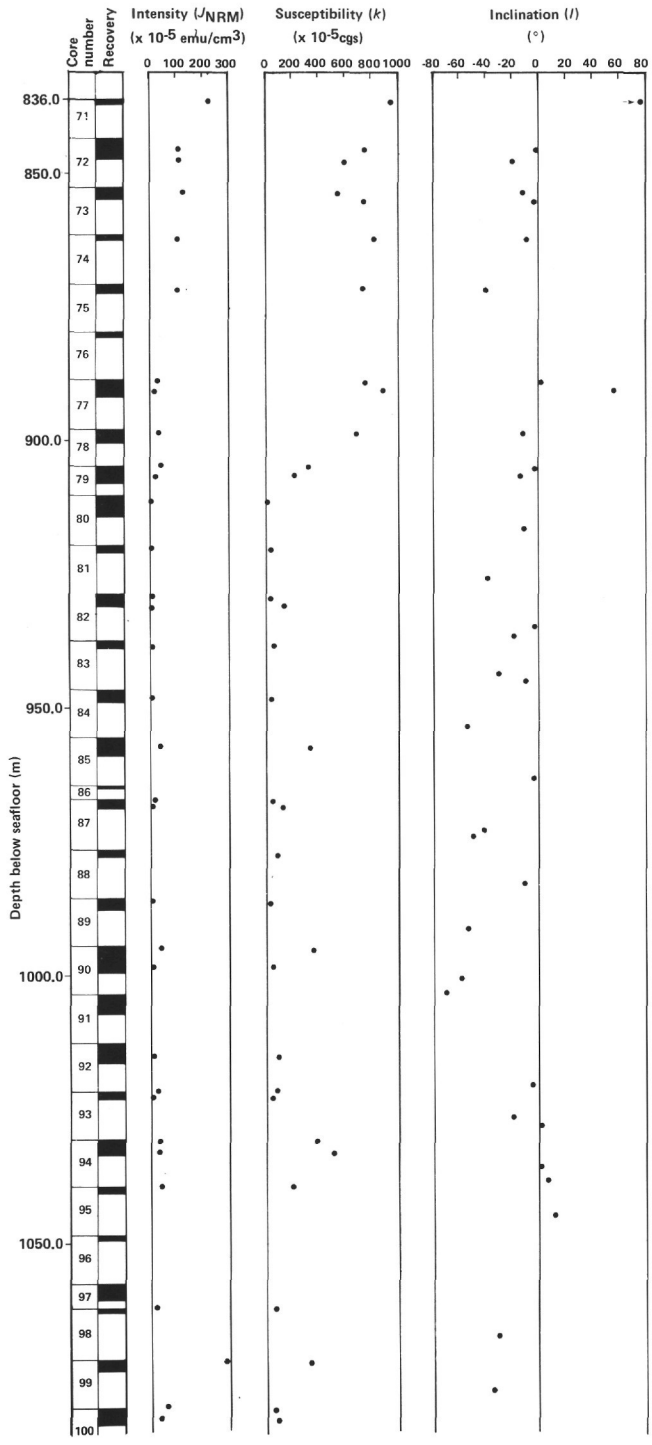

Figure 13. Shipboard measurements of magnetic intensities, susceptibilities, and inclinations of Leg 83 basalt samples.

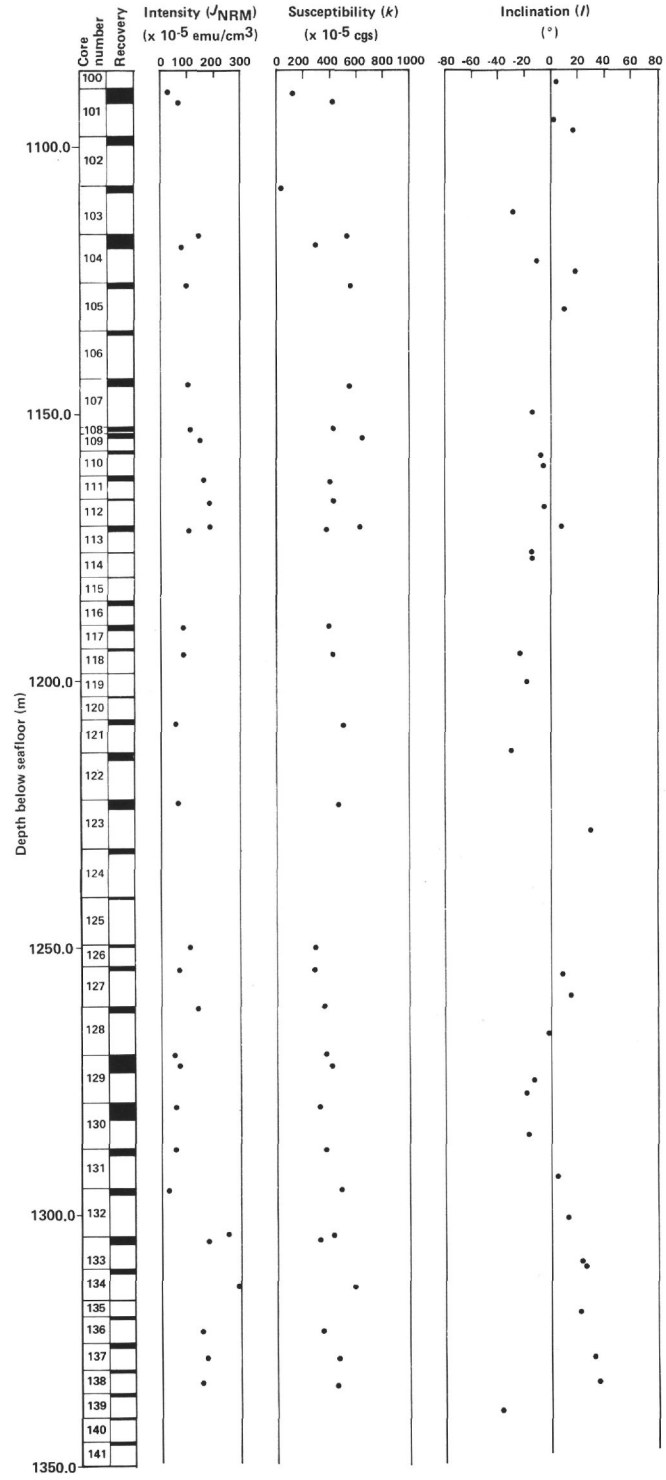

Figure 13. (Continued).

much lower. This in fact is indicated by the borehole televiewer records.

Most samples show negative inclinations, corresponding to reversed magnetization at this site (Fig. 13). There are a few alternating sequences of normal and reversed polarity downhole. Some 18 magnetic units have been defined, largely by the ranges of inclinations. They are numbered in accordance with the numbering system established during Legs 69 and 70 (Furuta and Levi, 1983). Their boundary zones correspond to lithologic boundaries, breccia and fracture zones, cooling margins or a drastic change in the character of alteration, often accompanied by distinct changes in J_{NRM} and k. Average values of J_{NRM}, k, and inclination (I) are given in Table 7.

The low sampling frequency and the absence of magnetic cleaning make the definition of these units most

Table 7. Magnetic units and average magnetic properties, Hole 504B, Leg 83.

Unit no.	Unit thickness: No. of cores (m)	N	J_{NRM} ($\times 10^{-5}$ emu/cm^3)	k ($\times 10^{-5}$ cgs)	I (NRM)
1	7 (7.5)	7	239.3	940	84.5
2	4 (36)	6	99.3 ± 32.4	687.8 ± 96.1	−15.75 ± 13.4
3	2 (18)	2	33.8 ± 13.1	812.0 ± 68.0	28.7 ± 27.8
4	3 (22)	4	36.6 ± 23.5	172.0 ± 216.0	−11.2 ± 4.3
5	4 (36)	5	2.8 ± 3.0	61.0 ± 35.5	−29.5 ± 17.9
6	7 (9)	7	60.9	323	−1.9
7	5 (39)	6	16.2 ± 20.0	115.0 ± 111.2	−48.5 ± 18.7
8	5 (45)	6	39.13 ± 32.4	208.2 ± 169.17	−2.2 ± 10.0
9	5 (41)	4	97.7 ± 108.2	144.3 ± 122.3	−23.2 ± 15.5
10	1 (9)	2	47.3 ± 18.5	257.0 ± 144.0	9.35 ± 6.9
11	4 (36)	4	78.9 ± 51.4	339.5 ± 208.0	−3.0 ± 17.8
12	9 (46)	7	141.2 ± 30.8	487.1 ± 95.2	−8.47 ± 7.5
13	7 (33)	3	76.6 ± 16.1	429.7 ± 39.7	−24.0 ± 4.5
14	4 (36)	1	60.8	455	29.7
15	2 (11.5)	2	83.0 ± 20.8	278.0 ± 1.0	12.0 ± 3.6
16	3 (26.5)	4	72.7 ± 34.3	356.0 ± 32.8	−11.5 ± 6.8
17	7 (44.5)	7	160.0 ± 88.0	416.6 ± 84.3	−22.3 ± 10.1
18	1 (4.5)	1	150.085	429	−38.6
					Absolute value
Hole average:	70 (514)	66	79.7 ± 70.0	360.0 ± 233.7	23.3 ± 24.95

tentative. Statistically, many of the averages given in Table 7 have no "real" meaning because of their large standard deviations and are only presented for qualitative distinction. (For example, several "units" each consist of only one sample.) Presumably, the statistical averages will improve after magnetic cleaning. Alternatively, the directions of some samples might be expected to change after cleaning. This would be consistent with the observation of secondary magnetic minerals in some thin sections (Cores 118–131, 1194 to 1296.5 m BSF; see Basement Alteration Petrography section).

Perhaps the most striking correlation is that between J_{NRM} and k and the extent of alteration downhole. The upper section of the hole above 898 m BSF (Core 78) has an average k of 743 × 10^{-5} cgs. A marked decrease in k occurs from 898 to 920 m BSF (Cores 77–80), where it reaches a minimum value (about 90 × 10^{-5} cgs) which persists with depth. This decrease corresponds to that interval where titanomagnetite becomes extensively replaced with sphene. Lower average k (96 × 10^{-5} cgs) and J_{NRM} (14 × 10^{-5} emu/cm^3) is measured from 910 m to 1040 m BSF (Cores 80–94), which corresponds with a region of more extensive alteration. Higher average k (373 × 10^{-5} cgs) and J_{NRM} (90 × 10^{-5} emu/cm$_3$) in the lower part of the hole below 1080 m BSF (Core 100) correlates with the observation that titanomagnetite is generally only partly replaced by sphene through this more massive region.

Throughout the hole inclinations are skewed toward negative values. Although the time-average inclination at Hole 504B would be expected to be very near zero, inadequate sampling could explain small deviations. However, the average inclinations throughout the hole (Legs 69 and 70 included) exhibit fluctuations in inclination which exceed those expected from normal secular variation. Previous reports (Furuta and Levi, 1983) have discussed this problem in detail and have proposed three mechanisms by which the anomalous inclinations might be produced: (1) geomagnetic excursions; (2) tectonic rotation; (3) stable secondary remanence.

It is not possible to find any definitive proof for either of these proposed mechanisms without first cleaning the Leg 83 samples and thus obtaining stable inclinations. However, the appearance of secondary magnetic minerals in the lower section of the hole (Cores 118–131; see Basement Alteration Petrography section) correlates well with the increase in J_{NRM} and k. This may provide support for the third proposed mechanism.

PHYSICAL PROPERTIES

Thermal Conductivity

Thermal conductivities of 59 homogeneous basalt samples—one from nearly every core—were measured using a Vacquier flat plate needle. The methodology used was calibrated by several measurements of a fused silica standard, with excellent duplication of the quoted value for the conductivity of the standard, 1.38 W/m-K. The basalt results—accurate to within ±5%—are significantly different from (but not inconsistent with) Legs 69 and 70 values in the upper 561.5 m of basement. In the upper part of the Leg 83 section, conductivities increase from the consistent Legs 69 and 70 mean of 1.7 to 2.0 W/m-K. Deeper than 650 m into basement, conductivity values are quite uniform at 2.0 ± 0.1 W/m-K.

Methods and Calibration

The theory for determination of sample conductivity with the half-space needle probe is analogous to that for the bare, whole-space needle probe given by Von Herzen and Maxwell (1959), with the exception that a geometric factor very nearly equal to two must be introduced. Thus, the conductivity K is obtained from the temporal temperature rise $T(t)$ on application of a constant heat source Q by

$$K \frac{Qf}{4\pi T} \ln(t) , \quad (1)$$

with $f \approx 2$. Several measurements of a Dow-Corning fused silica standard were made, before and among the

basalt measurements, both to check the instrumentation and to determine the factor f. Since the response to the conductivity instrument is linear over a limited temperature range ($\approx$20–30°C), f may vary slightly with measurement procedures used. All conductivity values were calculated using a two-point version of (1):

$$K \frac{Qf}{4\pi} \frac{\ln(t_2/t_1)}{(T_2 - T_1)}, \quad (2)$$

with t_2 = 2 min., t_1 = 0.7 min.

Ten measurements of the fused silica standard showed a high degree of consistency. Assuming the manufacturer's quoted conductivity value for the standard, 1.38 W/m-K (3.29 mcal/cm·s·°C), these measurements yielded mean f = 2.09 ± 0.03 S.D. Thus f was taken as 2.09 for all Leg 83 basalt measurements. Based on the consistency of the silica measurements, the absolute accuracy of the basalt values is well within the ±5% quoted for needle-probe values by Von Herzen and Maxwell (1959).

Results

The Leg 83 thermal conductivity values are listed in Table 8 and plotted in Figure 14. (All Hole 504B conductivity values are plotted in Figure 4 of Becker et al., this volume.) As noted above, a sharp depth gradient in sample conductivities occurs in the upper 10–15 cores of the Leg 83 section; below Core 80, Leg 83 values vary closely about a mean value of 2.04 W/m-K. The sharp difference in trends of Leg 70 and Leg 83 values is at first disturbing—possibly suggesting some experimental cause. However, the measurements on both legs were made with the same apparatus, calibrated by reliable standards—granite with a value determined by a divided bar apparatus on Leg 70, and fused silica on Leg 83. There is no experimental reason to doubt that either set of measurements was inaccurate by more than ± 5%, so the difference in conductivity values is taken to be real.

Other physical properties show a similar change in the upper part of the Leg 83 section, as do petrologic and logging results. In particular, the large-scale electrical resistivity experiment showed a very large increase in apparent resistivities with depth, immediately below the Leg 70 section. Taken together, all the results indicate that a real discontinuity or gradient in physical and chemical properties occurs at about 600 m into basement. It appears to be only coincidence that the Leg 70 drilling stopped just before this change became apparent.

For heat flow calculations, three different sample means (with standard deviations) were used for basalt conductivities:

Depth into basement (m)	K(W/m-K)
0–560	1.65 ± 0.7
560–640	1.83 ± 0.10
640–1075 m	2.04 ± 0.09

To obtain bulk crustal conductivities, a slight correction to these sample values for crustal porosity is necessary, as discussed by Becker et al. (this volume).

Laboratory Measurement of Sonic Velocity, Density, and Porosity

Physical and elastic properties were measured on 53 homogeneous basalt samples from nearly every core, as follows:

1. Compressional acoustic velocity was measured using the Hamilton Frame method. A rectangular sample was cut from the core so that a pair of parallel surfaces of the sample lay in the direction of the drilled core axis and the other pair of parallel surfaces lay in a plane perpendicular to the core axis. Acoustic velocities were determined along these two orientations. Calibration of the measuring device is achieved by measuring several standard samples provided by DSDP (quartz glass, aluminum plate of various thicknesses, and others). The maximum error of the measuring system thus obtained is about 1.5% (at room temperature, 23°C). However, in actual cases where the sample surface is rather rough when trimmed by a diamond saw wheel only, we may expect an error a bit larger than the estimate. Further discussion on this matter must await detailed shore-based studies.
2. Gravimetric density, porosity, and water content were obtained from a sample chip contiguous to the sonic velocity samples. Porosity and water content were obtained after samples were dehydrated by being exposed to air for one day at 110°C in an electric oven.
3. Gamma ray technique (2-min. GRAPE) was used to provide data supplementary to the gravimetric data. The corrected wet-bulk density is calculated according to the DSDP instruction manual for the GRAPE technique. The true wet-bulk density is obtained by combining the corrected wet-bulk density with the grain density data provided by the gravimetric method.

Results

All results of sonic velocity, wet-bulk density, and porosity measurements are plotted on Figure 15 and listed in Table 8. These plots include also data obtained from Holes 504, 504A, and the upper section of 504B of the previous Legs 69 and 70 (Cann, Langseth, Honnorez, Von Herzen, White, et al., 1983) to provide a clear picture of the variation in physical quantities from the ocean floor to the maximum depth reached by Hole 504B. Holes 504, 504A, and 504B are close enough together to allow us to compile their data in this manner.

The major features of the physical properties in Hole 504B of Leg 83 are characterized by uniform values (mean ± S.D.):

$$V_p = 6.17 \pm 0.38 \text{ km/s}$$
$$\rho = 2.93 \pm 0.07 \text{ g/cm}^3$$
$$\phi = 3.22 \pm 2.27\%.$$

Here, V_p represents an average value of the velocities measured both horizontally and vertically for each sample and ρ and ϕ are both based upon gravimetric measurement.

These values compare well with those obtained from the basalt samples of Holes 504A and 504B of Legs 69 and 70, where they are mostly bracketed by $5.5 < V_p <$

Table 8. Shipboard physical properties measurements, Hole 504B, Leg 83.

Core-Section (interval in cm)	Sub-bottom depth (m)	Sonic velocity (km/s)		2-min. GRAPE		Gravimetrics			Acoustic impedance (10^5 g/cm^2·s)	Thermal conductivity (W/m-K)
		Horizontal	Vertical (a)	Wet-bulk density (g/cm^3)	Porosity (%)	Wet-bulk density (g/cm^3) (b)	Porosity (%)	Water content (%)	Vertical (a) × (b)	
71-1,68-70	836.7	6.21	5.97	2.90	4.8	2.93	4.1	1.4	17.5	1.72
72-2, 27-29	845.3	5.88	5.99	2.91	5.1	2.95	3.2	1.1	17.7	—
73-1, 61-63	853.1	6.36	5.70	2.90	6.0	2.96	2.7	0.9	16.9	1.87
74-1, 78-80	862.3	6.43	5.69	2.78	11.9	—	—	—	—	1.76
75-1, 10-15	870.6	—	—	—	—	—	—	—	—	1.79
76-1, 24-26	879.8	5.64	5.98	2.80	10.3	2.90	4.9	1.7	17.3	—
77-3, 1-3	888.5	5.59	5.93	2.84	7.8	2.90	4.4	1.5	17.2	2.03
78-2, 60-62	898.1	5.76	5.54	2.83	7.3	2.86	5.8	2.1	15.8	1.86
79-2, 24-26	904.7	5.33	5.89	2.88	5.1	2.86	5.9	2.0	16.8	1.81
80-1, 2-4	910.0	4.74	4.57	2.93	—	2.66	13.6	5.1	12.2	1.82
82-3, 65-67	929.2	6.17	5.10	2.93	3.3	2.93	3.7	1.3	14.9	2.20
83-1, 126-128	938.8	6.23	5.96	2.95	—	2.77	6.5	2.3	16.5	2.16
84-2, 59-61	948.6	5.80	6.27	2.83	5.9	2.88	6.5	2.7	18.1	2.10
85-2, 80-82	957.8	6.26	6.02	2.96	3.3	2.93	2.2	0.7	17.9	2.05
87-2, 92-94	969.4	6.10	6.25	2.88	5.0	2.92	3.0	1.0	18.3	2.09
88-1, 65-67	977.2	6.55	5.88	2.84	3.9	2.75	8.4	3.1	16.2	2.14
89-2, 27-29	987.3	6.10	6.41	2.82	9.8	2.98	1.4	0.5	19.1	2.16
90-4, 72-74	999.7	6.13	5.89	2.90	2.3	2.90	2.3	0.8	17.1	2.14
91-2, 11-13	1005.1	6.43	6.27	2.99	1.3	2.95	2.9	1.0	18.5	2.00
92-1, 62-64	1013.1	6.36	6.33	2.87	6.1	2.94	2.6	0.9	18.6	1.90
93-3, 12-14	1024.6	6.12	6.32	2.94	2.1	2.92	2.6	0.9	18.5	2.06
94-1, 27-29	1030.8	6.29	6.25	2.94	6.3	2.97	2.2	0.8	18.6	2.03
95-1, 137-143	1040.9	—	—	—	—	—	—	—	—	2.25
96-1, 93-95	1049.4	6.12	6.18	2.88	6.9	2.96	3.2	1.1	18.3	2.04
97-1, 115-117	1058.7	6.13	6.44	2.80	11.0	2.95	3.1	1.1	19.0	2.05
98-1, 2-4	1062.0	6.33	6.53	2.84	8.3	2.95	2.9	1.0	19.3	1.95
99-1, 48-50	1072.0	6.33	6.10	2.90	2.8	2.88	3.5	1.2	17.6	2.13
100-1, 130-132	1081.8	5.78	6.03	2.85	7.8	2.93	3.3	1.1	17.7	1.92
101-2, 76-78	1090.3	6.21	6.46	—	—	2.95	2.4	0.8	19.1	2.08
102-1, 55-57	1099.0	6.49	6.16	2.88	6.7	2.95	2.7	0.9	18.2	1.98
103-1, 84-86	1108.4	6.48	6.03	2.84	8.4	2.96	2.4	0.8	17.8	2.07
104-2, 32-34	1116.8	6.44	6.38	2.81	9.6	2.97	1.5	0.5	18.9	2.07
106-1, 5-7	1134.6	6.94	6.55	2.75	10.6	2.89	2.2	0.8	18.9	1.91
107-2, 51-53	1144.0	6.35	6.53	2.96	2.6	2.96	2.4	0.8	19.3	2.03
108-1, 11-13	1152.6	6.02	6.37	3.02	1.1	3.00	1.7	0.6	19.1	2.01
109-1, 10-12	1153.6	6.74	6.14	3.03	—	2.96	1.4	0.5	18.2	2.07
111-1, 35-37	1161.9	5.46	5.55	2.80	6.7	2.78	7.4	2.7	15.4	1.87
112-1, 61-63	1166.6	6.76	6.47	2.98	3.5	3.00	2.2	0.7	19.4	2.05
113-1, 14-16	1171.2	6.42	6.45	2.97	1.5	2.95	2.5	0.8	19.0	1.98
116-1, 17-19	1185.2	6.14	6.26	2.98	2.5	2.98	2.8	1.0	18.7	1.94
117-1, 134-136	1190.8	6.62	6.36	2.97	3.0	3.00	1.4	0.5	19.1	2.11
118-1, 16-18	1194.2	6.81	6.28	2.98	3.5	3.03	1.3	0.4	19.0	2.18
120-1, 32-34	1203.3	6.87	6.40	2.85	8.5	2.94	3.6	1.2	18.8	1.90
121-1, 82-84	1208.3	5.93	6.13	2.88	2.6	2.87	2.9	1.0	17.7	2.02
122-1, 103-105	1214.5	5.83	6.48	2.92	4.1	2.94	2.6	0.9	19.1	1.87
123-1, 44-46	1222.9	6.53	6.84	2.93	4.1	2.96	2.2	0.7	20.2	2.02
124-1, 131-133	1232.8	6.48	6.73	2.87	6.1	2.95	2.2	0.9	19.9	1.94
125-1, 100-105	1241.0	—	—	—	—	—	—	—	—	1.96
126-1, 53-55	1250.0	6.37	5.90	2.96	3.0	3.00	1.3	0.4	17.7	2.03
127-1, 90-92	1254.4	6.46	6.02	2.95	1.5	2.96	1.1	0.4	17.8	2.13
128-1, 30-32	1261.8	6.60	6.43	2.97	1.5	2.99	0.7	0.2	19.2	2.09
129-1, 25-27	1270.3	5.98	6.03	2.92	3.0	2.95	1.7	0.6	17.8	2.06
130-1, 80-82	1280.0	6.48	6.28	2.97	2.0	2.99	0.5	0.2	18.8	2.11
131-1, 93-95	1288.4	5.97	6.31	2.97	2.6	3.01	1.4	0.5	18.9	2.03
132-2, 13-15	1295.2	6.16	6.15	2.97	3.1	2.99	1.4	0.5	18.4	2.08
133-2, 3-5	1304.0	6.39	6.21	3.16	—	2.99	1.7	0.6	18.6	2.17
136-1, 76-78	1322.8	6.59	6.53	2.94	3.8	2.98	1.2	0.4	19.5	2.10/2.15[a]
137-1, 56-58	1327.6	6.37	6.70	2.94	2.2	2.95	1.6	0.5	19.8	2.07
138-1, 26-28	1332.2	6.54	6.59	2.87	6.2	2.96	1.3	0.4	19.5	2.06
139-1, 37-39[b]	1336.9	6.79	—	—	—	—	—	—	—	—
140-1, 40-42[b]	1341.4	6.53	—	—	—	—	—	—	—	—
141-1, 2-4[b]	1345.5	6.44	—	—	—	—	—	—	—	—

Note: Dash indicates no measurement made.
[a] Different chunks.
[b] Samples not trimmed.

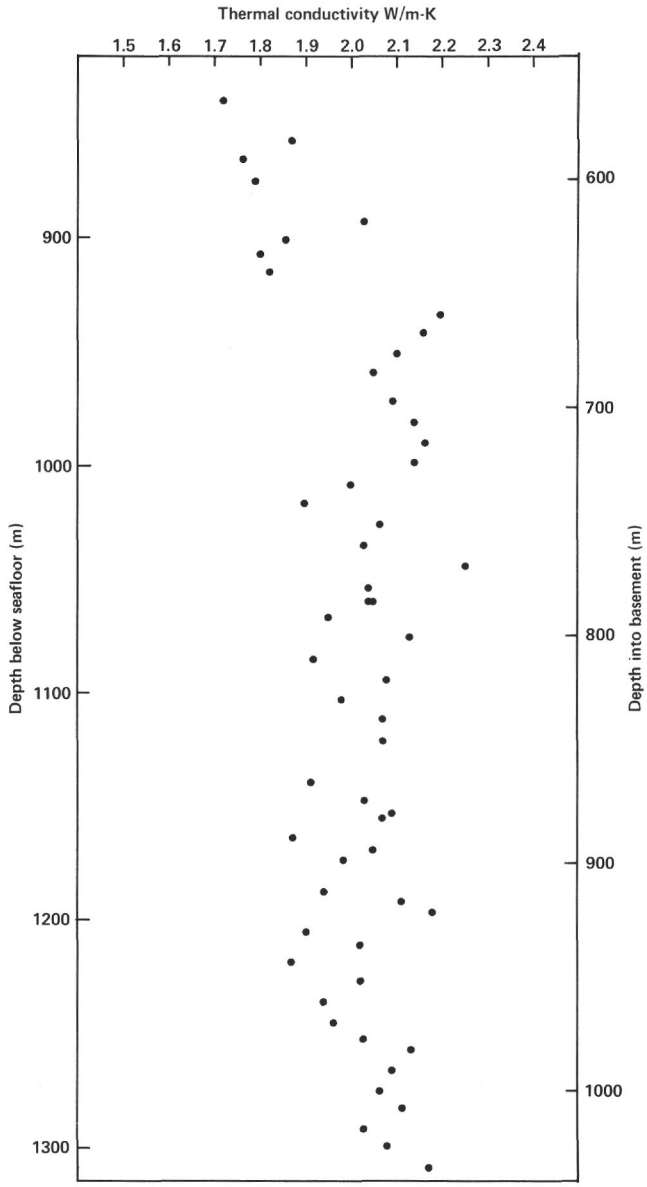

Figure 14. Shipboard measurements of thermal conductivities of Leg 83 basalt samples.

6.2 km/s, $2.8 < \rho < 3.1$ g/cm^3, and $0 < \phi < 10\%$, respectively.

TEMPERATURE MEASUREMENTS

Borehole Temperature before Leg 83 Drilling

The return to Hole 504B about two years after it was drilled on Legs 69 and 70 provided a unique opportunity to sample borehole temperatures and fluids, fully equilibrated from the disturbances of drilling. The first order of business after the Leg 83 reentry into Hole 504B was to lower the DSDP temperature probe four times, with concurrent and intervening water sampling. Negligible pumping accompanied these measurements, so the results are taken as representative of equilibrium downhole conditions.

Extensive temperature logging during Legs 69 and 70 (CRRUST, 1982; both papers by Becker et al., 1983; Becker et al., this volume) had revealed an extraordinary hydrologic downhole flow of bottom water into a shallow basement reservoir, superimposed on a dominantly conductive equilibrium geothermal gradient extending to a depth of 836 m. Based on these temperature measurements Becker, Langseth, and Von Herzen (1983) concluded (1) that the rate of downhole flow was on the order of 90 m/hr. (6000 L/hr.) as of December 1979; (2) that the downhole flow was directed into a relatively thin reservoir no deeper than 90 m into basement; and (3) that before Hole 504B was drilled heat transfer through the upper 836 m of ocean crust here was dominantly conductive, at the theoretical value of 200 mW/m^2 predicted from plate cooling models. The temperature measurements showed no clear evidence for presently active hydrothermal circulation; the downhole flow after drilling was *not* hydrothermal convection, but was convection forced by basement pore fluid underpressures (Anderson and Zoback, 1982; Becker, Langseth, Von Herzen, and Anderson, 1983).

The Leg 83 temperature measurements were primarily directed toward a reassessment of the geothermal and hydrologic conditions in the hole. In particular, the new measurements allowed evaluation of:

1. Whether or not the downhole flow had persisted over two years, and if so, at what rates.
2. The validity of the theoretical extrapolations from which it was concluded that a constant temperature gradient held in the basement, deeper than 450 m.

These were both confirmed, but significant slowing of the downhole flow rate was indicated.

Measurement Techniques

Water temperatures ahead of the bit were measured using the DSDP downhole temperature probe (T-probe), modified from a design of Yokota et al. (1980). This device monitors the resistance of a single thermistor protruding through the bit, at 128 discrete intervals, at a user-selected sampling rate of 1 or 2 min. It was used in two distinct configurations on Leg 83.

1. On the first and second lowerings in the upper part of the hole, where relatively low temperatures were expected, and where the chance of bridges in the hole was judged to be slim, the "normal" configuration was used. The thermistor extended about 1 m ahead of the bit, and resistances were measured over 30 to 0.01 kΩ range, to a nominal precision of 10 Ω. This is roughly equivalent to temperature resolution of 0.01°C at 0°C to 0.1°C at 50°C.
2. On the third and fourth lowerings, deeper in the hole, where higher temperatures were expected and where a greater chance of bridges existed, a shorter probe was used, which extended about 10 cm ahead of the bit. The instrument was modified to record thermistor resistances over 3000 to 1, to a nominal precision of 1 Ω. This is roughly equivalent to temperature resolution of 0.01°C at 50°C to 0.05°C at 100°C.

Since attaching the T-probe to the sand line limits the depth range of measurement to a single stand of pipe, it

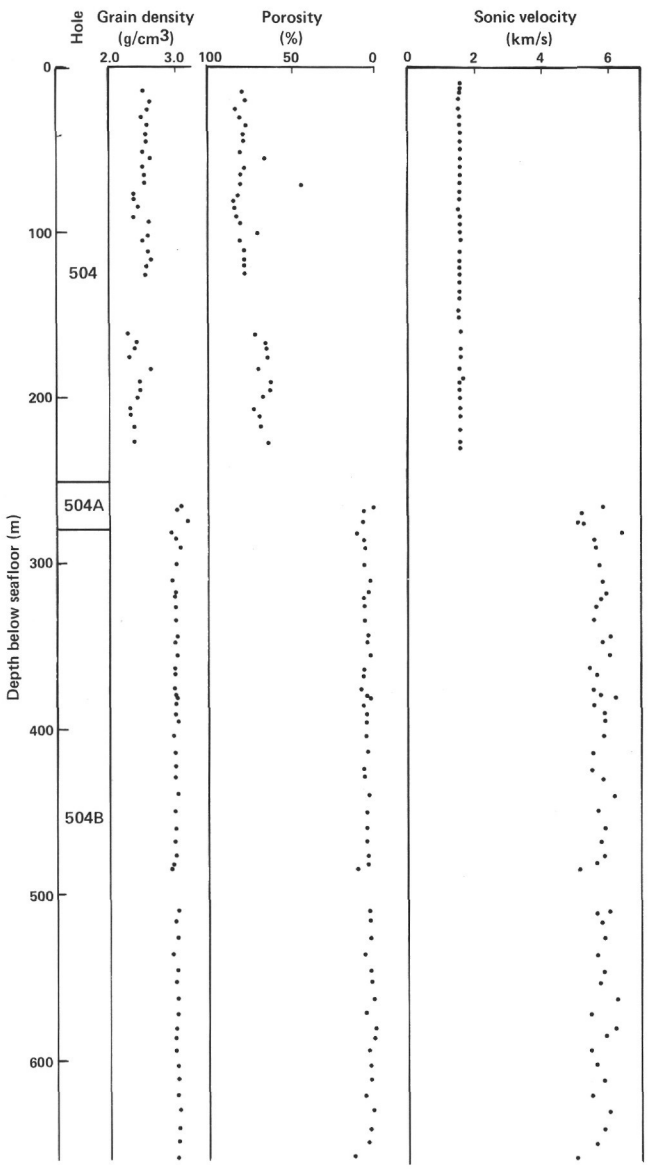

Figure 15. Shipboard measurements of densities, porosities, and sonic velocities of samples recovered from Holes 504, 504A, and 504B during Legs 69, 70, and 83.

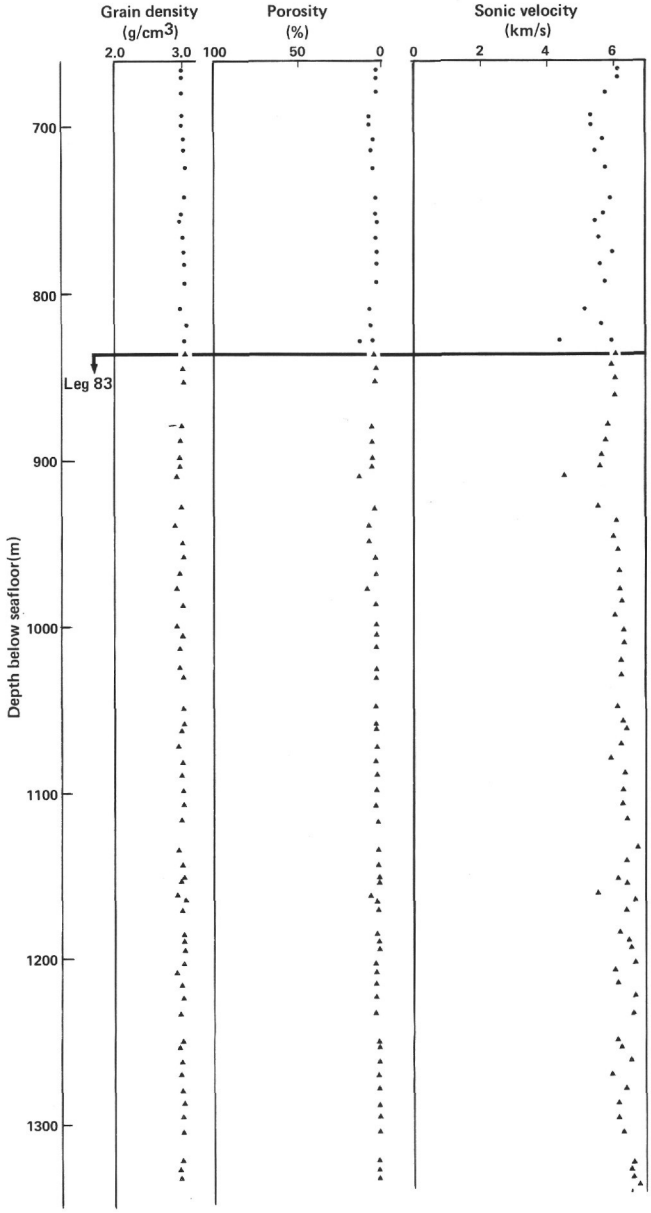

Figure 15. (Continued).

was impractical to cover the great range of hole depths with sand line measurements. Thus the instrument was allowed to free fall for each of the four lowerings, despite the greater danger of damage on impact with the bit. In fact, the thermistor probe was bent during the second station (with no noticeable effect on the quality of the data) and the recorder on-off switch failed in the "on" position during the fourth lowering, apparently a mechanical failure due to the impact.

After 25 min. was allowed for the free fall, the pipe was lowered one stand at a time, for several 5–10 min. stops at 29 m intervals. No pumping occurred during either free fall, or during the slow lowering of each stand. There was no evidence that the instrument disengaged from the bit because of the lack of pump pressure.

The various configurations and procedures used in the four heat flow lowerings are summarized in Table 9.

Calibrations and Precision of Temperature Measurements

The thermistor used had been calibrated about three years before, over the temperature range 0–100°C, nearly coincident with the range of downhole temperatures measured. Close duplication of the known bottom water temperature of 2.1°C, in the pipe at the mudline, as well as water ice point and boiling point checks on previous legs, suggests that measurement errors caused by possible drifting of the thermistor response are relatively minor compared to possible recorder errors and environmental disturbances.

The recorder resistance response was calibrated before and after each lowering against a 0.1% decade box. Although previously detected low-temperature recorder instabilities had been corrected and many components

Table 9. Summary of downhole temperature measurements made upon Leg 83 reentry of Hole 504B, before any drilling or pumping in the hole.

T-probe lowering	Depth range (m BSF)	Instrument	Sampling rate	Thermistor	Data quality
1	51–194	Low temp.	1 min.	14 (1 m)	Very good
2	194–451	Low temp.	2 min.	14 (1 m)	Good
3	507–650	High temp.	1 min.	10 (0.1 m)	Good
4	650–736	High temp.	1 min.	10 (0.1 m)	None: on/off switch failed in "on" position
Packer	793	Maximum-reading thermometer			Good

had been replaced by high-temperature versions, the before and after calibrations showed differences as large as 1 part in 100 resistance. This is roughly equivalent to about 0.2°C at low temperature to 0.5°C at high temperature; these values are here taken to be the limit of recorder precision for these measurements.

The temperature–time records for the first three thermistor lowerings are shown in Figure 16. The 5–10 min. stop at each depth should have been sufficient for the probe to reach equilibrium with ambient water temperature, particularly since only negligible frictional heating should have occurred as the probe was lowered through the water. It was expected that temperatures at each measurement point would possibly show slight increases with time as the probe equilibrated, or would be relatively constant. However, several of the temperature points unexpectedly showed regular decreases with time more characteristic of the dissipation of frictional heating or of penetration into sediments. Since frictional heating of the probe as it was lowered through water should not have been so significant, these cases are attributed to some combination of two factors:

1. Mixing of water in the vicinity of the probe, possibly either cool water from above, or initially displaced warm water from below.

2. Instability of the recorder at various ambient temperatures. This is also indicated by the mismatched mudline temperature readings during the second lowering. Although it is possible that the peak temperatures measured at these points were more representative of ambient conditions, preliminary equilibrium temperatures were assigned from the apparent asymptotes of the temperature–time curves.

Because these effects were more pronounced at higher temperatures, the accuracy of our high-temperature values is probably considerably less than that of low temperature values. The estimated accuracy of recorded temperatures ranges from about ±0.2°C near 0°C to about ±2°C near 100°C.

Results

Becker et al. (this volume) discuss the results of these measurements in detail. The Leg 83 equilibrium hole temperatures are superimposed on the Legs 69 and 70 results in Figure 17. Three important observations are immediately apparent from this figure:

1. Below 450 m, temperatures measured on Leg 83 verify the Leg 70 conclusion that a linear temperature gradient of 0.11°C/m exists in the deeper basement section. The linear temperature gradient argues against any significant, presently active hydrothermal circulation in the deep basement.

2. As on Legs 69 and 70, temperatures measured in the casing are significantly lower than those expected from adjacent sediment temperatures, indicating continued drawdown of bottom water into the hole. However, the Leg 83 casing temperatures are somewhat higher than the Leg 70 values, indicating a significant slowing of the downhole flow.

3. The depth at which temperature below the casing revert toward expected geothermal values is significantly shallower (20–30 m) during Leg 83 than during Leg 70. Since this break marks the level below which no significant downhole flow continues, the change in depth is consistent with a reduction of flow rate. See Becker, Langseth, Von Herzen, and Anderson (1983) and Becker et al. (this volume) for an estimate of the Leg 83 downhole flow rate and a detailed discussion of the underpressured reservoir in the basement.

Temperature Logs after Leg 83 Drilling

In the 11 days of experiments run after Leg 83 deepened Hole 504B to 1287.5 m, water temperatures in the hole were logged three times with the Schlumberger High-Resolution Thermometer (HRT). The first temperature log was run immediately after two hours of circulation, in order to assess its effectiveness in cooling the hole before temperature-sensitive tools were deployed. The second and third logs were run about 58 and 82 hr. after the last circulation disturbance to the hole, without any intervening pumping. Thus they could be extrapolated to correct for the circulation disturbance, to yield an estimate of the equilibrium geothermal conditions before drilling. The uncorrected temperature logs are shown in Figure 18. Becker et al. (this volume) analyze these data; in general their results confirm the conclusion of Legs 69 and 70 that heat transfer in the upper km of crust at Hole 504B is dominantly conductive.

PERMEABILITY

One of the most fundamental physical observations in any active convective system in a porous medium is the form and magnitude of the variation in permeability. Convection of seawater in the upper oceanic crust is now a well-documented physical observation, yet we know

virtually nothing about the permeability of the oceanic crust and how it varies with depth and age.

Since 1979 we have been measuring permeability (k) *in situ* in Deep Sea Drilling Project holes; first at Hole 504B, then at Hole 395A in the Atlantic. The return to Hole 504B on Leg 83 offered us a chance to determine the variation in k with depth, since on Leg 69 we measured values of 4×10^{-2} darcys over the depth interval 50–200 m into the basement and 4×10^{-3} darcys at 195–210 m into the basement (Anderson and Zoback, 1982). Also Becker, Langseth, Von Herzen and Anderson (1983) estimated 6×10^{-2} darcys for the upper ~100 m of basement.

Despite defective rubber packer elements which appear to have been devulcanized by the high borehole temperatures, we did succeed in making one measurement of k over the depth interval 250–1000 m into the basement. This permeability value, $1\text{–}2 \times 10^{-4}$ darcys, was almost three orders of magnitude *less* than the permeability in the upper section of basement (Fig. 19). A fit of permeability versus depth in Hole 504B yielded the following function:

$$k(z) = 0.11 \exp\left(\frac{-z}{50}\right),$$

with z in meters, k in darcys. See Anderson et al. (this volume) for detailed analysis of the Hole 504B permeability measurements.

BOREHOLE TELEVIEWER

Introduction

The ultrasonic borehole televiewer (BHTV) is the only wireline logging tool capable of providing a continuous image of the borehole wall. Although other logging techniques produce continuous records of various physical properties downhole, none of them can provide much information regarding the structural condition downhole. Because the televiewer makes a record of the smoothness of the walls of the borehole, discontinuities such as cracks and fractures are readily seen in the record. The BHTV is also sensitive to changes in formation reflectively, and thus changes in lithology, veins, bedding planes in sedimentary rock, and other features can sometimes be seen. Particularly in areas of low core recovery, the BHTV can provide an invaluable, continuous record with which to interpret the interrelationships of the rock units from which the cores have been drilled.

The televiewer contains a rotating piezoelectric transducer which emits ultra high frequency (1.2 MHz) acoustic pulses at a rate of 1500 times/s in a 3° focused beam as it rotates at 3 rev./s. The amplitude of the reflected signal is recorded on videotape and plotted as trace brightness on a three-axis oscilloscope as a function of the beam azimuth and vertical position in the hole. The scope trace is triggered as magnetic north by a fluxgate magnetometer in the tool.

As the tool is moved vertically in the hole (up- or downhole at 0.6 m/min.), a photograph of the traces on the scope yields a 360° view (north-to-north "picture") of the vertical section of the wall. A record of the smoothness or reflectivity of the borehole wall is obtained, so that hard, smooth surfaces produce white zones from high-amplitude reflectance, and fractures, voids, and soft material such as clays absorb or scatter much of the signal, resulting in low-amplitude reflectance that produces dark zones. Resolution of the tool depends on hole diameter, reflectivity of the formation, acoustic impedance of the wellbore fluid, and general wall conditions. In the Leg 83 records, fractures and other features can be clearly distinguished down to a 1-cm scale.

During Leg 83, two logging runs were made in the crustal section of Hole 504B using a U.S. Geological Survey BHTV. Since the original televiewer data were recorded and presented in depths below the rig floor, these depths are used here. Depths below seafloor are given in parentheses. The total interval logged was slightly over 1 km in depth. On the first logging run on 18 December 1981, the compass began to run erratically because of the high temperatures encountered downhole and 80 m of data were lost. During the period of highest temperatures encountered, the tool actually stopped, but increasing the AC power remedied the problem. At a depth of 4120 m below the rig floor (646.5 m BSF), the Sony video player stopped working. Because we were still receiving excellent signal returns, we finished logging the hole to the sediment/basalt interface with only Polaroid photograph recovery. Upon completion of this run, we attempted to relog the bottom 80 m that we had missed, but the tool would not work upon reaching the bottom, and we pulled it out of the hole.

The second logging run on 27 December was made using the ship's video machine for tape recording. Since the compass control was still inoperative, the entire second logging run was accomplished using a mechanical mark which maintains a trigger rate at three times per second but produces no orientation information. Again we were able to get excellent Polaroid photograph coverage of the logging run. Unfortunately, secondary recovery of data obtained during this run has proven difficult as the mechanical mark and the audio track were not recorded properly on the video tape.

The Polaroid photograph composites of the BHTV records are shown in Appendix A, Figure 1 of Newmark et al. (this volume). Those photographs shot below 4430 m depth (956.5 m BSF) are not compass-triggered and therefore their left margins are not north-oriented. Compass orientations are available, however, over the lower section of the hole from the first BHTV run. This run, which was of poorer quality, is not reproduced in this volume. There is no usable video record for that part of the hole shot above 4120 m (646.5 m BSF). The overall quality of the photographs is excellent. The major cause of data loss is that due to the heaving of the ship, which causes the tool to be either pulled up or dropped down at a much higher rate than the very slow logging rate it requires. This causes vertical streaks in the record, often up to a third of a meter in downhole depth. A second feature in the record is a general dark-light banding running vertically down the hole. We believe this may have been caused by the tool being off-center in the hole be-

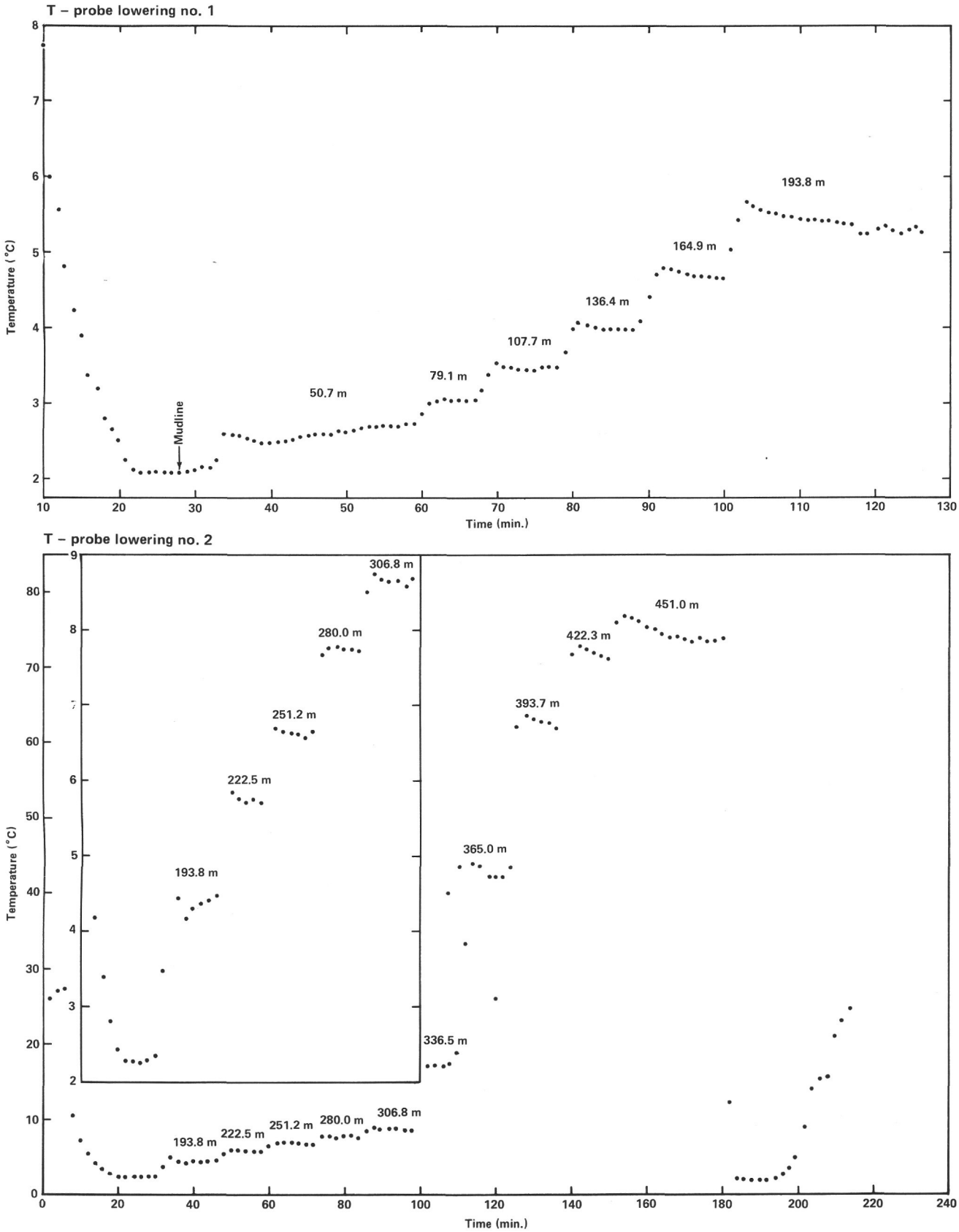

Figure 16. Corrected temperature–time records for the three lowerings of the DSDP temperature probe in Hole 504B before any Leg 83 disturbance to the hole. The records are annotated with the depths (in m below seafloor) of the discrete instrument stops of 5–10 min. duration. Part of the record for T-probe lowering no. 2 is shown in an inset at an expanded temperature scale.

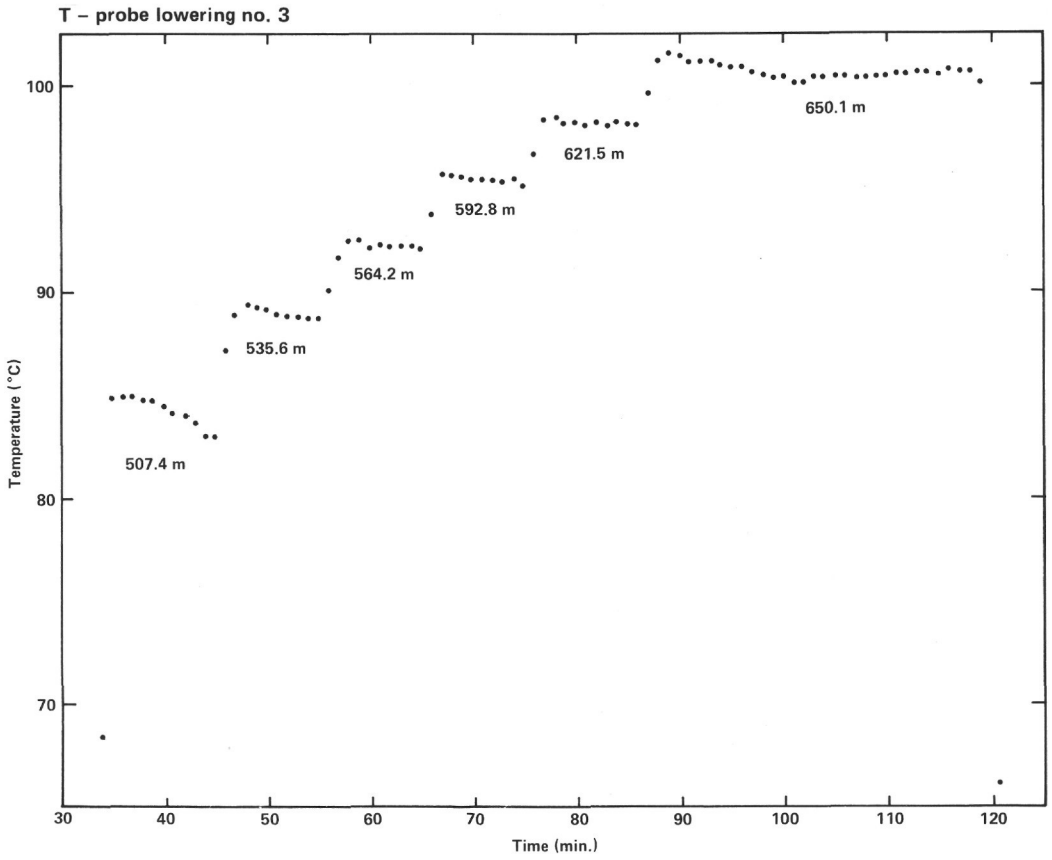

Figure 16. (Continued).

cause it is equipped with small-sized centralizers. Thus if the tool is rotating in the hole, the banding will seem to spiral down the record. This would be true in both the compass and the mechanically triggered records.

There are three lithologically distinct units that can be distinguished in Hole 504B: pillow basalt units, massive units, and brecciated units.

Pillow basalt units can be distinguished by the appearance of horizontally oriented ellipsoidal bodies, outlined by dark rims (less reflective), often up to nearly a meter across (about the width of the photograph) and up to a third of a meter high. Their centers tend to be brighter (more reflective). They are cut by numerous horizontal cracks and voids and tend to have a generally mottled appearance in the record. A good test for the presence of pillows is whether or not both sides of the ellipse are present. Only if both sides of the ellipse are seen can the feature be considered a pillow. (An ellipse cut by the edge of the photograph should be continued at the opposite edge.) Good examples of pillow units can be seen in the intervals 3910–3920, 3945–3950 and 3957–3962 m (436.5–446.5, 471.5–476.5, and 483.5–488.5 in BSF). They are not found below 4520 m (1046.5 m BSF).

Massive units are distinguished by their solid texture and the relative absence of voids and cracks. Since the BHTV records high-amplitude reflections as white, the massive units show up as being very bright on the records. Good examples are the intervals 3898–3994, 4006–4015, and 4048–4058 m (424.5–520.5, 532.5–541.5, and 574.5–584.5 m BSF). From 4445 to 4450 m (971.5–976.5 in BSF), there is a series of chatter marks down the wall in a massive unit, which may be an artifact of the drilling process.

Brecciated units are distinguished by their generally dark (low-reflective) and chaotic appearance in the records. They look much like pillow units except that they appear to have a more regular texture and are generally darker. Good examples are found in the intervals 4672–4677 and 4688–4692 m (1198.5–1203.5 and 1214.5–1218.5 m BSF).

There are numerous zones of intense subhorizontal fracturing throughout the hole. For example, from 3770 to 3775 m (296.5–301.5 m BSF), a massive unit appears fairly intact. However, from 3775 to 3787 m (301.5 to 313.5 m BSF) there are several zones of sometimes intense subhorizontal fracturing. From 3787 to 3797 m (313.5 to 323.5 m BSF) again appears to be fairly massive and solid, but below 3797 m (323.5 m BSF) another zone of intense subhorizontal fracturing occurs. It is common to find massive units bordered by such intense fracturing, such as at 4080 (606.5 m BSF), and below 4060 m (586.5 m BSF). Perhaps the most spectacularly fractured interval is the one called the "reservoir"; a good record of it is seen in the interval 3800–3830 m (326.5–356.5 m BSF).

When a planar feature such as a fracture plane intersects the borehole at anything but a purely horizontal or

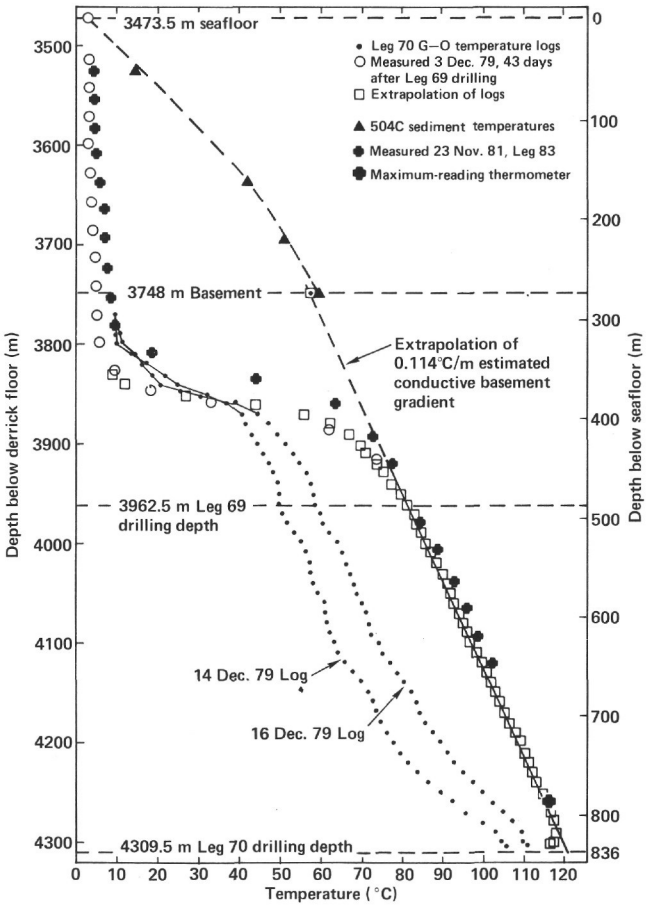

Figure 17. Hole 504B temperatures measured before and after Leg 70 drilling, with extrapolated equilibrium crustal temperatures. Superimposed are equilibrium temperatures measured during Leg 83, before any drilling disturbance.

vertical angle, a distinct sinusoidal pattern is seen. The steeper the dip, the more elongated the "nose" of the peaks. Although the BHTV records give a horizontal exaggeration of about 2:1; the sinusoidal pattern is readily identified, for example at 4002 and 4604 m (528.5 and 1130.5 m BSF). A steeply inclined intersection would produce a very long sinusoid "nose," or two long, vertical S-shapes. Such is the expected form of any dike contacts we might expect to find in the lower section of the hole. Indeed, such features can be seen in the intervals 4732–4734 and 4750–4754 m (1258.5–1260.5 and 1276.5–1280.5 m BSF). These features are perhaps the only support in the BHTV record for the existence of dikes in this hole.

Using the drilling records to correlate between the BHTV records and the recovered cores, it is possible to approximate the contacts between units with different lithologies. Changes in drilling rate seem to correlate well with changes from chaotic to massive units. In some cases, the dark and light bands in the BHTV record are offset at contacts, producing a rough S-shape across the photograph such as at 4728 m (1245.5 m BSF), which would correspond to the top of Lithologic Unit 131. Similarly, at 4687.5 m (1214.0 m BSF), a sinusoidal pattern may correlate with the chilled contact top of Lithologic Unit 121.

Correlation of the BHTV records with drilling records and recovered core provides constraints on the location of cored material in the section. This is particularly useful in instances of low recovery; on Leg 83, average recovery was 20% overall, 15% in the dikes.

The common practice in DSDP reports is to expand the lithologic units observed in the recovered cores to the entire cored interval in proportion to their recovered thicknesses. Because of the drilling process itself, the more massive material tends to be disproportionately represented.

We tried to improve upon this technique. We started by using the BHTV images to establish a pattern of pillow, massive, and brecciated units over a coring depth interval. The drilling torque records provided a time continuity of hard versus easy drilling for each core. Each recovered lithologic unit was then assigned to its appropriate position in the drilling history of the core, depending on its character. For example, a massive unit would be recovered during a period of hard drilling, whereas rubble would be recovered during a period of easier drilling.

Correlation of the temporal drilling history with the spatial pattern as revealed in the BHTV images allowed us more accurately to estimate both where each of the recovered units was located and the thickness of those units.

The two lithostratigraphic columns can be compared in Figure 20. On the left is the lithostratigraphic column derived on board from coring depth and the petrologic character of the recovered material. The low recovery is apparent. To the right we see the correlated lithostratigraphic column. The unit thicknesses are correlated. It is clear that the thickness of several lithologic units has been changed and the estimate of brecciation in each unit refined. This correlated lithostratigraphic column is a more accurate representation of the *in situ* locations of the recovered material.

LARGE-SCALE RESISTIVITY EXPERIMENT

The large-scale resistivity experiment is designed to monitor bulk crustal electrical resistivities, averaged over radial scales on the order of 10–100 m away from the hole. This scale is considerably larger than the effective penetration depths of conventional logging tools, so the large-scale results are much less affected by small-scale formation heterogeneities and physical drilling disturbance to the formation near the borehole. Since the electrical conductivity of seawater is on the order of 10–1000 times greater than that of basalt, the bulk resistivity of a seawater-saturated formation is strongly dependent on its bulk porosity. Thus the large-scale resistivity experiment can yield estimates of bulk porosities, at averaging scales large enough both to escape the effects of drilling disturbances near the hole and to include the effects of possible large-scale fracture porosity.

Despite fears about the capability of the cable to withstand temperatures near 100°C, the large-scale resistivity experiment was run successfully on Leg 83 over the

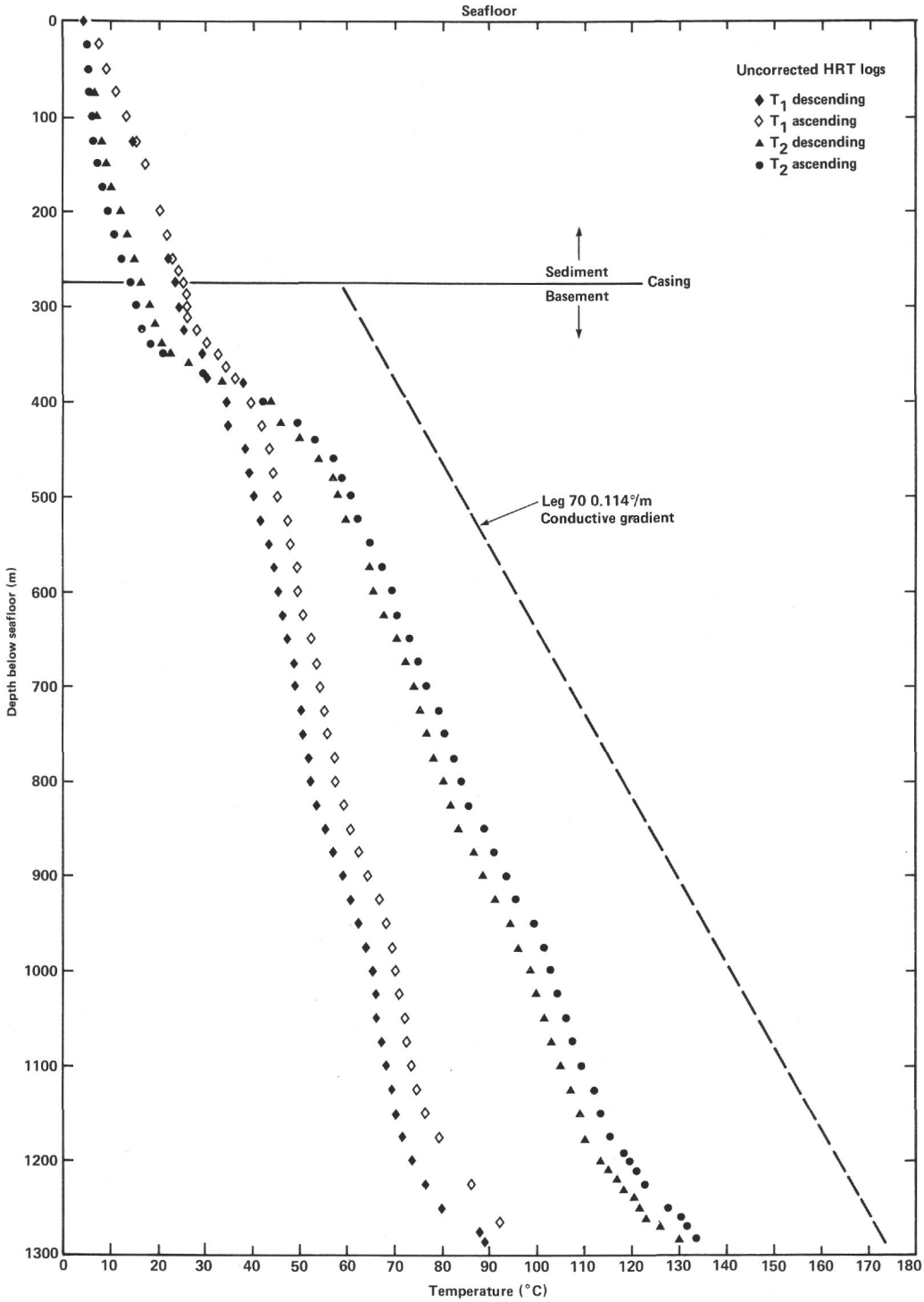

Figure 18. Uncorrected temperature logs measured within 3-1/2 days of the end of Leg 83 drilling and circulation in Hole 504B.

entire open section of Hole 504B. Excellent data were obtained throughout the upper km of basement, from the casing at 274.5 m sub-bottom down to 1287.5 m. In the Leg 70 section of the hole, the Leg 83 experimental results closely corroborated the results of a similar Leg 70 experiment (Von Herzen et al., 1983) with crustal resistivities on the order of 10 Ω-m, suggesting bulk porosities of about 15 to 5%, decreasing with depth. below the Leg 70 hole depth of 836 m, an extreme gradient in resistivity was observed, with a peak value of 750 Ω-m occurring at the bottom of the hole (see Fig. 21). This suggests a sharp decrease in bulk crustal porosities, to less than 1% one km into basement.

The large-scale resistivity experiments in Hole 504B are discussed in greater detail by Becker et al. (1982) and Becker (this volume).

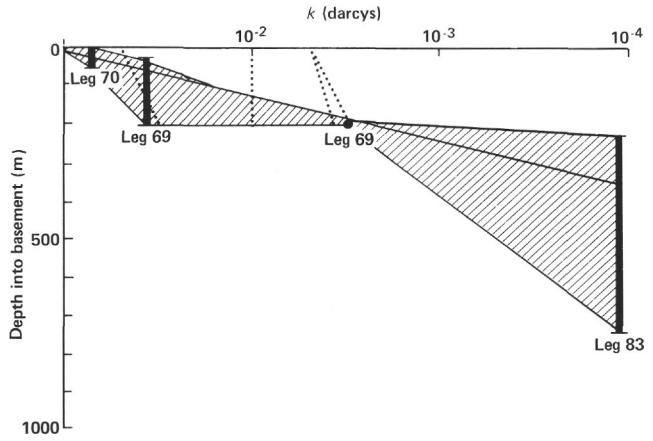

Figure 19. Bulk permeability values versus depth in Hole 504B. The vertical bars indicate the depth intervals over which the bulk permeability was measured. The solid line is the exponential fit of permeability to depth.

LOGGING

Interpretation of Deep Sea Drilling Project results in basaltic oceanic crust has always been hampered by low core recovery. The average recovery is ~30%, and drilling into the dike complex for the first time on Leg 83 has set new records for lowest percentage recovered (20% overall and <15% in the dikes). But geophysical logging does not merely fill gaps not cored. The suite of logs run on Leg 83 provides a scale of observation that spans the gap from cores (mm to cm resolution) to surface geophysics (hundreds of meters to kilometer resolution). A log "sees" cm to m variations both up and down the wellbore and radially away from the hole. Beyond providing a scaling factor for correlation of cores and surface geophysics, logs provide primary information on the *in situ* physics of the oceanic crust.

Leg 83 represents the first attempt to take the advanced capabilities of Schlumberger logging equipment beyond "routine" logging. The results have been most encouraging. In the future, ocean crustal logging could be right at the forefront in development of new techniques. Logs custom-made to the ocean crust can be designed and carried out with existing technology.

For example, the sonic logging sonde from Schlumberger sends back four complete waveforms for each transmitted sonic pulse. Previously, even in the oil industry, that waveform was recorded for processing back in the lab to "pick" shear wave arrivals. By changing the programmed gating and filtering package within the Schlumberger computer van, we were able to make the first ever (to our knowledge) real-time downhole S-wave log. Recording S-waves as well as P-waves gives us a direct measure of the variation in elastic properties of the country rock on a foot to foot scale through Poisson's ratio. Since fractured rock, clay, and other alteration products have very different elastic properties from solid fresh basalt, we would then take a major step toward understanding the fracture distribution and extent of alteration over the entire length of the wellbore.

What Logs See

Geophysical logs in various combinations are able to discriminate among different lithologies and structures. Four lithologies are distinguishable in Hole 504B: pillows, breccias, massive flows, and dikes. Additionally, structural features such as fracture zones, voids, alteration zones, and the area of invasion of the seawater drilling fluid into the formation are determinable from logs.

The primary parameters transmitted back to the surface, however, are porosity, density, electrical resistivity, and seismic velocity (a function of elastic properties). Each of the logs distinguishes lithologies and structures to *differing* extents. This is good because it allows the isolation of specific parameters through cross-correlation. For example, the neutron porosity log "sees" all the hydrogen in the wall rock, whether in alteration products as hydroxyl, in pore waters, or in the rock itself, whereas the gamma-ray density tool "sees" only rock and seawater. Hydroxyl (alteration) content versus depth can be isolated by examining the cross-plot of the two logs with depth. But the Schlumberger computer does this in a sophisticated way—correcting for temperature, pressure, hole size, and rugosity (wall roughness) at each data point. The result on Leg 83 was the first-ever alteration-analysis log for the oceanic crust.

Below we detail each log (Figs. 21 and 22) and its data quality before presenting the new logs and a brief interpretation. Depths are referred to the rig floor, 3473.5 m above the seafloor, with depths below seafloor given in parentheses.

Resistivity

A dual laterolog (DLL) was attempted but failed downhole so a dual induction log (DIT) with spherically focused laterolog (SFL) was sent down with natural gamma ray and SP logs in combination. As always in the oceanic crust, the latter two were virtually useless because of the low radioactive content of basalt and the use of seawater as a drilling fluid.

The problem with induction logs in seawater-basalt holes is that in resistive formations, the accuracy of these tools falls off dramatically. They measure electrical conductivity directly and so are strongly affected by seawater. In fact, the induction log produced poor results below 4000 m (526.5 m BSF) in the hole, the laterolog giving much more representative resistivities toward the bottom of the hole. The laterolog focuses a strong current into the wellbore and away from the annulus, thereby overcoming the seawater problem. Resistivity from the laterolog increases with depth in a manner similar to that of the long-spacing resistivity log (see Becker et al., this volume). Since penetration is 2–3 ft. into the wall, results similar to those of the long-spacing tool would imply uniform resistivity structure.

Proceeding downward from the surface, the aquifer from 3750 to 3850 m (276.5 to 376.5 m BSF) has very low resistivity (≈10 Ω-m) except for the massive flow at 3750–3800 m (306.5–326.5 m BSF). Then resistivity in-

creases to ≈50 Ω-m at 4000 m (526.5 m BSF), below which it kicks back to low resistivity. This low from 4000 to 4390 m (526.5 to 916.5 m BSF) is the most highly altered section of the hole. As with the long-spacing tool, there is a dramatic increase below 4390 m (916.5 m BSF). This point also is where an increase in thermal conductivity and a drop in magnetic susceptibility occurs in the solid rock cores. From there on down, the rock rather than the porous fracture pattern controls the bulk resistivity of the hole. A steady gradient increase in resistivity to the bottom of the hole peaks at over 200 Ω-m. Although Archie's Law breaks down at high resistivities, porosities must be ≈1% at the bottom of the hole (see Becker et al., 1982, and Becker, this volume).

Nuclear

Two very successful active-source nuclear logs were run in tandem with a temperature probe, three-armed caliper, and natural gamma ray log in Hole 504B on Leg 83.

The neutron porosity tool (CNL) has two detectors spaced so as to "see" 8 and 16 in. away from the source from a Am^{241}-Be emitter. The purpose is to compensate for hole rugosity and diameter changes. Porosity is calculated using a type curve. Since DSDP has never generated a basalt type curve, porosities (ϕ) are displayed relative to a tight limestone. Relative changes are real, however.

This tool measures how much the high-energy neutrons emitted by the source are slowed by collision with the nuclei of elements in the formation. The elements that have an atomic mass closest to that of the neutrons slow the neutrons more than elements that have fairly large atomic mass. Hydrogen, having about the same atomic mass as the neutrons, slows neutrons more readily than other elements. Therefore, what the neutron porosity tool predominantly measures is the hydrogen ion content in the formation. This tool then measures not only the porosity of the rock (ϕ) but hydroxyl content of the country rock and its alteration products in the country rock.

The other useful nuclear tool is the density log. This tool measures, again at a near and far receiver, the Compton scattering of a gamma ray flux emitted by a Cs^{127} source, which is directly a function of the electron density of the rock and matrix. This tool sees density (ρ_b) which is only a function of the density of pore fluid (ρ_f) times the percentage of that pore fluid (ϕ_f) plus the density of the remaining country rock (ρ_R):

$$\rho_b = \phi_f \rho_f + (1-\phi)\,\rho_R\ .$$

Density and porosity structure at Hole 504B show very low values in the aquifer with heavily altered (high ϕ, low ρ_b) zones from 4000 to 4150 and 4250 to 4390 m (526.5 to 676.5 and 776.5 to 916.5 m BSF). Again, there is a big density increase at 4390 m (916.5 m BSF), but neutron porosity stays high until 4500 m (1026.5 m BSF), indicating high alteration of the basalts in this zone.

The caliper log on this tool worked best of all. It shows washouts in the aquifer only with a sharp drop to gauge-hole at 3830 m (356.5 m BSF). From there on down, the hole is to gauge. It gets even tighter from 4520 m (1046.5 m BSF) to the bottom, remaining just above bit size.

Sonic

The Schlumberger sonic sonde used on Leg 83 is a two-transmitter (15 kHz, 15 times/s), two-receiver, long-spacing tool giving four channels of full-wave-form recording at 8, 10, 10, and 12 ft. spacing from the transmitter. The sonde is centralized top and bottom in the hole, giving the first truly high quality sonic logs on the *Challenger*. Several runs with two different sondes were made and the repeatability was excellent.

The sonic log was run in several modes. First a traditional P-wave first-arrival log was run. Then full-wave-form digitization of all four channels was recorded for deconvolution and stacking upon return to shore. This noise reduction will produce quality wave trains to quantify attenuation of the Stonely wave seen clearly on each of the wave-form tracks (Fig. 22). Additionally, an S-wave log was recorded *in situ* (Fig. 21), proving the routine capability for recording such logs on the *Challenger*. A moving-window gate was forced to cancel out the P-wave arrival and a noise amplitude trigger "fooled" the P-wave software into picking the larger-amplitude S-wave arrival. The log gave very satisfactory values up the hole but the rapid drop in velocity at the top of the hole caused us to make several gate resettings. The *steps* on the log occurred because we did not set the gate back quickly enough, thus forcing the first arrival to see the second or third ring of the S wave. This was only a problem at 3840–3850 m (366.5–376.5 m BSF), where 0.2 km/s must be added, at 3875–3910 m (401.5–436.5 m BSF) (−0.3 km/s), and at 4125–4155 m (651.5–681.5 m BSF), (−0.4 km/s). This can easily be corrected on shore.

Structurally, we see a low P- and S-wave velocity over the upper 100 m (aquifer S-velocity drops to 21.0 at some locations). Layer 2A consists of a steep velocity gradient over the upper 200 m of basalt. There is a low-velocity zone at 4050–4100 m (576.5–626.5 m BSF) that was completely missed by earlier Leg 70 sonic logging, and again, a velocity increase at 4390 m (916.5 m BSF) from which the velocity remains relatively constant to the bottom of the hole. S-wave velocities reach 3.4 km/s in the dyke complex, dropping to 3.0 at 4175 m (701.5 m BSF), then falling rapidly toward the surface. The S waves do not track with the P waves, indicating that a Poisson's ratio log is of great interest (Newmark et al., this volume).

The body wave logs show a strong Stoneley arrival from 4750 to 4390 m (1276.5 to 916.5 m BSF)—the depth above which attenuation begins. Attenuation zones upward from that depth (and two small ones below) correlate with zones of high alteration, dense fracturing, and low borehole televiewer reflectivity (Fig. 21). Signal in the reservoir is so attenuated that gain was increased

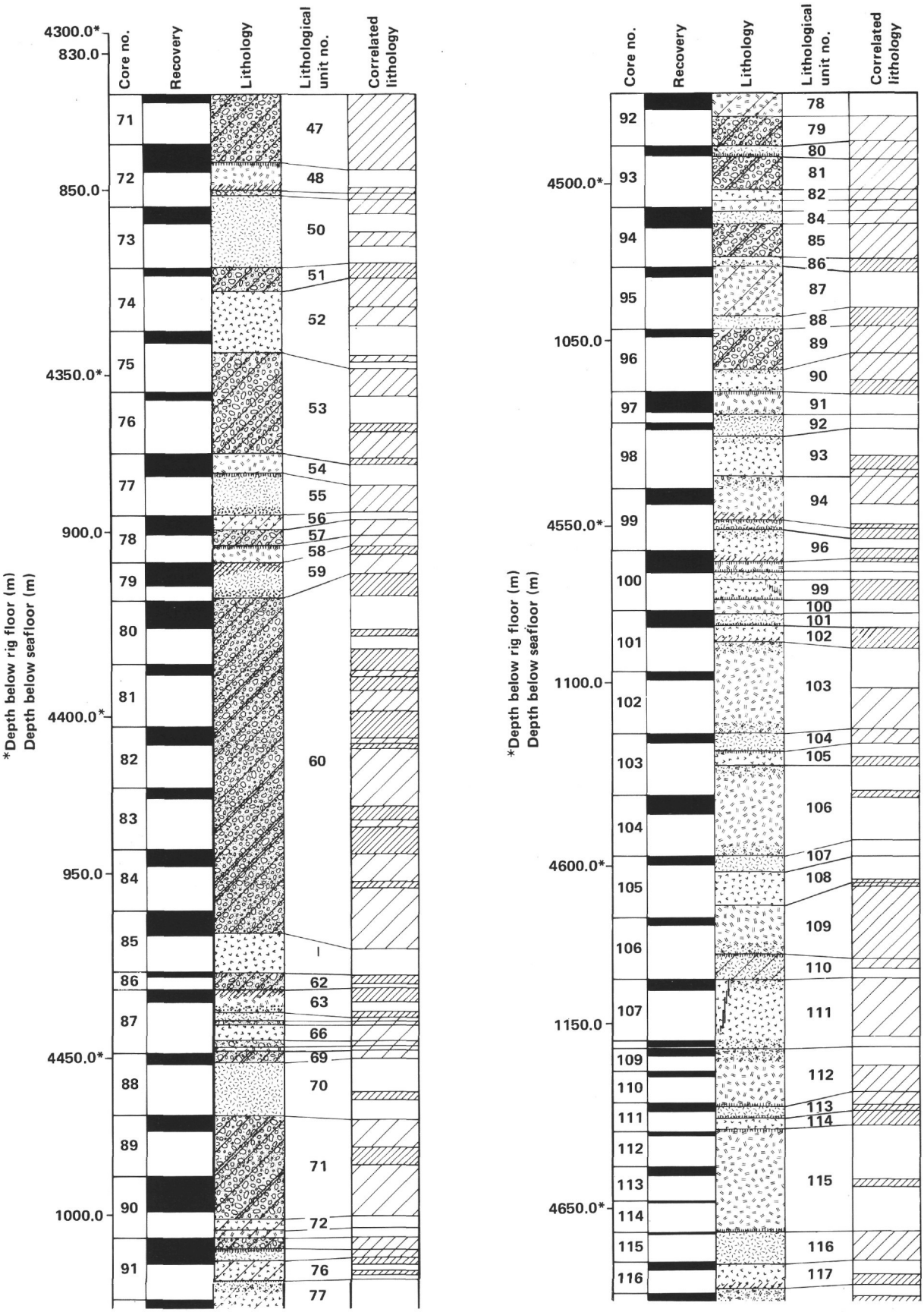

Figure 20. Lithostratigraphy of the Leg 83 section of Hole 504B (left), compared with the "correlated lithology" determined with the borehole televiewer (right).

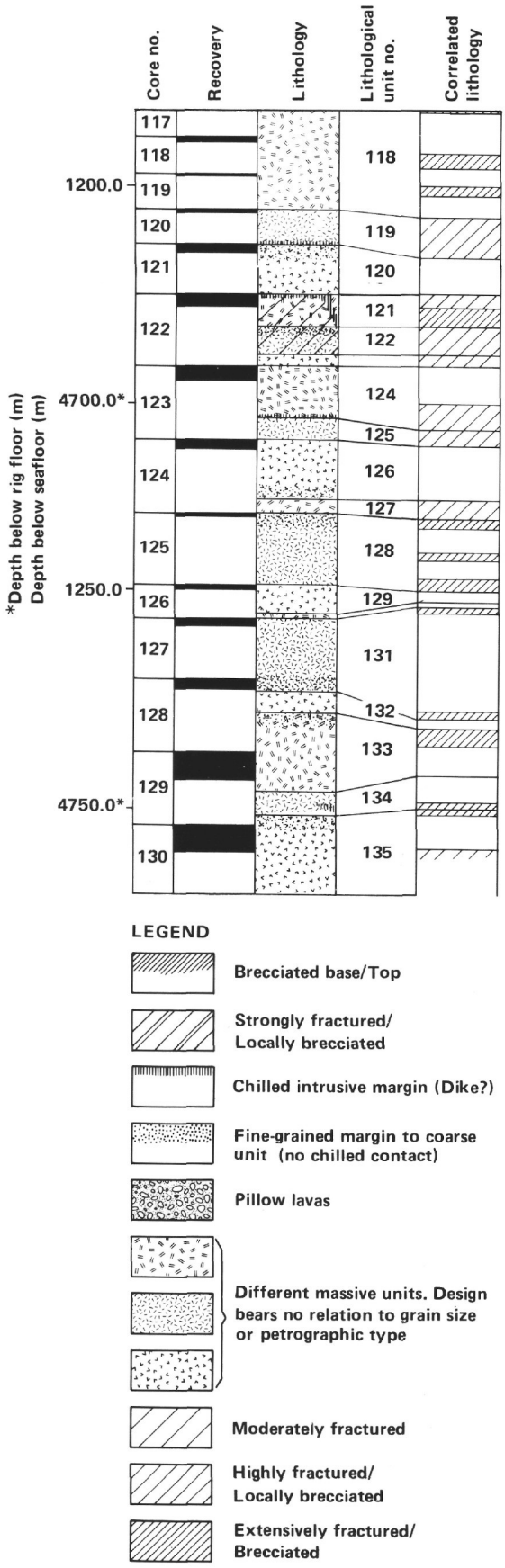

Figure 20. (Continued).

fivefold during the P-wave logging run from 3900 to 3750 m (426.5 to 276.5 m BSF).

Clay Analysis Log

Wanting to quantify alteration changes down the hole, we used a rapid shale-index cross-correlation program called DWQL, part of the Schlumberger CYBERLOOK processing package. This on-site program does a small-scale clay analysis. The technique is conceptually simple. Each log "sees" rock, pore fluid, and chemically bound water differently. The programs available on shore will use the entire suite of logs for cross-correlation. Here we used only two, the density and neutron porosity logs.

The neutron porosity log responds to all the hydrogen present in the oceanic crust (including hydroxyl):

$$\phi_N = S_w + V_{CL} + V_{NCL} + (1 - \phi - V_{CL})\,\phi_{NR}\,, \quad (1)$$

where

ϕ_N = neutron porosity,
ϕ = actual formation porosity,
S_w = water saturation,
V_{CL} = bulk-volume fraction hydrated minerals,
V_{NCL} = neutron log response to V_{CL} of 100% calibrated to ocean crustal cores,
ϕ_{NR} = neutron log response to 100% solid basalt.

The density log responds differently to porosity:

$$\phi_D = S_w + V_{CL}\,\phi_{DCL}\,, \quad (2)$$

where

$$\phi_{DCL} = \frac{\rho_R - \rho_{CL}}{\rho_R - \rho_W}\,.$$

The DWQL program cross-correlates ϕ_N and ϕ_D, determining a term ϕ_A. This term has been corrected for effects of temperature and pressure increases downhole, rugosity, and hole size. At each ϕ_A versus depth point, the program calculates the clay index V_{CL} from equations (1) and (2) and plots it as the alteration percentage at that depth. The only user inputs are ρ_R, ρ_{CL}, ϕ_R, and ϕ_{CL}. Those values are calibrated to the cores from Hole 504B; then the program plots out V_{CL}.

For example, suppose a large fracture system at 4050–4060 m (576.5–586.5 m BSF) is full of clay and zeolite minerals. Then ϕ_N is high because clay absorbs neutrons, but ϕ_D is also high because the formation is more dense than if seawater filled the fractures. The program will require a higher value of V_{CL} to solve for ϕ_N and for ϕ_D than for the opposite case, where, for example, at 3840–3850 m (366.5–376.5 m BSF) a fracture zone is filled with seawater and not alteration minerals. The ϕ_D, ϕ_N, and V_{CL} would be small. The interesting cases are those where ϕ_N and ϕ_D are asymmetrical. The program then is conservative and selects the smaller V_{CL} value.

The results from this analysis are extremely encouraging. The change at 4390 m (916.5 m BSF) shows up as a $\approx$ 10% drop in alteration pervasiveness below 916.5

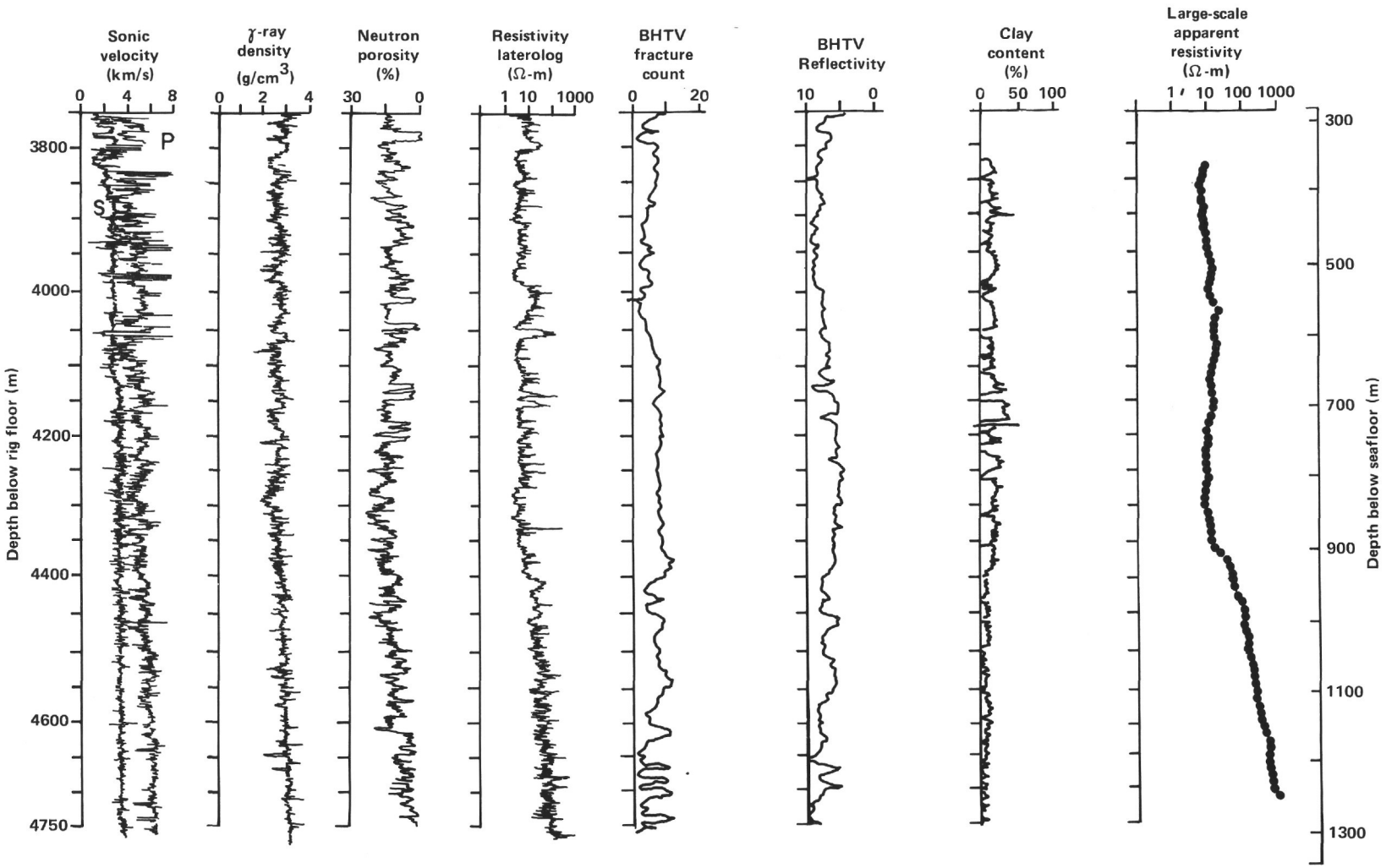

Figure 21. Leg 83 geophysical logs in Hole 504B. Note changes in slopes at the Layer 2A/2B and Layer 2B/2C boundaries, about 375 and 900 m below seafloor, respectively.

m, yet the remarkable zone of intense, high-temperature alteration at 4450 m (976.5 m BSF) is clearly present. In the aquifer, where the amount of alteration decreases and ϕ increases, the V_{CL} log also decreases relative to its value lower down in the more highly altered pillow zone.

Summary

Comparing the Leg 83 logging results with those during Leg 69 and 70, we find the earlier logs seriously in error in the worst cases (e.g., sonic), and only of fair quality in the best cases. The Schlumberger logs carried out on Leg 83—S-wave, body wave, borehole televiewer (see Newmark et al., this volume; Anderson et al., this volume) and alteration logs—go much farther than previously possible to define the physics of the upper oceanic crust in Hole 504B.

REFERENCES

Anderson, R. N., and Zoback, M. D., 1982. Permeability, underpressures, and convection in the oceanic crust near the Costa Rica Rift, eastern equatorial Pacific. *J. Geophys. Res.*, 87:2860–2868.

Anderson, R. N., Honnorez, J., Becker, K., Adamson, A. C., Alt, J. C., Emmermann, R., Kempton, P. D., Kinoshita, H., Laverne, C., Mottl, M., and Newmark, R. L., 1982. DSDP Hole 504B, the first reference section over 1 km through Layer 2 of the oceanic crust. Nature, *300*:589–594.

Becker, K., Von Herzen, R. P., Francis, T. J. G., Anderson, R. N., Honnorez, J., Adamson, A. C., Alt, J. C., Emmermann, R., Kempton, P. D., Kinoshita, H., Laverne, C., Mottl, M., and Newmark, R. L., 1982. *In situ* electrical resistivity and bulk porosity of the oceanic crust, Costa Rica Rift. *Nature, 300*:594–598.

Becker, K., Langseth, M. G., and Von Herzen, R., 1983. Deep crustal geothermal measurements, Hole 504B, Deep Sea Drilling Projects Legs 69 and 70. *In* Cann, J. R., Langseth, M. G., Honnorez, J., Von Herzen, R. P., White, S. M., et al., *Init. Repts. DSDP*, 69: Washington (U.S. Govt. Printing Office), 223–235.

Becker, K., Langseth, M. G., Von Herzen, R. P., and Anderson, R. N., 1983. Deep crustal geothermal measurements, Hole 504B, Costa Rica Rift. *J. Geophys. Res.*, 88:3447–3457.

Bougault, H., 1977. Major elements: analytical chemistry on board, and preliminary results. *In* Aumento, F., Melson, W. G., et al., *Init. Repts. DSDP*, 37: Washington (U.S. Govt. Printing Office), 643–657.

Cann, J. R., Langseth, M. G., Honnorez, J., Von Herzen, R. P., White, S. M., et al., 1983. *Init. Repts. DSDP*, 69: Washington (U.S. Govt. Printing Office).

CRRUST (Costa Rica Rift United Scientific Team), 1982. Geothermal regimes of the Costa Rica Rift, east Pacific, investigated by drilling, DSDP-IPOD Legs 68, 69 and 70. *Geol. Soc. Am. Bull.*, 93: 862–875.

Emmermann, R., and Puchelt, H., 1980. Major and trace element chemistry of basalts from Holes 417D and 418A, Deep Sea Drilling Project Legs 51–53. *In* Donnelly, T., Francheteau, J., Bryan, W., Robinson, A., Flower, M., Salisbury, M., et al., *Init. Repts. DSDP*, 51, 52, 53, Pt. 2: Washington (U.S. Govt. Printing Office), 987–1000.

Furuta, T., and Levi, S., 1983. Basement paleomagnetism of Hole 504B. *In* Cann, J. R., Langseth, M. G., Honnorez, J., Von Herzen, R. P., White, S. M., et al., *Init. Repts. DSDP*, 69: Washington (U.S. Govt. Printing Office), 697–703.

Hubberten, H.-W., Emmermann, R., and Puchelt, H., 1983. Geochemistry of basalts from Costa Rica Rift Sites 504 and 505 (Deep Sea Drilling Project Legs 69 and 70). *In* Cann, J. R., Langseth, M. G., Honnorez, J., Von Herzen, R. P., White, S. M., et al., *Init. Repts. DSDP*, 69: Washington (U.S. Govt. Printing Office), 791–803.

Kidd, R. G. W., and Cann, J. R., 1974. Chilling statistics indicate an ocean-floor spreading origin for the Troodos Complex, Cyprus. *Earth Planet. Sci. Lett.*, 24:151–155.

Kristmansdottir, H., 1975. Hydrothermal alteration of basaltic rocks in Icelandic geothermal areas. *Proc. Second U. N. Symp. on Devel. Use Geothermal Resources*, 1:441–445.

Liou, J. G., 1971. Laumontite equilibria. *J. Petrol.*, 12:370–411.

Melson, W. G., Rabinowitz, P. D., Natland, J. H., Bougault, H., and Johnson, H. P., 1979. Cruise objectives and major results, analytical procedures, and explanatory notes. *In* Melson, W. G., Rabinowitz, P. D., et al., *Init. Repts. DSDP*, 45: Washington (U.S. Govt. Printing Office), 5–20.

Moores, E. M., and Vine, F. J., 1971. The Troodos Massif, Cyprus and other ophiolites and oceanic crust: evaluation and implications. *Phil. Trans. R. Soc. Lond. A*, 268:589–603.

Natland, J. H., Adamson, A. C., Laverne, C., Melson, W. G., and O'Hearn, T., 1983. A compositionally nearly steady-state magma chamber at the Costa Rica Rift: Evidence from basalt glass and mineral data, DSDP Sites 501, 504, and 505. *In* Cann, J. R., Langseth, M. G., Honnorez, J., Von Herzen, R. P., White, S. M., et al., *Init. Repts. DSDP*, 69: Washington (U.S. Govt. Printing Office), 811–858.

Puchelt, H. R., and Emmermann, R., in press. Petrogenetic implications from tholeiite basalt glasses from the East Pacific Rise and the Galapagos Spreading Center. *Chem. Geol.*

Von Herzen, R. P., Francis, T. J. G., and Becker, K., 1983. *In situ* large-scale electrical resistivity of ocean crust, Hole 504B. *In* Cann, J. R., Langseth, M. G., Honnorez, J., Von Herzen, R. P., White, S. M., et al., *Init. Repts. DSDP*, 69: Washington (U.S. Govt. Printing Office), 237–244.

Von Herzen, R. P., and Maxwell, A. E., 1959. The measurement of thermal conductivity of deep-sea sediments by a needle-probe method. *J. Geophys. Res.*, 64:1557–1563.

Williams, H., and Malpas, J., 1972. Sheeted dykes and brecciated dyke rocks within transported igneous complexes, Bay of Islands, western Newfoundland. *Can. J. Earth Sci.*, 9:1216–1229.

Yokota, T., Kinoshita, H., and Yueda, S., 1980. New DSDP (Deep Sea Drilling Project) downhole temperature probe utilizing IC RAM (memory) elements. *Bull. Earth. Res. Inst. Tokyo*, 54:441–462.

Date of Initial Receipt: 1 January 1983
Date of Acceptance: 19 August 1983

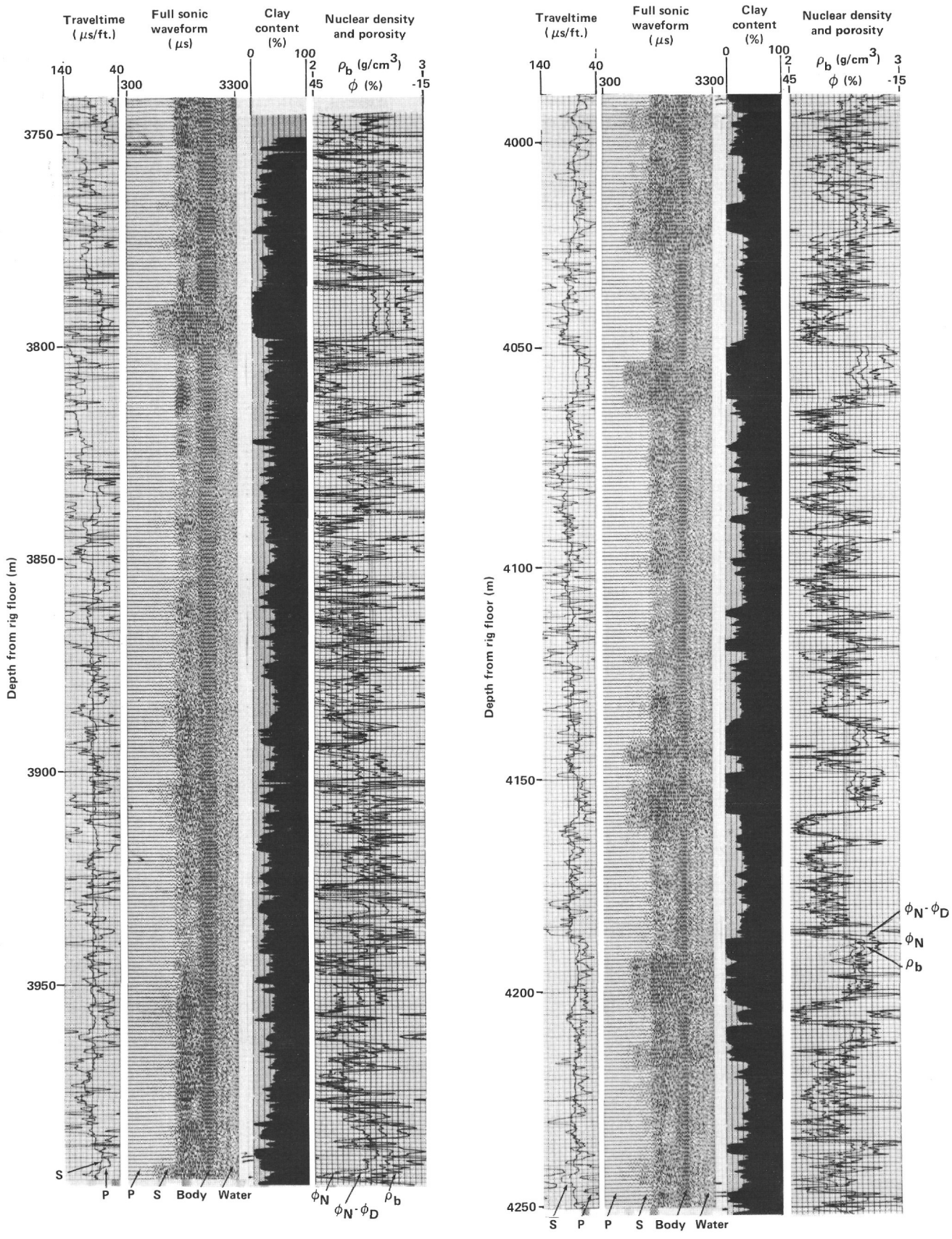

Figure 22. Leg 83 Schlumberger logs from Hole 504B.

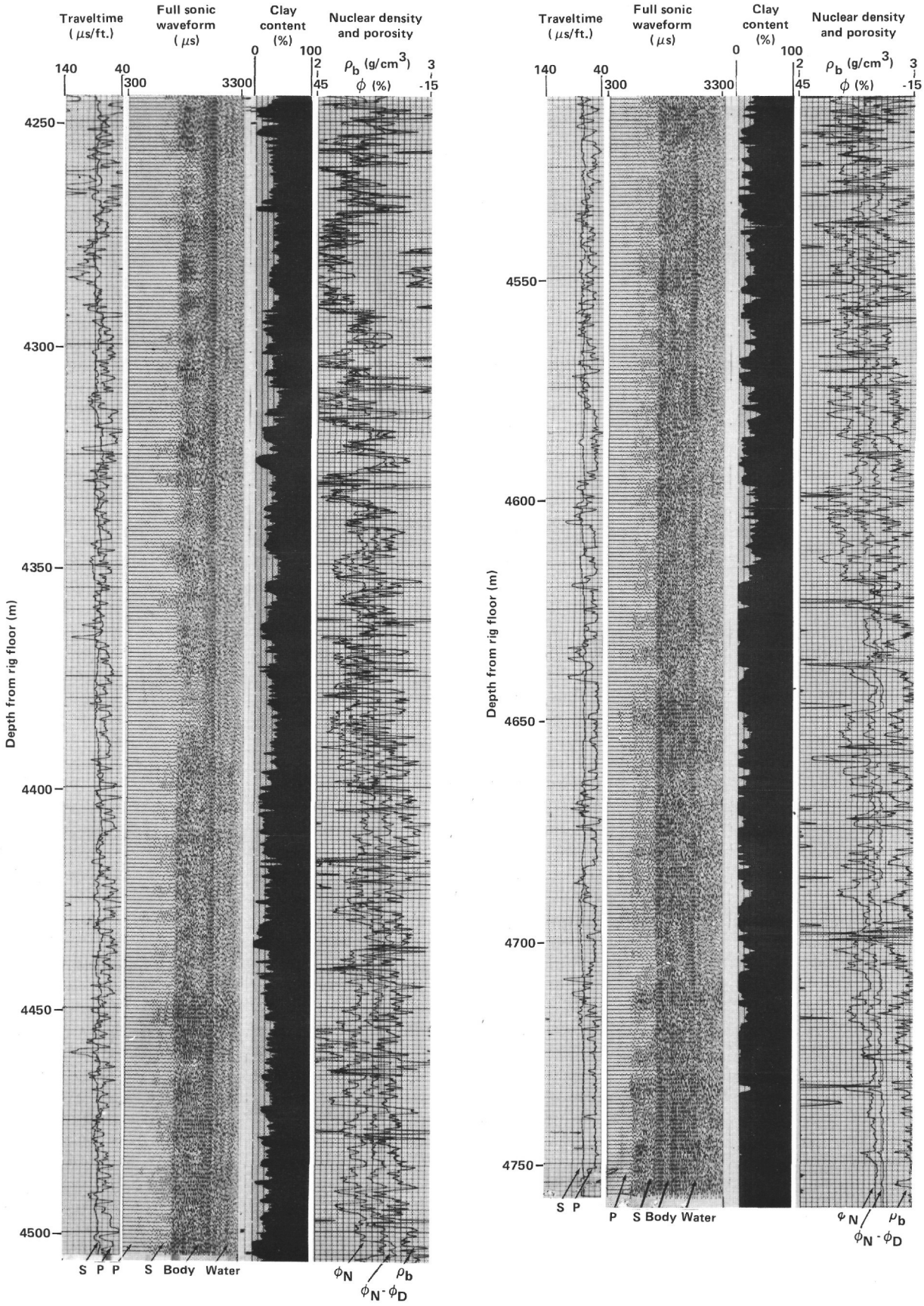

Figure 22. (Continued).

cm
0
50
100
150
Core-Section
Piece Number
Graphic Representation
Orientation
Shipboard Studies
Alteration
71-1
Unit 47
PP
T
72-1
TS
T
M
Unit 48
Unit 47
72-2
Void
PP
T
Unit 48
72-3
XRF
XRD
T
Unit 49
Unit 48
72-4
Unit 50
73-1
XRF
XRD
PP
M
Unit 50
73-2
XRD
T
M
Unit 50

Unit 47 (836.0–846.0 m).

This unit consists of a series of pillow lavas, individual pillows separated by glassy rims and/or fine grained areas, on the top/bottom of oriented samples. All the pillows are composed of a moderately olivine-plagioclase-clinopyroxene phyric basalt of a relatively uniform grayish-green color. In most pillows, phenocrysts constitute about 10% of the rock of which olivine (2–3 mm) forms 2–3% plagioclase (2–3 mm) 4–10% as euhedral crystals and glomerocrystic clumps, and clinopyroxene (2 mm) about 2% in total. All phenocrysts are euhedral, the feldspars often exhibiting normal or oscillatory zoning. Textures are intergranular to subophitic in pillow centers, grading into variolitic at glassy margins. Veins are abundant (average width of less than 2 mm), filled with dark green clay minerals (saponite?) often with a radiate form. Rarely, a white fibrous mineral can be found in association with the green clays. Pyrite is common on fractured surfaces. Adjacent to some veins and in all fine-grained pillow margins, the basalt appears pale gray in color. Olivine is completely replaced by dark green clay minerals. Rare breccias are also cemented by green clays which are visually identical to those filling both the veins and pseudomorphs.

Unit 48 (846.0–850.0 m).

This unit comprises a homogeneous, fine-grained, dark grayish-green, moderately olivine-plagioclase-clinopyroxene phyric basalt. An intrustive contact (confirmed by thin section study) delineates the upper margin of the unit (dike?), while the lower is highly brecciated and exact relationships with the subsequent pillow hyaloclastic breccias are unclear. Phenocrysts constitute about 10–12% of the rock of which olivine (1–4 mm) forms 3–5%, plagioclase (0.4–2 mm) 5%, and clinopyroxene (approximately 1 mm) about 1%. Feldspar phenocrysts occur as single euhedral crystals (An_{72-83}), or in glomerocryst clumps where oscillatory zoning is apparent. Clinopyroxene phenocrysts are on the whole subhedral. A few small euhedral crystals of chrome spinel are recognizable in thin section. Textures are subophitic. Groundmass and phenocryst olivine are replaced by dark and light green clays in a concentric arrangement, previously observed during Leg 70. Fractures filled by dark green radiating clays, and a white mineral, are common. Pyrite is evident on most broken vein surfaces.

Unit 49 (850.0–850.8 m).

This unit consists of a thin series of pillow lavas recognized by grain size and from the occurrence of chilled pillow margins and hyaloclastic breccias. The basalt is a dark greenish-gray color, and is moderately olivine-plagioclase phyric. Phenocrysts form about 8–9% of the rock, of which olivine (2–4 mm) forms approximately 5%, and plagioclase (3 mm) 3–4% in total. The pillows are fine-grained throughout. Olivine is completely altered to a dark green mineral, which also cements the hyaloclastic breccia and replaces the glass in pillow rims. Pyrite is disseminated on fracture surfaces.

Unit 50 (850.8–861.2 m).

This unit is a massive (dike/flow?) uniformly fine-grained, dark grayish-green, moderately olivine-plagioclase-clinopyroxene phyric basalt. Phenocrysts form about 7–10% of the rock, of which olivine (2–3 mm) forms 2–3%, plagioclase as euhedral phenocrysts (two phases, 0.8–1 mm An_{72-76} and 1.5–2 mm An_{82}) 3% in total, and as glomerocrysts (2–3 mm diameter) 2%, and clinopyroxene (approximately 2 mm) about 2–3%. Feldspars and clinopyroxenes distinctly larger than the equilibrium phenocrysts occur in subophitic to ophitic relationships. The feldspars in these aggregates are normal to slightly oscillatory zoned and, in common with the associated clinopyroxene, are partially resorbed. These have been interpreted as xenoliths from other dikes. Groundmass texture and grain size varies on the scale of millimeters in some thin sections, ranging from very fine granular to subophitic and ophitic textures. Olivine is totally altered to dark green clay minerals. Fractures are filled with similar colored clays which can be radiate in habit. Some veins show a multi-stage filling, pale green clays and calcite (XRD), associated with the more abundant dark green material. Iron sulfides are commonly associated with vein surfaces.

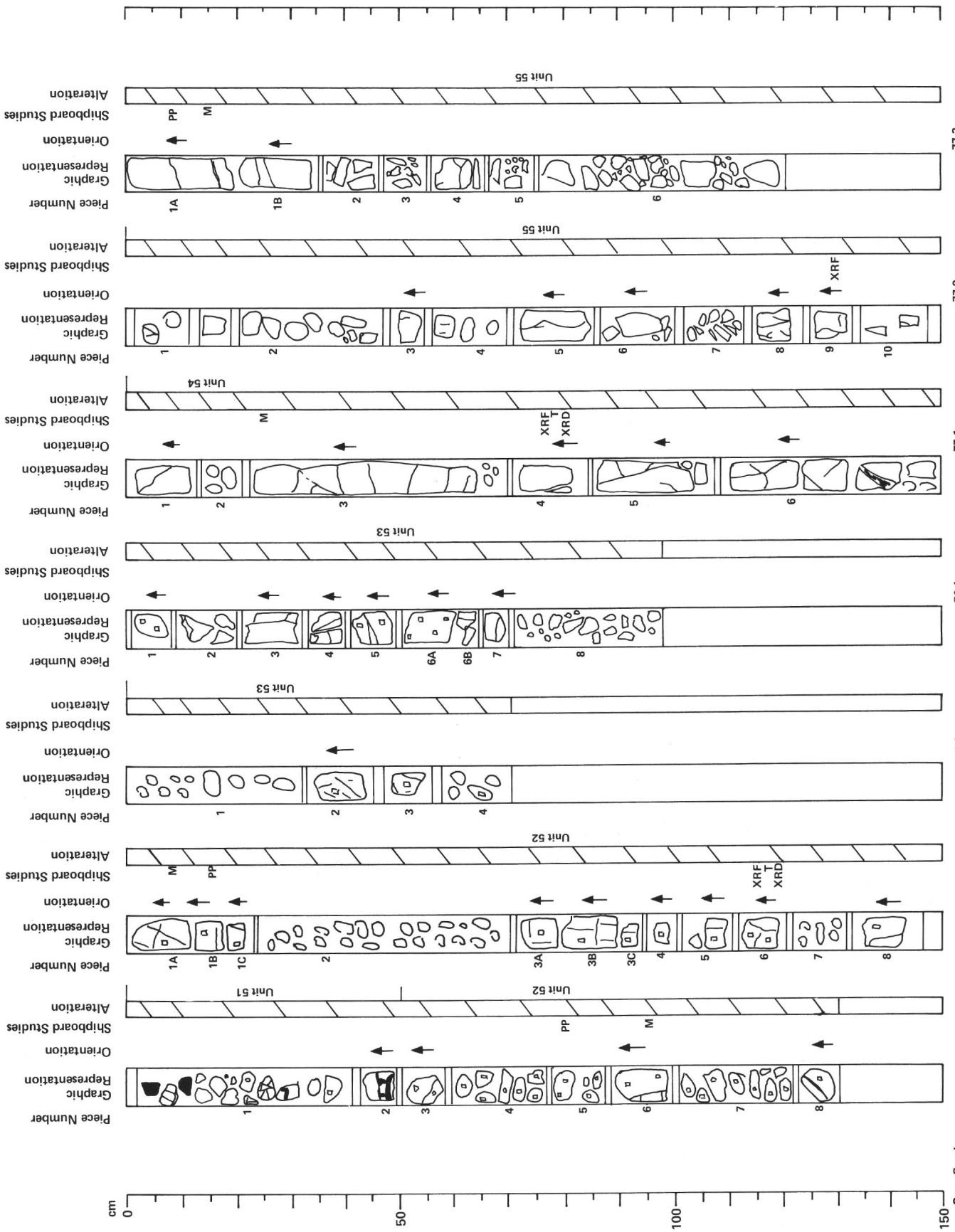
Core-Section
Piece Number
Graphic Representation
Orientation
Shipboard Studies
Alteration
74-1
75-1
75-2
76-1
77-1
77-2
77-3
Unit 51
Unit 52
Unit 53
Unit 54
Unit 55
XRF
XRD
T
PP
M
cm
0
50
100
150

Unit 51 (861.2–864.8 m).
This unit consists of a thin, pillow lava sequence composed of a sparsely to moderately olivine-plagioclase phyric basalt. All are fine-grained, grayish-green in color. Olivine phenocrysts vary in size from 0.5–3 mm, and are completely altered to dark green clays. Plagioclase phenocrysts tend to be smaller, only 0.5–2 mm in size. Much of the recovered material is heavily veined by dark green clays, or alternatively by a white fibro-radiated mineral (zeolite?) enveloped by dark green clay. Pillow rims tend to be aphyric, their glass areas completely altered to dark green clay, sulfides and a white mineral.

Unit 52 (864.8–873.8 m).
This unit is a massive (dike/flow?) uniformly fine-grained, grayish-green, aphyric to sparsely olivine-plagioclase phyric basalt. Olivine phenocrysts are up to 1.5 mm in size pseudomorphed by green clays, the plagioclase phenocrysts averaging 2 mm in size. Veins (average width 1 mm) are generally filled by green clays, accessory white minerals evident in some pieces. Iron sulfides are associated with vein surfaces.

Unit 53 (873.8–888.5 m).
This unit consists of a thick pillow lava sequence recognized from the fine-grained nature of the rock, the occasional quenched pillow margins (non-oriented), and the overall fractured appearance of the recovered material. The pillows vary from aphyric to sparsely-moderately olivine-plagioclase phyric basalt. In the latter cases, phenocrysts constitute from about 1–4% of the total rock of which olivine (1–3 mm) forms up to 1%, and plagioclase (less than 2 mm) about 3%. Clinopyroxene phenocrysts (0.6–0.8 mm) have been identified in thin section forming about 0.5% of the rock, but these were not recognized in hand specimen. Textures are subophitic in thin sections studied. The olivine is completely altered to green clays. Veins are filled by green clays, occasionally with a white mineral forming their centers. A reddish alteration band was observed on two pieces, varying from 5 mm to 10 mm in width.

Unit 54 (888.5–891.5 m).
This is a massive, uniformly textured aphyric, medium-grained, doleritic basalt. The lower margin to the unit lies against an intruded basalt from Unit 55 (intrusive contact confirmed by thin section). This contact is inclined at about 50° and appears extremely sharp. There is no evidence of fining towards the upper margin of the unit (dike/flow?). Veins and veinlets (less than 1 mm on average) are filled with bluish-green clays, together with common sulfides. There are also rare white minerals in a few fractures.

Unit 55 (891.5–897.5 m).
This unit is a massive, fine- to medium-grained, aphyric basalt. The top of the unit is chilled against Unit 54, steadily coarsening towards the center and possibly fining slightly towards its base (dike?). Textures are subophitic. Fractures (less than 1 mm on average) are filled by dark green clays with common sulfides. Slickensides are evident on some fracture surfaces.

cm
0
50
100
150
Core-Section
Piece Number
Graphic Representation
Orientation
Shipboard Studies
Alteration
78-1
78-2
79-1
79-2
79-3
Unit 56
Unit 57
Unit 58
Unit 59
XRD
M
T
XRF
PP

Unit 56 (897.5–899.7 m).
This unit consists of a fine-grained, grayish-green, aphyric basalt. There is no definite contact or decrease in grain size evident at the top of the unit. The lower margin is brecciated and lies adjacent to a chilled pillow margin and hyaloclastic breccia, both assigned to Unit 57. The whole of the unit is strongly fractured, veining so common as to approach a breccia towards it bottom. The veins/cement (up to 2 mm wide) are filled by light green clays, and in some areas by epidote and white minerals (quartz/calcite?). Iron sulfides are common in veins.

Unit 57 (899.7–902.0 m).
This unit consists of a thin, pillow-lava sequence. The upper contact is recognized by a chilled pillow margin and hyaloclastic breccia, and the lower by a chilled pillow margin intruded by later dike material (Unit 58). All the pillows are of the same grayish-green, aphyric, fine-grained basalt. Textures are subophitic. Veining is very intense, particularly in the brecciated areas towards the top of the unit. Fractures (2–12 mm) are filled by light and dark green clays, epidote and various white minerals. Pyrite is common in all fractures.

Unit 58 (902.0–904.5 m).
This unit is probably an intrusive dike. A sharp chilled contact delineates the upper margin, Unit 58 having been intruded into the preceeding pillow lavas of Unit 57 (confirmed by thin section). The actual inclination of this contact is unclear, since one of the two chilled pieces which form it, is disoriented. The unit coarsens towards its center (medium-grained), and fines at the base. The rock is grayish-green, sparsely olivine-plagioclase phyric. Phenocrysts form about 2% of the rock of which olivine (0.8–2 mm) forms about 1%, and plagioclase (1–2 mm) less than 1% in total. The plagioclase commonly occurs in glomerocrystic aggregates. All phenocrysts are euhedral in a subophitic groundmass. Alteration appears to be less intense than in the proceeding unit, possibly because fracturing is not as severe in competent lithologies. Olivine and glass in the chilled margins are altered to dark green clays, with associated pyrite.

Unit 59 (904.5–909.5 m).
This unit is a massive, aphyric to sparsely olivine-plagioclase phyric basalt. The top and center of the unit are uniformly fine-grained, becoming progressively finer towards the base (no chilled contact). The top is highly brecciated (approximately 30 cm), possibly corresponding to the rubble surface of a submarine lava flow. The overall color is a grayish-green. Phenocrysts form about 2% of the rock, olivine (0.5–2 mm) and plagioclase (up to 2 mm) phenocrysts in roughly equal proportions. Olivine phenocrysts are euhedral and completely altered to chlorite. Plagioclase phenocrysts occur either as separate subhedral crystals or sometimes as groups in glomerocrystic clumps. Textures are described as intergranular to intersertal. This unit is heavily veined, their width varying from 0.5 mm to 5 mm (average 2 mm). Veins are mostly filled by dark green chlorite, but can also be composite with white minerals, epidote and abundant pyrite. The breccia is cemented by similar green clays.

cm
0
50
100
150
CORE/SECTION
Piece Number
Graphic Representation
Orientation
Shipboard Studies
Alteration
Cuttings
1
2
3B
3A
3C
4
5
6
7A
7B
7C
7D
PP
M
XRD
Unit 60
80-1
1
2
3
4
5
6
7
8
9
10
11
12
Unit 60
80-2
1
2
3
4A
4B
5
6
7
8A
8B
8C
8D
8E
8F
8G
XRD
XRF
T
Unit 60
80-3
1A
1B
1C
2
T
Unit 60
80-4
1
2
3
4
5
6
7
8
9
10
11
12
13
14
15
16
17
T
M
Unit 60
81-1

Unit 60 (909.5–958.5 m).

This unit consists of a thick sequence of pillow lavas recovered in six consecutive cores (80 through 85). Numerous chilled pillow margins (several confirmed by thin section) and hyaloclastic breccias are distributed throughout the unit. Fracturing was so intense in some of the recovered material, from both the pillow margins and interiors, that recovery was reduced to rubble at several horizons. The upper sections of the unit (approximately Cores 80 through 83) consist of a sparsely to moderately olivine-plagioclase phyric basalt. Phenocryst contents can vary from 2% (sparsely phyric) to 6–8% (moderately phyric) depending on the pillows. In the sparsely phyric pillows, olivine (0.5–2 mm) and plagioclase (up to 2 mm) phenocrysts are in roughly equal proportions. In the more moderately phyric basalts the plagioclase content increases to about 5%, and the olivine to about 3% in total. Rare chrome spinel can be recognized in thin section as subhedral/euhedral micro-phenocrysts (0.2 mm). Olivine phenocrysts are euhedral and replaced by chlorite, plagioclase phenocrysts (exhibiting replacement by albite in varying degrees) commonly occur in glomerocrystic aggregates. Towards the base of the unit (Cores 84 and 85) the phenocrysts assemblages of the pillows change to include clinopyroxene; these are moderately olivine-plagioclase-clinopyroxene phyric basalts. The amounts of olivine and plagioclase phenocrysts in these pillows are similar to those described in the pillows from higher in the sequence and are again variably phyric but with anhedral/subhedral clinopyroxene phenocrysts (0.2–3 mm) forming an additional 1–5% of the rock. In both groups textures are dependent on the distance from the pillow margins or interior (see petrography chapter). All the pillows are of a similar pale grayish-green to green color. Alteration is intense most fractures and all the hyaloclastic breccias are cemented by clays and various other alteration minerals. Clays are generally a bluish-green or a dark green in color (chlorite). Laumontite, quartz, talc, and calcite, sometimes cutting earlier clay veins, and epidote are also common throughout the pillow sequence. Pyrite is abundant, often cementing the breccias together with chlorite. Sphalerite is present in some veins, but is not common.

cm
0
50
100
150
Core-Section
Piece Number
Graphic Representation
Orientation
Shipboard Studies
Alteration
Void
M
T
Unit 60
XRF
PP
82-1
82-2
82-3
83-1
83-2
84-1
84-2

cm
0
50
100
150
Core-Section
Piece Number
Graphic Representation
Orientation
Shipboard Studies
Alteration
Empty
Unit 60
Unit 61
Unit 62
Unit 63
Unit 64
Unit 65
Unit 66
Unit 67
Unit 68
Unit 69
Unit 70
Cuttings
XRD
XRF
T
M
PP
85-1
85-2
85-3
86-1
87-1
87-2
88-1

Unit 61 (958.5–964.5 m).
This is a massive, uniformly medium-grained, sparsely olivine-plagioclase-clinopyroxene phyric basalt unit (flow/dike?). Phenocrysts form about 3% of the rock, olivine (1.5–2 mm), plagioclase (2–3 mm) and clinopyroxene (1–1.5 mm) in roughly equal proportions. All phenocrysts are subhedral in a subophitic groundmass. Olivine is completely replaced by chlorite, plagioclase partially altered to albite(?). Fractures are few (average width of less than 1 mm) and are filled with dark green clay minerals (chlorite?) and minor white material. Pyrite is disseminated throughout the rock and in veins, but is less common than in the preceeding pillow unit.

Unit 62 (964.5–967.0 m).
This is a thin, pillow-lava sequence with a single pillow margin at the top and brecciated, fine-grained material at the base. The unit consists of a olivine-plagioclase-clinopyroxene phyric basalt which is greenish-gray in color. Phenocryst content varies from 2–4% of which olivine (less than 1 mm) forms less than 1%, plagioclase (less than 1.5 mm) between 1% and 2%, and clinopyroxene (less than 1 mm) less than 1% in total. Olivine phenocrysts are euhedral to subhedral and completely replaced by dark green chlorite. The plagioclase phenocrysts are subhedral and partially altered, the clinopyroxene varies from subhedral to anhedral in form. Veins are abundant filled by dark green clays, some may be cut by later veins filled with white minerals. Pyrite is disseminated throughout the unit.

Unit 63 (967.0–970.2 m).
This massive unit probably represents a submarine flow. There is a fining of grain size towards both the top and bottom of the unit, in addition to what is described as a cataclastite zone in the top 40 cm. The unit consists of a grayish-green colored, aphyric to sparsely olivine-plagioclase-clinopyroxene basalt. Phenocrysts form about 2–3% of the rock of which olivine (approximately 2 mm), plagioclase (0.4–1.3 mm) and clinopyroxene (0.8–1.5 mm) are present in roughly equal proportions. The clinopyroxene was mostly recognized in thin section as rounded equant to tabular crystals, present only in one hand specimen as ophitic crystals 3–5 mm across. Textures are described as intersertal to subophitic. Most fractures/veins (1–2 mm average) are filled by dark green chlorite, but a few have centers composed of white minerals. There are a few veins filled entirely by white minerals. Pyrite is disseminated throughout the rock, but is particularly evident in the white veins together with limited chalcopyrite.

Unit 64 (970.2–971.4 m).
This is a thin massive unit composed of an aphyric to sparsely olivine-plagioclase phyric basalt. The unit has the same characteristics as those of the preceeding unit, but is distinct in being medium grained and lacking cooling margins. Alteration is identical to that in Unit 63.

Unit 65 (971.4–972.0 m).
This unit is an extremely thin, pillow-lava sequence. It consists of a very fine-grained, aphyric basalt. There are no quench margins in the material recovered and assignment to a pillow unit has been made on the basis of their extremely fine grain size. Alteration characteristics are the same as in the two preceeding units.

Unit 66 (972.0–974.3 m).
This massive unit is composed of a uniformly medium- to coarse-grained, grayish-green, aphyric basalt. There are no chilled contacts and no evidence of fining. Textures are described as subophitic. Groundmass olivine is completely altered to chlorite. Veins are not common and are filled by either chlorite, epidote or laumontite, or a combination of all three. Pyrite and chalcopyrite are present in the rock.

Unit 67 (974.3–975.2 m).
This unit is a thin, pillow-lava sequence recognized from the very fine grain size (chilled margin?) and fractured appearance. The pillows are composed of a gray-colored, sparsely olivine phyric basalt in which olivine phenocrysts (2 mm average size) form about 2% of the rock. Olivine is completely altered to dark green chlorite. Veining is more common than in the preceeding unit, filled by the same alteration minerals as before.

Unit 68 (975.2–975.8 m).
This unit is a thin massive flow or dike composed of a sparsely olivine-plagioclase phyric basalt. The unit is uniformly medium-coarse grained. Phenocrysts form about 2% of the rock. The olivine is completely altered to dark green chlorite. There are no fractures or veins in the material recovered.

Unit 69 (975.8–977.5 m).
This unit is a thin pillow lava sequence with an unoriented chilled pillow margin at its base. The remainder of the material is very fine-grained pieces either highly fractured or reduced to rubble. All the pillows are a uniform, greenish-gray color, aphyric basalt. Marginal areas are slightly paler gray in color. Alteration is the same as in the two preceeding units.

Unit 70 (977.5–985.5 m).
This unit is composed of a massive, aphyric to sparsely plagioclase-clinopyroxene phyric basalt (dike/flow?). It is greenish-gray in color and uniformly medium-grained. Phenocrysts form less than 2% of the rock. The plagioclase phenocrysts are subhedral (less than 1.5 mm) and slightly less abundant than the anhedral clinopyroxene (less than 1.5 mm) phenocrysts. Textures are subophitic to intergranular. Olivine (less than 1 mm) is present as a component of the groundmass (less than 2%), completely replaced by dark green chlorite. Fractures are filled by chlorite and white minerals (quartz and laumontite). Pyrite is particularly common on broken vein surfaces.

cm
0
50
100
150
Core-Section
Piece Number
Graphic Representation
Orientation
Shipboard Studies
Alteration
89-1
89-2
90-1
90-2
90-3
90-4
90-5
Unit 71
Unit 72
Unit 73
XRF
M
PP
T
XRD

Unit 71 (985.5–1000.5 m).

This unit consists of a series of pillow lavas about 15 m thick. There are numerous chilled pillow margins (oriented/unoriented) and hyaloclastic breccias. Recovered material is locally highly fractured with large amounts reduced to rubble. There are several cases of breccias containing angular fragments of material now separated by clays which must have previously fitted together. All the pillows are fine-grained, grayish-green/greenish-gray in color. Compositions vary through the unit, moderately olivine-plagioclase phyric and aphyric basalt pillows forming an alternating series from top to bottom. Phenocrysts form about 3–6% of the phyric pillows of which olivine (0.5–4 mm) and plagioclase (0.4–2 mm) each form 1–3% in total. The latter are often only recognizable in thin section. Groundmass olivine and olivine phenocrysts are altered to dark green chlorite. Textures are typical for pillow lavas (see petrography chapters). Alteration is particularly intense in brecciated areas and the hyaloclastites. Cementing by chlorite and epidote is most common, but quartz and laumontite can also be present. A similar suite of alteration minerals fills veins penetrating the pillow centers. Pyrite, chalcopyrite and sphalerite can be found in some veins.

Unit 72 (1000.5–1002.0 m).

This unit is a massive, aphyric to sparsely plagioclase phyric basalt dike or flow. It is uniformly fine-grained, greenish-gray in color. In thin section plagioclase phenocrysts form about 2% of the rock in a subophitic groundmass. A few grains of chrome spinel can be seen. The unit is locally tectonically deformed/brecciated and heavily veined, filled mainly by quartz with some chlorite and epidote. Pyrite is disseminated throughout the rock. A chilled vertical intrusive margin whose affinities could not be determined, occurs about half way down the unit over a distance of 20 cm. Unit 72 chills against a host which was not recovered during drilling. The margin is strongly tectonized and veined and confirmation of its intrusive nature has not been possible.

Unit 73 (1002.0–1003.2 m).

This unit is a massive, strongly brecciated, fine-grained aphyric basalt. Fragments are cemented with green clay (chlorite?), white minerals, and epidote. Pyrite is common disseminated throughout the rock.

cm
0
50
100
150
Core-Section
Piece Number
Graphic Representation
Orientation
Shipboard Studies
Alteration
91-1
91-2
91-3
91-4
92-1
92-2
92-3
Unit 74
Unit 75
Unit 76
Unit 77
Unit 78
Unit 79
XRF
M
PP
XRD
T

Unit 74 (1003.2–1004.8 m).
This unit is a highly brecciated, pillow-lava sequence. There are several chilled pillow margins. The rock is a very fine-grained sparsely plagioclase-olivine phyric basalt. The breccia is cemented by chlorite and minor white minerals. A tan to pinkish mineral was also observed. Sulfides and epidote are present as a minor component of the breccias.

Unit 75 (1004.8–1006.8 m).
This unit is probably a thin (2 m) dike as its upper surface has a chilled margin. The remainder of the unit becomes progressively coarser grained towards the base. It consists of a sparsely olivine-plagioclase-clinopyroxene phyric basalt. Fractures are common towards the top of the unit, less so towards the bottom. They are filled with chlorite and sometimes with lighter green alteration zones immediately adjacent to vein surfaces. Large vugs (approximately 1 cm in diameter) in one piece are filled with calcite. Common sulfides are disseminated in the rock.

Unit 76 (1006.8–1009.7 m).
This unit is a massive, strongly brecciated, uniformly fine-grained, aphyric basalt. Brecciated areas are cemented by dark green chlorite, epidote, a tan to pinkish mineral, common sulfides, and minor quartz. Most fractures/veins are filled by chlorite, but a late series of veins filled with white minerals and epidote sometimes cut these.

Unit 77 (1009.7–1014.0 m).
This is a massive unit composed of an aphyric basalt. The upper section of the unit is very fine-grained, but becomes coarser towards the base. This coarsening (almost doleritic in some areas) is associated with the appearance of phenocrysts in the lower 70 cm, the unit finally developing into a sparsely olivine-plagioclase phyric basalt. Textures are intergranular to subophitic. Groundmass olivine is altered to dark green chlorite. In thin section interstitial areas are seen to be filled by chlorite, accounting for the pronounced green color of the rock. The whole of the unit is highly fractured (mostly oblique), but particularly badly at the top where it is described as a breccia. Fractures (up to 2 mm) are filled mostly by chlorite, but occasionally a later phase of white veins (quartz/laumontite?) are seen to cut these. Minor epidote and the pinkish-tan mineral first observed in Unit 75 are also present. Pyrite is disseminated throughout the rock.

Unit 78 (1014.0–1017.2 m).
This is a massive unit composed of a sparsely to moderately olivine-plagioclase-clinopyroxene phyric basalt. Phenocrysts form about 8% of the rock of which euhedral olivine phenocrysts (0.4–1.2 mm) form less than 1%, euhedral plagioclase phenocrysts (0.2–1.6 mm) about 4% and anhedral clinopyroxene phenocrysts (0.3–1.6 mm) about 3% in total. The latter are resorbed and are commonly twinned. Plagioclase crystals can also occur in small (0.4–0.6 mm) glomerophyric clusters. The unit is fine-grained throughout with a horizontal, chilled, intrusive margin at the base (confirmed by thin section), Unit 78 intrudes into the earlier pillow Unit 79. Textures are described as intergranular to very fine-grained, immature plumose towards the dike margin. The unit is highly fractured approaching a breccia (tectonic?) in several localized areas. Veins (approximately 1–2 mm, maximum 5 mm) and breccias are filled/cemented with a variety of minerals, mainly epidote, chlorite, and laumontite. These can occur alone or together in a variety of different combinations.

Unit 79 (1017.2–1021.5 m).
This unit consists of a series of pillow lavas. The uppermost pillows are composed of a sparsely to moderately olivine-plagioclase-clinopyroxene phyric basalt, the lower pillows composed of an aphyric basalt. In the phyric pillows, phenocrysts form about 3–4% of the rock. Euhedral to subhedral olivine phenocrysts (0.2–1.5 mm) form less than 1% of the rock and subhedral plagioclase phenocrysts (0.2–2 mm) about 2–3% in total. Anhedral clinopyroxene phenocrysts (0.4–1.5 mm) recognized only in thin section, form less than 1%. Textures are described as intergranular to subophitic. There are several oriented pillow margins and abundant hyaloclastic breccias. The unit is generally fine-grained and of a grayish-green color. Olivine when present is completely altered to dark green chlorite. Numerous fractures are filled with chlorite, epidote, quartz, and laumontite, some of which may show cross-cutting relationships. Chlorite forms the main cement to the breccias. Sulfides are common accessories in veins, particularly in the upper pillows.

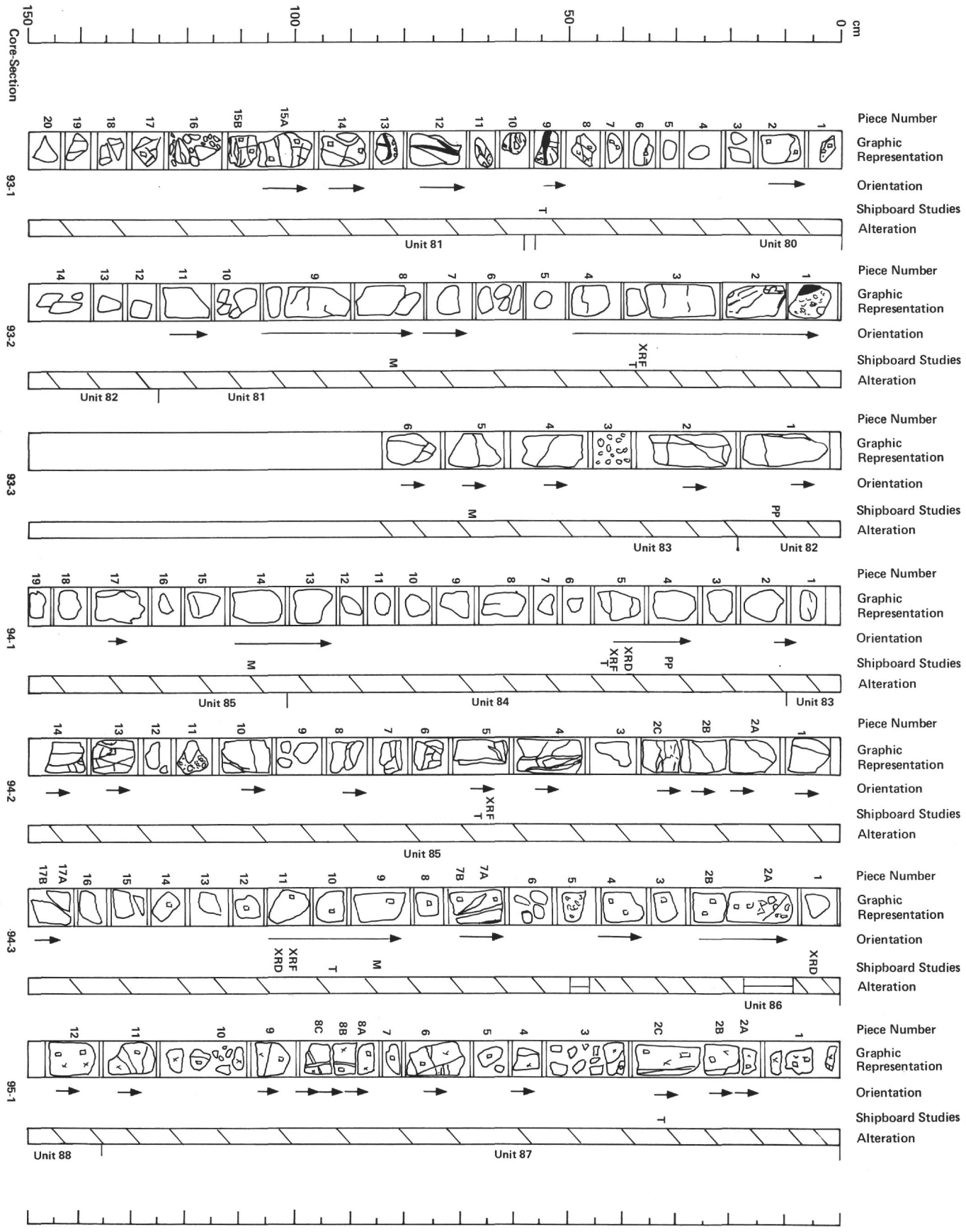
150
100
50
0
cm
Core-Section
Piece Number
Graphic Representation
Orientation
Shipboard Studies
Alteration
93-1
Unit 81
Unit 80
93-2
Unit 82
Unit 81
93-3
Unit 83
Unit 82
94-1
Unit 85
Unit 84
Unit 83
94-2
Unit 85
94-3
Unit 86
95-1
Unit 88
Unit 87

Unit 80 (1021.5–1023.2 m).
This unit is probably a dike. A chilled intrusive margin (confirmed by thin section) forms the base to the unit. It is composed of a sparsely to moderately olivine-plagioclase-clinopyroxene phyric basalt, grayish-green in color. Phenocrysts form 2–5% of the rock, olivine (0.8–2 mm) forming between 1% and 3%, plagioclase (1–2 mm) about 2% and clinopyroxene (0.4–2 mm) less than 1% in total. Olivine phenocrysts are subhedral and completely replaced by chlorite. Plagioclase occurs as single subhedral to euhedral phenocrysts, and as small but rare glomerocrysts. Most clinopyroxene phenocrysts are subhedral to euhedral and twinned. Several contain small plagioclase laths (0.08 x 0.16 mm) as inclusions, and these are anhedral (xenocrysts?). Fracturing is not intense, veins are filled with chlorite, epidote, and quartz. Pyrite is disseminated throughout the rock, but is not particularly abundant.

Unit 81 (1023.2–1028.0 m).
This unit consists of a series of pillow lavas. The uppermost pillows are moderately olivine-plagioclase-clinopyroxene phyric. Phenocrysts form about 5% of the rock of which olivine (up to 2 mm) forms 3%, plagioclase (1–2 mm) about 2% and clinopyroxene (approximately 1 mm) less than 1% in total. Pillows lower in the sequence are only very sparsely olivine-plagioclase-clinopyroxene phyric to aphyric. The lowermost pillows are the same as those at the top, but only sparsely phyric, olivine, and clinopyroxene phenocrysts both forming less than 1% of the rock and plagioclase phenocrysts about 2%. Olivine is completely altered to dark green chlorite. The unit is mostly fine-grained but with several very fine-grained areas and two chilled pillow margins (oriented). Hyaloclastic breccias are common throughout the unit, cemented by dark and light green chlorite. The unit is heavily veined, small horizontal veins abundant in localized areas, probably the result of concentrated shearing. Fractures are filled by chlorite, epidote, and quartz, the latter often present as a late phase, white veins cutting earlier chlorite-filled fractures.

Unit 82 (1028.0–1029.6 m).
This unit is a massive, uniformly medium-grained, moderately olivine-plagioclase phyric basalt (dike/flow?). It is greenish-gray in color. Olivine phenocrysts (1–5 mm) are completely replaced by dark green chlorite. Veins (0.5–3 mm wide) are filled mainly with white minnerals with occasional epidote centers. Dark green chlorite is not a common vein component.

Unit 83 (1029.6–1031.0 m).
This unit is a uniformly fine-grained massive aphyric basalt (dike/flow?). It is greenish-gray in color. Alteration characteristics are the same as in Unit 82.

Unit 84 (1031.0–1033.0 m).
This unit consists of a massive relatively coarse-grained, sparsely olivine phyric to aphyric basalt. The coarseness of the unit makes it quite distinct from all preceeding units encountered during Leg 83 drilling, which have been much finer-grained than this. Olivine is recognized only in hand specimen and is totally replaced by a dark green mineral (not chlorite). Megascopically plagioclase forms radiate clusters, giving a speckled appearance to the rock due to their size. Clinopyroxene is also represent, but is insufficiently large to be considered a phenocryst. In thin section textures are described as ophitic to subophitic. The unit has very few fractures and its gray color adds to the general appearance of being less altered than many of the preceeding units.

Unit 85 (1033.0–1037.9 m).
This unit consists of a thin, pillow-lava sequence, with several fine-grained areas (pillow margins?) and associated coarser-grained regions (pillow interiors?) recovered during drilling. There are no chilled margins in the unit, but typical localized breccias (hyaloclastic and tectonic) are associated with the unit. The pillows are composed of a moderately olivine-plagioclase-clinopyroxene phyric basalt and are greenish-gray in color. The proportion of phenocrysts in the rock varies between 6–9%, olivine (1–5 mm) forming around 4–5%, plagioclase (3–5 mm) about 2–3% and clinopyroxene (4–7 mm) less than 1% in total. Textures are described as intersertal to subophitic away from chilled margins. The olivine phenocrysts (euhedral) and groundmass olivine are completely altered, replaced by a dark green clay mineral with occasional small (less than 0.5 mm) pyrite grains in association. The plagioclase phenocrysts (equant and tabular) are often difficult to recognize in hand specimen. Clinopyroxene phenocrysts are elongate in hand specimen but rounded in thin section. The breccias may well be a mixture of hyaloclastic and tectonic breccias, cemented by dark and light green clay minerals. A very distinct and sharp contact can separate these two differently colored clays. Veining is common (0.5–3 mm wide) particularly at the top of the unit. These are generally filled with the same light and dark green clay minerals together with pyrite. White veins and epidote veins are found in two pieces at the top of the unit. Pyrite and occasional grains of chalcopyrite are disseminated throughout the rock.

Unit 86 (1037.9–1039.5 m).
This unit is composed of a massive, sparsely to moderately olivine-clinopyroxene phyric basalt. It is uniformly medium-grained. The lowermost 20 cm appear almost aphyric, but elsewhere phenocrysts form about 3% of the rock of which euhedral olivine crystals (0.6–1.5 mm) form 2%, and subhedral clinopyroxene phenocrysts (0.6–0.8 mm) about 1% in total. In thin section microphenocrysts of plagioclase are recognizable forming glomerophyric areas, in addition to abundant plagioclase laths. Textures are described as subophitic. Olivine is replaced by dark green chlorite in both phenocrysts and groundmass. Fractures are few, filled by a dark green mineral. Sulfides are disseminated in the whole rock.

Unit 87 (1039.5–1046.5 m).
This unit is a massive, uniformly medium-grained, greenish-gray, sparsely to moderately olivine-plagioclase-clinopyroxene phyric basalt. The upper part of the unit is more phyric than the lower part. Phenocrysts form between 3% and 8% of the rock, of which olivine phenocrysts (0.5–4 mm) form about 5% (in thin section this figure is much lower, estimated at about 1%) and plagioclase (2 mm) about 2% in the more phyric areas, olivine phenocrysts (0.5–4 mm) form about 5% of the rock in hand specimen (in thin section this figure is much lower, estimated at about 1%), and plagioclase (2 mm) about 2%. Clinopyroxene phenocrysts (2–3 mm) are recognizable only in hand specimen in the upper part of the unit (approximately 50 cm), and form about 1% of the rock. In thin section, they are considered to be more abundant, nearer to 5% in total. These are subhedral phenocrysts and are smaller (0.6–2 mm) than those seen megascopically. In the sparsely phyric areas of the unit, in addition to the absence of clinopyroxene phenocrysts, olivine (3 mm) forms only a trace or up to about 2% of the rock, and plagioclase phenocrysts about the same. All the phenocrysts are subhedral in an intergranular to intersertal groundmass. Olivine is completely altered to dark green chlorite. The unit is fractured with veins from 1 mm to 7 mm wide filled by a variety of minerals (chlorite, epidote, laumontite, and minor calcite). Pyrite is rare.

Unit 88 (1046.5–1048.5 m).
This unit is a thin flow or dike composed of a sparsely olivine-plagioclase phyric basalt. It is coarse/medium-grained and greenish-gray in color. Olivine phenocrysts are up to 2 mm in size, completely altered to dark green chlorite. Alteration charcteristics are the same as in Unit 87.

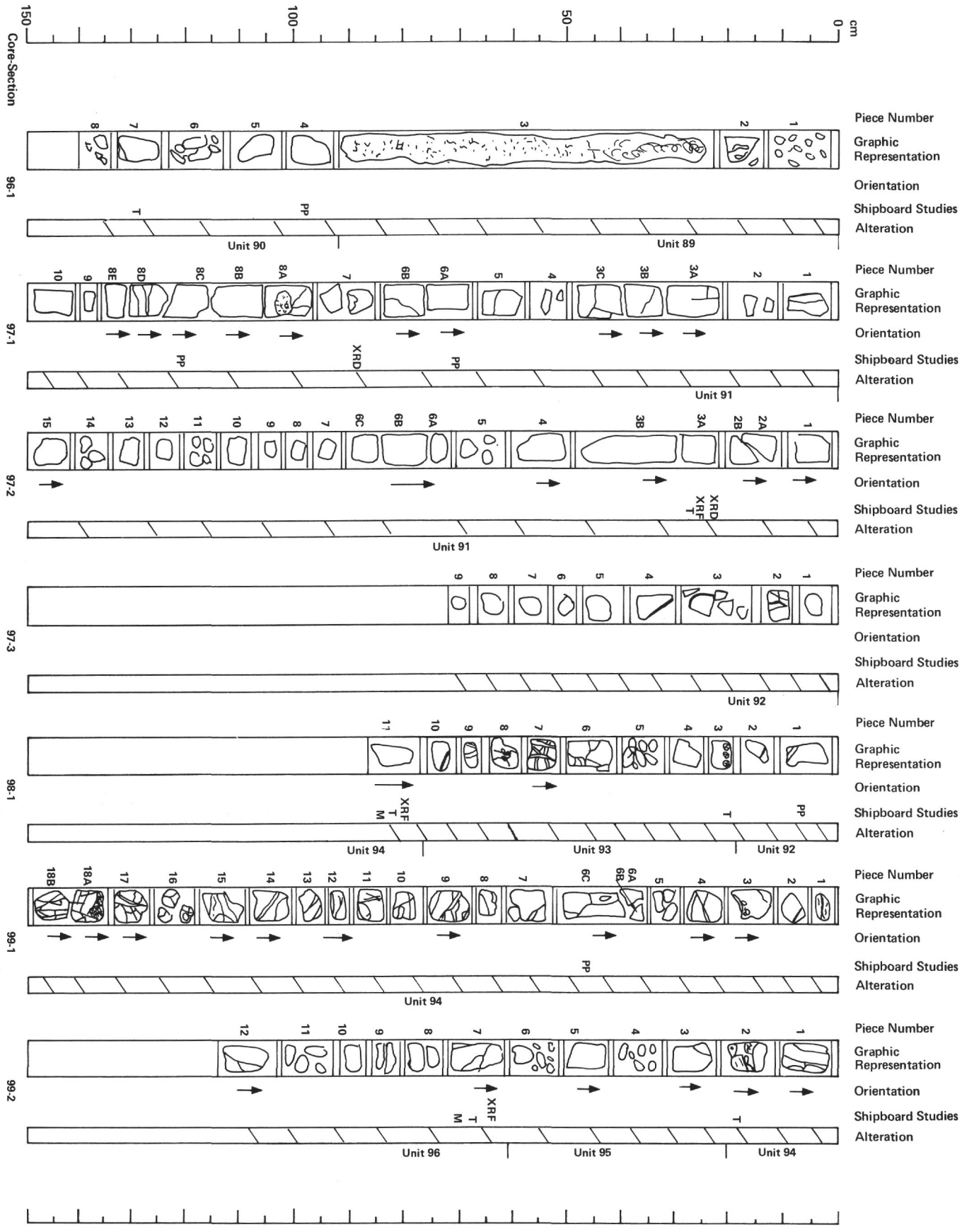
150
100
50
0
cm
Core-Section
Piece Number
Graphic Representation
Orientation
Shipboard Studies
Alteration
96-1
T
PP
Unit 90
Unit 89
97-1
XRD
PP
Unit 91
97-2
XRD
XRF
T
Unit 91
97-3
Unit 92
98-1
XRF
T
M
T
PP
Unit 94
Unit 93
Unit 92
99-1
PP
Unit 94
99-2
XRF
T
M
T
Unit 96
Unit 95
Unit 94

Unit 89 (1048.5–1054.0 m).
This unit is a pillow-lava sequence which has been badly disturbed by drilling (the core barrel was dropped to the bottom of the hole during the drilling of Core 96 resulting in the granulation of much of the recovered material). The upper part of the unit is a fine-grained aphyric basalt, probably from close to a pillow margin. Below this is a similarly fine-grained, sparsely olivine-plagioclase phyric basalt pillow section. The majority of the unit consists of drill cuttings which are felt to represent pillow material (a massive unit may well resist severe brecciation caused by the dropping of a core barrel). The condition of the material recovered in the unit precludes any information as to the degree of alteration.

Unit 90 (1054.0–1057.5 m).
This unit is a massive, variably phyric dike or flow. The top and bottom are both finer grained than the center which is a medium-grained aphyric basalt. The margins are sparsely phyric containing olivine, plagioclase, and clinopyroxene phenocrysts. These form from 3% to 4% of the rock of which olivine (1.2–1.6 mm) forms less than 1%, plagioclase (0.8–2 mm) about 2% and clinopyroxene (1–1.5 mm) 1% in total. Groundmass olivine and the euhedral olivine phenocrysts are completely replaced by chlorite. The plagioclase phenocrysts are subhedral and normally zoned. Groundmass plagioclase is often rimmed, probably representing late stage differentiate material. Clinopyroxene phenocrysts (augite) are anhedral. Textures are subophhitic. In thin section, about 1–2% of sulfides are disseminated throughout the groundmass.

Unit 91 (1057.5–1061.0 m).
This is a massive unit with an extremely fine-grained zone (chilled intrusive contact?) forming its upper margin, and evidence of fining towards its base. Unit 91 is probably a dike which has intruded the preceeding massive Unit 90. The upper margin is grayish-green in color and distinct from the majority of the unit, which is aphyric, in being composed of a sparsely to moderately olivine-plagioclase phyric basalt. Olivine phenocrysts (1–2 mm) are replaced by dark green clays (chlorite?), sometimes with associated crystals of pyrite (less than 0.5 mm). Plagioclase phenocrysts are up to 1.5 mm in size. Away from the upper margin the unit is aphyric, gradually coarsening to a medium/coarse-grained center and fining again slightly towards the base. A few olivine crystals are seen in hand specimen in the finer rocks at the base. The lower sections of the unit are a dark grayish-green in color. Textures are subophitic to intergranular away from the margins. Veins are rare and very thin, filled by pale greenish-gray minerals at the top of the unit and dark green minerals at the base. In the central part of the unit there are coarse grained areas which are more strongly altered than the basalts surrounding them. One sample contains large vugs (up to 3 cm) filled by a white fibro-radiating mineral (laumontite?). There are minor disseminated sulfides throughout the unit.

Unit 92 (1061.0–1064.0 m).
This unit is a massive flow or dike composed of an aphyric to sparsely olivine-plagioclase phyric basalt. The upper 30 cm is fine-grained, gradually becoming coarser and more uniform (medium-grained) towards the center and base. Veins are filled mostly by chlorite, but some can have centers filled by white minerals (laumonite and quartz?) and a minor, acicular, tan-colored mineral. Pyrite is common in veins towards the base of the unit.

Unit 93 (1064.0–1069.7 m).
This unit is massive and uniformly fine-grained. The top is aphyric, grading downwards into a moderately olivine-plagioclase phyric basalt. The unit has a coarse variolitic texture in the top few centimeters of the aphyric zone. This was probably originally adjacent to a chilled margin (intrusive?) which was not recovered during drilling. Away from this margin textures are subophitic. The unit is heavily veined (average 2 mm wide). These are often filled with a mixture of minerals, most commonly rims of dark green chlorite with centers filled by white minerals. Pyrite is common in these veins, but is also disseminated in the whole rock. Complex crosscutting vein relationships are evident in the bottom part of the unit.

Unit 94 (1069.7–1076.2 m).
This is a massive aphyric basalt unit, distinguished from the preceeding aphyric Unit 93 by a sudden change in grain size. The upper part of the unit is medium-grained, gradually becoming finer towards the base where the unit is intruded by a later basalt dike (Unit 95). Fracturing is common, particularly in the lower section of the unit and at the contact where the basalt is highly brecciated (flow breccia/tectonic?). Veins can be filled by a variety of different minerals including dark green chlorite, a white mineral (laumontite?), a colorless radial prismatic mineral (quartz?) and common epidote. Sometimes these can be layered with a rim of dark green clay lined by epidote with centers composed of a prismatic white mineral. Sulfides are particularly common on broken vein surfaces.

Unit 95 (1076.2–1077.5 m).
This unit is a thin dike. The upper margin forms an intrusive contact (confirmed by thin section), Unit 95 chilled against the highly brecciated base of Unit 94 over a distance of about 5 cm. The remainder of the unit is a very fine-grained (chilled) aphyric to very sparsely olivine-plagioclase-clinopyroxene phyric basalt, light gray in color. Phenocrysts are recognized only in thin section as microphenocrysts forming 1–2% of the rock. The olivine microphenocrysts (0.1–0.3 mm) are euhedral and totally replaced by chlorite, forming considerably less than 1% of the rock. Euhedral plagioclase microphenocrysts (0.04–0.4 mm) form about 1% of the basalt, and subhedral clinopyroxene microphenocrysts (0.1–0.3 mm) less than 1% in total. Close to the margin textures are equigranular (0.1–0.3 mm) quenched. In thin section an intensely altered zone (chloritized) 1–2 mm wide is present at the contact between host and dike. Cracks are common in the unit, mostly subhorizontal with brecciation towards the base. Cracks are filled with dark green chlorite with associated epidote (± quartz).

Unit 96 (1077.5–1082.2 m).
This unit is composed of a massive, aphyric to sparsely olivine phyric basalt. It is greenish-gray to gray in color. The unit has a fine-grained upper margin which gradually coarsens towards the base. Two pieces which have fine-grained rims, described as chilled in hand specimen, occur roughly in the center of the unit. Their relationship to the remainder of the unit is unclear, but possibly they indicate the close proximity of a chilled intrusive margin. The unit is strongly fractured, particularly in the bottom 20 cm which is brecciated (flow breccia?). The bottom of the unit is defined by a chilled intrusive contact, Unit 97 having been intruded into Unit 96. The center of the unit is sparsely olivine phyric grading into aphyric margins. Phenocrysts form 1–2% of the rock and are composed entirely of olivine (average size 2 mm) which are completely replaced by dark green chlorite. Textures are intergranular. Fine fractures predominant away from the brecciated base of the unit. These are mainly filled by dark green clay (chlorite?), but some contain quartz with a white mineral (laumontite?) together with epidote.

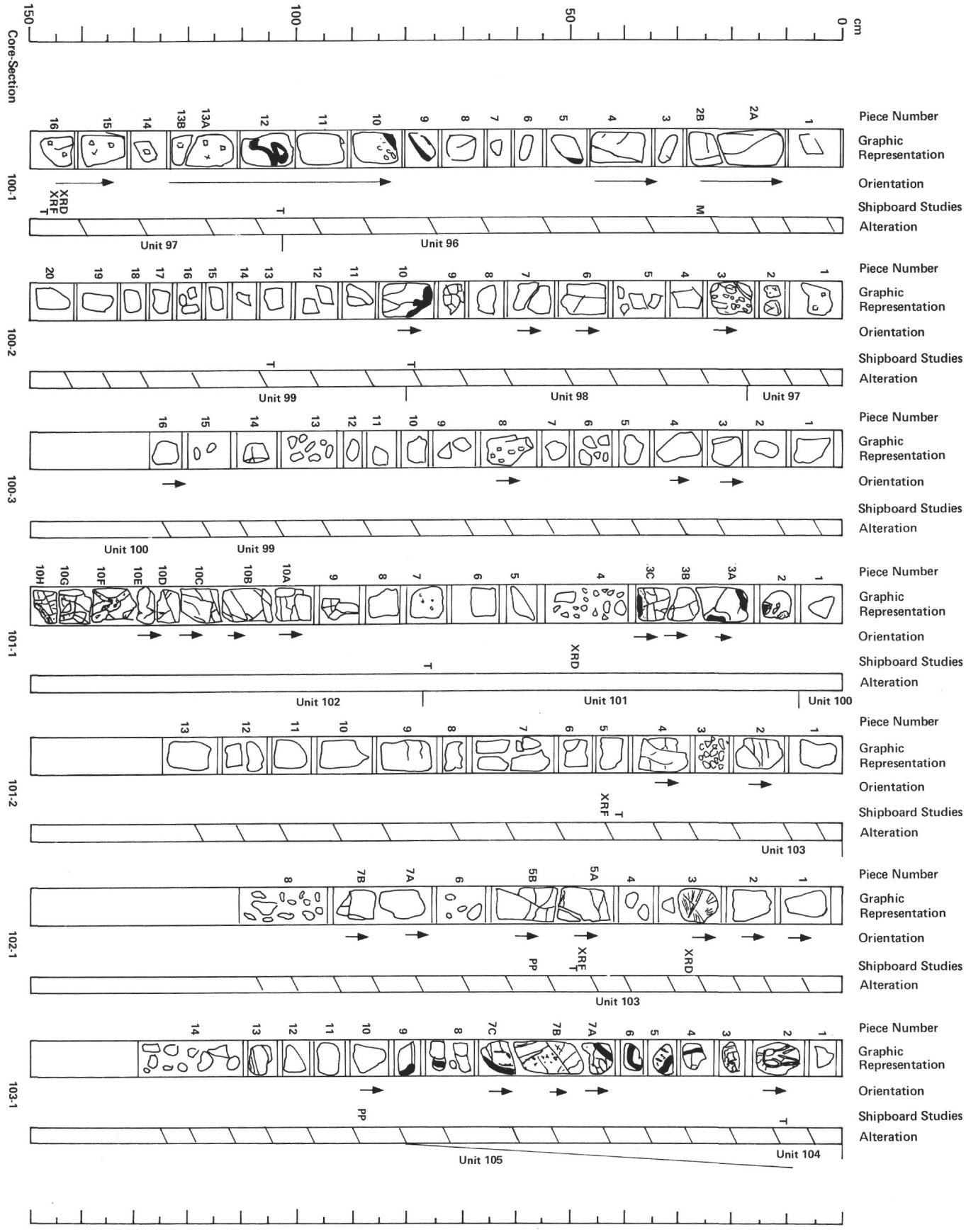
150
100
50
0
cm
Core-Section
Piece Number
Graphic Representation
Orientation
Shipboard Studies
Alteration
100-1
XRD
XRF
T
T
M
Unit 97
Unit 96
100-2
T
T
Unit 99
Unit 98
Unit 97
100-3
Unit 100
Unit 99
101-1
XRD
T
Unit 102
Unit 101
Unit 100
101-2
XRF
T
Unit 103
102-1
PP
XRF
T
XRD
Unit 103
103-1
PP
T
Unit 105
Unit 104

Unit 97 (1082.2–1083.8 m).
This unit is probably a dike. Chilled intrusive contacts form the upper and lower margins to the unit (Unit 97 intruding into Units 96 and 98), with the center composed of a uniformly fine/medium-grained, moderately olivine-plagioclase-clinopyroxene phyric basalt. The lower contact of the unit and the upper part of Unit 98 are both strongly brecciated. The margin has been assigned to Unit 97 but this is open to some interpretation. Phenocrysts form 6–10% of the rock of which olivine (0.5–2 mm) forms 1–2%, plagioclase (0.3–3 mm) 3–5% and clinopyroxene (0.4–6 mm) 1–3% in total. All the phenocrysts are subhedral except for a few clinopyroxene crystals which are euhedral. Textures are intergranular. Groundmass olivine and olivine phenocrysts are completely altered to chlorite. A network of small veins are filled by a blue-green clay mineral (chlorite?).

Unit 98 (1083.8–1084.8 m).
This unit is composed of a massive, sparsely olivine-plagioclase-clinopyroxene phyric basalt. The upper few centimeters are fine-grained and brecciated and include several fragments of chilled basalt. These are probably part of the chilled margin of Unit 97. In hand specimen there appears to be a few clots of subophitic clinopyroxene and plagioclase in the coarser parts of the unit. The breccia is cemented by dark and light green clays, the dark green clays often acting as rims to the lighter material. Epidote is found together with minor pyrite in fractured areas of the unit.

Unit 99 (1084.8–1088.0 m).
This is a massive unit composed of a gray colored, sparsely olivine-plagioclase-clinopyroxene phyric basalt. It is uniformly fine-grained with a brecciated base which includes chilled basalt. This material has been assigned to Unit 99 although it could possibly be the upper brecciated chilled intrusive margin of Unit 100. Phenocrysts form about 3–4% of the rock. Olivine phenocrysts (0.4–3 mm) are rare, but can occasionally form up to 1%, plagioclase phenocrysts (0.4–1.7 mm) form about 2% and clinopyroxene phenocrysts (0.2–0.8 mm) 1% or less. Olivine phenocrysts (euhedral) are completely altered to dark green chlorite. The plagioclase phenocrysts sometimes occur in glomerocrystic aggregates up to 2 mm in diameter. The clinopyroxene phenocrysts are anhedral and show late stage nucleation and crystallization on their rims. Textures are fine-grained intergranular to subophitic. The phenocryst content in the lower part of the unit can vary locally, approaching aphyric in some areas. Veins are small (less than 1.5 mm) and sparse, filled by chlorite with occasional laumontite and an unidentified white mineral. Pyrite is disseminated throughout the rock and is often associated with the chlorite replacing olivine phenocrysts. A thin gray-colored, chilled finger of basalt intrudes close to the upper margin of Unit 99. It is separated from the host by a vein of chlorite. The basalt is almost aphyric with only isolated phenocrysts of olivine (0.8 mm) and plagioclase (0.04–0.4 mm). These are euhedral and subhedral respectively. This basalt is different from both the host and the basalts of the immediately adjacent units.

Unit 100 (1088.0–1089.8 m).
This is a massive unit composed of a blackish-gray, aphyric basalt. The unit is uniformly fine-grained. The upper margin is brecciated and intruded by the later basalt dike of Unit 99 (chilled basalt fragments included in the breccia have been assigned to Unit 99). Alteration charcteristics are the same as in the preceeding unit.

Unit 101 (1089.8–1091.5 m).
This unit is probably a dike. It is composed of a grayish-green, sparsely olivine-plagioclase-clinopyroxene phyric basalt. The bottom of the unit if formed by a chilled intrusive contact (confirmed by thin section study), Unit 101 apparently intruding into Unit 102, although the contact is located on an unoriented sample. The unit coarsens slightly towards the center (medium-grained) and top. Phenocrysts form up to 5% of the rock of which olivine (0.1–0.3 mm) forms 1%, plagioclase (0.2–0.8 mm) about 3% and clinopyroxene (0.2–0.8 mm) less than 1%. The olivine phenocrysts are euhedral and completely replaced by chlorite. Immediately adjacent to the chilled margin the texture varies from very fine-grained to immature sheaf over the distance of about 1 cm. The unit is quite strongly fractured. Localized breccias are present in some parts of the unit. Alteration as a consequence is intense, thin veins (0.5–1 mm) are filled by a dark green clay mineral (chlorite?) and an unidentified white mineral. Veins located within the breccias are larger (up to 1 cm), filled by the same dark green clay and white minerals, but with additional epidote and laumontite and abundant pyrite. A small irregular finger of fine-grained, light gray basalt intrudes into the upper 20 cm of the unit. This probably represents a small offshoot from the margin of a nearby dike.

Unit 102 (1091.5–1094.0 m).
This is a massive unit composed of a gray, sparsely olivine-plagioclase-clinopyroxene phyric basalt. The unit is fine-grained throughout. The top is defined by a chilled intrusive contact, Unit 101 having intruded and chilled against Unit 102. Phenocrysts form up to 4% of the rock of which olivine (4–6 mm) forms less than 1%, plagioclase (0.5–2 mm) 1–2%, and clinopyroxene (0.5–2 mm) about 1% in total. Olivine phenocrysts are skeletal and completely replaced by chlorite, but unlike Unit 99, have no associated pyrite. Clinopyroxene was only recognized in thin section as resorbed subhedral crystals. Evidently they were not seen in hand specimen. Textures are fine-grained intergranular towards the top of the unit. The bottom 30 cm is heavily brecciated. There appear to be two different elements present – very fine-grained, light gray, aphryic basalt (intrusive?) and a slightly coarser, but still fine-grained, darker gray, aphyric basalt (host?). Exact relationships are unclear, but possibly this breccia includes a chilled contact. The cement is not abundant, and is replaced by a dark green mineral (chlorite?). A sparse white mineral (laumontite) occurs in thin veins (less than 1 mm).

Unit 103 (1094.0–1107.5 m).
This is a massive unit composed of a gray-colored, aphyric to sparsely olivine-plagioclase phyric basalt. It has fine-grained margins (about 30 cm wide) and a medium-grained center with occasional coarse-grained patches. Phenocrysts form 2–3% of the rock of which olivine (1–3 mm) forms less than 1% and plagioclase (up to 2 mm) about 1% or 2%. The olivine phenocrysts are euhedral and completely replaced by dark green chlorite. Plagioclase phenocrysts are subhedral and form glomerocrystic aggregates. Extremely rare clinopyroxene phenocrysts (less than 1.5 mm) were identified in thin section, but apparently overlooked during hand specimen description. Textures are intergranular to subophitic. The unit is not strongly altered or veined. Veins when present are thin (less than 1.5 mm) and are filled with dark green chlorite and white scolecite (white radiating crystals up to 6 mm long). Pyrite is associated with chlorite in cracks.

Unit 104 (1107.5–1110.2 m).
Units 104 and 105 are separated by a complicated and irregular chilled intrusive margin which runs vertically over a distance of about 70 cm at the top of Core 103, Section 1. The host rock (situated to the left of the contact on archive photographs) has been assigned to Unit 104, and the intruding dike to Unit 105. The contact is fractured and locally brecciated. About 10 cm from the top of the unit the breccia partially obscures a second intrusive contact distinct from that mentioned above. A dark gray, fine-grained, aphyric to sparsely plagioclase-clinopyroxene phyric basalt is surrounded by a chilled, light gray, sparsely olivine-plagioclase-clinopyroxene phyric basalt (Unit 104 basalt). The aphyric basalt is intruded by several altered glass fingers, intruded prior to brecciation. The light gray basalt forming Unit 104 contains about 4% phenocrysts of which less than 1% are olivine (0.3–0.45 mm), 2% plagioclase (0.3–2.5 mm) and about 1% clinopyroxene (0.4–1.5 mm). The olivine phenocrysts are euhedral and replaced by chlorite. Both the plagioclase and clinopyroxene phenocrysts are subhedral, the latter sometimes ophitically enclosing plagioclase crystals. There are a few equant, euhedral (less than 0.05 mm) chrome spinel crystals scattered through the groundmass. Away from the aphyric basalt at the top of the unit, the rock becomes greenish-gray in color although still fine-grained. Towards the base, Unit 105 is chilled against a fine-grained aphyric basalt. This could be a slightly different part of the phyric Unit 104, or alternatively part of an adjacent dike. The brecciation of the unit has led to intense alteration, glass fragments (present in the uppermost breccia), veins and the breccia cements are composed of dark green chlorite with accessory laumontite and pyrite.

Unit 105 (1110.2–1112.0 m).
An irregular vertical chilled intrusive contact separates this unit which is intrusive, from Unit 104, the host. The relationships between these two are complex and difficult to ascertain. The dike (Unit 105) is a pale gray in color and composed of a moderately olivine-plagioclase phyric basalt. Close to the margin phenocrysts tend to cluster about a plane parallel to the contact. Fractures are common, sufficiently intense in some areas to cause localized brecciation. As a consequence, alteration is intense, veins and breccias filled and cemented by the same alteration minerals as in Unit 104. The bottom of the unit is also defined by a intrusive/fine-grained contact, Unit 106 intruding into Unit 105.

cm
0
50
100
150
Core-Section
Piece Number
Graphic Representation
Orientation
Shipboard Studies
Alteration
104-1
104-2
104-3
105-1
106-1
107-1
107-2
Unit 106
Unit 107
Unit 108
Unit 109
Unit 110
Unit 111
XRD
PP
T
XRF
M

Unit 106 (1112.0–1125.5 m).
This is a thick (13.5 m) massive unit composed of a sparsely to moderately olivine-plagioclase-clinopyroxene phyric basalt. The top is fine-grained, possibly chilled against Unit 106 (the contact is not oriented and could equally be the bottom margin of Unit 105). The unit coarsens rapidly towards the center, becoming medium/coarse-grained, and then fines slightly again towards the base. Particularly in the center of the unit, recovery was excellent with large (up to 30 cm) intact lengths of core retrieved. Towards the margins, 5–10 cm lengths were more common. Individual olivine phenocrysts (up to 2 mm) can be recognized by the naked eye forming 1–3% of the rock. Textures are medium- to coarse-grained subophitic, the plagioclase and clinopyroxene crystals seen in clusters in hand specimen. Olivine is completely altered to dark green chlorite. The unit has very few fractures or veins, but when present, they show an interesting symmetrical alteration of the surrounding basalt walls, particularly in the center of the unit. Most veins are filled by dark green chlorite, the immediately adjacent (up to 4 mm) walls are altered to a dark gray color (unaltered rock is a lighter gray) and outwards from this is a zone where the basalt is green/gray in color (up to 5 cm). A similar type of alteration occurs near the base of the unit. Here it is much more patchy and appears to have attacked the interstices in selected areas, accentuating the plagioclase clusters. Pyrite is disseminated in the rock.

Unit 107 (1125.5–1128.0 m).
This is a massive, uniformly fine-grained, aphyric basalt unit (no chilled contacts). Veins are sparse and very thin (less than 0.5 mm), filled with dark or light green minerals (chlorite?). A lighter gray matrix is evident in the basalt around some of the dark green veins, contrasting with the darker gray of the rock. A limited amount of pyrite can also be found in association with the dark green veins.

Unit 108 (1128.0–1133.0 m).
This is a massive unit composed of an aphyric to sparsely olivine-plagioclase-clinopyroxene phyric basalt. It is uniformly medium-grained, except for the base which is slightly coarser. The unit is gray in color. Phenocrysts form about 3–4% of the rock of which olivine (0.4–3 mm) forms 1–2% and plagioclase (0.3–1.2 mm) about 1%. A few crystals of clinopyroxene are evident, but are not common. Olivine phenocrysts are euhedral and completely altered to dark green chlorite (no associated pyrite). The plagioclase and clinopyroxene phenocrysts are both subhedral, the latter with resorbed edges and exhibiting twinning. The groundmass plagioclase is unusual in being rather elongate (length to width ratio approximately 8:1) and forms radiate patterns with 2 or 3 other laths. Textures are intergranular. Alteration is the same as in the preceeding unit with minor epidote and laumontite filling vein centers.

Unit 109 (1133.0–1139.8 m).
This is a massive unit composed of an aphyric basalt. The top and center of the unit are uniformly medium-grained, gradually becoming finer grained towards the base. There are no chilled contacts. Textures are subophitic to ophitic; olivine (0.1–0.5 mm) are present as anhedral to subhedral crystals, completely replaced by chlorite. Plagioclase occurs as laths (0.04–2 mm) and clinopyroxene in the form of anhedral grains (0.5–1.6 mm). The upper part of the unit is quite heavily fractured, containing numerous small veins (less than 1 mm) filled with dark green chlorite, and wider veins (1.0–5.0 mm wide) filled with a white mineral (laumontite?). There are no sulfides in the rock or veins.

Unit 110 (1139.8–1143.5 m).
This is a massive unit composed of a moderately olivine-plagioclase phyric basalt. The top 10 cm of the unit are strongly brecciated. The elements of the breccia include many fine-grained fragments which may have originated from a chilled margin. Possibly Unit 110 represents a dike which has intruded into the basalt of Unit 109. The center and bottom of the unit are fine- to medium-grained and strongly fractured/slightly brecciated. Olivine phenocrysts are up to 2 mm in size and replaced by dark green chlorite. Plagioclase phenocrysts are up to 3 mm in size. Chlorite acts as the cement to the breccia and as a filling to veins, the latter exhibiting a zonation affect on the surrounding basalts, i. e. the rock immediately adjacent to the vein is black compared to the gray of the fresh basalt.

Unit 111 (1143.5–1153.5 m).
This is a massive unit composed of a dark gray, aphyric basalt. Textures are subophitic to intergranular. The upper and lower margins of the unit are fine-grained (for approximately 30 cm), both gradually coarsening towards a medium-grained center. The top 40 cm are strongly brecciated and intruded by a later, pale gray aphyric basalt dike. This forms a vertical chilled intrusive contact over a distance of 25 cm, some 2 cm wide. The intrusive material is not brecciated which would suggest the intense fracturing of the host was a prelude to dike intrusion. The breccia is cemented mostly by chlorite, but with minor epidote and white minerals. Away from the breccia there are very few cracks and veins are rare. The latter when present are up to 1 mm wide, filled by chlorite with light greenish-gray alteration halos. Occasionally quartz may accompany the chlorite. In the central portion of the unit there are millimeter to centimeter-sized irregularly shaped vugs filled with chlorite.

cm
0
50
100
150
Core-Section
Piece Number
Graphic Representation
Orientation
Shipboard Studies
Alteration
PP
XRD
XRF
T
M
Unit 111
108-1
Unit 112
109-1
Unit 113
Unit 114
Unit 115
110-1
111-1
112-1
113-1
114-1

Unit 112 (1153.5–1162.2 m).
This is a massive unit composed of a dark gray, aphyric to very sparsely olivine-plagioclase-clinopyroxene phyric basalt. The unit is uniformly fine- to medium-grained with a chilled intrusive contact at the base (confirmed by thin section study). The unit is probably a dike. Unit 112 appears to have intruded into Unit 113, although the contact is located on an unoriented sample. The phenocryst content of the core can vary from less than 1% up to 2–3%. Olivine phenocrysts (0.3–1 mm) form considerably less than 1% of the rock as subhedral crystals completely replaced by a green mineral (smectite/chlorite?). Plagioclase phenocrysts (0.4–1 mm) form about 1% as subhedral/platy crystals, and anhedral clinopyroxene phenocrysts (0.3–1 mm) less than 1% in total. Textures are intergranular to locally very mature sheaf. The unit is cut by some minor veinlets filled with quartz and/or chlorite. Pyrite occurs in minor amounts disseminated throughout the rock.

Unit 113 (1162.2–1164.0 m).
This unit is composed of a greenish-gray, moderately to highly olivine-plagioclase phyric basalt. The lower contact is formed by a chilled intrusive margin (confirmed by thin section study) in which Unit 113 intrudes into Unit 114 (the recovery in this area of the hole suggests the presence of a series of parallel dikes). The contact is sharp, inclined between 50° and vertical. The upper margin of the unit is delineated by a further chilled intrusive contact in which Unit 112 intrudes Unit 113. The unit is medium-grained at the top and center, but fines toward the base. An isolated fine-grained area occurs towards the center of the unit, about 5 cm long and about 2 cm wide (i. e. approximately one-third the width of the core). Olivine phenocrysts in this zone are preferentially clustered in a similar manner to those close to a chilled contact in Unit 105. Presumably a chilled contact must lie a few centimeters to one side of the core at this location. Phenocrysts form about 7–9% of the rock of which olivine phenocrysts (0.5–3 mm) form about 3–5% and plagioclase phenocrysts (up to 2.5 mm) about 4%. All phenocrysts are euhedral. A few euhedral microphenocrysts of chrome spinel (0.03–0.2 mm) can be seen in thin section. Some of these are slightly resorbed and occur at the edge of the olivines. Textures are subophitic. Olivine is replaced by a dark green and/or a light green mineral. Plagioclase phenocrysts are replaced by a light green, slightly transparent mineral (clay + laumontite?) in hand specimen. Veins are thin (less than 0.5 mm), filled with a light green mineral. Occasionally these can have light gray halos, up to 5 mm wide, in the surrounding rock.

Unit 114 (1164.0–1165.5 m).
This is a massive unit composed of a uniformly medium-grained, gray colored, sparsely to moderately olivine-plagioclase-clinopyroxene phyric basalt. The upper and lower margins consist of chilled intrusive contacts, Units 113 and 115 intruding into Unit 114. The upper contact is sharp, inclined between 50° and vertical. The lower contact is less clear, but fine-grained (chilled?) material forms an approximately vertical association with the lower part of Unit 114. Phenocrysts form about 4% of the rock of which olivine (up to 2 mm) forms 1–2%, plagioclase (0.2–1.5 mm) about 3% and clinopyroxene (0.8–2 mm) about 1%. The latter were only recognized in thin section. Olivine is completely altered to dark green chlorite which also fills rare thin veins (less than 1 mm wide) together with a white mineral.

Unit 115 (1165.5–1180.5 m).
This is a thick (15 m), massive unit composed of a dark gray, aphyric to sparsely olivine-plagioclase phyric basalt. The upper margin is formed by fine-grained (chilled?) basalt in an almost vertical association with Unit 114. This has been interpreted as an intrusive contact with Unit 115 intruding Unit 114. Away from the margin the unit coarsens steadily towards the center (medium-grained) and then fines toward the base. The bottom of the unit is formed by a chilled contact, Unit 115 have intruded against a fine-grained breccia cemented with quartz (there is no specific chilled contact between Units 115 and 116. The latter is massive and starts at the top of a new core.). The phenocryst content of the unit varies locally from aphyric, particularly near the upper margin, to sparsely phyric. Phenocrysts form about 2% of the rock, olivine (up to 2 mm) and plagioclase (up to 3 mm) present in roughly equal amounts. The olivine phenocrysts are subhedral and completely altered to dark green chlorite with occasional light green centers. The plagioclase phenocrysts are euhedral and platy. The unit is cut by small veinlets (less than 1 mm) filled by chlorite and/or a white mineral (laumontite?). Sulfides are disseminated throughout the rock.

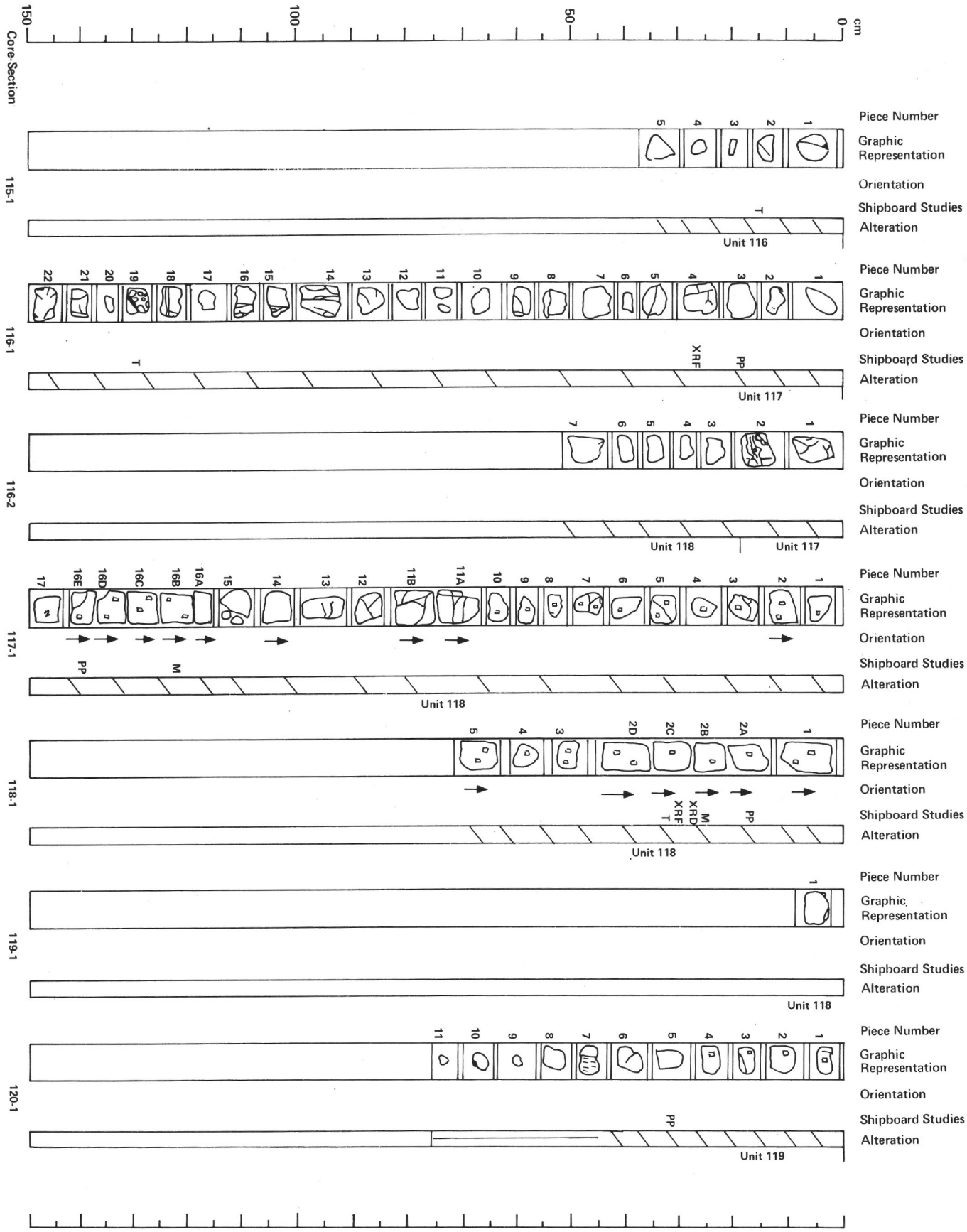
150
100
50
0
cm
Core-Section
115-1
Piece Number
Graphic Representation
Orientation
Shipboard Studies
Alteration
T
Unit 116
116-1
Piece Number
Graphic Representation
Orientation
Shipboard Studies
Alteration
T
XRF
PP
Unit 117
116-2
Piece Number
Graphic Representation
Orientation
Shipboard Studies
Alteration
Unit 118
Unit 117
117-1
Piece Number
Graphic Representation
Orientation
Shipboard Studies
Alteration
PP
M
Unit 118
118-1
Piece Number
Graphic Representation
Orientation
Shipboard Studies
Alteration
T
XRF
XRD
M
PP
Unit 118
119-1
Piece Number
Graphic Representation
Orientation
Shipboard Studies
Alteration
Unit 118
120-1
Piece Number
Graphic Representation
Orientation
Shipboard Studies
Alteration
PP
Unit 119

Unit 116 (1180.5–1185.2 m).
This is a massive unit composed of a fine-grained, gray-colored, sparsely olivine-plagioclase-clinopyroxene phyric basalt. It is unclear whether the breccia at the bottom of Core 114, Section 1, into which Unit 115 intrudes is part of this unit or not. There is no contact at the bottom of the unit. Phenocrysts form about 3% of the rock; olivine (up to 2 mm), plagioclase (up to 2 mm) and clinopyroxene (up to 2.5 mm) are present in roughly equal amounts. Clinopyroxene phenocrysts were recognized only in thin section. Groundmass textures are intersertal Olivine is completely altered to dark green chlorite. Plagioclase phenocrysts appear slightly altered (pale green) in hand specimen, particularly when close to veins. Occasional small veins (approximately 1 mm) are filled with chlorite and/or a pale green/white mineral.

Unit 117 (1185.2–1189.0 m).
This is a massive unit composed of a gray-colored, aphyric to very sparsely olivine-plagioclase ± clinopyroxene phyric basalt. The unit is uniformly fine-grained. The bottom 15 cm of the unit, and a small area approximately two-thirds of the way down from the upper margin, are strongly brecciated, including many chilled basalt fragments. The exact relationship of this material to the remainder of the unit is unclear. The dhilled material in the central part of the unit would suggest a possible lithological division at this horizon between two petrologically identical units. Alternatively, this brecciated material may represent an offshoot from a nearby dike, and be unrelated to the majority of the unit. Thin section study has not helped to alleviate the problem; the material is too highly brecciated to determine to which unit the fine-grained fragments belong. The situation at the base is no simpler, but for simplicity the breccia and fine-grained (chilled?) fragments have been included in Unit 117 (there is no actual chilled contact against Unit 118). Phenocrysts form about 3% of the rock of which olivine (2–4 mm) forms about 1% and plagioclase (2–4 mm) about 2%. Clinopyroxene phenocrysts are rare. Olivine is completely replaced by dark green chlorite. Away from the breccias the unit is still quite heavily veined, although the rock as a whole is not heavily altered. Veins (2–3 mm wide) are filled by green chlorite with occasional accessory white minerals. Wider veins (up to 1 cm in the breccias) often have dark green borders and lighter green centers, with or without white minerals. There are minor disseminated sulfides in the rock.

Unit 118 (1189.0–1203.0 m).
This is a massive unit composed of a sparsely to moderately olivine-plagioclase-clinopyroxene phyric basalt. The top is fine-grained gradually coarsening towards a uniformly medium-grained center and base. Phenocrysts form about 2–3% of the rock; olivine (up to 3 mm) and plagioclase (up to 4 mm) are present in roughly equal proportions. Clinopyroxene phenocrysts (up to 1.5 mm) are rare and recognized only in thin section. Olivine is completely replaced by dark green clay mineral with associated sulfides. Cracks are sparse, filled by a light green to light gray mineral.

Unit 119 (1203.0–1207.5 m).
This is a massive unit composed of a dark gray, sparsely olivine-plagioclase phyric basalt. It is uniformly fine-grained. Two breccias are situated at the center and base of the unit which include chilled basalt fragments. Their exact relationship to the rest of the unit is unclear, but possibly the brecciated chilled material at the center of the unit may be the edge of, or an offshoot from an adjacent dike. The chilled material at the base is probably the intrusive margin of Unit 119, although there is no actual contact with Unit 120. Olivine phenocrysts are up to about 1 mm in size and completely replaced by clay minerals, or sometimes by a reddish colored mineral. Plagioclase phenocrysts are about 2 mm long. Alteration is particularly intense in the brecciated areas; the remainder of the unit is only moderately fractured and less altered. Veins and breccias are filled and cemented by dark green clay minerals and a rare white mineral. Minor amounts of sulfides are disseminated through the rock.

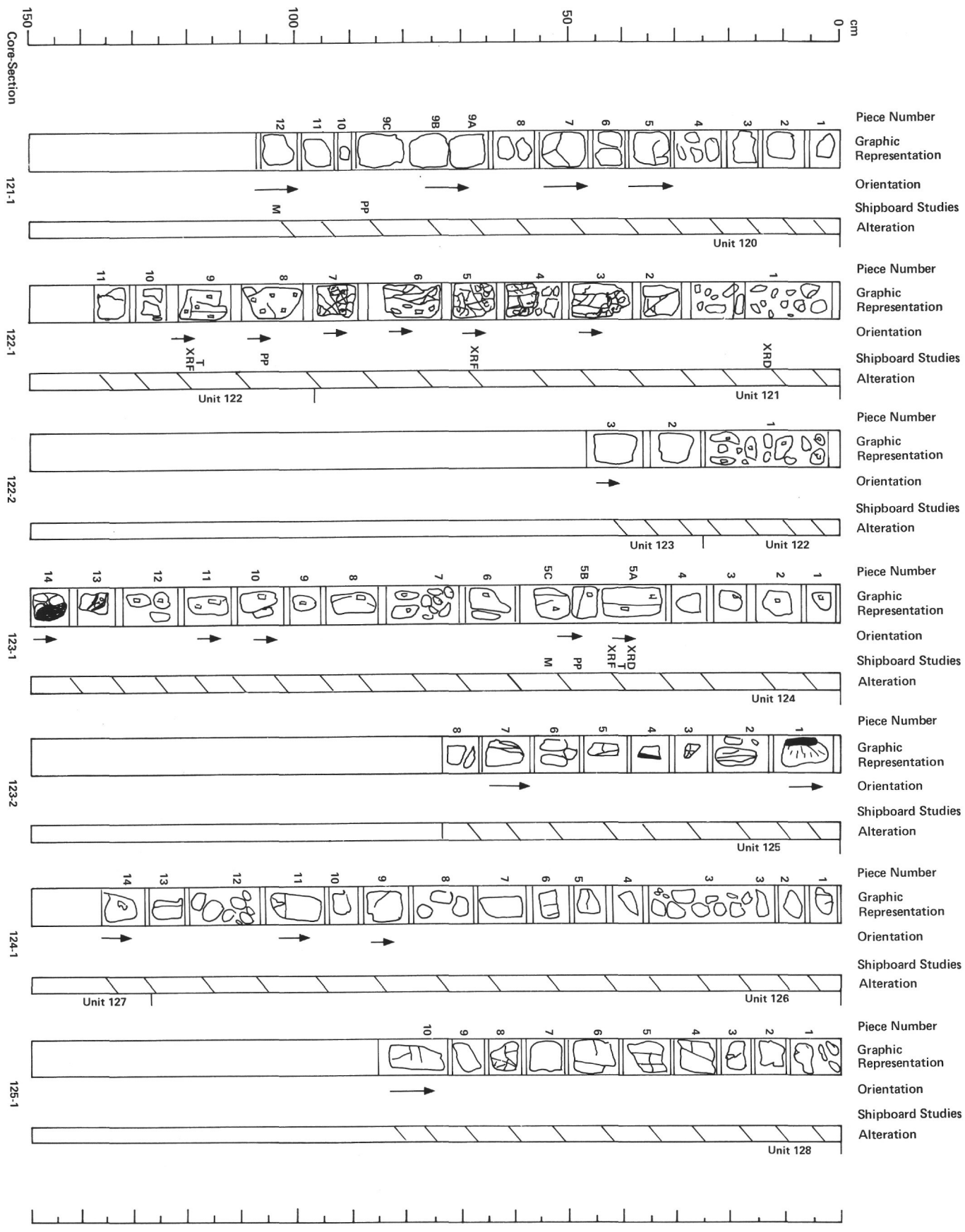
150
100
50
0
cm
Core-Section
121-1
122-1
122-2
123-1
123-2
124-1
125-1
Piece Number
Graphic Representation
Orientation
Shipboard Studies
Alteration
Unit 120
Unit 121
Unit 122
Unit 123
Unit 124
Unit 125
Unit 126
Unit 127
Unit 128
M
PP
XRF
T
XRD

Unit 120 (1207.5–1213.5 m).
This is a massive unit composed of an aphyric to sparsely olivine-plagioclase phyric basalt. The top of the unit is very fine-grained, olivine phyric, rapidly becoming aphyric away from the margin for a distance of about 50 cm. In the medium-grained center and bottom of the unit the basalt becomes sparsely olivine-plagioclase phyric. Phenocrysts can then form up to 2–3% of the rock, olivine (0.5 mm average) being slightly more abundant than plagioclase (up to 2 mm). A few small clinopyroxene phenocrysts (up to 1 mm) were recognized in thin section, but overlooked in hand specimen. Textures are subophitic. Olivine is completely altered to a dark green clay mineral with associated sulfides. Veins are rare, but patchy alteration areas up to 2 mm diameter are reasonably common. Patches appear as irregularly shaped, green areas surrounded by lighter green halos.

Unit 121 (1213.5–1217.5 m).
This is a massive unit composed of a fine-grained, greenish-gray, aphyric basalt. The entire unit is strongly brecciated. Rubble forms the upper 20 cm and includes several chilled basalt fragments which presumably formed an upper intrusive contact to the unit at one time. A small chilled finger of basalt intrudes into the unit close to the base. Veins which coalesce to form the breccias vary in size from 0.5 mm to 1.5 mm and are filled with dark green chlorite. A white platy mineral (anhydrite?) appears in several cracks occasionally associated with clay mineral and accessory pyrite. Some clay mineral veins contain small (0.5 mm) globules composed of a white mineral.

Unit 122 (1217.5–1221.0 m).
This is a massive unit composed of a dark gray, moderately olivine-plagioclase phyric basalt. It is uniformly fine-grained, possibly with a slightly finer top (no chilling). Phenocrysts form about 7% of the rock of which olivine (1–2 mm) forms about 5% and plagioclase (1–3 mm) about 2%. Both are subhedral in shape in a plumose groundmass. Olivine is completely altered to dark green clay. The unit is covered by a network of very fine fractures. Most of these are empty. Exceptions are filled by a light green mineral with occasional white platy or blocky mineral.

Unit 123 (1221.0–1222.5 m).
This is a massive unit composed of a medium-grained, very sparsely olivine-plagioclase phyric basalt. There are no contacts. Olivine phenocrysts (less than 2 mm) are completely altered to a dark green mineral with lighter green mineral cores.

Unit 124 (1222.5–1228.8 m).
This is a massive unit composed of a dark gray, sparsely olivine-plagioclase phyric basalt. The bottom of the unit has intruded into and chilled against a fine- to medium-grained aphyric basalt, forming an almost vertical contact (it is unclear whether this aphyric basalt forms the upper margin of Unit 125). Alteration is intense along this contact (possibly altered glass). The aphyric basalt also contains a small intruded finger of glass (possibly part of Unit 124), now altered to clay. Away from the contact the unit is uniformly fine-grained. Phenocrysts form about 4–5% of the rock of which olivine (up to 2 mm) forms less than 1% and plagioclase (up to 3 mm) 3–4% in total. Textures are fine-grained intergranular. Olivine phenocrysts are euhedral and completely replaced by dark green and reddish-brown minerals (talc/smectite?). Veins can be filled with chlorite or with a white mineral (anhydrite?).

Unit 125 (1228.8–1231.5 m).
This unit is composed of an aphyric basalt. The top is formed by a chilled margin; the unit gradually becomes coarser grained towards the center and bottom (fine- to medium-grained). Fracture surfaces are coated with clays and white minerals. These white minerals often fills the centers of veins (1–3 mm wide) with clay forming the walls. Minor sulfides are usually associated with the green chlorite.

Unit 126 (1231.5–1238.8 m).
This is a massive unit composed of a dark greenish-gray, sparsely olivine-plagioclase phyric basalt. The top is fine-grained gradually coarsening toward the center and base (medium-grained). Olivine phenocrysts are up to 3 mm and are completely altered to green clay. The unit has very few cracks (average width of less than 1 mm). When present they are filled by clay, often with paler-green alteration halos.

Unit 127 (1238.8–1240.5 m).
This is a massive unit composed of a uniformly medium-grained, moderately olivine-plagioclase phyric basalt. It differs from the bottom of the preceeding unit in being more phyric and containing vugs (up to 5 mm) filled with clay. Clay also replaces olivine phenocrysts. Veining is the same as in Unit 126.

Unit 128 (1240.5–1249.5 m).
This is a massive unit composed of an aphyric to very sparsely olivine phyric basalt. The top is fine-grained coarsening downwards into a medium-grained center and base. Olivine phenocrysts (approximately 2 mm) are sparse and totally altered to a dark green mineral surrounded by halos of lighter green alteration. The unit is cut by a network of fine veins filled by clay and white minerals with associated sulfides. Veins are frequently surrounded by a light green halo up to about 5 mm wide.


Core-Section
cm
0
50
100
150
126-1
127-1
128-1
128-2
129-1
129-2
129-3
Piece Number
Graphic Representation
Orientation
Shipboard Studies
Alteration
Unit 129
Unit 130
Unit 131
Unit 132
Unit 133
Unit 134
Unit 135
XRD
XRF
T
PP
M

Unit 129 (1249.5–1253.0 m).
This is a massive unit composed of a moderately olivine-plagioclase-clinopyroxene phyric basalt. The top of the unit is slightly coarser grained than the center and base which are fine- to medium-grained. Phenocrysts form about 6–7% of the rock, olivine (2–3 mm) and plagioclase (2 mm) forming about 2–3% each and clinopyroxene (2–5 mm) about 1%. A few chrome spinel microphenocrysts (0.4 mm) are evident in thin section. Textures are intergranular. Olivine phenocrysts are completely replaced by dark green clay (saphonite?) which fill the cores, and a pale green fibrous mineral (talc?) forming the rims. Pyrite is often associated with the pseudomorphs. The upper part of the unit contains several areas with pale-colored patches in the groundmass, presumably the affect of diffuse alteration. There is a limited amount of veinings; veins are mostly filled with dark green minerals and white crystalline anhydrite.

Unit 130 (1253.0–1253.5 m).
This is a thin (0.5 m), fine-grained, massive unit very similar to Unit 129. It differs only slightly in being sparsely phyric rather than moderately olivine-plagioclase-clinopyroxene phyric. Alteration characteristics are the same as in Unit 129, but without any pale-colored patchy areas.

Unit 131 (1253.5–1262.5 m).
This is a massive unit composed of a gray-colored, sparsely to moderately olivine-plagioclase-clinopyroxene phyric basalt. It has a medium- to coarse-grained top with a fine-grained base (no contact). Phenocrysts form 4–7% of the rock, olivine (0.5–4 mm) forming 2–4%, plagioclase (0.5–3 mm) about 2–3% and clinopyroxene (up to 6 mm long) less than 1%. Olivine phenocrysts are euhedral or subhedral and completely replaced by dark green or light green clays (saponite[?] and talc[?] respecitively). The latter, together with minor grains of pyrite, usually forms a rim to the pseudomorph. The plagioclase and clinopyroxene phenocrysts are subhedral. Textures are subophitic. Veins are rare and thin (less than 0.5 mm), filled by dark green or light green minerals.

Unit 132 (1262.5–1265.2 m).
This is a massive unit composed of a gray-colored, uniformly medium-grained, sparsely to moderately olivine-plagioclase-clinopyroxene phyric basalt. Phenocrysts form 4–5% of the rock, olivine (up to 2 mm) and clinopyroxene (up to 10 mm) each forming about 1–2%, and plagioclase (up to 3 mm) 2–3%. The olivine phenocrysts are completely altered to talc with opaques and minor smectite. Clinopyroxene phenocrysts are rounded, occasionally with inclusions of plagioclase. In hand specimen they often exhibit alignment. Textures are intergranular to subophitic. Veins are rare. Fracturing is unusual in having two distinct sets, one vertical and one subvertical.

Unit 133 (1265.2–1274.8 m).
This is a massive unit composed of a dark gray, sparsely to moderately olivine-plagioclase-clinopyroxene phyric basalt. The top of the unit is fine-grained (no contact), becoming gradually coarser towards the center and base (medium- to coarse-grained. The upper 30 cm are almost aphyric, the remainder of the unit contains up to 7 or 8% phenocrysts. Olivine (3–4 mm) is the most abundant phase, forming up to 3% of the rock; plagioclase (up to 4 mm) and clinopyroxene (up to 6 mm) phenocrysts are in roughly equal proportions, forming up to 2% each. Olivine phenocrysts are euhedral and completely replaced by dark green and light green clays. The center of the pseudomorphs are rounded and composed of dark green clay (saponite?); the rims are altered to the lighter green mineral (talc?) together with magnetite. Olivine crystals also have spherical inclusions which are probably melt inclusions. Plagioclase phenocrysts are subhedral. Clinopyroxene phenocrysts are anhedral, mostly as large ophitic or subophitic crystals. Groundmass textures are subophitic to ophitic. Alteration of the rock appears to be minimal with very few veins; the veins are filled mainly by dark green clay minerals. Minor sulfides are disseminated through the rock.

Unit 134 (1274.8–1277.8 m).
This is a massive unit composed of a dark gray, moderately olivine-plagioclase-clinopyroxene phyric basalt. Textures are intergranular to intersertal. Olivine phenocrysts (1 mm) are extremely rare, completely replaced by dark green clays. Alteration can also affect the groundmass surrounding the olivine pseudomorphs giving the illusion of larger phenocrysts. Pale green halos surround these areas. Vug-like bodies, distinct from the olivine pseudomorphs but with the same alteration characteristics, give the rock a spotted appearance. Veins are more common than in the preceeding unit. Often these are filled by several minerals, usually dark green chlorite forming the vein walls with centers composed of a white mineral (laumontite?). Pale green-gray halos penetrate the surrounding rock for up to 3 mm. Pyrite is common in the veins. Approximately halfway down the unit a small, chilled intrusive finger of a plagioclase-clinopyroxene phyric basalt can be seen. This presumably is an offshoot from an adjacent dike missed during drilling.

cm
0
50
100
150
Core-Section
Piece Number
Graphic Representation
Orientation
Shipboard Studies
Alteration
130-1
130-2
130-3
131-1
131-2
132-1
132-2
Unit 135
Unit 136
Unit 137
XRD
PP
M
XRF
T
Void

Unit 135 (1277.8–1287.5 m).
This is a massive unit composed of a dark gray, moderately olivine-plagioclase-clinopyroxene phyric basalt. The top of the unit is slightly finer grained than the center and base which are both fine- to medium-grained. Phenocrysts form about 4–6% of the rock of which olivine (1–3 mm) forms 1–2%, plagioclase (up to 2 mm) about 2–4% and clinopyroxene (up to 6 mm) 1–3%. Olivine phenocrysts are euhedral, the cores having been replaced by dark green saponite and rims by talc. Plagioclase and clinopyroxene phenocrysts are subhedral. A few small (0.2 mm) microphenocrysts of chrome spinel are recognizable in thin section. Textures are subophitic. Very few veins/fractures disect the unit. These are usually filled with dark blue-green clays, sometimes with grayish alteration zones up to 5 mm wide. Pyrite occurs in small patches (up to 4 mm) on broken vein surfaces.

Unit 136 (1287.5–1295.0 m).
This is a massive unit composed of a dark gray, moderately olivine-plagioclase-clinopyroxene phyric basalt. The top and center of the unit are uniformly fine-grained, rapidly fining even further towards a 20 cm thick zone (aphyric) at the bottom of the unit, presumably close to a contact. Phenocrysts form 7–8% of the rock of which olivine (up to 4 mm) forms about 2%, plagioclase (up to 5 mm) about 3% and clinopyroxene (up to 6 mm) about 2–3% in total. The olivine phenocrysts are euhedral and completely altered to dark green clays (in thin section they comprise a pale brown core with colorless rim). Plagioclase phenocrysts are euhedral, often forming glomero-crystic aggregates. Clinopyroxene phenocrysts are anhedral. Groundmass textures are subophitic. The unit is sparsely veined towards the top, veins becoming more common towards the base. They are filled with dark green (chlorite?) and white minerals. Minor amounts of pyrite are disseminated through the rock.

Unit 137 (1295.0–1304.0 m).
This is a massive unit composed of a gray, sparsely olivine-plagioclase-clinopyroxene phyric basalt. The unit has a fine- to medium-grained top and bottom with a medium- to coarse-grained center. Phenocrysts form about 3% of the rock in the upper two thirds of the unit, slightly less towards the base. Of these, olivine (1 mm) is the most abundant, forming about 2% of the rock; the plagioclase (less than 1 mm) and clinopyroxene (up to 2 mm) form less than 1% each. Olivine phenocrysts are replaced by two minerals, one which is light green and forms the core and the other which is dark green and forms the rims. Pyrite is associated with olivine alteration. Veins are small (0.5 mm) and not common, but those present are filled with green chlorite, pyrite, and a white mineral, the latter usually in the vein centers. Isolated areas of the unit show an unusual pervasive alteration where vein minerals are disseminated throughout the groundmass.

cm
0
50
100
150
Core-Section
Piece Number
Graphic Representation
Orientation
Shipboard Studies
Alteration
133-1
133-2
134-1
135-1
136-1
137-1
138-1
Void
XRD
M
T
PP
Unit 137
Unit 138
Unit 139
Unit 140
Unit 141
Unit 142
Unit 143
Unit 144

Unit 138 (1304.0–1313.0 m).
This is a massive unit composed of a moderately olivine-plagioclase-clinopyroxene phyric basalt. The top 50 cm are fine-grained, gradually coarsening towards the center and bottom of the unit, which are medium-grained. The unit tends to be less phyric near to the bottom. Those parts which are moderately phyric have a phenocryst content of about 5–6%, olivine (average 2 mm), plagioclase (up to 2 mm) and clinopyroxene (up to 8 mm) present in roughly equal proportions. Textures are subophitic to intergranular. Olivine is completely altered to a dark green mineral. Fractures are sparse; these tend to be horizontal in orientation, particularly near the base. They are not always filled with secondary minerals as in other units. When they are, the mineral is usually dark green, often with pale gray alteration zones extending for up to 5 mm away from the vein walls. A white fibrous mineral can act as a late-stage filling to the green veins. Particularly towards the bottom of the unit, pervasive alteration of the basalt is locally intense, occurring as single and/or coalesced vug-like bodies or elongate vein-like areas. These have centers composed of a speckled mass of light green, dark green, and white minerals, surrounded by a pale gray halo (see alteration chapter).

Unit 139 (1313.0–1317.5 m).
This unit is composed of a uniformly fine- to medium-grained, sparsely to moderately olivine-plagioclase-clinopyroxene phyric basalt. Phenocrysts can form up to a maximum of 7% of the rock, olivine (up to 5 mm) forming about 1%, plagioclase (up to 3 mm) 4–5% and clinopyroxene (up to 10 mm) about 2%. The large clinopyroxene phenocrysts make this unit quite distinct from those above and below it. Olivine phenocrysts are euhedral, completely replaced by a dark green mineral (chlorite?) with occasional pyrite grains. Plagioclase phenocrysts are subhedral to euhedral exhibitng normal zoning with distinct cores and rims. Some form glomerocrystic aggregates. The clinopyroxene phenocrysts are subhedral to anhedral; the large crystals ophitically enclose small plagioclase grains and exhibit late stage nucleation of plagioclase at their rims. Textures are subophitic to intergranular. Veins are rare and thin (less than 0.5 mm), filled by a dark green mineral. Light grayish-green alteration halos (up to 15 mm wide) occur around some of these veins.

Unit 140 (1317.5–1322.0 m).
This is a massive unit composed of a uniformly medium-grained, greenish-gray, sparsely olivine-plagioclase-clinopyroxene phyric basalt. The unit is distinguished from the preceeding one by its lack of large clinopyroxene phenocrysts and by a unusual pervasive alteration of the groundmass. Here large green patches (up to 20 cm^3) of highly altered basalt penetrate the rock. The contact between these patches and the surrounding fresher basalt is diffuse, and is recognized by a lighter gray zone. Veins are not particularly common, but can be up to 3 mm wide. These are filled by a dark green mineral which coats the walls; vein centers are composed of a white mineral (zeolite?) together with minor amounts of pyrite. Light greenish-gray alteration halos (up to 8 mm wide) can accompany these veins. Minor amounts of pyrite are disseminated through the rock.

Unit 141 (1322.0–1323.0 m).
This is a massive unit composed of a dark gray, aphryic basalt. It has a fine-grained top which coarsens very slightly towards the bottom. A few thin veinlets (less than 1 mm) filled with a dark green mineral dissect the unit. Narrow (less than 0.5 mm), greenish-gray, alteration halos are associated with these. Minor sulfides are disseminated through the unit.

Unit 142 (1323.0–1325.0 m).
This is a massive unit composed of a dark gray uniformly fine- to medium-grained, moderately olivine-plagioclase-clinopyroxene phyric basalt. The olivine phenocrysts (up to 4 mm) are relatively abundant; they are completely replaced by either a dark green mineral, by a light green mineral, or by a combination of both. Plagioclase phenocrysts are up to 4 mm in size. Clinopyroxene phenocrysts are recognized in hand specimen as large (up to 8 mm) prismatic crystals. Veins are rare, usually less than 1 mm wide. When present they often exhibit pervasive alteration of the surrounding basalt walls where green, white (zeolite?) and transparent minerals permeate the groundmass to form 1 cm wide alteration halos.

Unit 143 (1325.0–1332.0 m).
This is a massive unit composed of a dark gray, highly olivine-plagioclase-clinopyroxene phyric basalt. The unit is uniformly fine- to medium-grained, with a slightly finer zone at the top. Olivine phenocrysts (up to 5 mm) are replaced by green and dark reddish-brown minerals. Plagioclase phenocrysts are up to 5 mm in size. Particularly abundant clinopyroxene phenocrysts characterize the unit. Seen in hand specimen they appear as large, (up to 10 mm) green, prismatic crystals. Very few veins disect the unit, but when present they are filled with white minerals, sometimes with adjacent alteration halos. Rare pyrite grains are disseminated in the groundmass.

Unit 144 (1332.0–1337.5 m).
This is a massive unit composed of a gray-colored, sparsely olivine-plagioclase phyric basalt. The top of the unit is medium-grained, gradually fining towards a chilled intrusive contact at the base of the unit. The contact is not oriented, but it would appear Unit 144 has intruded into and chilled against Unit 145. Phenocrysts form about 1–2% of the rock of which olivine (up to 2 mm) forms less than 1% and plagioclase about 1–2% in total. Olivine is replaced by a dark green mineral with minor amounts of pyrite. Veining is not intense (average width of 1 mm), but when present veins are filled by a white fibrous-platy mineral (anhydrite?), a pale greenish mineral and a dark green mineral. In the case of the dark green veins, alteration zones up to 1 cm wide penetrate the surrounding rock.

cm
0
50
100
150
Core-Section
Piece Number
Graphic Representation
Orientation
Shipboard Studies
Alteration
Unit 144
Unit 145
Unit 145
Unit 146
Unit 147
XRD
139-1
140-1
141-1

Unit 145 (1337.5–1345.5 m).
This is a massive unit composed of a dark gray to greenish-gray, sparsely to moderately olivine-plagioclase-clinopyroxene phyric basalt. The upper part of the unit is fine-grained and intruded by Unit 144. The center is medium-grained and the base fine-grained. The lower part of the unit tends to be less phyric than the upper with no clinopyroxene phenocrysts evident in hand specimen. The unit is extensively altered, veins filled by dark green clays with minor amounts of a white platy mineral (anhydrite?). Towards the base of the unit an additional white mineral appears which is fibrous and prismatic (zeolite?). A small intrusive finger of chilled, sparsely olivine phyric basalt glass, intrudes into the center of the unit. It is strongly altered.

Unit 146 (1345.5–1347.3 m).
This is a massive unit composed of a dark gray, sparsely to moderately olivine-plagioclase-clinopyroxene phyric basalt. It has a fine-grained top, gradually coarsening towards the base. Olivine phenocrysts are up to 6 mm, completely replaced by dark green and reddish-brown minerals. Plagioclase phenocrysts and clinopyroxene phenocrysts are 3 cm and 4 cm long, respectively. Minor amounts of sulfide are disseminated through the rock.

Unit 147 (1347.3–1350.0 m).
This is a massive unit composed of a uniformly fine-grained, greenish-gray, moderately olivine-plagioclase ± clinopyroxene phyric basalt. The unit is strongly altered, disected by many thin veins (less than 1.5 mm) which are filled with a dark green and a light green mineral. Sulfides are rare.

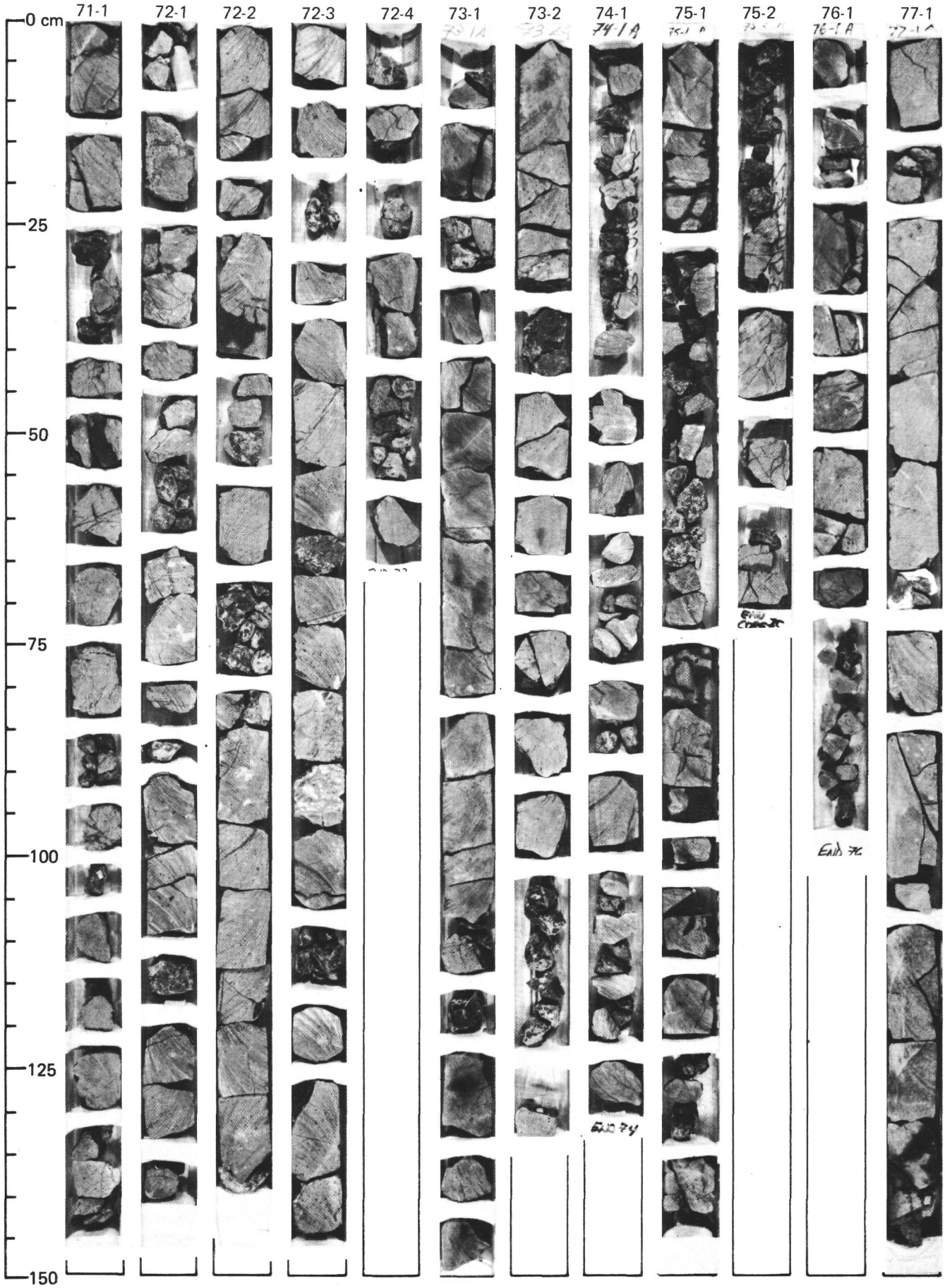
0 cm
25
50
75
100
125
150
71-1
72-1
72-2
72-3
72-4
73-1
73-2
74-1
75-1
75-2
76-1
77-1

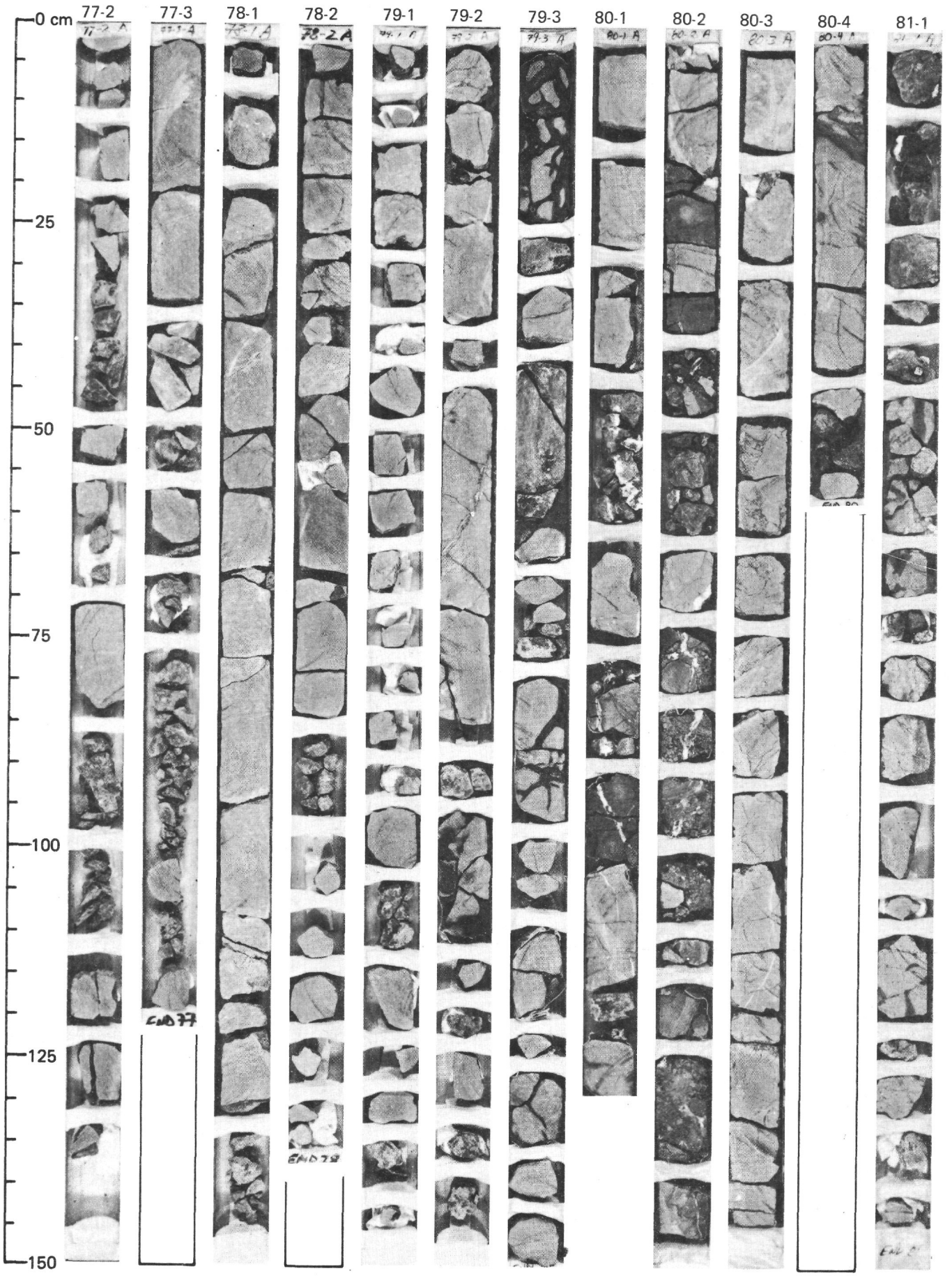
0 cm
25
50
75
100
125
150
77-2
77-3
78-1
78-2
79-1
79-2
79-3
80-1
80-2
80-3
80-4
81-1

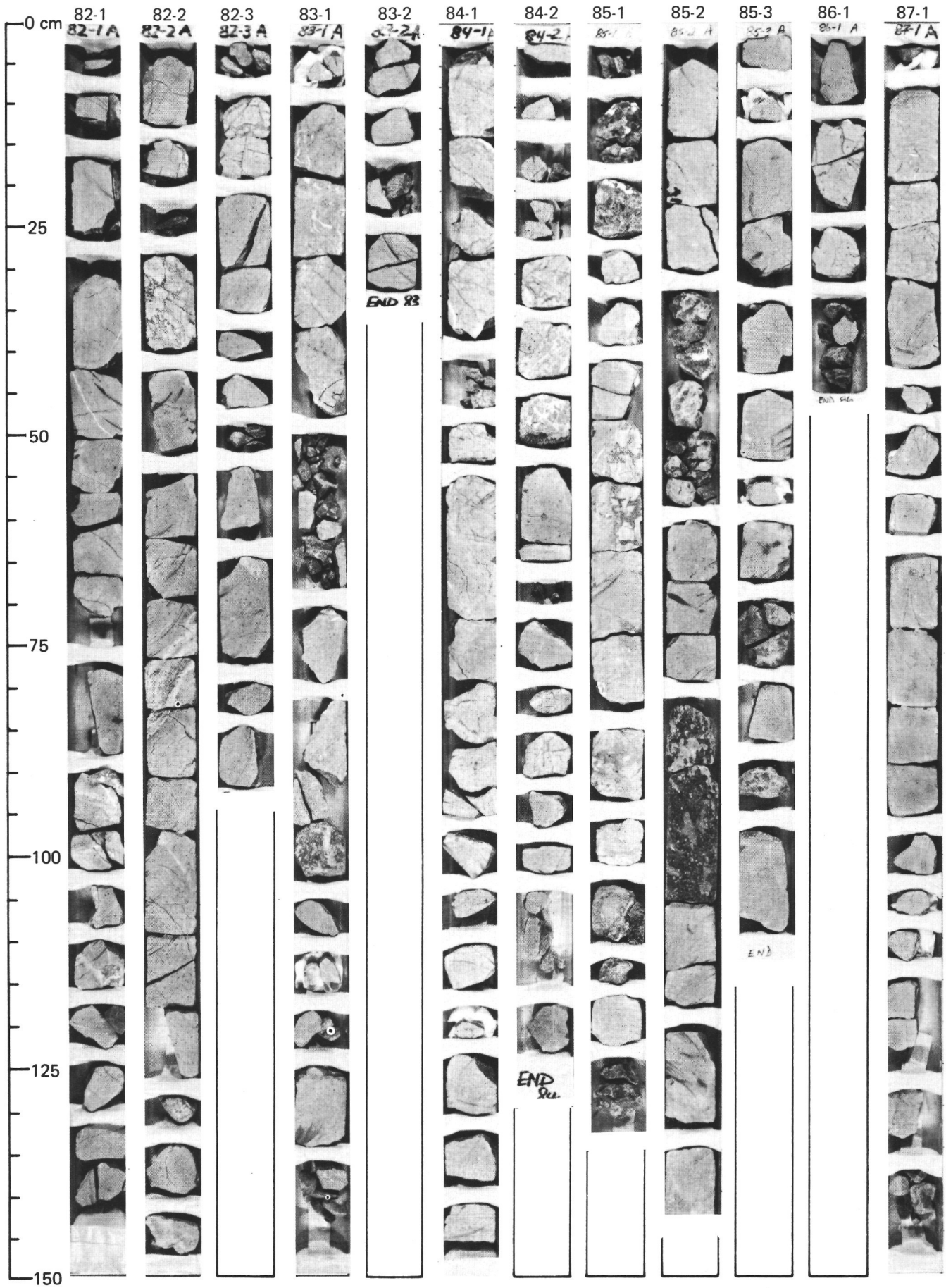
0 cm
25
50
75
100
125
150
82-1
82-2
82-3
83-1
83-2
84-1
84-2
85-1
85-2
85-3
86-1
87-1
END

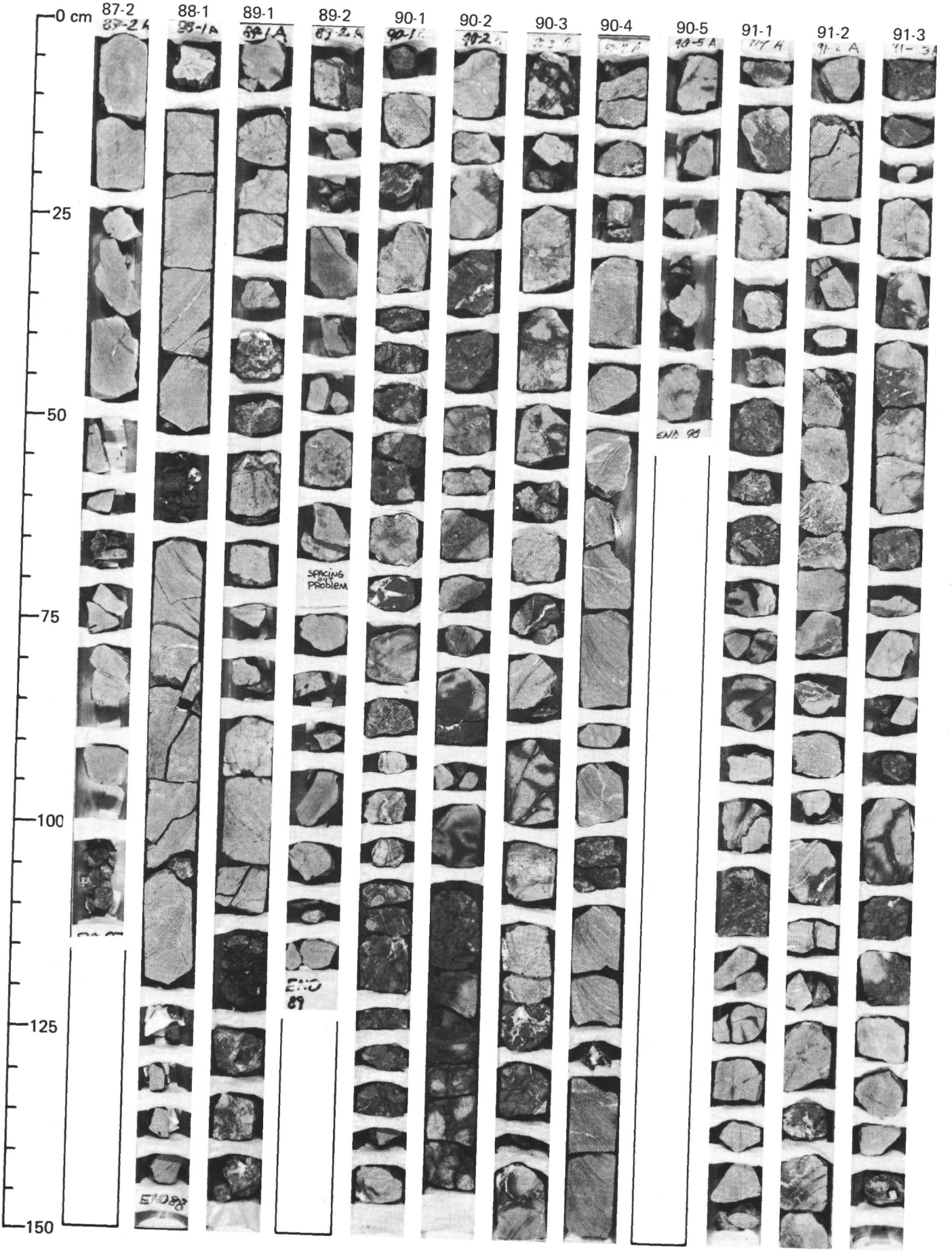
0 cm
87-2
88-1
89-1
89-2
90-1
90-2
90-3
90-4
90-5
91-1
91-2
91-3
25
50
75
100
125
150
SPACING NOT PROBLEM
END 89
END 88

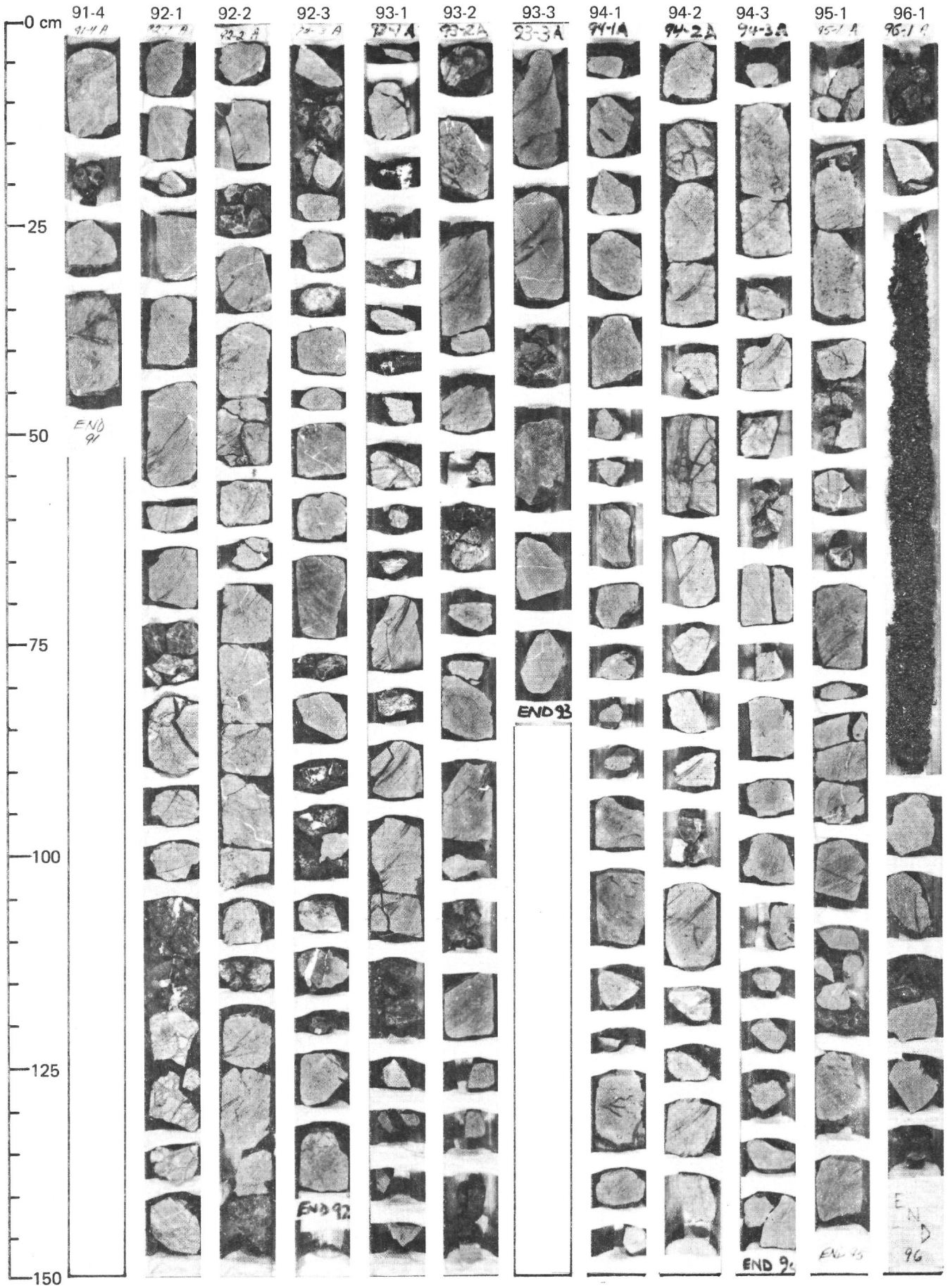
0 cm
25
50
75
100
125
150
91-4
92-1
92-2
92-3
93-1
93-2
93-3
94-1
94-2
94-3
95-1
96-1
END 91
END 92
END 93
END 96

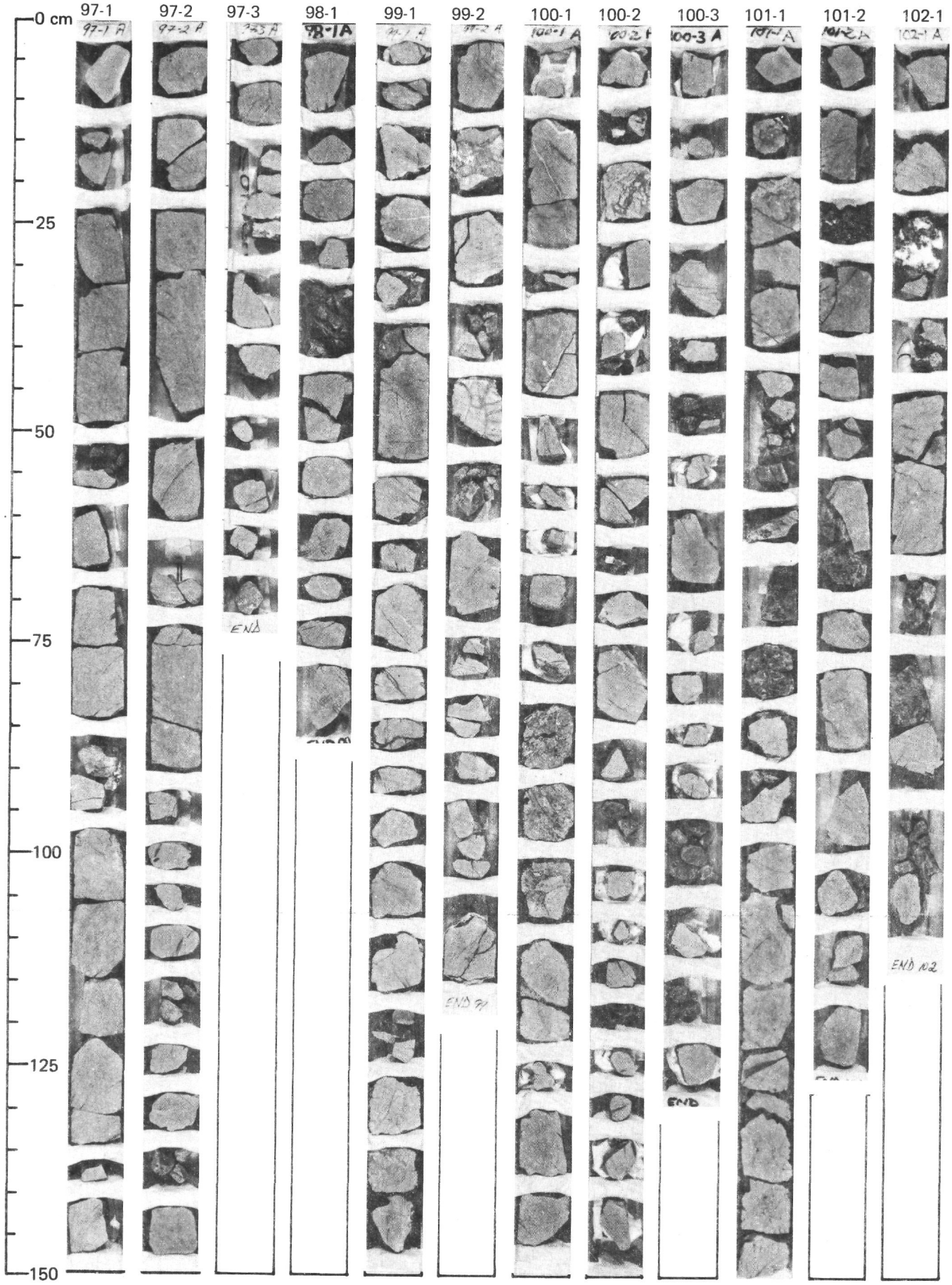
0 cm
25
50
75
100
125
150
97-1
97-2
97-3
98-1
99-1
99-2
100-1
100-2
100-3
101-1
101-2
102-1
END
END 102

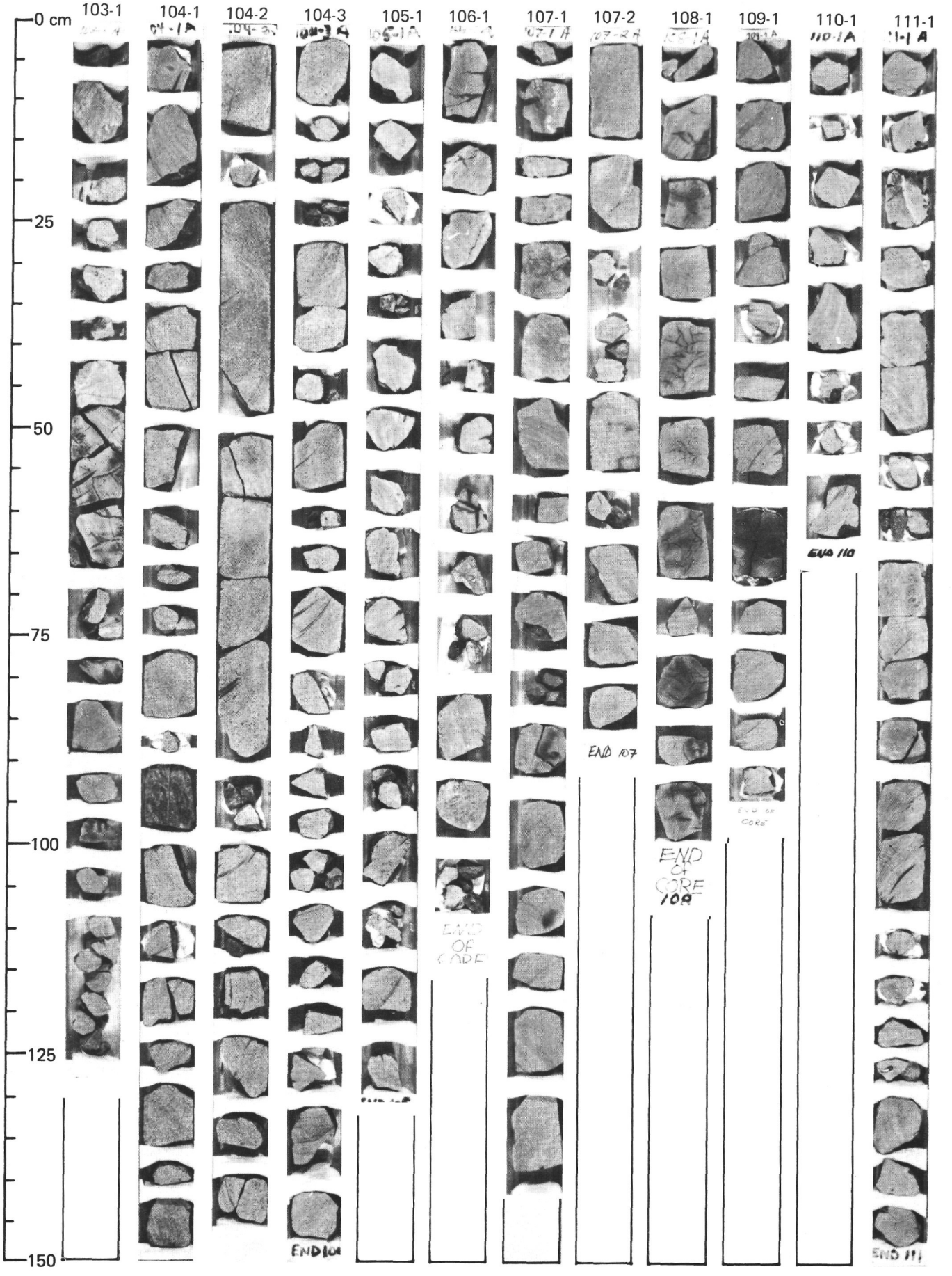
0 cm
25
50
75
100
125
150
103-1
104-1
104-2
104-3
105-1
106-1
107-1
107-2
108-1
109-1
110-1
111-1
END 110
END 107
END OF CORE
END OF CORE 108
END 104
END 111

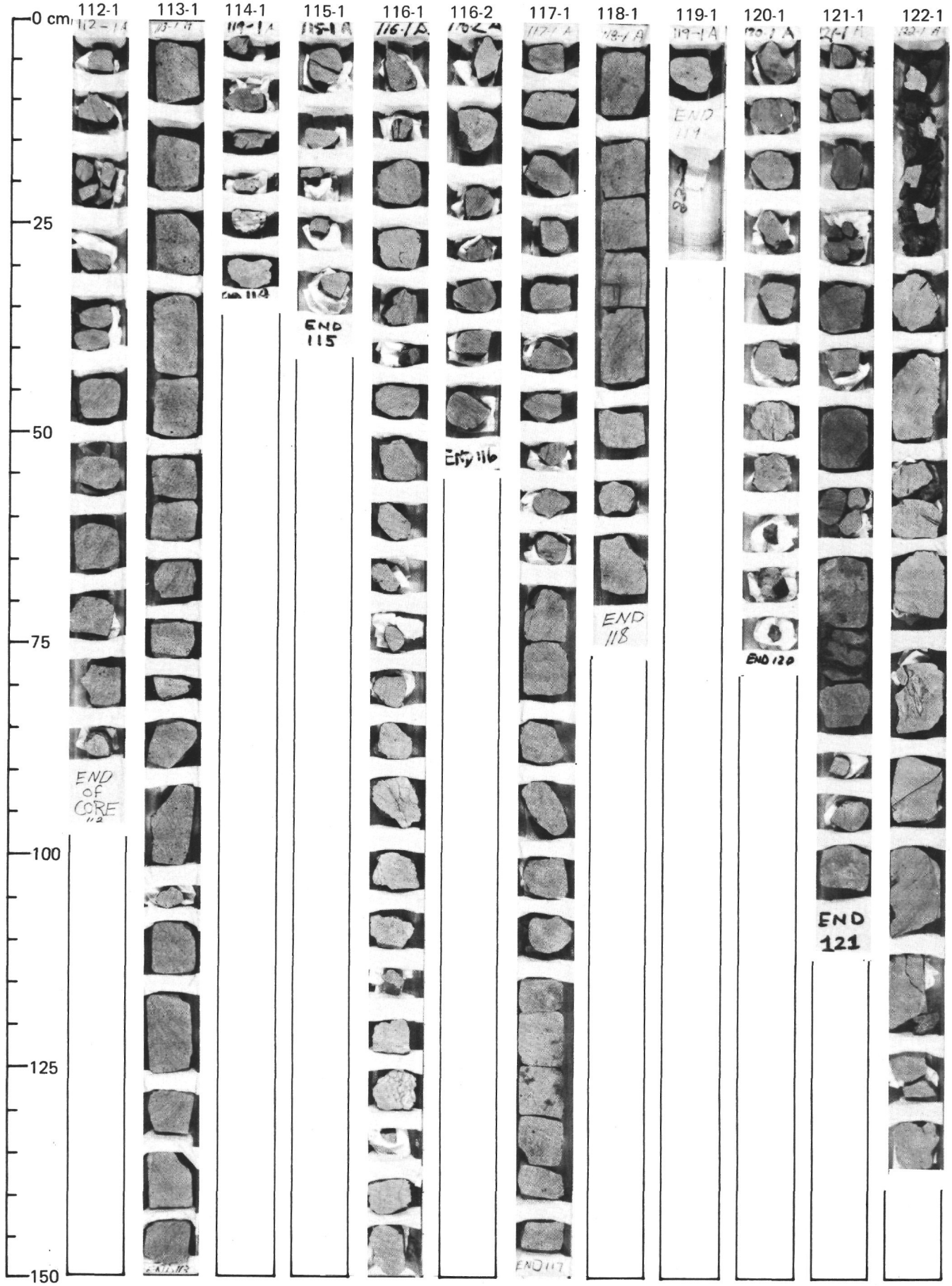
0 cm
25
50
75
100
125
150
112-1
113-1
114-1
115-1
116-1
116-2
117-1
118-1
119-1
120-1
121-1
122-1
END of CORE
END 115
END 116
END 118
END 120
END 121

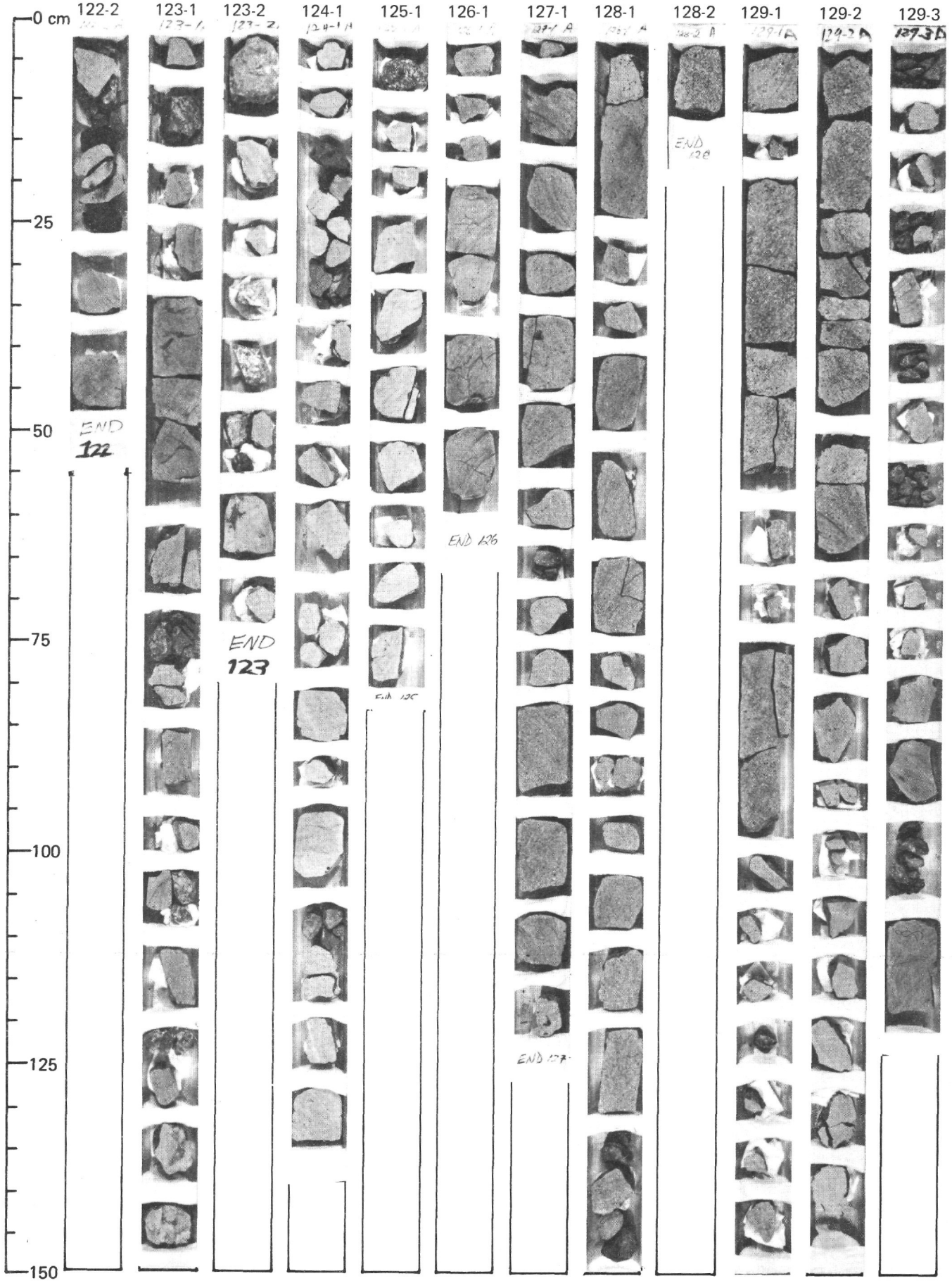
0 cm
25
50
75
100
125
150
122-2
123-1
123-2
124-1
125-1
126-1
127-1
128-1
128-2
129-1
129-2
129-3
END 122
END 123
END 126
END 127
END 128

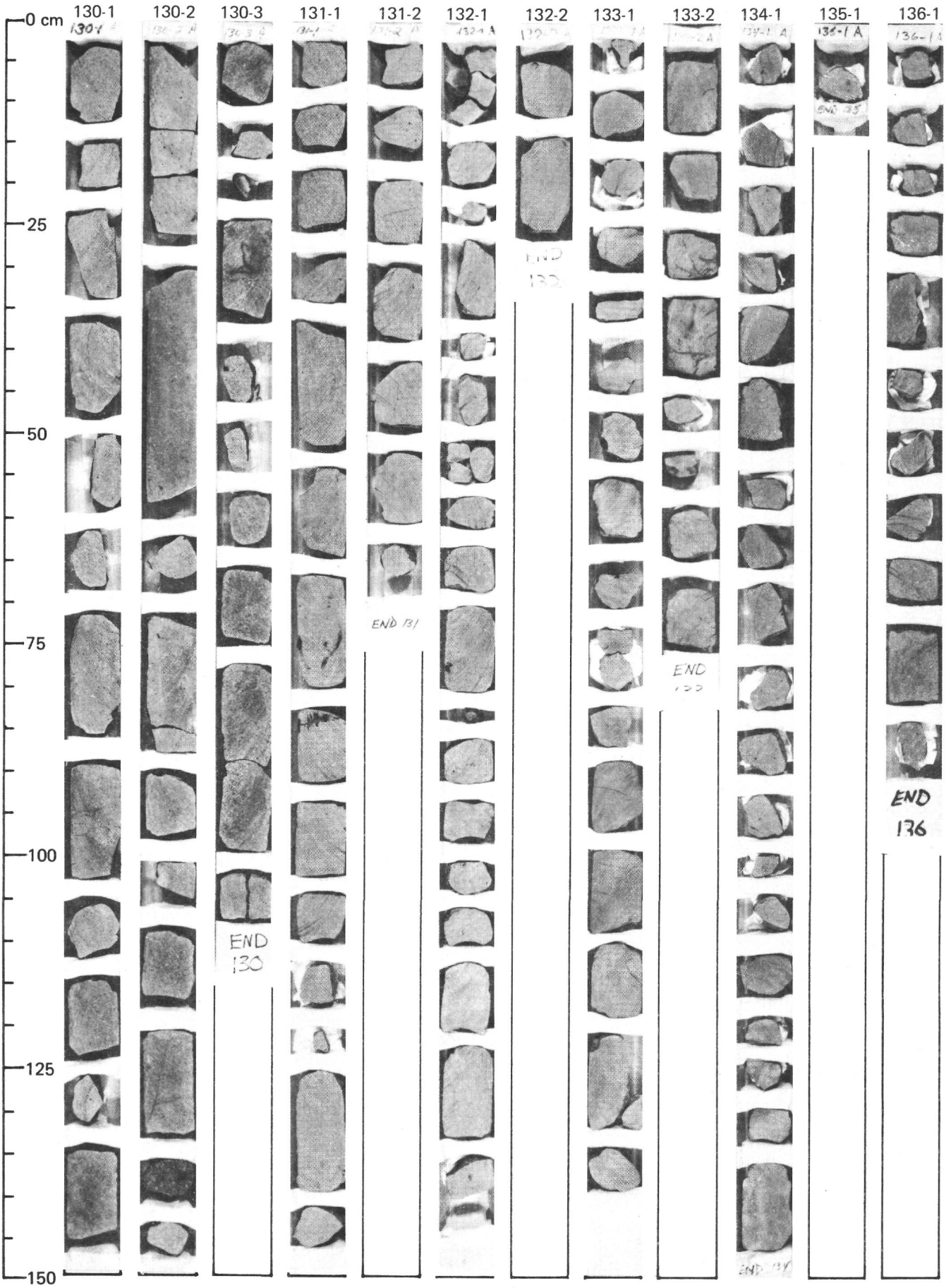
0 cm
25
50
75
100
125
150
130-1
130-2
130-3
131-1
131-2
132-1
132-2
133-1
133-2
134-1
135-1
136-1
END 130
END 131
END 132
END 133
END 135
END 136

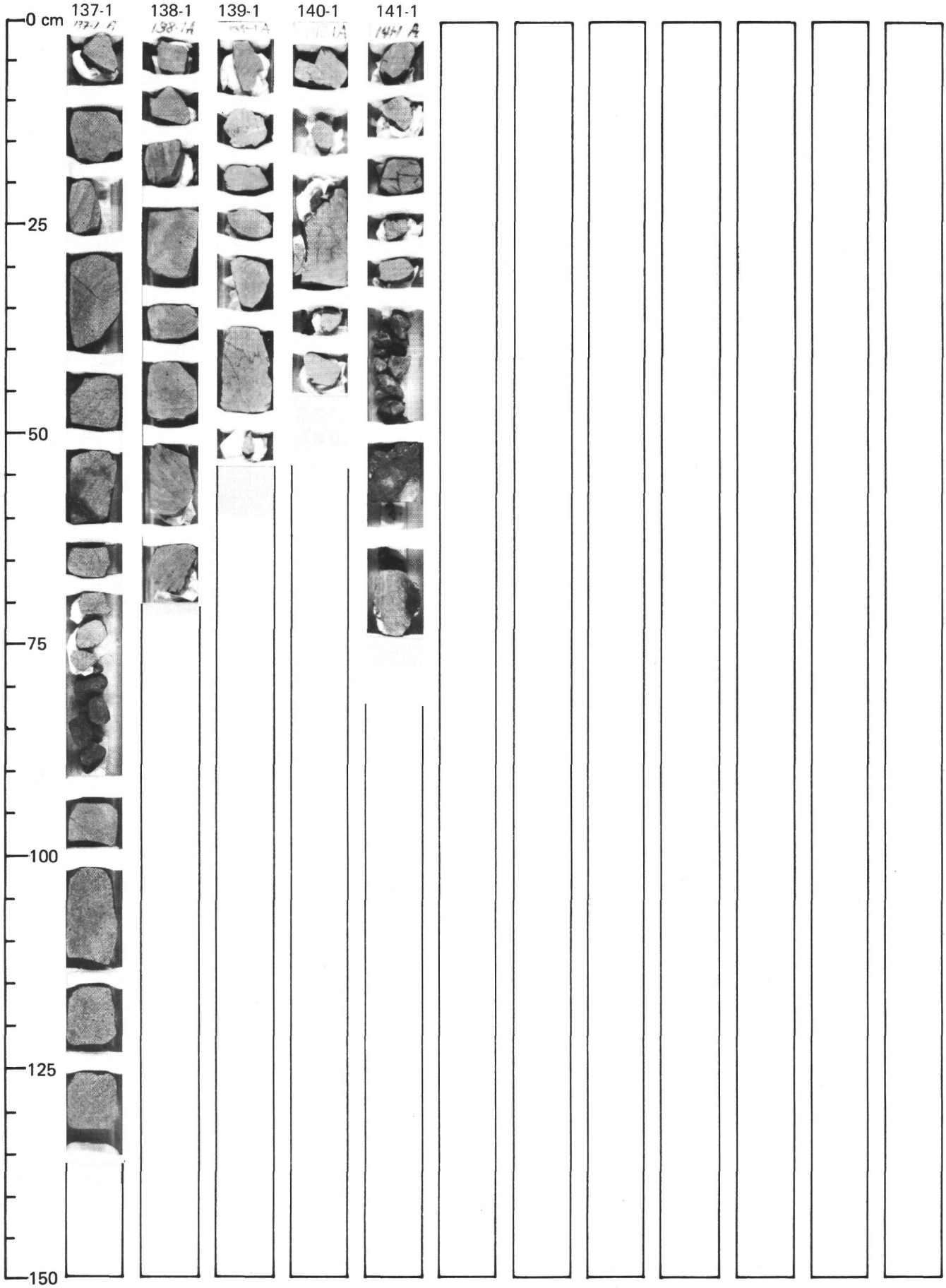
0 cm
137-1
138-1
139-1
140-1
141-1
25
50
75
100
125
150